

# **Gamma-Ray Bursts**



# Contents

<b>1. Topics</b>	<b>17</b>
<b>2. Participants</b>	<b>19</b>
2.1. ICRA Net participants . . . . .	19
2.2. Past collaborators . . . . .	19
2.3. Ongoing collaborations . . . . .	20
2.4. Students . . . . .	21
<b>3. Brief description</b>	<b>23</b>
3.1. The space, time and energetics of GRBs . . . . .	23
3.2. The black hole and GRB uniqueness . . . . .	23
3.3. The blackholic energy . . . . .	26
3.4. The limits on the energetics of GRBs . . . . .	28
3.5. The “canonical” GRB: short vs long GRBs . . . . .	29
3.6. Brief summary of recent progresses . . . . .	32
<b>4. Selected publications before 2005</b>	<b>35</b>
4.1. Refereed journals . . . . .	35
4.2. Conference proceedings . . . . .	41
<b>5. Publications (2005–2011)</b>	<b>45</b>
5.1. Refereed journals . . . . .	45
5.2. Conference proceedings . . . . .	56
<b>6. Brief reminder of the fireshell model</b>	<b>79</b>
6.1. The optically thick phase . . . . .	81
6.2. The transparency point . . . . .	82
6.3. The optically thin phase . . . . .	87
6.4. Extended afterglow luminosity and spectrum . . . . .	88
6.5. The new class of “disguised” short GRBs . . . . .	93
6.6. The “fireshell” model and GRB progenitors . . . . .	95
<b>7. Evidence for broadening of the spectral energy distribution of GRBs within the fireshell model</b>	<b>97</b>
7.1. Introduction . . . . .	97
7.2. The Fireshell Model . . . . .	98

7.3.	The source luminosity and the spectrum . . . . .	99
7.3.1.	Thermal case . . . . .	100
7.3.2.	The “modified” thermal spectrum . . . . .	101
7.4.	Comparison with observational data . . . . .	103
7.4.1.	GRB 080319B . . . . .	103
7.4.2.	GRB 050904 . . . . .	103
7.5.	Conclusions . . . . .	106
<b>8.</b>	<b>On the nature of GRB 050509b: a disguised short GRB</b>	<b>109</b>
8.1.	Introduction . . . . .	109
8.2.	Fireshell model . . . . .	110
8.3.	Data analysis of GRB 050509b . . . . .	114
8.3.1.	Scenario 1 . . . . .	114
8.3.2.	Scenario 2 . . . . .	114
8.4.	The theoretical spectrum and Amati relation . . . . .	117
8.5.	Discussion . . . . .	121
8.6.	Conclusion . . . . .	122
<b>9.</b>	<b>A new class of very energetic GRBs within the fireshell model</b>	<b>125</b>
9.1.	GRB 080319B . . . . .	125
9.2.	GRB 050904 . . . . .	126
<b>10.</b>	<b>GRB 090423 : a canonical GRB at redshift 8.1</b>	<b>137</b>
10.1.	GRB 090423 in the fireshell model . . . . .	138
10.1.1.	The fragmentation of the fireshell . . . . .	140
10.1.2.	GRB 090423 considered as a disguised short GRB . . . . .	141
10.2.	A new component in the afterglow scenario . . . . .	142
10.3.	Discussions and conclusions . . . . .	146
<b>11.</b>	<b>The high-energy emission in the fireshell scenario</b>	<b>149</b>
11.1.	Spectral analysis of the P-GRB candidates . . . . .	152
<b>12.</b>	<b>A double component in the prompt emission of GRB 090618</b>	<b>157</b>
12.1.	Introduction . . . . .	157
12.1.1.	A brief description of the fireshell scenario . . . . .	157
12.2.	Data analysis . . . . .	158
12.2.1.	Data reduction and light curve . . . . .	158
12.2.2.	Spectral analysis: identification of the P-GRB . . . . .	158
12.3.	Results . . . . .	159
12.3.1.	From 0 to 50s . . . . .	159
12.3.2.	The second episode as an independent GRB . . . . .	160
12.3.3.	The first 50 s emission is not a GRB . . . . .	161
12.4.	A different emission process . . . . .	161

<b>13. Evidences for a double component in GRB 101023</b>	<b>163</b>
13.1. Introduction . . . . .	163
13.1.1. Fireshell Scenario . . . . .	163
13.2. Data analysis . . . . .	164
13.2.1. Data reduction . . . . .	164
13.2.2. light curve . . . . .	164
13.3. Redshift determination . . . . .	164
13.4. Spectral analysis . . . . .	166
13.4.1. Episode 1: Temperature and radius evolution . . . . .	168
13.5. Conclusions . . . . .	169
<b>A. On the GRB-SN association</b>	<b>173</b>
A.1. GRB 980425 / SN 1998bw / URCA-1 . . . . .	173
A.2. GRB 030329 / SN 2003dh / URCA-2 . . . . .	176
A.3. GRB 031203 / SN 2003lw / URCA-3 . . . . .	177
A.4. The GRB / SN / URCA connection . . . . .	177
A.5. URCA-1, URCA-2 and URCA-3 . . . . .	179
<b>B. Collisions in the slowing down phase of the prompt emission</b>	<b>183</b>
B.1. Dynamics of the Collision and determination of $\gamma_2$ . . . . .	184
B.2. $\gamma_2$ - $\gamma_0$ correlation . . . . .	187
<b>C. Applications to various sources from previous year report</b>	<b>191</b>
C.1. Application to GRB 970228 . . . . .	191
C.1.1. The analysis of GRB 970228 prompt emission . . . . .	192
C.1.2. Rescaling the CBM density . . . . .	194
C.1.3. GRB 970228 and the Amati relation . . . . .	196
C.1.4. Conclusions . . . . .	196
C.2. Application to GRB 060614 . . . . .	199
C.2.1. The fit of the observed luminosity . . . . .	201
C.2.2. Open issues in current theoretical models . . . . .	204
C.2.3. Conclusions . . . . .	206
C.3. Application to GRB 071227: an additional case of a <i>disguised</i> short burst . . . . .	208
C.3.1. The interpretation of GRB 071227 light curves . . . . .	209
C.3.2. GRB 071227 within the Amati relation . . . . .	212
C.3.3. Conclusions . . . . .	214
C.4. Application to GRB 011121 . . . . .	216
C.4.1. A widely debated issue: the interpretation of flares . . . . .	216
C.4.2. The first step on the first flare: analysis of GRB 011121 . . . . .	218
C.5. Application to GRB 031203 . . . . .	219
C.5.1. The initial conditions . . . . .	220
C.5.2. The GRB luminosity in fixed energy bands . . . . .	220
C.5.3. The “prompt emission” . . . . .	220

C.5.4. The instantaneous spectrum . . . . .	222
C.5.5. The time-integrated spectrum vs. the observed data . .	224
C.6. Application to GRB 050315 . . . . .	226
C.6.1. The fit of the observations . . . . .	226
C.6.2. The instantaneous spectrum . . . . .	230
C.6.3. Problems with the definition of “long” GRBs . . . . .	232
C.7. Application to GRB 060218 . . . . .	232
C.7.1. The fit of the observed data . . . . .	234
C.7.2. The procedure of the fit . . . . .	236
C.7.3. The fireshell fragmentation . . . . .	237
C.7.4. Binaries as progenitors of GRB-SN systems . . . . .	241
C.7.5. Conclusions . . . . .	241
C.8. Application to GRB060607A: prompt emission, X-ray flares and late afterglow phase. . . . .	242
C.8.1. GRB060607A prompt emission light curve . . . . .	244
C.8.2. GRB spectrum . . . . .	246
C.8.3. The X-ray flares . . . . .	250
C.8.4. The decaying afterglow regime . . . . .	252
C.8.5. Conclusions . . . . .	254
<b>Bibliography</b>	<b>257</b>

# 1. Topics

- The “canonical” GRB: “genuine short” vs long vs “disguised short” GRBs
- “Disguised short” GRB host galaxies: correlation between offset and extended afterglow peak luminosity
- The theoretical explanation of the “Amati relation”
- The “Amati relation” as a tool to identify “disguised short” GRBs
- “Genuine short” GRBs: Possible identifications and selection effects
- A modified spectral energy distribution for highly energetic GRBs
- The observed spectra of the P-GRBs
- GRB prompt emission spectra below 5 keV: challenges for future missions
- Interpretation of the ultra high energy emission from GRBs observed by Fermi and AGILE
- Analysis of different families of progenitors for GRBs with different energetics
- GRBs at redshift  $z > 6$
- GRBs originating from a multiple collapse
- Prompt emission and X-ray flares: the clumpiness of CBM
- Microphysical description of the interaction between the fireshell and the CBM
- Theoretical interpretation of the “plateau” phase in the X-ray afterglow
- Possible existence of a “proto-black hole” emission as first Episode of GRBs.
- Redshift estimators for GRBs with no measured redshift.



## 2. Participants

### 2.1. ICRANet participants

- David Arnett
- Maria Grazia Bernardini
- Carlo Luciano Bianco
- Letizia Caito
- Pascal Chardonnet
- Massimo Della Valle
- Barbara Patricelli
- Remo Ruffini
- Gregory Vereshchagin
- She-Sheng Xue

### 2.2. Past collaborators

- Sabrina Casanova (MPIK, Germany)
- Demetrios Christodoulou (ETH Zurich, Switzerland)
- Alessandra Corsi (INAF-IASF Roma, Italy)
- Valeri Chechetkin
- Maria Giovanna Dainotti
- Thibault Damour (IHES, France)
- Walter Ferrara
- Federico Fraschetti (CEA Saclay, France)
- Roberto Guida

- Vahe Gurzadyan (Yerevan Physics Institute, Armenia)
- Massimiliano Lattanzi (Oxford Astrophysics, UK)
- Nino Panagia
- Elena Pian
- Giuliano Preparata (Università di Milano, Italy)
- Jay D. Salmonson (Livermore Lab, USA)
- Jim Wilson (Livermore Lab, USA)

### 2.3. Ongoing collaborations

- Alexey Aksenov (ITEP, Russia)
- Lorenzo Amati (INAF-IASF Bologna, Italy)
- Joao Braga (INPE, Brazil)
- Sandip Kumar Chakrabarti (S.N. Bose National Centre and Indian Centre for Space Physics, India)
- Alessandro Chieffi (INAF-IASF Roma, Italy)
- Guido Chincarini (Universit di Milano “Bicocca”, Italy)
- Stefano Covino (OAB, Italy)
- Filippo Frontera (Universit di Ferrara, Italy)
- Dafne Guetta (OAR, Italy)
- Cristiano Guidorzi (OAB, Italy)
- Stanislav Kelner (MEPhI, Russia, and MPIK, Germany)
- Marco Limongi (OAR, Italy)
- Vanessa Mangano (INAF-IASF Palermo, Italy)
- Susanna Vergani (Dunsink Observatory, Ireland)
- Francesco Vissani (INFN, Italy)

## 2.4. Students

- Andrey Baranov (IRAP PhD, Russia)
- Riccardo Belvedere (IRAP PhD, Italy)
- Gustavo de Barros (IRAP PhD, Brazil)
- Wen-Biao Han (IRAP PhD, China)
- Luca Izzo (IRAP PhD, Italy)
- Vincenzo Liccardo (IRAP PhD, Italy)
- Marco Muccino (IRAP PhD, Italy)
- Ana Virginia Penacchioni (IRAP PhD, Argentina)
- Giovanni Pisani (IRAP PhD, Italy)
- Luis Juracy Rangel Lemos (IRAP PhD, Brazil)
- Ivan Siutsou (IRAP PhD, Belarus)
- Vineeth Valsan (IRAP PhD, India)



## 3. Brief description

### 3.1. The space, time and energetics of GRBs

The new era of GRBs started with the discovery of Beppo-SAX of the existence of the afterglow of GRBs (Costa et al., 1997). This fortunate discovery, as it is well known, led to the optical identification of GRB sources and to the determination of their distances and of their energetics. After that pioneering work a large number of missions including HETE-II, INTEGRAL, KONUS-Wind, Suzaku, Swift have given a wealth of information of GRB sources, giving details of their cosmological redshifts, their energetics and their spectra. It has been then possible to draw a figure (see Fig. 3.1) representing these sources as well as giving a diagram of the number of GRBs at selected redshift value (Fig. 3.2), where there are represented all the 140 GRBs with such characteristics.

### 3.2. The black hole and GRB uniqueness

It has become evident from the theoretical analysis of these sources that we are witnessing a vast number of progenitors to the GRB phenomena. In particular, we can identify a family of progenitors formed by a binary system of a neutron star and a companion star in the late phase of thermonuclear evolution. These systems lead to the less energetic GRB sources which have the characteristic signature of being associated to a supernovae explosion. A specific model has been studied by our group following the idea of induced gravitational collapse, see section A. The emission of GRB in this case originates from a black hole with the smallest possible mass: the one originating from a neutron star going over to its critical mass. This naturally explains why these sources are the less energetic ones.

There is also evidence for GRBs originating from binary neutron star-white dwarf system, and from neutron star-neutron star binary systems (see e.g. GRB 060614 in section C.2, GRB 071227 in section C.3 and GRB 050509B in section 8). And there is mounting evidence for a different family of black holes linked to more energetic gravitational collapse of a massive core around  $10 M_{\odot}$  (see e.g. GRB 080916C and GRB 050904 in section 9 as well as GRB 090423 at  $z \sim 8.1$  in section 10, GRB 080916C and GRB 090902B in section 11)).

### 3. Brief description

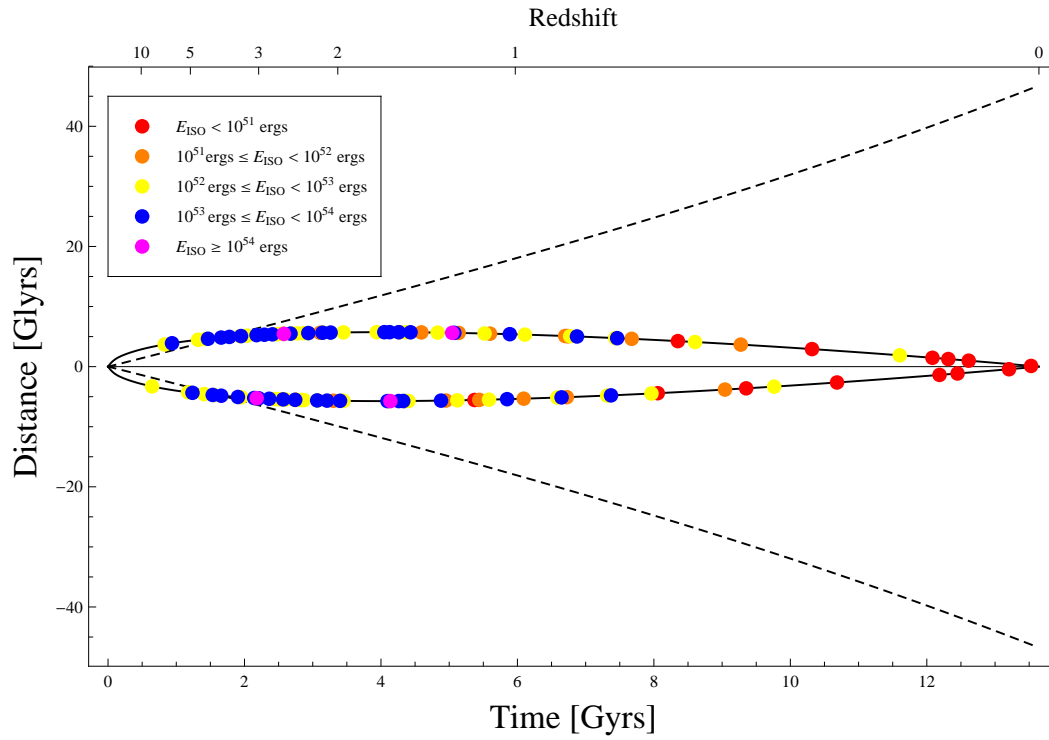


Figure 3.1.: GRB Distribution in distance and in energy.

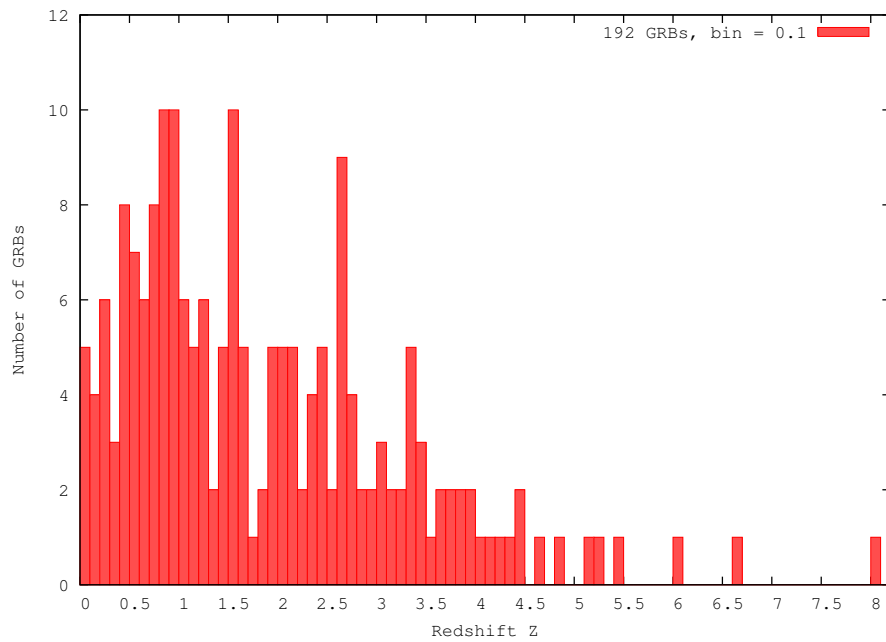


Figure 3.2.: Histogram of GRB redshifts.

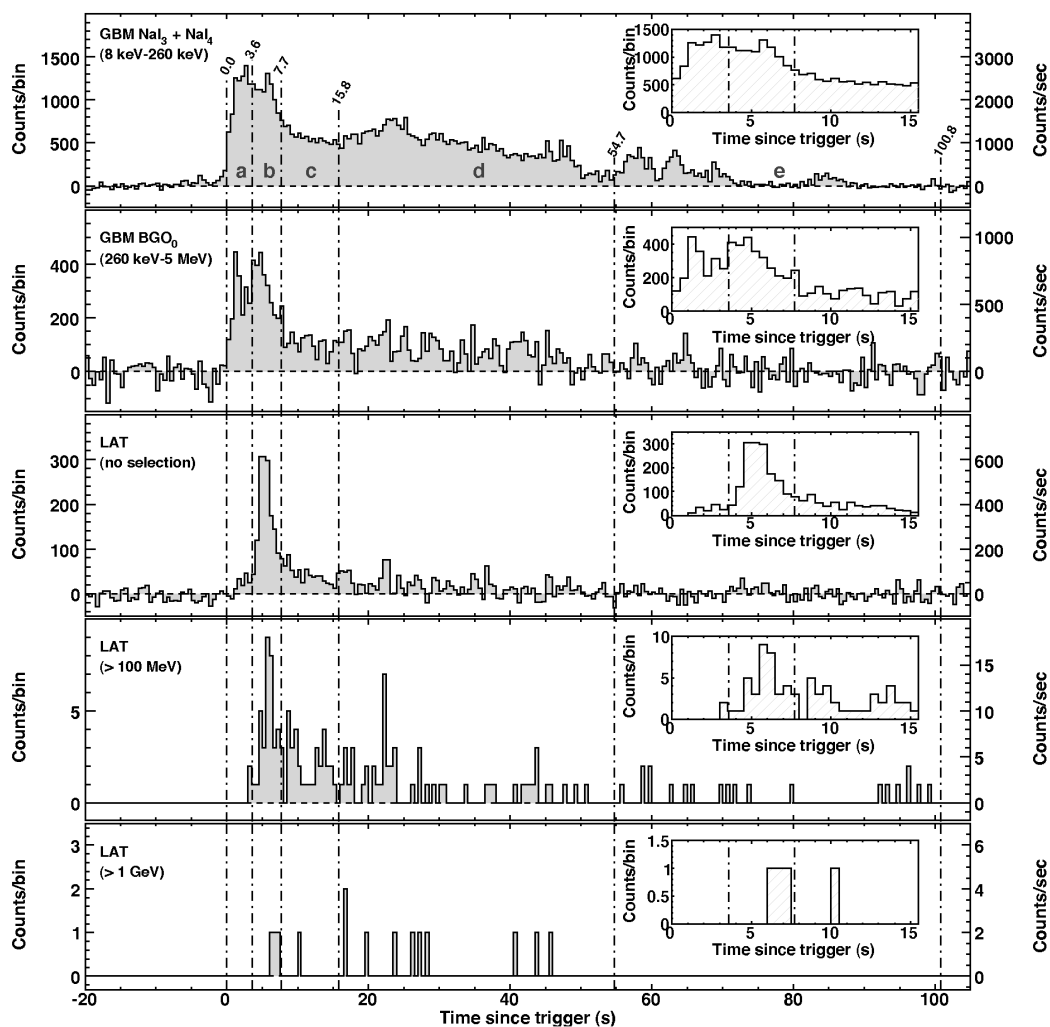
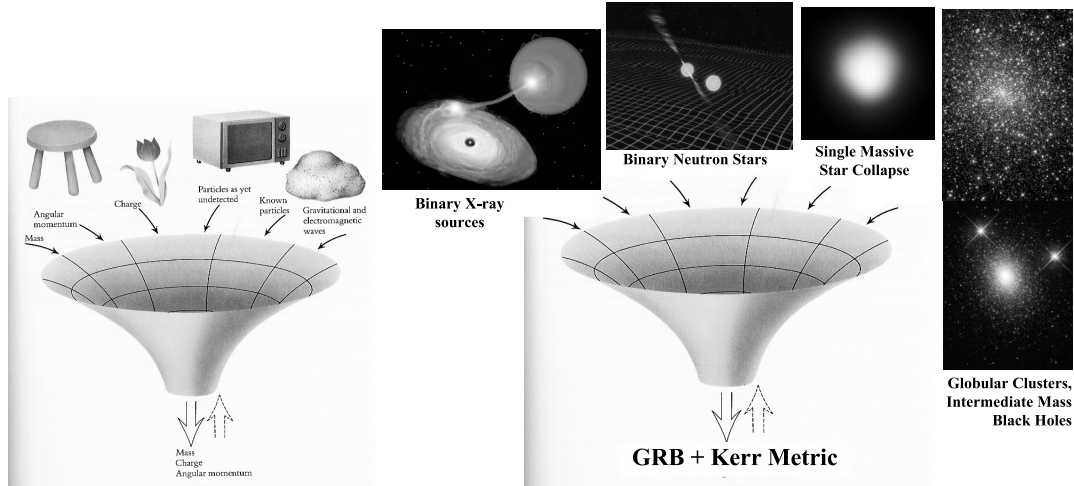


Figure 3.3.: Fermi observations of GRB 080916C

After the pioneering observations of the AGILE satellite and the Fermi mission it appears that there is an additional family of sources, extremely energetic, giving rise not only to emission in the X- and  $\gamma$ -rays, but also in the GeV region (see Fig. 3.3).

One may wonder how such a variety of astrophysical scenarios and of initial conditions may lead to a unified picture of GRBs.

The fundamental point is that all the above mentioned processes (see Fig. 3.4) are leading to the formation of a black hole, characterized uniquely by the three parameters of mass, charge and angular momentum. The emission process of GRBs occurs when this standard final configuration is approached. Therefore, the differences are uniquely in the energetics, but it is clear that the underlying physical process is the same. We report in the following progress in this understanding based on the theoretical analysis of specific sources



**Figure 3.4.:** **Left:** The Black Hole Uniqueness theorem (see e.g. Ref. Ruffini and Wheeler, 1971). **Right:** The GRB uniqueness.

which we have accomplished in this year.

### 3.3. The blackholic energy

It is now clear that the basic mechanism of acceleration of the GRBs is the electron-positron plasma created in the process of gravitational collapse to a black hole. The latest developments on these topics have been presented in the Reports on pages 559 and 1333, where we have also reported progresses in the understanding of dyadospheres and dyado-torii of black holes. We have also formalized the understanding of the crucial thermalization process of such electron-positron plasma and its interaction with the baryons, see the report on page 1333. We also obtained recent results on the dynamical evolution of such an electron-positron plasma, in presence of selected profiles of baryons (see Fig. 3.5, details in the report on page 1333).

The understanding of all these processes is crucial for describing the extraction of the blackholic energy, see the report on page 1. Similarly important is the use of the electron-positron plasma for the acceleration of baryons up to Lorentz gamma factors  $\gamma \sim 10^3 - 10^4$ . Far from being academic topic of researches, such concepts find their natural observational consequence in the study of the structure of the signal emitted when the electron-positron-baryon plasma reaches transparency in the emission of the Proper-GRB (see below).

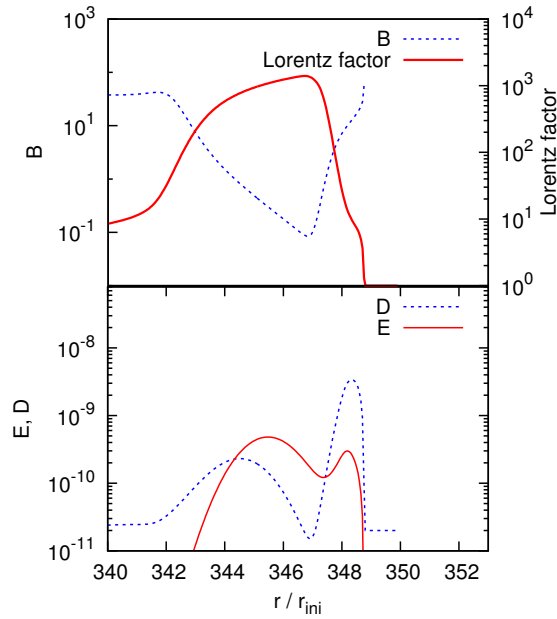


**Figure 3.5.:** Detailed structure of the spatial distribution of Lorentz factor and baryonic loading (upper panel), energy and matter density (lower panel) is shown for the hybrid case and for the moment  $t = 434$ . The  $B$  parameter changes 8 orders of magnitude in the extension of the shell.  $B$  is plotted until the point where Lorentz factor is equal one. Now we can see two shells for both densities  $E$  and  $D$ . Details in the report on page 1333.

### 3.4. The limits on the energetics of GRBs

One of the crucial steps which made possible the identification of the first black hole in our Galaxy has been the establishing an upper limits on the neutron star mass on general principles: 1) the validity of General Relativity, 2) the velocity of sound smaller than the speed of light, and 3) the existence of a fiducial density. This is today considered a classic result (see the report on page 1). What we have attempted now (presented in the talk by R. Ruffini at XII Marcel Grossmann Meeting) is to find a similar argument on the upper limit of the energetics of GRBs, quite independent of any details of the process, and uniquely based on the properties of the black holes and of the vacuum polarization process.

In brief, we recall that, in the process of gravitational collapse, a massive object of mass  $M$  reaches a minimum dimension  $R$  given by

$$R \sim d \frac{GM}{c^2}, \quad (3.4.1)$$

where  $d$  is a number of the order of 1-2 for black holes and close to 10 in the case of neutron stars. The gravitational energy at disposal is of the order of

$$E_{grav} \sim \frac{Mc^2}{d}, \quad (3.4.2)$$

and the average density of such an object is given by

$$\langle \rho \rangle \sim 1.86^2 \frac{m_n}{\frac{4}{3}\pi d^3 \left(\frac{\hbar}{m_n c}\right)^3 \left(\frac{M}{M_\odot}\right)^2}. \quad (3.4.3)$$

Since the process of vacuum polarization necessarily occur at nuclear densities, see report on page 429, we have

$$\langle \rho \rangle > \rho_{nucl} \sim \frac{m_n}{\frac{4}{3}\pi d^3 \left(\frac{\hbar}{m_n c}\right)^3}. \quad (3.4.4)$$

And the necessary condition that  $\langle \rho \rangle > \rho_{nucl}$  imposes an upper limit on the mass of the collapsing object:

$$\frac{M}{M_\odot} < 1.86 d^{-3/2} \left(\frac{m_n}{m_\pi}\right)^{3/2}. \quad (3.4.5)$$

This implies that the mass of a neutron star should be in the range  $0.1 < \frac{M_{NS}}{M_\odot} < 3.2$ , while for black holes  $M_{BH} < 32.5 d^{3/2} M_\odot = 11.5 M_\odot$ . We can then conclude that an absolute upper limit to the energy of GRBs is  $E < 1.1 \times 10^{55}$

ergs.

A larger value observed in a GRB would imply either a violation of a very basic physical law, or, more likely, a multiple structure in the gravitational collapse process as proposed by Ruffini and Wheeler in 1971, see Rees et al. (1974) and Fig. 3.6.

### 3.5. The “canonical” GRB: short vs long GRBs (GRB991216 and GRB 050315 as the prototypes)

As we recall later (see section 6) in our “canonical GRB” scenario there are only two free parameters characterizing the source (Ruffini et al., 2000, 2001b, 2007a):

- the total energy  $E_{e^\pm}^{tot}$  of the  $e^\pm$  plasma forming the self-accelerating optically thick fireshell
- the fireshell baryon loading  $B \equiv M_B c^2 / E_{e^\pm}^{tot}$ , where  $M_B$  is the total baryons’ mass.

These two parameters fully determine the optically thick self-acceleration phase of the fireshell, which lasts until the transparency condition is reached and the Proper-GRB (P-GRB) is emitted. After the transparency point the self-acceleration phase ends and it remains only an optically thin fireshell of baryonic matter ballistically expanding with an initially ultrarelativistic velocity and losing its kinetic energy via the interaction with the CircumBurst Medium (CBM).

Therefore, we define a “canonical GRB” light curve with two sharply different components (see Fig. 3.7 and Ruffini et al., 2001b, 2007a; Bernardini et al., 2007; Bianco et al., 2008a,b):

- **The P-GRB**, which is emitted when the optically thick fireshell becomes transparent. It depends only on  $E_{e^\pm}^{tot}$  and  $B$ . It has the imprint of the black hole formation, an harder spectrum and no spectral lag (Bianco et al., 2001; Ruffini et al., 2005d).
- **the extended afterglow**, which is due to the collision between the left-over optically thin fireshell and the CBM (Ruffini et al., 2001b, 2007a; Bianco and Ruffini, 2004, 2005b,a). It depends on  $E_{e^\pm}^{tot}$  and  $B$  but its temporal structure depends also on the additional parameters describing the effective CBM distribution: its density  $n_{cbm}$  and the ratio  $\mathcal{R} \equiv A_{eff} / A_{vis}$  between the effective emitting area of the fireshell  $A_{eff}$  and its total visible area  $A_{vis}$ . It presents a clear hard-to-soft spectral evolution in time and it is composed by a rising part, a peak and a decaying

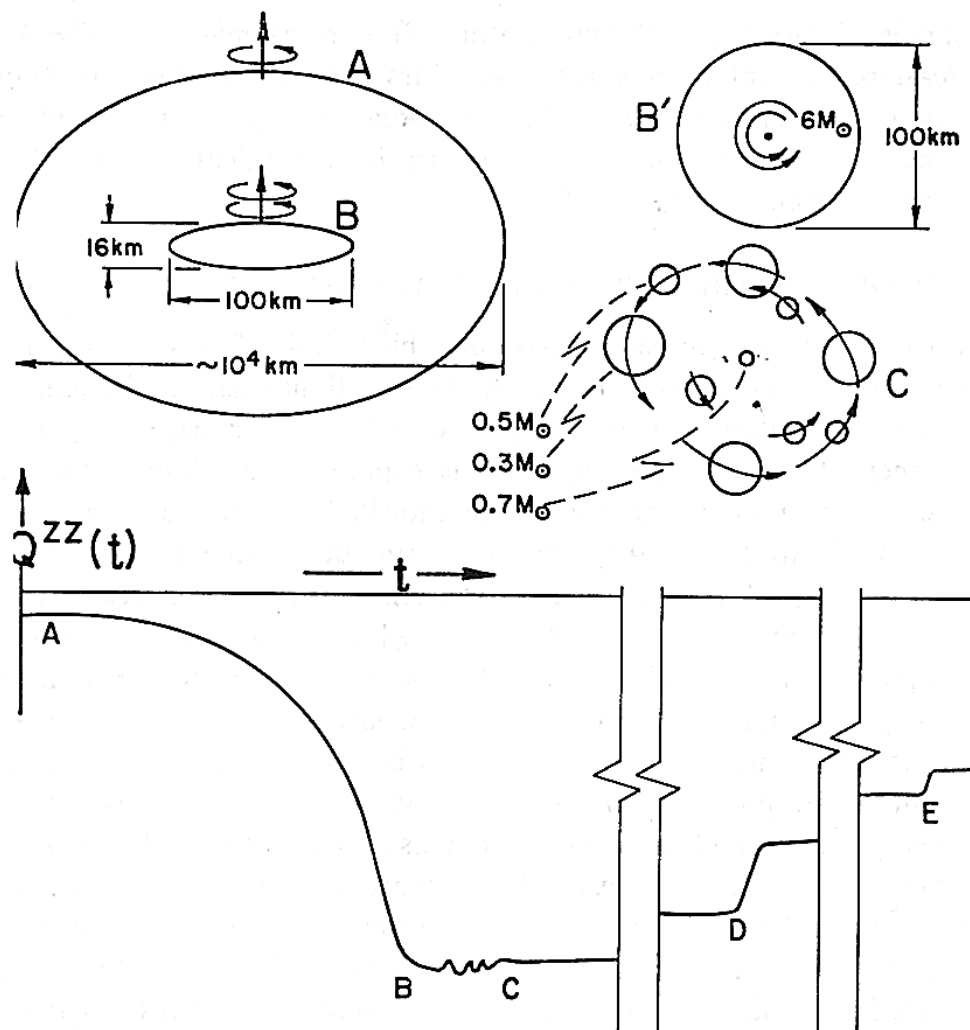


**Figure 33** A rotating star with dense core A collapses to a pancake neutron star B; it fragments C; the fragments lose energy in periodic and splash gravitational radiation and recombine. The lower curve gives a schematic representation of the quadrupole moment as a function of time. Between B and C impulse radiation is created in the act of fragmentation not adequately described by the one indicated component of the quadrupole moment tensor. Between C and D multiply periodic radiation is given out until at D two fragments have lost enough angular momentum so that they combine with a splash of gravitational radiation; similarly at E, etc.

**Figure 3.6.:** The Pursuit & Plunge scenario, from Rees et al. (1974).

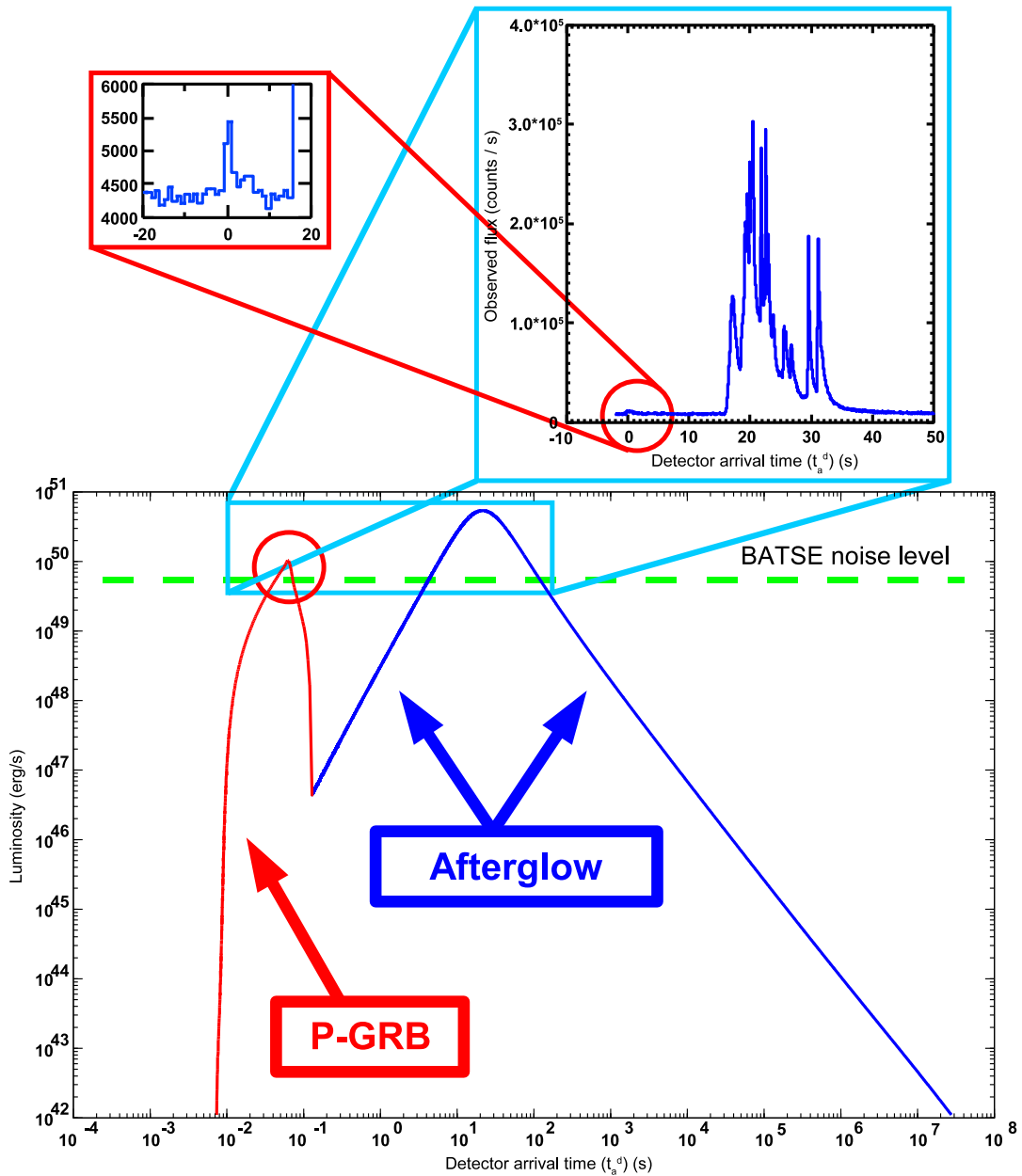


**Figure 3.7.:** The “canonical GRB” light curve theoretically computed for GRB 991216. The prompt emission observed by BATSE is identified with the peak of the afterglow, while the small precursor is identified with the P-GRB. For this source we have  $E_{e^{\pm}}^{tot} = 4.83 \times 10^{53}$  ergs,  $B \simeq 3.0 \times 10^{-3}$  and  $\langle n_{cbm} \rangle \sim 1.0$  particles/cm<sup>3</sup>. Details in Ruffini et al. (2001b, 2002, 2007a).

tail (Ruffini et al., 2002, 2004b, 2005c; Bernardini et al., 2005a; Ruffini et al., 2006b; Dainotti et al., 2007).

We clarify that what in the literature is called “prompt emission” within our theory is composed by both the P-GRB and the peak of the extended afterglow (see Fig. 3.7).

The ratio between the total time-integrated luminosity of the P-GRB (namely, its total energy) and the corresponding one of the afterglow is the crucial quantity for the identification of GRBs’ nature (Ruffini et al., 2001b):

- When  $B \leq 10^{-5}$  we have a P-GRB dominated event (in the limit  $B \rightarrow 0$  the afterglow vanishes).
- In the opposite limit, for  $10^{-4} \leq B \leq 10^{-2}$  we have an afterglow dominated GRB, and this is indeed the case of most of the GRBs we have recently examined (see Fig. 3.8).

## 3.6. Brief summary of recent progresses

Major progresses have been accomplished this year in the following aspects:

- In well identifying the origin of the new GRB family which we have defined as “disguised short” GRBs, the prototype being GRB 970228 (see section C.1) confirmed by GRB 060614 (see section C.2), by GRB 071227 (see section C.3), and by GRB 050509B (see section 8); all these objects appear to be related to progenitors formed by binary systems of neutron stars or a neutron star and a white dwarf (see section 6.6).
- In identifying the offset of disguised GRB host galaxies as a key parameter to classify this kind of sources (see section 6.5, C.3 and 8).
- In understanding the role of the “Amati” relation for the disguised short GRBs (see sections C.3.2 and 8.4).
- In studying the possible selection effect preventing the identification of “genuine” short GRBs (see section 8).
- In evidencing a broadening of the spectral energy distribution within the fireshell model for highly energetic GRBs ( $\sim 10^{53} - 10^{54}$  ergs) (see section 7).
- In identifying a new family of very energetic sources (GRB 080319B and GRB 050904, see section 9); both these sources are at an energy of  $10^{54}$  ergs and they offer unprecedented opportunities since one is located at  $z \sim 1$  and the other at  $z \sim 6.3$ : the nearby source allow a most

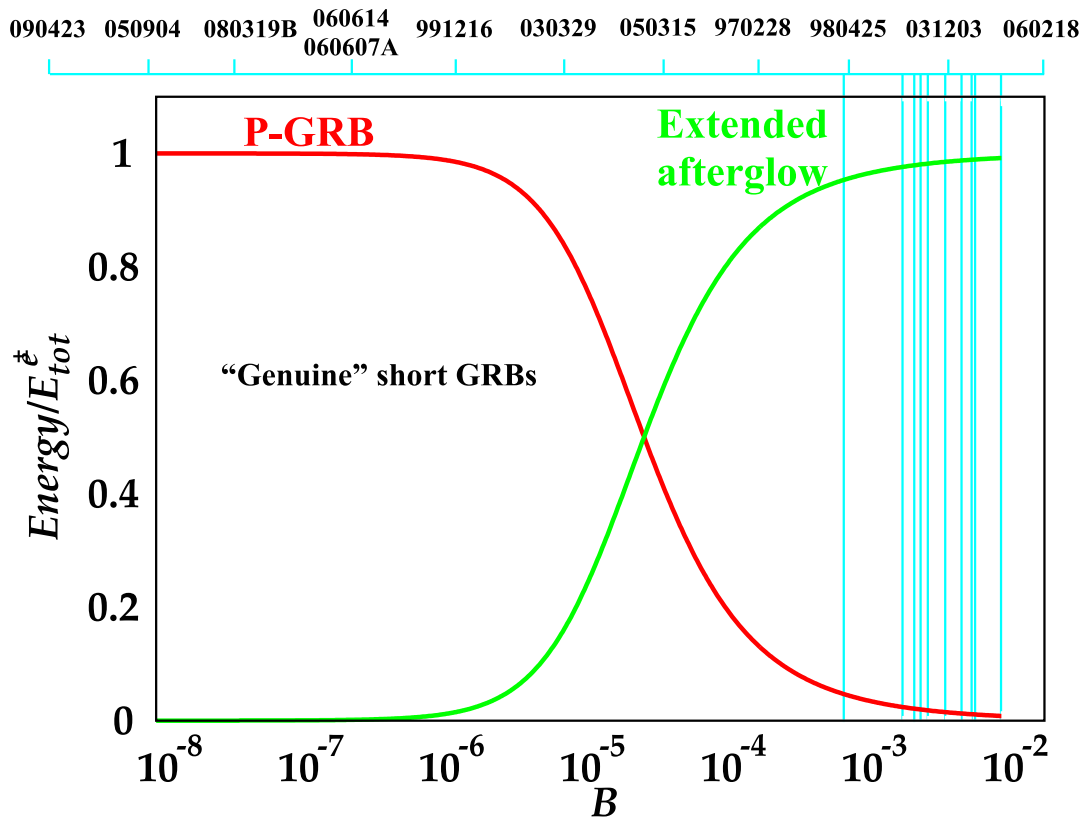


**Figure 3.8.:** Here the energies emitted in the P-GRB (red line) and in the afterglow (green line), in units of the total energy of the plasma, are plotted as functions of the  $B$  parameter. When  $B \leq 10^{-5}$ , the P-GRB becomes predominant over the afterglow, giving rise to a P-GRB dominated GRB. In the figure are also marked in blue the values of the  $B$  parameters corresponding to some GRBs we analyzed.

significant high-quality data on very short time scale which has allowed to reach a deeper understanding of the instantaneous spectrum vs. the average one. Both of them appear to originate from a collapse of a black hole of 10 solar masses. Still members of this family appears to be GRB 090423 at  $z \sim 8$  (see section 10) and GRB 060607A (see section C.8).

- New outlook has been brought to this field by the Fermi and AGILE satellites and the very exciting preliminary results have been obtained on GRB 080916C and GRB 090902B (see section 11).
- In studying the P-GRB observed spectra (see section 11).
- Particularly exciting is the new possibility of having components yet to be observed in GRB sources. In fact, we have shown that it is not possible to interpret GRB 090618 and GRB 101023 within the framework of the traditional single component GRB model. We argue that the observation of the first episode of duration of around 50s could not be a part of a canonical GRB, while the residual emission could be modeled easily with the models existing in literature. This led to the definition of the novel concept of “proto-black hole emission” (see sections 12 and 13).

We have reached a new understanding of these family of sources thanks to the knowledge we had acquired previously on GRB 011121, GRB 031203, GRB 050315, GRB 060218, GRB 970228, GRB 060607A, GRB 060614, GRB 071227 whose details can be found in appendix C.

# 4. Selected publications before 2005

## 4.1. Refereed journals

1. D. Christodoulou, R. Ruffini; "Reversible Transformations of a Charged Black Hole"; *Physical Review D*, 4, 3552 (1971).

A formula is derived for the mass of a black hole as a function of its "irreducible mass", its angular momentum, and its charge. It is shown that 50% of the mass of an extreme charged black hole can be converted into energy as contrasted with 29% for an extreme rotating black hole.

2. T. Damour, R. Ruffini; "Quantum electrodynamical effects in Kerr-Newman geometries"; *Physical Review Letters*, 35, 463 (1975).

Following the classical approach of Sauter, of Heisenberg and Euler and of Schwinger the process of vacuum polarization in the field of a "bare" Kerr-Newman geometry is studied. The value of the critical strength of the electromagnetic fields is given together with an analysis of the feedback of the discharge on the geometry. The relevance of this analysis for current astrophysical observations is mentioned.

3. G. Preparata, R. Ruffini, S.-S. Xue; "The dyadosphere of black holes and gamma-ray bursts"; *Astronomy & Astrophysics*, 338, L87 (1999).

The "dyadosphere" has been defined as the region outside the horizon of a black hole endowed with an electromagnetic field (abbreviated to EMBH for "electromagnetic black hole") where the electromagnetic field exceeds the critical value, predicted by Heisenberg & Euler for  $e^\pm$  pair production. In a very short time ( $\sim O(\hbar/mc^2)$ ) a very large number of pairs is created there. We here give limits on the EMBH parameters leading to a Dyadosphere for  $10M_\odot$  and  $10^5M_\odot$  EMBH's, and give as well the pair densities as functions of the radial coordinate. We here assume that the pairs reach thermodynamic equilibrium with a photon gas and estimate the average energy per pair as a function of the EMBH mass. These data give the initial conditions for the analysis of an enormous pair-electromagnetic-pulse or "P.E.M. pulse" which naturally leads to relativistic expansion. Basic energy requirements for gamma ray bursts (GRB), including GRB971214 recently observed at  $z=3.4$ , can be accounted for by processes occurring in the dyadosphere. In this letter we do not address the prob-

lem of forming either the EMBH or the dyadosphere: we establish some inequalities which must be satisfied during their formation process.

4. R. Ruffini, J.D. Salmonson, J.R. Wilson, S.-S. Xue; "On the pair electromagnetic pulse of a black hole with electromagnetic structure"; *Astronomy & Astrophysics*, 350, 334 (1999).

We study the relativistically expanding electron-positron pair plasma formed by the process of vacuum polarization around an electromagnetic black hole (EMBH). Such processes can occur for EMBH's with mass all the way up to  $6 \times 10^5 M_{\odot}$ . Beginning with a idealized model of a Reissner-Nordstrom EMBH with charge to mass ratio  $\zeta = 0.1$ , numerical hydrodynamic calculations are made to model the expansion of the pair-electromagnetic pulse (PEM pulse) to the point that the system is transparent to photons. Three idealized special relativistic models have been compared and contrasted with the results of the numerically integrated general relativistic hydrodynamic equations. One of the three models has been validated: a PEM pulse of constant thickness in the laboratory frame is shown to be in excellent agreement with results of the general relativistic hydrodynamic code. It is remarkable that this precise model, starting from the fundamental parameters of the EMBH, leads uniquely to the explicit evaluation of the parameters of the PEM pulse, including the energy spectrum and the astrophysically unprecedented large Lorentz factors (up to  $6 \times 10^3$  for a  $10^3 M_{\odot}$  EMBH). The observed photon energy at the peak of the photon spectrum at the moment of photon decoupling is shown to range from 0.1 MeV to 4 MeV as a function of the EMBH mass. Correspondingly the total energy in photons is in the range of  $10^{52}$  to  $10^{54}$  ergs, consistent with observed gamma-ray bursts. In these computations we neglect the presence of baryonic matter which will be the subject of forthcoming publications.

5. R. Ruffini, J.D. Salmonson, J.R. Wilson, S.-S. Xue; "On the pair-electromagnetic pulse from an electromagnetic black hole surrounded by a baryonic remnant"; *Astronomy & Astrophysics*, 359, 855 (2000).

The interaction of an expanding Pair-Electromagnetic pulse (PEM pulse) with a shell of baryonic matter surrounding a Black Hole with electromagnetic structure (EMBH) is analyzed for selected values of the baryonic mass at selected distances well outside the dyadosphere of an EMBH. The dyadosphere, the region in which a super critical field exists for the creation of  $e+e-$  pairs, is here considered in the special case of a Reissner-Nordstrom geometry. The interaction of the PEM pulse with the baryonic matter is described using a simplified model of a slab of constant thickness in the laboratory frame (constant-thickness approximation) as well as performing the integration of the general relativistic hydrodynamical equations. The validation of the constant-thickness approximation, already presented in a previous paper Ruffini et al. (1999) for a PEM pulse in vacuum, is here generalized to the presence of baryonic matter. It is found that for a baryonic shell of mass-energy less than 1% of the total

energy of the dyadosphere, the constant-thickness approximation is in excellent agreement with full general relativistic computations. The approximation breaks down for larger values of the baryonic shell mass, however such cases are of less interest for observed Gamma Ray Bursts (GRBs). On the basis of numerical computations of the slab model for PEM pulses, we describe (i) the properties of relativistic evolution of a PEM pulse colliding with a baryonic shell; (ii) the details of the expected emission energy and observed temperature of the associated GRBs for a given value of the EMBH mass;  $10^3 M_{\odot}$ , and for baryonic mass-energies in the range  $10^{-8}$  to  $10^{-2}$  the total energy of the dyadosphere.

6. C.L. Bianco, R. Ruffini, S.-S. Xue; "The elementary spike produced by a pure  $e^+e^-$  pair-electromagnetic pulse from a Black Hole: The PEM Pulse"; *Astronomy & Astrophysics*, 368, 377 (2001).

In the framework of the model that uses black holes endowed with electromagnetic structure (EMBH) as the energy source, we study how an elementary spike appears to the detectors. We consider the simplest possible case of a pulse produced by a pure  $e^+e^-$  pair-electro-magnetic plasma, the PEM pulse, in the absence of any baryonic matter. The resulting time profiles show a *Fast-Rise-Exponential-Decay* shape, followed by a power-law tail. This is obtained without any special fitting procedure, but only by fixing the energetics of the process taking place in a given EMBH of selected mass, varying in the range from 10 to  $10^3 M_{\odot}$  and considering the relativistic effects to be expected in an electron-positron plasma gradually reaching transparency. Special attention is given to the contributions from all regimes with Lorentz  $\gamma$  factor varying from  $\gamma = 1$  to  $\gamma = 10^4$  in a few hundreds of the PEM pulse travel time. Although the main goal of this paper is to obtain the elementary spike intensity as a function of the arrival time, and its observed duration, some qualitative considerations are also presented regarding the expected spectrum and on its departure from the thermal one. The results of this paper will be comparable, when data will become available, with a subfamily of particularly short GRBs not followed by any afterglow. They can also be propedeutical to the study of longer bursts in presence of baryonic matter currently observed in GRBs.

7. R. Ruffini, C.L. Bianco, P. Chardonnet, F. Fraschetti, S.-S. Xue; "Relative spacetime transformations in Gamma-Ray Bursts"; *The Astrophysical Journal*, 555, L107 (2001).

The GRB 991216 and its relevant data acquired from the BATSE experiment and RXTE and Chandra satellites are used as a prototypical case to test the theory linking the origin of gamma ray bursts (GRBs) to the process of vacuum polarization occurring during the formation phase of a black hole endowed with electromagnetic structure (EMBH). The relative space-time transformation paradigm (RSTT paradigm) is presented. It relates the observed signals of GRBs to their past light cones, defining the events on the worldline of the

source essential for the interpretation of the data. Since GRBs present regimes with unprecedentedly large Lorentz  $\gamma$  factor, also sharply varying with time, particular attention is given to the constitutive equations relating the four time variables: the comoving time, the laboratory time, the arrival time at the detector, duly corrected by the cosmological effects. This paradigm is at the very foundation of any possible interpretation of the data of GRBs.

8. R. Ruffini, C.L. Bianco, P. Chardonnet, F. Fraschetti, S.-S. Xue; "On the interpretation of the burst structure of Gamma-Ray Bursts"; *The Astrophysical Journal*, 555, L113 (2001).

Given the very accurate data from the BATSE experiment and RXTE and Chandra satellites, we use the GRB 991216 as a prototypical case to test the EMBH theory linking the origin of the energy of GRBs to the electromagnetic energy of black holes. The fit of the afterglow fixes the only two free parameters of the model and leads to a new paradigm for the interpretation of the burst structure, the IBS paradigm. It leads as well to a reconsideration of the relative roles of the afterglow and burst in GRBs by defining two new phases in this complex phenomenon: a) the injector phase, giving rise to the proper-GRB (P-GRB), and b) the beam-target phase, giving rise to the extended afterglow peak emission (E-APE) and to the afterglow. Such differentiation leads to a natural possible explanation of the bimodal distribution of GRBs observed by BATSE. The agreement with the observational data in regions extending from the horizon of the EMBH all the way out to the distant observer confirms the uniqueness of the model.

9. R. Ruffini, C.L. Bianco, P. Chardonnet, F. Fraschetti, S.-S. Xue; "On a possible Gamma-Ray Burst-Supernova time sequence"; *The Astrophysical Journal*, 555, L117 (2001).

The data from the Chandra satellite on the iron emission lines in the afterglow of GRB 991216 are used to give further support for the EMBH theory, which links the origin of the energy of GRBs to the extractable energy of electromagnetic black holes (EMBHS), leading to an interpretation of the GRB-supernova correlation. Following the relative space-time transformation (RSTT) paradigm and the interpretation of the burst structure (IBS) paradigm, we introduce a paradigm for the correlation between GRBs and supernovae. The following sequence of events is shown as kinematically possible and consistent with the available data: a) the GRB-progenitor star  $P_1$  first collapses to an EMBH, b) the proper GRB (P-GRB) and the peak of the afterglow (E-APE) propagate in interstellar space until the impact on a supernova-progenitor star  $P_2$  at a distance  $\leq 2.69 \times 10^{17}$  cm, and they induce the supernova explosion, c) the accelerated baryonic matter (ABM) pulse, originating the afterglow, reaches the supernova remnants 18.5 hours after the supernova explosion and gives rise to the iron emission lines. Some considerations on the dynamical implementation of the paradigm are presented. The concept of induced supernova

explosion introduced here specifically for the GRB-supernova correlation may have more general application in relativistic astrophysics.

10. R. Ruffini, C.L. Bianco, P. Chardonnet, F. Frascchetti, S.-S. Xue; "On the physical processes which lie at the bases of time variability of GRBs"; *Il Nuovo Cimento B*, 116, 99 (2001).

The relative-space-time-transformation (RSTT) paradigm and the interpretation of the burst-structure (IBS) paradigm are applied to probe the origin of the time variability of GRBs. Again GRB 991216 is used as a prototypical case, thanks to the precise data from the CGRO, RXTE and Chandra satellites. It is found that with the exception of the relatively inconspicuous but scientifically very important signal originating from the initial "proper gamma ray burst" (P-GRB), all the other spikes and time variabilities can be explained by the interaction of the accelerated-baryonic-matter pulse with inhomogeneities in the interstellar matter. This can be demonstrated by using the RSTT paradigm as well as the IBS paradigm, to trace a typical spike observed in arrival time back to the corresponding one in the laboratory time. Using these paradigms, the identification of the physical nature of the time variability of the GRBs can be made most convincingly. It is made explicit the dependence of a) the intensities of the afterglow, b) the spikes amplitude and c) the actual time structure on the Lorentz gamma factor of the accelerated-baryonic-matter pulse. In principle it is possible to read off from the spike structure the detailed density contrast of the interstellar medium in the host galaxy, even at very high redshift.

11. R. Ruffini, C.L. Bianco, P. Chardonnet, F. Frascchetti, S.-S. Xue; "On the structures in the afterglow peak emission of gamma ray bursts"; *The Astrophysical Journal*, 581, L19 (2002).

Using GRB 991216 as a prototype, it is shown that the intensity substructures observed in what is generally called the "prompt emission" in gamma ray bursts (GRBs) do originate in the collision between the accelerated baryonic matter (ABM) pulse with inhomogeneities in the interstellar medium (ISM). The initial phase of such process occurs at a Lorentz factor  $\gamma \sim 310$ . The crossing of ISM inhomogeneities of sizes  $\Delta R \sim 10^{15}$  cm occurs in a detector arrival time interval of  $\sim 0.4$  s implying an apparent superluminal behavior of  $\sim 10^5 c$ . The long lasting debate between the validity of the external shock model vs. the internal shock model for GRBs is solved in favor of the first.

12. R. Ruffini, C.L. Bianco, P. Chardonnet, F. Frascchetti, S.-S. Xue; "On the structure of the burst and afterglow of Gamma-Ray Bursts I: the radial approximation"; *International Journal of Modern Physics D*, 12, 173 (2003).

We have recently proposed three paradigms for the theoretical interpretation of gamma-ray bursts (GRBs). (1) The relative space-time transformation (RSTT) paradigm emphasizes how the knowledge of the entire world-line of the source

from the moment of gravitational collapse is a necessary condition in order to interpret GRB data. (2) The interpretation of the burst structure (IBS) paradigm differentiates in all GRBs between an injector phase and a beam-target phase. (3) The GRB-supernova time sequence (GSTS) paradigm introduces the concept of *induced supernova explosion* in the supernovae-GRB association. In the introduction the RSTT and IBS paradigms are enunciated and illustrated using our theory based on the vacuum polarization process occurring around an electromagnetic black hole (EMBH theory). The results are summarized using figures, diagrams and a complete table with the space-time grid, the fundamental parameters and the corresponding values of the Lorentz gamma factor for GRB 991216 used as a prototype. In the following sections the detailed treatment of the EMBH theory needed to understand the results of the three above letters is presented. We start from the considerations on the dyadosphere formation. We then review the basic hydrodynamic and rate equations, the equations leading to the relative space-time transformations as well as the adopted numerical integration techniques. We then illustrate the five fundamental eras of the EMBH theory: the self acceleration of the  $e^+e^-$  pair-electromagnetic plasma (PEM pulse), its interaction with the baryonic remnant of the progenitor star, the further self acceleration of the  $e^+e^-$  pair-electromagnetic radiation and baryon plasma (PEMB pulse). We then study the approach of the PEMB pulse to transparency, the emission of the proper GRB (P-GRB) and its relation to the “short GRBs”. Particular attention is given to the free parameters of the theory and to the values of the thermodynamical quantities at transparency. Finally the three different regimes of the afterglow are described within the fully radiative and radial approximations: the ultrarelativistic, the relativistic and the nonrelativistic regimes. The best fit of the theory leads to an unequivocal identification of the “long GRBs” as extended emission occurring at the afterglow peak (E-APE). The relative intensities, the time separation and the hardness ratio of the P-GRB and the E-APE are used as distinctive observational test of the EMBH theory and the excellent agreement between our theoretical predictions and the observations are documented. The afterglow power-law indexes in the EMBH theory are compared and contrasted with the ones in the literature, and no beaming process is found for GRB 991216. Finally, some preliminary results relating the observed time variability of the E-APE to the inhomogeneities in the interstellar medium are presented, as well as some general considerations on the EMBH formation. The issue of the GSTS paradigm will be the object of a forthcoming publication and the relevance of the iron-lines observed in GRB 991216 is shortly reviewed. The general conclusions are then presented based on the three fundamental parameters of the EMBH theory: the dyadosphere energy, the baryonic mass of the remnant, the interstellar medium density. An in depth discussion and comparison of the EMBH theory with alternative theories is presented as well as indications of further developments beyond the radial approximation, which will be the subject of paper II in this series. Future needs for specific

GRB observations are outlined.

13. R. Ruffini, C.L. Bianco, P. Chardonnet, F. Frascchetti, V. Gurzadyan, S.-S. Xue; "On the instantaneous spectrum of gamma ray bursts"; *International Journal of Modern Physics D*, 13, 843 (2004).

A theoretical attempt to identify the physical process responsible for the afterglow emission of Gamma-Ray Bursts (GRBs) is presented, leading to the occurrence of thermal emission in the comoving frame of the shock wave giving rise to the bursts. The determination of the luminosities and spectra involves integration over an infinite number of Planckian spectra, weighted by appropriate relativistic transformations, each one corresponding to a different viewing angle in the past light cone of the observer. The relativistic transformations have been computed using the equations of motion of GRBs within our theory, giving special attention to the determination of the equitemporal surfaces. The only free parameter of the present theory is the "effective emitting area" in the shock wave front. A self consistent model for the observed hard-to-soft transition in GRBs is also presented. When applied to GRB 991216 a precise fit ( $\chi^2 \simeq 1.078$ ) of the observed luminosity in the 2–10 keV band is obtained. Similarly, detailed estimates of the observed luminosity in the 50–300 keV and in the 10–50 keV bands are obtained.

## 4.2. Conference proceedings

1. R. Ruffini; "Beyond the critical mass: The dyadosphere of black holes"; in "Black Holes and High Energy Astrophysics", H. sato, N. Sugiyama, Editors; p. 167; Universal Academy Press (Tokyo, Japan, 1998).

The "dyadosphere" (from the Greek word "duas-duados" for pairs) is here defined as the region outside the horizon of a black hole endowed with an electromagnetic field (abbreviated to EMBH for "electromagnetic black hole") where the electromagnetic field exceeds the critical value, predicted by Heisenberg and Euler for  $e^+e^-$  pair production. In a very short time ( $\sim O(\hbar/mc^2)$ ), a very large number of pairs is created there. I give limits on the EMBH parameters leading to a Dyadosphere for  $10M_\odot$  and  $10^5M_\odot$  EMBH's, and give as well the pair densities as functions of the radial coordinate. These data give the initial conditions for the analysis of an enormous pair-electromagnetic-pulse or "PEM-pulse" which naturally leads to relativistic expansion. Basic energy requirements for gamma ray bursts (GRB), including GRB971214 recently observed at  $z = 3.4$ , can be accounted for by processes occurring in the dyadosphere.

2. R. Ruffini, C.L. Bianco, P. Chardonnet, F. Frascchetti, L. Vitagliano, S.-S. Xue; "New perspectives in physics and astrophysics from the theoretical understanding of Gamma-Ray Bursts"; in "COSMOLOGY AND

GRAVITATION: Xth Brazilian School of Cosmology and Gravitation; 25th Anniversary (1977-2002)", Proceedings of the Xth Brazilian School on Cosmology and Gravitation, Mangaratiba, Rio de Janeiro (Brazil), July - August 2002, M. Novello, S.E. Perez Bergliaffa, Editors; AIP Conference Proceedings, 668, 16 (2003).

If due attention is given in formulating the basic equations for the Gamma-Ray Burst (GRB) phenomenon and in performing the corresponding quantitative analysis, GRBs open a main avenue of inquiring on totally new physical and astrophysical regimes. This program is very likely one of the greatest computational efforts in physics and astrophysics and cannot be actuated using shortcuts. A systematic approach is needed which has been highlighted in three basic new paradigms: the relative space-time transformation (RSTT) paradigm, the interpretation of the burst structure (IBS) paradigm, the GRB-supernova time sequence (GSTS) paradigm. From the point of view of fundamental physics new regimes are explored: (1) the process of energy extraction from black holes; (2) the quantum and general relativistic effects of matter-antimatter creation near the black hole horizon; (3) the physics of ultrarelativistic shock waves with Lorentz gamma factor  $\gamma > 100$ . From the point of view of astronomy and astrophysics also new regimes are explored: (i) the occurrence of gravitational collapse to a black hole from a critical mass core of mass  $M \gtrsim 10M_{\odot}$ , which clearly differs from the values of the critical mass encountered in the study of stars "catalyzed at the endpoint of thermonuclear evolution" (white dwarfs and neutron stars); (ii) the extremely high efficiency of the spherical collapse to a black hole, where almost 99.99% of the core mass collapses leaving negligible remnant; (iii) the necessity of developing a fine tuning in the final phases of thermonuclear evolution of the stars, both for the star collapsing to the black hole and the surrounding ones, in order to explain the possible occurrence of the "induced gravitational collapse". New regimes are as well encountered from the point of view of nature of GRBs: (I) the basic structure of GRBs is uniquely composed by a proper-GRB (P-GRB) and the afterglow; (II) the long bursts are then simply explained as the peak of the afterglow (the E-APE) and their observed time variability is explained in terms of inhomogeneities in the interstellar medium (ISM); (III) the short bursts are identified with the P-GRBs and the crucial information on general relativistic and vacuum polarization effects are encoded in their spectra and intensity time variability. A new class of space missions to acquire information on such extreme new regimes are urgently needed.

3. R. Ruffini, C.L. Bianco, P. Chardonnet, F. Fraschetti, S.-S. Xue; "The EMBH Model in GRB 991216 and GRB 980425"; in Proceedings of "Third Rome Workshop on Gamma-Ray Burst in the Afterglow Era", 17-20 September 2002; M. Feroci, F. Frontera, N. Masetti, L. Piro, Editors; ASP Conference Series, 312, 349 (2004).

This is a summary of the two talks presented at the Rome GRB meeting by C.L. Bianco and R. Ruffini. It is shown that by respecting the Relative Space-Time Transformation (RSTT) paradigm and the Interpretation of the Burst Structure (IBS) paradigm, important inferences are possible: a) in the new physics occurring in the energy sources of GRBs, b) on the structure of the bursts and c) on the composition of the interstellar matter surrounding the source.

4. M.G. Bernardini, C.L. Bianco, P. Chardonnet, F. Frascchetti, R. Ruffini, S.-S. Xue; "A New Astrophysical 'Triptych': GRB030329/SN2003dh/URCA-2"; in "GAMMA-RAY BURSTS: 30 YEARS OF DISCOVERY", Proceedings of the Los Alamos "Gamma Ray Burst Symposium", Santa Fe, New Mexico, 8-12 September 2003, E.E. Fenimore, M. Galassi, Editors; AIP Conference Proceedings, 727, 312 (2004).

We analyze the data of the Gamma-Ray Burst/Supernova GRB030329/SN2003dh system obtained by HETE-2, R-XTE, XMM and VLT within our theory for GRB030329. By fitting the only three free parameters of the EMBH theory, we obtain the luminosity in fixed energy bands for the prompt emission and the afterglow. Since the Gamma-Ray Burst (GRB) analysis is consistent with a spherically symmetric expansion, the energy of GRB030329 is  $E = 2.1 \times 10^{52}$  erg, namely  $\sim 2 \times 10^3$  times larger than the Supernova energy. We conclude that either the GRB is triggering an induced-supernova event or both the GRB and the Supernova are triggered by the same relativistic process. In no way the GRB can be originated from the supernova. We also evidence that the XMM observations, much like in the system GRB980425/SN1998bw, are not part of the GRB afterglow, as interpreted in the literature, but are associated to the Supernova phenomenon. A dedicated campaign of observations is needed to confirm the nature of this XMM source as a newly born neutron star cooling by generalized URCA processes.

5. F. Frascchetti, M.G. Bernardini, C.L. Bianco, P. Chardonnet, R. Ruffini, S.-S. Xue; "The GRB980425-SN1998bw Association in the EMBH Model"; in "GAMMA-RAY BURSTS: 30 YEARS OF DISCOVERY", Proceedings of the Los Alamos "Gamma Ray Burst Symposium", Santa Fe, New Mexico, 8-12 September 2003, E.E. Fenimore, M. Galassi, Editors; AIP Conference Proceedings, 727, 424 (2004).

Our GRB theory, previously developed using GRB 991216 as a prototype, is here applied to GRB 980425. We fit the luminosity observed in the 40–700 keV, 2–26 keV and 2–10 keV bands by the BeppoSAX satellite. In addition the supernova SN1998bw is the outcome of an "induced gravitational collapse" triggered by GRB 980425, in agreement with the GRB-Supernova Time Sequence (GSTS) paradigm. A further outcome of this astrophysically exceptional sequence of events is the formation of a young neutron star generated by the SN1998bw event. A coordinated observational activity is recommended to

further enlighten the underlying scenario of this most unique astrophysical system.

6. A. Corsi, M.G. Bernardini, C.L. Bianco, P. Chardonnet, F. Fraschetti, R. Ruffini, S.-S. Xue; "GRB 970228 Within the EMBH Model"; in "GAMMA-RAY BURSTS: 30 YEARS OF DISCOVERY", Proceedings of the Los Alamos "Gamma Ray Burst Symposium", Santa Fe, New Mexico, 8-12 September 2003, E.E. Fenimore, M. Galassi, Editors; AIP Conference Proceedings, 727, 428 (2004).

We consider the gamma-ray burst of 1997 February 28 (GRB 970228) within the ElectroMagnetic Black Hole (EMBH) model. We first determine the value of the two free parameters that characterize energetically the GRB phenomenon in the EMBH model, that is to say the dyadosphere energy,  $E_{dya} = 5.1 \times 10^{52}$  ergs, and the baryonic remnant mass  $M_B$  in units of  $E_{dya}$ ,  $B = M_B c^2 / E_{dya} = 3.0 \times 10^{-3}$ . Having in this way estimated the energy emitted during the beam-target phase, we evaluate the role of the InterStellar Medium (ISM) number density ( $n_{ISM}$ ) and of the ratio  $\mathcal{R}$  between the effective emitting area and the total surface area of the GRB source, in reproducing the observed profiles of the GRB 970228 prompt emission and X-ray (2-10 keV energy band) afterglow. The importance of the ISM distribution three-dimensional treatment around the central black hole is also stressed in this analysis.

# 5. Publications (2005–2011)

## 5.1. Refereed journals

1. R. Ruffini, C.L. Bianco, P. Chardonnet, F. Fraschetti, V. Gurzadyan, S.-S. Xue; “Emergence of a filamentary structure in the fireball from GRB spectra”; *International Journal of Modern Physics D*, 14, 97 (2005).

It is shown that the concept of a fireball with a definite filamentary structure naturally emerges from the analysis of the spectra of Gamma-Ray Bursts (GRBs). These results, made possible by the recently obtained analytic expressions of the equitemporal surfaces in the GRB afterglow, depend crucially on the single parameter  $R$  describing the effective area of the fireball emitting the X-ray and gamma-ray radiation. The X-ray and gamma-ray components of the afterglow radiation are shown to have a thermal spectrum in the co-moving frame of the fireball and originate from a stable shock front described self-consistently by the Rankine-Hugoniot equations. Precise predictions are presented on a correlation between spectral changes and intensity variations in the prompt radiation verifiable, e.g., by the Swift and future missions. The highly variable optical and radio emission depends instead on the parameters of the surrounding medium. The GRB 991216 is used as a prototype for this model.

2. R. Ruffini, M.G. Bernardini, C.L. Bianco, P. Chardonnet, F. Fraschetti, V. Gurzadyan, M. Lattanzi, L. Vitagliano, S.-S. Xue; “Extracting energy from black holes: ‘long’ and ‘short’ GRBs and their astrophysical settings”; *Il Nuovo Cimento C*, 28, 589 (2005).

The introduction of the three interpretational paradigms for Gamma-Ray Bursts (GRBs) and recent progress in understanding the X- and gamma-ray luminosity in the afterglow allow us to make assessments about the astrophysical settings of GRBs. In particular, we evidence the distinct possibility that some GRBs occur in a binary system. This subclass of GRBs manifests itself in a “trypitch”: one component formed by the collapse of a massive star to a black hole, which originates the GRB; a second component by a supernova and a third one by a young neutron star born in the supernova event. Similarly, the understanding of the physics of quantum relativistic processes during the gravitational collapse makes possible precise predictions about the structure of short GRBs.

3. M.G. Bernardini, C.L. Bianco, P. Chardonnet, F. Frascchetti, R. Ruffini, S.-S. Xue; “Theoretical interpretation of luminosity and spectral properties of GRB 031203”; *The Astrophysical Journal*, 634, L29 (2005).

The X-ray and gamma-ray observations of the source GRB 031203 by INTEGRAL are interpreted within our theoretical model. In addition to a complete spacetime parameterization of the GRB, we specifically assume that the afterglow emission originates from a thermal spectrum in the comoving frame of the expanding baryonic matter shell. By determining the two free parameters of the model and estimating the density and filamentary structure of the ISM, we reproduce the observed luminosity in the 20-200 keV energy band. As in previous sources, the prompt radiation is shown to coincide with the peak of the afterglow, and the luminosity substructure is shown to originate in the filamentary structure of the ISM. We predict a clear hard-to-soft behavior in the instantaneous spectra. The time-integrated spectrum over 20 s observed by INTEGRAL is well fitted. Despite the fact that this source has been considered “unusual”, it appears to us to be a normal low-energy GRB.

4. R. Ruffini, M.G. Bernardini, C.L. Bianco, P. Chardonnet, F. Frascchetti, S.-S. Xue; Evidence for isotropic emission in GRB991216; *Advances in Space Research*, 38, 1291 (2006).

The issue of the possible presence or absence of jets in GRBs is here re-examined for GRB991216. We compare and contrast our theoretically predicted afterglow luminosity in the 2–10 keV band for spherically symmetric versus jetted emission. At these wavelengths the jetted emission can be excluded and data analysis confirms spherical symmetry. These theoretical fits are expected to be improved by the forthcoming data of the Swift mission.

5. R. Ruffini, M.G. Bernardini, C.L. Bianco, P. Chardonnet, F. Frascchetti, R. Guida, S.-S. Xue; “GRB 050315: A step toward understanding the uniqueness of the overall GRB structure”; *The Astrophysical Journal*, 645, L109 (2006).

Using the Swift data of GRB 050315, we are making progress toward understanding the uniqueness of our theoretically predicted gamma-ray burst (GRB) structure, which is composed of a proper GRB (P-GRB), emitted at the transparency of an electron-positron plasma with suitable baryon loading, and an afterglow comprising the so-called prompt emission due to external shocks. Thanks to the Swift observations, the P-GRB is identified, and for the first time we can theoretically fit detailed light curves for selected energy bands on a continuous timescale ranging over 10<sup>6</sup> s. The theoretically predicted instantaneous spectral distribution over the entire afterglow is presented, confirming a clear hard-to-soft behavior encompassing, continuously, the “prompt emission” all the way to the latest phases of the afterglow.

6. C.L. Bianco, L. Caito, R. Ruffini; “Theoretical interpretation of GRB 011121”; *Il Nuovo Cimento B*, 121, 1441 (2006).

GRB011121 is analyzed as a prototype to understand the “flares” recently observed by Swift in the afterglow of many GRB sources. Detailed theoretical computation of the GRB011121 light curves in selected energy bands are presented and compared and contrasted with observational BeppoSAX data.

7. R. Ruffini, M.G. Bernardini, C.L. Bianco, P. Chardonnet, F. Frascetti, R. Guida, S.-S. Xue; “GRB 050315: A step toward the uniqueness of the overall GRB structure”; *Il Nuovo Cimento B*, 121, 1367 (2006).

Using the *Swift* data of GRB 050315, we progress on the uniqueness of our theoretically predicted Gamma-Ray Burst (GRB) structure as composed by a proper-GRB (P-GRB), emitted at the transparency of an electron-positron plasma with suitable baryon loading, and an afterglow comprising the so called “prompt emission” as due to external shocks. Thanks to the *Swift* observations, we can theoretically fit detailed light curves for selected energy bands on a continuous time scale ranging over  $10^6$  seconds. The theoretically predicted instantaneous spectral distribution over the entire afterglow confirms a clear hard-to-soft behavior encompassing, continuously, the “prompt emission” all the way to the latest phases of the afterglow. Consequences of the instrumental threshold on the definition of “short” and “long” GRBs are discussed.

8. M.G. Bernardini, C.L. Bianco, L. Caito, P. Chardonnet, A. Corsi, M.G. Dainotti, F. Frascetti, R. Guida, R. Ruffini, S.-S. Xue; GRB970228 as a prototype for short GRBs with afterglow; *Il Nuovo Cimento B*, 121, 1439 (2006).

GRB970228 is analyzed as a prototype to understand the relative role of short GRBs and their associated afterglows, recently observed by Swift and HETE-II. Detailed theoretical computation of the GRB970228 light curves in selected energy bands are presented and compared with observational BeppoSAX data.

9. M.G. Dainotti, M.G. Bernardini, C.L. Bianco, L. Caito, R. Guida, R. Ruffini; “GRB060218 and GRBs associated with Supernovae Ib/c”; *Astronomy & Astrophysics*, 471, L29 (2007).

*Context:* The *Swift* satellite has given continuous data in the range 0.3–150 keV from 0 s to  $10^6$  s for GRB060218 associated with SN2006aj. This Gamma-Ray Burst (GRB) which has an unusually long duration ( $T_{90} \sim 2100$  s) fulfills the Amati relation. These data offer the opportunity to probe theoretical models for GRBs connected with Supernovae (SNe).

*Aims:* We plan to fit the complete  $\gamma$ - and X-ray light curves of this long duration GRB, including the prompt emission, in order to clarify the nature of the progenitors and the astrophysical scenario of the class of GRBs associated with SNe Ib/c.

*Methods:* We apply our “fireshell” model based on the formation of a black hole, giving the relevant references. It is characterized by the precise equations of motion and equitemporal surfaces and by the role of thermal emission.

*Results:* The initial total energy of the electron-positron plasma  $E_{e^\pm}^{tot} = 2.32 \times 10^{50}$  erg has a particularly low value, similar to the other GRBs associated with SNe. For the first time, we observe a baryon loading  $B = 10^{-2}$  which coincides with the upper limit for the dynamical stability of the fireshell. The effective CircumBurst Medium (CBM) density shows a radial dependence  $n_{cbm} \propto r^{-\alpha}$  with  $1.0 \lesssim \alpha \lesssim 1.7$  and monotonically decreases from 1 to  $10^{-6}$  particles/cm<sup>3</sup>. This behavior is interpreted as being due to a fragmentation in the fireshell. Analogies with the fragmented density and filling factor characterizing Novae are outlined. The fit presented is particularly significant in view of the complete data set available for GRB060218 and of the fact that it fulfills the Amati relation.

*Conclusions:* We fit GRB060218, usually considered as an X-Ray Flash (XRF), as a “canonical GRB” within our theoretical model. The smallest possible black hole, formed by the gravitational collapse of a neutron star in a binary system, is consistent with the especially low energetics of the class of GRBs associated with SNe Ib/c. We provide the first evidence for a fragmentation in the fireshell. This fragmentation is crucial in explaining both the unusually large  $T_{90}$  and the consequently inferred abnormally low value of the CBM effective density.

10. M.G. Bernardini, C.L. Bianco, L. Caito, M.G. Dainotti, R. Guida, R. Ruffini; “GRB970228 and a class of GRBs with an initial spikelike emission”; *Astronomy & Astrophysics*, 474, L13 (2007).

*Context:* The discovery by *Swift* and HETE-2 of an afterglow emission associated possibly with short GRBs opened the new problematic of their nature and classification. This issue has been further enhanced by the observation of GRB060614 and by a new analysis of the BATSE catalog which led to the identification of a new class of GRBs with “an occasional softer extended emission lasting tenths of seconds after an initial spikelike emission”.

*Aims:* We plan a twofold task: a) to fit this new class of “hybrid” sources within our “canonical GRB” scenario, where all GRBs are generated by a “common engine” (i.e. the gravitational collapse to a black hole); b) to propose GRB970228 as the prototype of the above mentioned class, since it shares the same morphology and observational features.

*Methods:* We analyze *BeppoSAX* data on GRB970228 within the “fireshell” model and we determine the parameters describing the source and the CircumBurst Medium (CBM) needed to reproduce its light curves in the 40–700 keV and 2–26 keV energy bands.

*Results:* We find that GRB970228 is a “canonical GRB”, like e.g. GRB050315, with the main peculiarity of a particularly low average density of the CBM  $\langle n_{cbm} \rangle \sim 10^{-3}$  particles/cm<sup>3</sup>. We also simulate the light curve corresponding

to a rescaled CBM density profile with  $\langle n_{cbm} \rangle = 1$  particle/cm<sup>3</sup>. From such a comparison it follows that the total time-integrated luminosity is a faithful indicator of the nature of GRBs, contrary to the peak luminosity which is merely a function of the CBM density.

*Conclusions:* We call attention on discriminating the short GRBs between the “genuine” and the “fake” ones. The “genuine” ones are intrinsically short, with baryon loading  $B \lesssim 10^{-5}$ , as stated in our original classification. The “fake” ones, characterized by an initial spikelike emission followed by an extended emission lasting tenths of seconds, have a baryon loading  $10^{-4} \lesssim B \lesssim 10^{-2}$ . They are observed as such only due to an underdense CBM consistent with a galactic halo environment which deflates the afterglow intensity.

11. R. Guida, M.G. Bernardini, C.L. Bianco, L. Caito, M.G. Dainotti, R. Ruffini; “The Amati relation in the “fireshell” model”; *Astronomy & Astrophysics*, 487, L37 (2008).

*Context:* The cosmological origin of gamma-ray bursts (GRBs) has been firmly established, with redshifts up to  $z = 6.29$ . They are possible candidates for use as “distance indicators” for testing cosmological models in a redshift range hardly achievable by other cosmological probes. Asserting the validity of the empirical relations among GRB observables is now crucial for their calibration.

*Aims:* Motivated by the relation proposed by Amati and collaborators, we look within the “fireshell” model for a relation between the peak energy  $E_p$  of the  $\nu F_\nu$  total time-integrated spectrum of the afterglow and the total energy of the afterglow  $E_{aft}$ , which in our model encompasses and extends the prompt emission.

*Methods:* The fit within the fireshell model, as for the “canonical” GRB050315, uses the complete arrival time coverage given by the Swift satellite. It is performed simultaneously, self-consistently, and recursively in the four BAT energy bands (15–25 keV, 25–50 keV, 50–100 keV, and 100–150 keV), as well as in the XRT one (0.2–10 keV). It uniquely determines the two free parameters characterizing the GRB source, the total energy  $E_{tot}^{e^\pm}$  of the  $e^\pm$  plasma and its baryon loading  $B$ , as well as the effective CircumBurst Medium (CBM) distribution. We can then build two sets of “gedanken” GRBs varying the total energy of the electron-positron plasma  $E_{tot}^{e^\pm}$  and keeping the same baryon loading  $B$  of GRB050315. The first set assumes the one obtained in the fit of GRB050315 for the effective CBM density. The second set assumes instead a constant CBM density equal to the average value of the GRB050315 prompt phase.

*Results:* For the first set of “gedanken” GRBs we find a relation  $E_p \propto (E_{aft})^a$ , with  $a = 0.45 \pm 0.01$ , whose slope strictly agrees with the Amati one. Such a relation, in the limit  $B \rightarrow 10^{-2}$ , coincides with the Amati one. Instead, no correlation is found in the second set of “gedanken” GRBs.

*Conclusions:* Our analysis excludes the proper GRB (P-GRB) from the prompt emission, extends all the way to the latest afterglow phases, and is independent of the assumed cosmological model, since all “gedanken” GRBs are at

the same redshift. The Amati relation, on the other hand, includes the P-GRB, focuses only on the prompt emission, being therefore influenced by the instrumental threshold that fixes the end of the prompt emission, and depends on the assumed cosmology. This might explain the intrinsic scatter observed in the Amati relation.

12. L. Caito, M.G. Bernardini, C.L. Bianco, M.G. Dainotti, R. Guida, R. Ruffini; “GRB060614: a “fake” short GRB from a merging binary system”; *Astronomy & Astrophysics*, 489, 501 (2009).

*Context:* GRB060614 observations by VLT and by Swift have infringed the traditionally accepted gamma-ray burst (GRB) collapsar scenario that purports the origin of all long duration GRBs from supernovae (SN). GRB060614 is the first nearby long duration GRB clearly not associated with a bright Ib/c SN. Moreover, its duration ( $T_{90} \sim 100$  s) makes it hardly classifiable as a short GRB. It presents strong similarities with GRB970228, the prototype of a new class of “fake” short GRBs that appear to originate from the coalescence of binary neutron stars or white dwarfs spiraled out into the galactic halo. *Aims:* Within the “canonical” GRB scenario based on the “fireshell” model, we test if GRB060614 can be a “fake” or “disguised” short GRB. We model the traditionally termed “prompt emission” and discriminate the signal originating from the gravitational collapse leading to the GRB from the process occurring in the circumburst medium (CBM). *Methods:* We fit GRB060614 light curves in Swift’s BAT (15 – 150 keV) and XRT (0.2 – 10 keV) energy bands. Within the fireshell model, light curves are formed by two well defined and different components: the proper-GRB (P-GRB), emitted when the fireshell becomes transparent, and the extended afterglow, due to the interaction between the leftover accelerated baryonic and leptonic shell and the CBM. *Results:* We determine the two free parameters describing the GRB source within the fireshell model: the total  $e^\pm$  plasma energy ( $E_{tot}^{e^\pm} = 2.94 \times 10^{51}$  erg) and baryon loading ( $B = 2.8 \times 10^{-3}$ ). A small average CBM density  $\sim 10^{-3}$  particles/cm<sup>3</sup> is inferred, typical of galactic halos. The first spikelike emission is identified with the P-GRB and the following prolonged emission with the extended afterglow peak. We obtain very good agreement in the BAT (15 – 150 keV) energy band, in what is traditionally called “prompt emission”, and in the XRT (0.2 – 10 keV) one. *Conclusions:* The *anomalous* GRB060614 finds a natural interpretation within our canonical GRB scenario: it is a “disguised” short GRB. The total time-integrated extended afterglow luminosity is greater than the P-GRB one, but its peak luminosity is smaller since it is deflated by the peculiarly low average CBM density of galactic halos. This result points to an old binary system, likely formed by a white dwarf and a neutron star, as the progenitor of GRB060614 and well justifies the absence of an associated SN Ib/c. Particularly important for further studies of the final merging process are the temporal structures in the P-GRB down to 0.1 s.

13. M.G. Bernardini, C.L. Bianco, L. Caito, M.G. Dainotti, R. Guida, R. Ruffini; “GRB970228 in the “canonical GRB” scenario”; *Journal of the Korean Physical Society*, 56, 1575 (2010).

Within the “fireshell” model, we define a “canonical GRB” light curve with two sharply different components: the proper-GRB (P-GRB), emitted when the optically thick fireshell of an electron-positron plasma originating from the phenomenon reaches transparency, and the afterglow, emitted due to the collision between the remaining optically thin fireshell and the circumburst medium (CBM). On the basis of the recent understanding of GRB970228 as the prototype for a new class of GRBs with “an occasional softer extended emission lasting tenths of seconds after an initial spikelike emission”, we outline our “canonical GRB” scenario, originating from the gravitational collapse to a black hole, with special emphasis on the discrimination between “genuine” and “fake” short GRBs. Furthermore, we investigate how the GRB970228 analysis provides a theoretical explanation for the apparent absence of such a correlation for the GRBs belonging to this new class.

14. L. Caito, M.G. Bernardini, C.L. Bianco, M.G. Dainotti, R. Guida, R. Ruffini; “GRB060614: a preliminary result”; *Journal of the Korean Physical Society*, 56, 1579 (2010).

The explosion of GRB 060614 produced a deep break in the GRB scenario and opened new horizons of investigation because it can’t be traced back to any traditional scheme of classification. In fact, it manifests peculiarities both of long bursts and of short bursts, and above all, it is the first case of a long-duration near GRB without any bright Ib/c associated Supernova. We will show that, in our canonical GRB scenario, this “anomalous” situation finds a natural interpretation and allows us to discuss a possible variation in the traditional classification scheme, introducing a distinction between “genuine” and “fake” short bursts.

15. M.G. Dainotti, M.G. Bernardini, C.L. Bianco, L. Caito, R. Guida, R. Ruffini; “The astrophysical tryptic: GRB, SN and URCA can be extended to GRB060218?”; *Journal of the Korean Physical Society*, 56, 1588 (2010).

The *Swift* satellite has given continuous data in the range 0.3–150 keV from 0 s to  $10^6$  s for GRB060218 associated with SN2006aj. This GRB is the fourth GRB spectroscopically associated with SNe after the cases of GRB980425-SN1998bw, GRB031203-SN2003lw, GRB 030329-SN2003dh. It has an unusually long duration ( $T_{90} \sim 2100$  s). These data offer the opportunity to probe theoretical models for Gamma-Ray Bursts (GRBs) connected with Supernovae (SNe). We plan to fit the complete  $\gamma$ - and X-ray light curves of this long duration GRB, including the prompt emission, in order to clarify the nature of the progenitors and the astrophysical scenario of the class of GRBs associated to SNe Ib/c. We apply our “fireshell” model based on the formation of a black hole, giving

the relevant references. The initial total energy of the electron-positron plasma  $E_{e^\pm}^{tot} = 2.32 \times 10^{50}$  erg has a particularly low value similarly to the other GRBs associated with SNe. For the first time we observe a baryon loading  $B = 10^{-2}$  which coincides with the upper limit for the dynamical stability of the fireshell. The effective CircumBurst Medium (CBM) density shows a radial dependence  $n_{cbm} \propto r^{-\alpha}$  with  $1.0 \lesssim \alpha \lesssim 1.7$  and monotonically decreases from 1 to  $10^{-6}$  particles/cm<sup>3</sup>. Such a behavior is interpreted as due to a fragmentation in the fireshell. Such a fragmentation is crucial in explaining both the unusually large  $T_{90}$  and the consequently inferred abnormal low value of the CBM effective density. We fit GRB060218, usually considered as an X-Ray Flash (XRF), as a “canonical GRB” within our theoretical model. The smallest possible black hole, formed by the gravitational collapse of a neutron star in a binary system, is consistent with the especially low energetics of the class of GRBs associated with SNe Ib/c. We present the URCA process and the connection between the GRBs associated with SNe extended also to the case of GRB060218.

16. L. Izzo, M.G. Bernardini, C.L. Bianco, L. Caito, B. Patricelli, R. Ruffini; “GRB 090423 at Redshift 8.1: a Theoretical Interpretation”; *Journal of the Korean Physical Society*, 57, 551 (2010).

GRB 090423 is the farthest gamma ray burst ever observed, with a redshift of about 8.1. We present within the fireshell scenario a complete analysis of this GRB. We model the prompt emission and the first rapid flux decay of the afterglow emission as being to the canonical emission of the interaction in the interval  $0 \leq t \leq 440$  s by using accelerated baryonic matter with the circumburst medium. After the data reduction of the Swift data in the BAT (15 - 150 keV) and XRT (0.2 - 10 keV) energy bands, we interpret the light curves and the spectral distribution in the context of the fireshell scenario. We also confirm in this source the existence of a second component, a plateau phase, as being responsible for the late emission in the X-ray light curve. This extra component originates from the fact that the ejecta have a range of the bulk Lorentz  $\Gamma$  factor, which starts to interact each other ejecta at the start of the plateau phase.

17. L. Caito, L. Amati, M.G. Bernardini, C.L. Bianco, G. De Barros, L. Izzo, B. Patricelli, R. Ruffini; “GRB 071227: an additional case of a disguised short burst”; *Astronomy & Astrophysics*, 521, A80 (2010).

*Context:* Observations of gamma-ray bursts (GRBs) have shown an hybridization between the two classes of long and short bursts. In the context of the fireshell model, the GRB light curves are formed by two different components: the *proper* GRB (P-GRB) and the extended afterglow. Their relative intensity is linked to the fireshell baryon loading  $B$ . The GRBs with P-GRB predominance are the short ones, the remainders are long. A new family of *disguised* short bursts has been identified: long bursts with a protracted low instantaneous luminosity due to a low density CircumBurst Medium (CBM). In the 15–150

keV energy band GRB 071227 exhibits a short duration (about 1.8s) spike-like emission followed by a very soft extended tail up to one hundred seconds after the trigger. It is a faint ( $E_{iso} = 5.8 \times 10^{50}$ ) nearby GRB ( $z = 0.383$ ) that does not have an associated type Ib/c bright supernova (SN). For these reasons, GRB 071227 has been classified as a short burst not fulfilling the Amati relation holding for long burst. *Aims:* We check the classification of GRB 071227 provided by the fireshell model. In particular, we test whether this burst is another example of a *disguised* short burst, after GRB 970228 and GRB 060614, and, for this reason, whether it fulfills the Amati relation. *Methods:* We simulate GRB 071227 light curves in the *Swift* BAT 15–50 keV bandpass and in the XRT (0.3–10 keV) energy band within the fireshell model. *Results:* We perform simulations of the tail in the 15–50 keV bandpass, as well as of the first part of the X-ray afterglow. This infers that:  $E_{tot}^{e^{\pm}} = 5.04 \times 10^{51}$  erg,  $B = 2.0 \times 10^{-4}$ ,  $E_{P-GRB}/E_{aft} \sim 0.25$ , and  $\langle n_{cbm} \rangle = 3.33$  particles/cm<sup>3</sup>. These values are consistent with those of “long duration” GRBs. We interpret the observed energy of the first hard emission by identifying it with the P-GRB emission. The remaining long soft tail indeed fulfills the Amati relation. *Conclusions:* Previously classified as a short burst, GRB 071227 on the basis of our analysis performed in the context of the fireshell scenario represents another example of a *disguised* short burst, after GRB 970228 and GRB 060614. Further confirmation of this result is that the soft tail of GRB 071227 fulfills the Amati relation.

18. M.G. Bernardini, C.L. Bianco, L. Caito, L. Izzo, B. Patricelli, R. Ruffini; “Analysis of GRB060607A within the fireshell model: prompt emission, X-ray flares and late afterglow phase”; *Astronomy & Astrophysics*, submitted to.

*Context:* GRB060607A is a very distant ( $z = 3.082$ ) and energetic event ( $E_{iso} \sim 10^{53}$  erg). Its main peculiarity is that the peak of the near-infrared (NIR) afterglow has been observed with the REM robotic telescope. This NIR peak has been interpreted as the afterglow onset within the fireball forward shock model, and the initial Lorentz gamma factor of the emitting system has been inferred. *Aims:* We analyze GRB060607A within the fireshell model. We emphasize the central role of the prompt emission in determining the initial Lorentz gamma factor of the extended afterglow and we interpret the X-ray flares as produced by the interaction of the optically thin fireshell with overdense CircumBurst Medium (CBM) clumps. *Methods:* We deal only with the *Swift* BAT and XRT observations, that are the basic contribution to the GRB emission and that are neglected in the treatment adopted in the current literature. The numerical modeling of the fireshell dynamics allows to calculate all its characteristic quantities, in particular the exact value of the Lorentz gamma factor at the transparency. *Results:* We show that the theoretically computed prompt emission light curves are in good agreement with the observations in all the *Swift* BAT energy bands as well as the spectra integrated over different time intervals. The flares observed in the decaying phase of the X-ray afterglow are

also reproduced by the same mechanism, but in a region in which the typical dimensions of the clumps are smaller than the visible area of the fireshell and most energy lies in the X-ray band due to the hard-to-soft evolution. *Conclusions:* We show that it is possible to obtain flares with  $\Delta t/t$  compatible with the observations when the three-dimensional structure of the CBM clumps is duly taken into account. We stop our analysis at the beginning of the X-ray plateau phase, since we suppose this originates from the instabilities developed in the collision between different subshells within a structured fireshell.

19. G. de Barros, M. G. Bernardini, C.L. Bianco, L. Caito, L. Izzo, B. Patricelli, R. Ruffini; “On the nature of GRB 050509b: a disguised short GRB”; *Astronomy & Astrophysics*, 529, A130 (2011)

*Context:* GRB 050509b, detected by the *Swift* satellite, is the first case where an X-ray afterglow has been observed associated with a short gamma-ray burst (GRB). Within the fireshell model, the canonical GRB light curve presents two different components: the proper-GRB (P-GRB) and the extended afterglow. Their relative intensity is a function of the fireshell baryon loading parameter  $B$  and of the CircumBurst Medium (CBM) density ( $n_{CBM}$ ). In particular, the traditionally called short GRBs can be either “genuine” short GRBs (with  $B \lesssim 10^{-5}$ , where the P-GRB is energetically predominant) or “disguised” short GRBs (with  $B \gtrsim 3.0 \times 10^{-4}$  and  $n_{CBM} \ll 1$ , where the extended afterglow is energetically predominant). *Aims:* We verify whether GRB 050509b can be classified as a “genuine” short or a “disguised” short GRB, in the fireshell model. *Methods:* We investigate two alternative scenarios. In the first, we start from the assumption that this GRB is a “genuine” short burst. In the second attempt, we assume that this GRB is a “disguised” burst. *Results:* If GRB 050509b were a genuine short GRB, there should initially be very hard emission which is ruled out by the observations. The analysis that assumes that this is a disguised short GRB is compatible with the observations. The theoretical model predicts a value of the extended afterglow energy peak that is consistent with the Amati relation. *Conclusions:* GRB 050509b cannot be classified as a “genuine” short GRB. The observational data are consistent with a “disguised” short GRB classification, i.e., a long burst with a weak extended afterglow “deflated” by the low density of the CBM. We expect that all short GRBs with measured redshifts are disguised short GRBs because of a selection effect: if there is enough energy in the afterglow to measure the redshift, then the proper GRB must be less energetic than the afterglow. The Amati relation is found to be fulfilled only by the extended afterglow excluding the P-GRB.

20. L. Caito, M.G. Bernardini, C.L. Bianco, L. Izzo, B. Patricelli, R. Ruffini; “GRB 071227: another disguised short burst”; *International Journal of Modern Physics D*, 20, 1931 (2011).

Observations of Gamma-ray Bursts (GRBs) put forward in the recent years have revealed, with increasing evidence, that the historical classification be-

tween long and short bursts has to be revised. Within the Fireshell scenario, both short and long bursts are canonical bursts, consisting of two different phases. First, a Proper-GRB (P-GRB), that is the emission of photons at the transparency of the fireshell. Then, the Extended Afterglow, multiwavelength emission due to the interaction of the baryonic remnants of the fireshell with the CircumBurst Medium (CBM). We discriminate between long and short bursts by the amount of energy stored in the first phase with respect to the second one. Within the Fireshell scenario, we have introduced a third intermediate class: the disguised GRBs. They appear like short bursts, because their morphology is characterized by a first, short, hard episode and a following deflated tail, but this last part — coincident with the peak of the afterglow — is energetically predominant. The origin of this peculiar kind of sources is inferred to a very low average density of the environment (of the order of  $10^{-3}$ ). After GRB 970228 and GRB 060614, we find in GRB 071227 a third example of disguised burst.

21. L. Izzo, M.G. Bernardini, C.L. Bianco, L. Caito, B. Patricelli, L.J. Rangel Lemos, R. Ruffini; “GRB 080916C and the high-energy emission in the fireshell scenario”; *International Journal of Modern Physics D*, 20, 1949 (2011).

In this paper we discuss a possible explanation for the high energy emission (up to  $\sim$  GeV) seen in GRB 080916C. We propose that the GeV emission is originated by the collision between relativistic baryons in the fireshell after the transparency and the nucleons located in molecular clouds near the burst site. This collision should give rise pion production, whose immediate decay provides high energy photons, neutrinos and leptons. Using a public code (SYBILL) we simulate these relativistic collisions in their simple form, so that we can draw our preliminar results in this paper. We will present moreover our hypothesis that the delayed onset of this emission identifies in a complete way the P-GRB emission.

22. B. Patricelli, M.G. Bernardini, C.L. Bianco, L. Caito, L. Izzo, R. Ruffini, G. Vereshchagin; “A new spectral energy distribution of photons in the fireshell model of GRBs”; *International Journal of Modern Physics D*, 20, 1983 (2011).

The analysis of various Gamma-Ray Bursts (GRBs) having a low energetics (an isotropic energy  $E_{iso} \lesssim 10^{53}$  ergs) within the fireshell model has shown how the  $N(E)$  spectrum of their prompt emission can be reproduced in a satisfactory way by a convolution of thermal spectra. Nevertheless, from the study of very energetic bursts ( $E_{iso} \lesssim 10^{54}$  ergs) such as, for example, GRB 080319B, some discrepancies between the numerical simulations and the observational data have been observed. We investigate a different spectrum of photons in the comoving frame of the fireshell in order to better reproduce the spectral properties of GRB prompt emission within the fireshell model. We introduce

a phenomenologically modified thermal spectrum: a thermal spectrum characterized by a different asymptotic power-law index in the low energy region. Such an index depends on a free parameter  $\alpha$ , so that the pure thermal spectrum corresponds to the case  $\alpha = 0$ . We test this spectrum by comparing the numerical simulations with the observed prompt emission spectra of various GRBs. From this analysis it has emerged that the observational data can be correctly reproduced by assuming a modified thermal spectrum with  $\alpha = -1.8$ .

## 5.2. Conference proceedings

1. R. Ruffini, M.G. Bernardini, C.L. Bianco, P. Chardonnet, F. Fraschetti, V. Gurzadyan, L. Vitagliano, S.-S. Xue; “The Blackholic energy: long and short Gamma-Ray Bursts (New perspectives in physics and astrophysics from the theoretical understanding of Gamma-Ray Bursts, II)”; in Proceedings of the XIth Brazilian School on Cosmology and Gravitation, Mangaratiba, Rio de Janeiro (Brazil), July–August 2004, M. Novello, S.E. Perez Bergliaffa, Editors; AIP Conference Proceedings, 782, 42 (2005).

We outline the confluence of three novel theoretical fields in our modeling of Gamma-Ray Bursts (GRBs): 1) the ultrarelativistic regime of a shock front expanding with a Lorentz gamma factor  $\sim 300$ ; 2) the quantum vacuum polarization process leading to an electron-positron plasma originating the shock front; and 3) the general relativistic process of energy extraction from a black hole originating the vacuum polarization process. There are two different classes of GRBs: the long GRBs and the short GRBs. We here address the issue of the long GRBs. The theoretical understanding of the long GRBs has led to the detailed description of their luminosities in fixed energy bands, of their spectral features and made also possible to probe the astrophysical scenario in which they originate. We are specially interested, in this report, to a subclass of long GRBs which appear to be accompanied by a supernova explosion. We are considering two specific examples: GRB980425/SN1998bw and GRB030329/SN2003dh. While these supernovae appear to have a standard energetics of  $10^{49}$  ergs, the GRBs are highly variable and can have energetics  $10^4 - 10^5$  times larger than the ones of the supernovae. Moreover, many long GRBs occurs without the presence of a supernova. It is concluded that in no way a GRB can originate from a supernova. The precise theoretical understanding of the GRB luminosity we present evidence, in both these systems, the existence of an independent component in the X-ray emission, usually interpreted in the current literature as part of the GRB afterglow. This component has been observed by Chandra and XMM to have a strong decay on scale of months. We have named here these two sources respectively URCA-1 and URCA-2, in honor of the work that George Gamow and Mario Shoenberg did in 1939 in this town of Urca identifying the basic mechanism, the Urca pro-

cesses, leading to the process of gravitational collapse and the formation of a neutron star and a supernova. The further hypothesis is considered to relate this X-ray source to a neutron star, newly born in the Supernova. This hypothesis should be submitted to further theoretical and observational investigation. Some theoretical developments to clarify the astrophysical origin of this new scenario are outlined. We turn then to the theoretical developments in the short GRBs: we first report some progress in the understanding the dynamical phase of collapse, the mass-energy formula and the extraction of blackholc energy which have been motivated by the analysis of the short GRBs. In this context progress has also been accomplished on establishing an absolute lower limit to the irreducible mass of the black hole as well as on some critical considerations about the relations of general relativity and the second law of thermodynamics. We recall how this last issue has been one of the most debated in theoretical physics in the past thirty years due to the work of Bekenstein and Hawking. Following these conceptual progresses we analyze the vacuum polarization process around an overcritical collapsing shell. We evidence the existence of a separatrix and a dyadosphere trapping surface in the dynamics of the electron-positron plasma generated during the process of gravitational collapse. We then analyze, using recent progress in the solution of the Vlasov-Boltzmann-Maxwell system, the oscillation regime in the created electron-positron plasma and their rapid convergence to a thermalized spectrum. We conclude by making precise predictions for the spectra, the energy fluxes and characteristic time-scales of the radiation for short-bursts. If the precise luminosity variation and spectral hardening of the radiation we have predicted will be confirmed by observations of short-bursts, these systems will play a major role as standard candles in cosmology. These considerations will also be relevant for the analysis of the long-bursts when the baryonic matter contribution will be taken into account.

2. R. Ruffini, M.G. Bernardini, C.L. Bianco, P. Chardonnet, F. Frascetti, V. Gurzadyan, L. Vitagliano, S.-S. Xue; "Black hole physics and astrophysics: The GRB-Supernova connection and URCA-1 URCA-2"; in Proceedings of the Tenth Marcel Grossmann Meeting on General Relativity, Rio de Janeiro, Brazil, July 2003, M. Novello, S.E. Perez-Bergliaffa, Editors; p. 369; World Scientific, (Singapore, 2006).

We outline the confluence of three novel theoretical fields in our modeling of Gamma-Ray Bursts (GRBs): 1) the ultrarelativistic regime of a shock front expanding with a Lorentz gamma factor  $\sim 300$ ; 2) the quantum vacuum polarization process leading to an electron-positron plasma originating the shock front; and 3) the general relativistic process of energy extraction from a black hole originating the vacuum polarization process. There are two different classes of GRBs: the long GRBs and the short GRBs. We here address the issue of the long GRBs. The theoretical understanding of the long GRBs has led to the detailed description of their luminosities in fixed energy bands, of

their spectral features and made also possible to probe the astrophysical scenario in which they originate. We are specially interested, in this report, to a subclass of long GRBs which appear to be accompanied by a supernova explosion. We are considering two specific examples: GRB980425/SN1998bw and GRB030329/SN2003dh. While these supernovae appear to have a standard energetics of  $10^{49}$  ergs, the GRBs are highly variable and can have energetics  $10^4 - 10^5$  times larger than the ones of the supernovae. Moreover, many long GRBs occurs without the presence of a supernova. It is concluded that in no way a GRB can originate from a supernova. The precise theoretical understanding of the GRB luminosity we present evidence, in both these systems, the existence of an independent component in the X-ray emission, usually interpreted in the current literature as part of the GRB afterglow. This component has been observed by Chandra and XMM to have a strong decay on scale of months. We have named here these two sources respectively URCA-1 and URCA-2, in honor of the work that George Gamow and Mario Shoenberg did in 1939 in this town of Urca identifying the basic mechanism, the Urca processes, leading to the process of gravitational collapse and the formation of a neutron star and a supernova. The further hypothesis is considered to relate this X-ray source to a neutron star, newly born in the Supernova. This hypothesis should be submitted to further theoretical and observational investigation. Some theoretical developments to clarify the astrophysical origin of this new scenario are outlined.

3. M.G. Bernardini, C.L. Bianco, P. Chardonnet, F. Frascchetti, R. Ruffini, S.-S. Xue; "General features of GRB 030329 in the EMBH model"; in Proceedings of the Tenth Marcel Grossmann Meeting on General Relativity, Rio de Janeiro, Brazil, July 2003, M. Novello, S.E. Perez-Bergliaffa, Editors; p. 2459; World Scientific, (Singapore, 2006).

GRB 030329 is considered within the EMBH model. We determine the three free parameters and deduce its luminosity in given energy bands comparing it with the observations. The observed substructures are compared with the predictions of the model: by applying the result that substructures observed in the extended afterglow peak emission (E-APE) do indeed originate in the collision of the accelerated baryonic matter (ABM) pulse with the inhomogeneities in the interstellar medium around the black-hole, masks of density inhomogeneities are considered in order to reproduce the observed temporal substructures. The induced supernova concept is applied to this system and the general consequences that we are witnessing are the formation of a cosmological thriptych of a black hole originating the GRB 030329, the supernova SN2003dh and a young neutron star. Analogies to the system GRB 980425–SN1998bw are outlined.

4. R. Ruffini, M.G. Bernardini, C.L. Bianco, P. Chardonnet, A. Corsi, F. Frascchetti, S.-S. Xue; "GRB 970228 and its associated Supernova in the

EMBH model"; in Proceedings of the Tenth Marcel Grossmann Meeting on General Relativity, Rio de Janeiro, Brazil, July 2003, M. Novello, S.E. Perez-Bergliaffa, Editors; p. 2465; World Scientific, (Singapore, 2006).

The  $\gamma$ -ray burst of 1997 February 28 is analyzed within the Electromagnetic Black Hole model. We first estimate the value of the total energy deposited in the dyadosphere,  $E_{dya}$ , and the amount of baryonic matter left over by the EMBH progenitor star,  $B = M_B c^2 / E_{dya}$ . We then consider the role of the interstellar medium number density  $n_{ISM}$  and of the ratio  $R$  between the effective emitting area and the total surface area of the  $\gamma$ -ray burst source, in reproducing the prompt emission and the X-ray afterglow of this burst. Some considerations are also done concerning the possibility of explaining, within the theory, the observed evidence for a supernova in the optical afterglow.

5. F. Frascchetti, M.G. Bernardini, C.L. Bianco, P. Chardonnet, R. Ruffini, S.-S. Xue; "Inferences on the ISM structure around GRB980425 and GRB980425-SN1998bw association in the EMBH Model"; in Proceedings of the Tenth Marcel Grossmann Meeting on General Relativity, Rio de Janeiro, Brazil, July 2003, M. Novello, S.E. Perez-Bergliaffa, Editors; p. 2451; World Scientific, (Singapore, 2006).

We determine the four free parameters within the EMBH model for GRB 980425 and deduce its luminosity in given energy bands, its spectra and its time variability in the prompt radiation. We compute the basic kinematical parameters of GRB 980425. In the extended afterglow peak emission the Lorentz  $\gamma$  factor is lower than the critical value 150 which has been found in Ruffini et al. (2002) to be necessary in order to perform the tomography of the ISM surrounding the GRB as suggested by Dermer & Mitman (1999). The detailed structure of the density inhomogeneities as well as the effects of radial apparent superluminal effects are evaluated within the EMBH model. Under the assumption that the energy distribution of emitted radiation is thermal in the comoving frame, time integrated spectra of EMBH model for prompt emission are computed. The induced supernova concept is applied to this system and general consequences on the astrophysical and cosmological scenario are derived.

6. R. Ruffini, M.G. Bernardini, C.L. Bianco, P. Chardonnet, F. Frascchetti, R. Guida, S.-S. Xue; "GRB 050315: A step in the proof of the uniqueness of the overall GRB structure"; in "GAMMA-RAY BURSTS IN THE SWIFT ERA: Sixteenth Maryland Astrophysics Conference", Washington, DC, USA, November 29th - December 2nd 2005, Stephen S. Holt, Neil Gehrels, John A. Nousek, Editors; AIP Conference Proceedings, 836, 103 (2006).

Using the Swift data of GRB 050315, we progress in proving the uniqueness of our theoretically predicted Gamma-Ray Burst (GRB) structure as composed by a proper-GRB, emitted at the transparency of an electron-positron plasma

with suitable baryon loading, and an afterglow comprising the “prompt radiation” as due to external shocks. Detailed light curves for selected energy bands are theoretically fitted in the entire temporal region of the Swift observations ranging over  $10^6$  seconds.

7. R. Ruffini, M.G. Bernardini, C.L. Bianco, P. Chardonnet, F. Fraschetti, S.-S. Xue; “Theoretical Interpretation of GRB 031203 and URCA-3”; in “Relativistic Astrophysics and Cosmology - Einsteins Legacy”, B. Aschenbach, V. Burwitz, G. Hasinger, B. Leibundgut, Editors; Springer-Verlag (2007).
8. R. Ruffini, M.G. Bernardini, C.L. Bianco, L. Caito, P. Chardonnet, M.G. Dainotti, F. Fraschetti, R. Guida, M. Rotondo, G. Vereshchagin, L. Vitagliano, S.-S. Xue; “The Blackholic energy and the canonical Gamma-Ray Burst”; in Proceedings of the XIIth Brazilian School on Cosmology and Gravitation, Mangaratiba, Rio de Janeiro (Brazil), September 2006, M. Novello, S.E. Perez Bergliaffa, Editors; AIP Conference Proceedings, 910, 55 (2007).

Gamma-Ray Bursts (GRBs) represent very likely “the” most extensive computational, theoretical and observational effort ever carried out successfully in physics and astrophysics. The extensive campaign of observation from space based X-ray and  $\gamma$ -ray observatory, such as the *Vela*, CGRO, BeppoSAX, HETE-II, INTEGRAL, *Swift*, R-XTE, *Chandra*, XMM satellites, have been matched by complementary observations in the radio wavelength (e.g. by the VLA) and in the optical band (e.g. by VLT, Keck, ROSAT). The net result is unprecedented accuracy in the received data allowing the determination of the energetics, the time variability and the spectral properties of these GRB sources. The very fortunate situation occurs that these data can be confronted with a mature theoretical development. Theoretical interpretation of the above data allows progress in three different frontiers of knowledge: **a)** the ultrarelativistic regimes of a macroscopic source moving at Lorentz gamma factors up to  $\sim 400$ ; **b)** the occurrence of vacuum polarization process verifying some of the yet untested regimes of ultrarelativistic quantum field theories; and **c)** the first evidence for extracting, during the process of gravitational collapse leading to the formation of a black hole, amounts of energies up to  $10^{55}$  ergs of blackholic energy — a new form of energy in physics and astrophysics. We outline how this progress leads to the confirmation of three interpretation paradigms for GRBs proposed in July 2001. Thanks mainly to the observations by *Swift* and the optical observations by VLT, the outcome of this analysis points to the existence of a “canonical” GRB, originating from a variety of different initial astrophysical scenarios. The communality of these GRBs appears to be that they all are emitted in the process of formation of a black hole with a negligible value of its angular momentum. The following sequence of events appears to be canonical: the vacuum polarization process in the dyadosphere with the

creation of the optically thick self accelerating electron-positron plasma; the engulfment of baryonic mass during the plasma expansion; adiabatic expansion of the optically thick “fireshell” of electron-positron-baryon plasma up to the transparency; the interaction of the accelerated baryonic matter with the interstellar medium (ISM). This leads to the canonical GRB composed of a proper GRB (P-GRB), emitted at the moment of transparency, followed by an extended afterglow. The sole parameters in this scenario are the total energy of the dyadosphere  $E_{dya}$ , the fireshell baryon loading  $M_B$  defined by the dimensionless parameter  $B \equiv M_B c^2 / E_{dya}$ , and the ISM filamentary distribution around the source. In the limit  $B \rightarrow 0$  the total energy is radiated in the P-GRB with a vanishing contribution in the afterglow. In this limit, the canonical GRBs explain as well the short GRBs. In these lecture notes we systematically outline the main results of our model comparing and contrasting them with the ones in the current literature. In both cases, we have limited ourselves to review already published results in refereed publications. We emphasize as well the role of GRBs in testing yet unexplored grounds in the foundations of general relativity and relativistic field theories.

9. R. Ruffini, M.G. Bernardini, C.L. Bianco, L. Caito, P. Chardonnet, M.G. Dainotti, F. Frascchetti, R. Guida, G. Vereshchagin, S.-S. Xue; “The role of GRB 031203 in clarifying the astrophysical GRB scenario”; in Proceedings of the 6<sup>th</sup> Integral Workshop - The Obscured Universe, Moscow, (Russia), July 2006, S. Grebenev, R. Sunyaev, C. Winkler, A. Parmar, L. Ouweland, Editors; ESA Special Publication, SP-622, 561 (2007).

The luminosity and the spectral distribution of the afterglow of GRB 031203 have been presented within our theoretical framework, which envisages the GRB structure as composed by a proper-GRB, emitted at the transparency of an electron-positron plasma with suitable baryon loading, and an afterglow comprising the “prompt emission” as due to external shocks. In addition to the GRB emission, there appears to be a prolonged soft X-Ray emission lasting for  $10^6$ – $10^7$  seconds followed by an exponential decay. This additional source has been called by us URCA-3. It is urgent to establish if this component is related to the GRB or to the Supernova (SN). In this second case, there are two possibilities: either the interaction of the SN ejecta with the interstellar medium or, possibly, the cooling of a young neutron star formed in the SN 2003lw process. The analogies and the differences between this triptych GRB 031203 / SN 2003lw / URCA-3 and the corresponding ones GRB 980425 / SN 1998bw / URCA-1 and GRB 030329 / SN 2003dh / URCA-2, as well as GRB 060218 / SN 2006aj are discussed.

10. M.G. Bernardini, C.L. Bianco, L. Caito, M.G. Dainotti, R. Guida, R. Ruffini; “GRB970228 and the class of GRBs with an initial spikelike emission: do they follow the Amati relation?”; in Relativistic Astrophysics Proceedings of the 4<sup>th</sup> Italian-Sino Workshop, Pescara (Italy), July 2007, C.L.

Bianco, S.-S. Xue, Editors; AIP Conference Proceedings, 966, 7 (2008).

On the basis of the recent understanding of GRB050315 and GRB060218, we return to GRB970228, the first Gamma-Ray Burst (GRB) with detected afterglow. We proposed it as the prototype for a new class of GRBs with “an occasional softer extended emission lasting tenths of seconds after an initial spikelike emission”. Detailed theoretical computation of the GRB970228 light curves in selected energy bands for the prompt emission are presented and compared with observational *BeppoSAX* data. From our analysis we conclude that GRB970228 and likely the ones of the above mentioned new class of GRBs are “canonical GRBs” have only one peculiarity: they exploded in a galactic environment, possibly the halo, with a very low value of CBM density. Here we investigate how GRB970228 unveils another peculiarity of this class of GRBs: they do not fulfill the “Amati relation”. We provide a theoretical explanation within the fireshell model for the apparent absence of such correlation for the GRBs belonging to this new class.

11. C.L. Bianco, M.G. Bernardini, L. Caito, M.G. Dainotti, R. Guida, R. Ruffini; “The “Fireshell” Model and the “Canonical” GRB Scenario; in *Relativistic Astrophysics Proceedings of the 4<sup>th</sup> Italian-Sino Workshop, Pescara (Italy), July 2007*, C.L. Bianco, S.-S. Xue, Editors; AIP Conference Proceedings, 966, 12 (2008).

In the “fireshell” model we define a “canonical GRB” light curve with two sharply different components: the Proper-GRB (P-GRB), emitted when the optically thick fireshell of electron-positron plasma originating the phenomenon reaches transparency, and the afterglow, emitted due to the collision between the remaining optically thin fireshell and the CircumBurst Medium (CBM). We outline our “canonical GRB” scenario, originating from the gravitational collapse to a black hole, with a special emphasis on the discrimination between “genuine” and “fake” short GRBs.

12. L. Caito, M.G. Bernardini, C.L. Bianco, M.G. Dainotti, R. Guida, R. Ruffini; “GRB 060614: A Progress Report”; in *Relativistic Astrophysics Proceedings of the 4<sup>th</sup> Italian-Sino Workshop, Pescara (Italy), July 2007*, C.L. Bianco, S.-S. Xue, Editors; AIP Conference Proceedings, 966, 16 (2008).

The explosion of GRB 060614, detected by the Swift satellite, produced a deep break in the GRB scenario opening new horizons of investigation, because it can't be traced back to any traditional scheme of classification. In fact, it manifests peculiarities both of long bursts and of short bursts. Above all, it is the first case of long duration near GRB without any bright Ib/c associated Supernova. We will show that, in our canonical GRB scenario, this “anomalous” situation finds a natural interpretation and allows us to discuss a possible variation to the traditional classification scheme, introducing the distinction between “genuine” and “fake” short bursts.

13. M.G. Dainotti, M.G. Bernardini, C.L. Bianco, L. Caito, R. Guida, R. Ruffini; “GRB 060218 and the Binaries as Progenitors of GRB-SN Systems”; in *Relativistic Astrophysics Proceedings of the 4<sup>th</sup> Italian-Sino Workshop, Pescara (Italy), July 2007*, C.L. Bianco, S.-S. Xue, Editors; AIP Conference Proceedings, 966, 25 (2008).

We study the Gamma-Ray Burst (GRB) 060218: a particularly close source at  $z = 0.033$  with an extremely long duration, namely  $T_{90} \sim 2000$  s, related to SN 2006aj. This source appears to be a very soft burst, with a peak in the spectrum at 4.9 keV, therefore interpreted as an X-Ray Flash (XRF). It fullfills the Amati relation. I present the fitting procedure, which is time consuming. In order to show its sensitivity I also present two examples of fits with the same value of  $B$  and different value of  $E_{e^\pm}^{tot}$ . We fit the X- and  $\gamma$ -ray observations by *Swift* of GRB 060218 in the 0.1–150 keV energy band during the entire time of observations from 0 all the way to  $10^6$  s within a unified theoretical model. The free parameters of our theory are only three, namely the total energy  $E_{e^\pm}^{tot}$  of the  $e^\pm$  plasma, its baryon loading  $B \equiv M_B c^2 / E_{e^\pm}^{tot}$ , as well as the CircumBurst Medium (CBM) distribution. We justify the extremely long duration of this GRB by a total energy  $E_{e^\pm}^{tot} = 2.32 \times 10^{50}$  erg, a very high value of the baryon loading  $B = 1.0 \times 10^{-2}$  and the effective CircumBurst Medium (CBM) density which shows a radial dependence  $n_{cbm} \propto r^{-\alpha}$  with  $1.0 \leq \alpha \leq 1.7$  and monotonically decreases from 1 to  $10^{-6}$  particles/cm<sup>3</sup>. We recall that this value of the  $B$  parameter is the highest among the sources we have analyzed and it is very close to its absolute upper limit expected. By our fit we show that there is no basic differences between XRFs and more general GRBs. They all originate from the collapse process to a black hole and their difference is due to the variability of the three basic parameters within the range of full applicability of the theory. We also think that the smallest possible black hole, formed by the gravitational collapse of a neutron star in a binary system, is consistent with the especially low energetics of the class of GRBs associated with SNe Ib/c.

14. R. Guida, M.G. Bernardini, C.L. Bianco, L. Caito, M.G. Dainotti, R. Ruffini; “The Amati Relation within the Fireshell Model”; in *Relativistic Astrophysics Proceedings of the 4<sup>th</sup> Italian-Sino Workshop, Pescara (Italy), July 2007*, C.L. Bianco, S.-S. Xue, Editors; AIP Conference Proceedings, 966, 46 (2008).

In this work we show the existence of a spectral-energy correlation within our “fireshell” model for GRBs. The free parameters of the model are the total energy  $E_{tot}^{e^\pm}$  of the  $e^\pm$  plasma and its baryon loading  $B \equiv M_B c^2 / E_{tot}^{e^\pm}$ , characterizing the source, and the parameters describing the effective CircumBurst medium (CBM) distribution, namely its particle number density  $\rho$  and its effective emitting area  $R$ . We build a sample of pseudo-GRBs, i.e. a set of theoretically simulated light curves, varying the total energy of the electron-positron plasma  $E_{tot}^{e^\pm}$  and keeping the same baryon loading; the parametrization used

to describe the distribution of the CircumBurst medium is the same as well for all the pseudo-GRBs. The values of these parameters ( $B$ ,  $\rho$  and  $R$ ) used in this work are equal to the ones assumed to fit GRB050315, a *Swift* burst representing a good example of what in the literature has been addressed as “canonical light curve”. For each GRB of the sample we calculate the  $\nu F_\nu$  spectrum integrating the theoretically computed light curve over the total time, namely from our  $T_0$ , the end of the Proper-GRB (P-GRB), up to the end of our afterglow phase, when the fireshell Lorentz gamma factor is close to unity; we exclude the P-GRB from this spectral computation because, following our “canonical” GRB scenario, this component of the GRB emission is physically different from the other component, that is our afterglow component, so one should take care in no mixing them. We find that the maximum of this spectrum, that is the observed peak energy  $E_{p,tot}$ , correlates with the initial electron-positron plasma energy  $E_{tot}^{e\pm}$  in a way very similar to the Amati one:  $E_{p,tot} \propto (E_{tot}^{e\pm})^{0.5}$ .

15. R. Guida, M.G. Bernardini, C.L. Bianco, L. Caito, M.G. Dainotti, R. Ruffini; “Theoretical interpretation of the Amati relation within the fireshell model”; in GAMMA-RAY BURSTS 2007: Proceedings of the Santa Fe Conference, Santa Fe (NM, USA), November 2007, M. Galassi, D. Palmer, E. Fenimore, Editors; AIP Conference Proceedings, 1000, 60 (2008).

We discuss within our theoretical “fireshell” model for Gamma-Ray Bursts (GRBs) the theoretical interpretation of the phenomenological correlation between the isotropic-equivalent radiated energy of the prompt emission  $E_{iso}$  and the cosmological rest-frame  $\nu F_\nu$  spectrum peak energy  $E_p$  observed by Amati and collaborators. Possible reasons for some of the outliers of this relation are given.

16. L. Caito, M.G. Bernardini, C.L. Bianco, M.G. Dainotti, R. Guida, R. Ruffini; “GRB 060614: a Fake Short Gamma-Ray Burst”; in GAMMA-RAY BURSTS 2007: Proceedings of the Santa Fe Conference, Santa Fe (NM, USA), November 2007, M. Galassi, D. Palmer, E. Fenimore, Editors; AIP Conference Proceedings, 1000, 301 (2008).

The explosion of GRB 060614 produced a deep break in the GRB scenario and opened new horizons of investigation because it can’t be traced back to any traditional scheme of classification. In fact, it manifests peculiarities both of long bursts and of short bursts and, above all, it is the first case of long duration near GRB without any bright Ib/c associated Supernova. We will show that, in our canonical GRB scenario, this “anomalous” situation finds a natural interpretation and allows us to discuss a possible variation to the traditional classification scheme, introducing the distinction between “genuine” and “fake” short bursts.

17. C.L. Bianco, M.G. Bernardini, L. Caito, M.G. Dainotti, R. Guida, R. Ruffini; “Short and canonical GRBs”; in GAMMA-RAY BURSTS 2007: Proceed-

ings of the Santa Fe Conference, Santa Fe (NM, USA), November 2007, M. Galassi, D. Palmer, E. Fenimore, Editors; AIP Conference Proceedings, 1000, 305 (2008).

Within the “fireshell” model for the Gamma-Ray Bursts (GRBs) we define a “canonical GRB” light curve with two sharply different components: the Proper-GRB (P-GRB), emitted when the optically thick fireshell of electron-positron plasma originating the phenomenon reaches transparency, and the afterglow, emitted due to the collision between the remaining optically thin fireshell and the CircumBurst Medium (CBM). We outline our “canonical GRB” scenario, with a special emphasis on the discrimination between “genuine” and “fake” short GRBs.

18. C.L. Bianco, M.G. Bernardini, L. Caito, M.G. Dainotti, R. Guida, R. Ruffini, G. Vereshchagin, S.-S. Xue; “The Equations of motion of the “fireshell””; in OBSERVATIONAL EVIDENCE FOR BLACK HOLES IN THE UNIVERSE: Proceedings of the 2<sup>nd</sup> Kolkata Conference, Kolkata (India), February 2008, S.K. Chakrabarti, A.S. Majumdar, Editors; AIP Conference Proceedings, 1053, 259 (2008).

The Fireshell originating a Gamma-Ray Burst (GRB) encompasses an optically thick regime followed by an optically thin one. In the first one the fireshell self-accelerates from a Lorentz gamma factor equal to 1 all the way to 200-300. The physics of this system is based on the continuous annihilation of electron-positron pairs in an optically thick  $e^+e^-$  plasma with a small baryon loading. In the following regime, the optically thin fireshell, composed by the baryons left over after the transparency point, ballistically expands into the CircumBurst Medium (CBM). The dynamics of the fireshell during both regimes will be analyzed. In particular we will re-examine the validity of the constant-index power-law relation between the fireshell Lorentz gamma factor and its radial coordinate, usually adopted in the current literature on the grounds of an “ultrarelativistic” approximation. Such expressions are found to be mathematically correct but only approximately valid in a very limited range of the physical and astrophysical parameters and in an asymptotic regime which is reached only for a very short time, if any.

19. M.G. Bernardini, C.L. Bianco, L. Caito, M.G. Dainotti, R. Guida, R. Ruffini; “The “Canonical” GRBs within the fireshell model”; in OBSERVATIONAL EVIDENCE FOR BLACK HOLES IN THE UNIVERSE: Proceedings of the 2<sup>nd</sup> Kolkata Conference, Kolkata (India), February 2008, S.K. Chakrabarti, A.S. Majumdar, Editors; AIP Conference Proceedings, 1053, 267 (2008).

Within the fireshell model we define a “canonical” GRB light curve with two sharply different components: the Proper-GRB (P-GRB), emitted when the optically thick fireshell of electron-positron plasma originating the phenomenon reaches transparency, and the afterglow, emitted due to the collision between

the remaining optically thin fireshell and the CircumBurst Medium (CBM). On the basis of the recent understanding of GRB970228 as the prototype for a new class of GRBs with “an occasional softer extended emission lasting tenths of seconds after an initial spikelike emission” we outline our “canonical” GRB scenario, originating from the gravitational collapse to a black hole, with a special emphasis on the discrimination between short GRBs and the ones appearing as such due to their peculiar astrophysical setting.

20. M.G. Dainotti, M.G. Bernardini, C.L. Bianco, L. Caito, R. Guida, R. Ruffini; “GRB 060218: the density mask and its peculiarity compared to the other sources”; in OBSERVATIONAL EVIDENCE FOR BLACK HOLES IN THE UNIVERSE: Proceedings of the 2<sup>nd</sup> Kolkata Conference, Kolkata (India), February 2008, S.K. Chakrabarti, A.S. Majumdar, Editors; AIP Conference Proceedings, 1053, 283 (2008).

The Swift satellite has given continuous data in the range 0.3150 keV from 0 s to 106 s for GRB060218 associated with SN2006aj. It has an unusually long duration ( $T_{90} \sim 2100$  s). We plan to fit the complete  $\gamma$ - and X-ray light curves of this long duration GRB, including the prompt emission and we give peculiar attention to the afterglow lightcurve in order to better constrain the density mask. We apply our “fireshell” model based on the formation of a black hole, giving the relevant references. The initial total energy of the electron-positron plasma  $E_{e^\pm}^{tot} = 2.32 \times 10^{50}$  erg has a particularly low value similarly to the other GRBs associated with SNe. For the first time we observe a baryon loading  $B = 10^{-2}$  which coincides with the upper limit for the dynamical stability of the fireshell. The effective CircumBurst Medium (CBM) density shows a radial dependence  $n_{cbm} \propto r^{-a}$  with  $1.0 \leq a \leq 1.7$  and monotonically decreases from 1 to  $10^{-6}$  particles/cm<sup>3</sup>. Such a behavior is interpreted as due to a fragmentation in the fireshell. Such a fragmentation is crucial in explaining both the unusually large  $T_{90}$  and the consequently inferred abnormal low value of the CBM effective density. We present the comparison between the density mask of this source and the ones of a normal GRB 050315 and a fake short, GRB 970228, making some assumptions on the CBM behaviour in the surrounding of the Black hole.

21. L. Caito, M.G. Bernardini, C.L. Bianco, M.G. Dainotti, R. Guida, R. Ruffini; “GRB 060614 in the canonical fireshell model”; in OBSERVATIONAL EVIDENCE FOR BLACK HOLES IN THE UNIVERSE: Proceedings of the 2<sup>nd</sup> Kolkata Conference, Kolkata (India), February 2008, S.K. Chakrabarti, A.S. Majumdar, Editors; AIP Conference Proceedings, 1053, 291 (2008).

Gamma-Ray Burst (GRB) 060614 is the first nearby long duration GRB clearly not associated to any bright Ib/c Supernova. The explosion of this burst undermines one of the fundamental assumptions of the standard scenario and opens new horizons and hints of investigation. GRB 060614, hardly classifiable as a short GRB, is not either a “typical” long GRB since it occurs in a low

star forming region. Moreover, it presents deep similarities with GRB 970228, which is the prototype of the “fake” short bursts, or better canonical GRBs disguised as short ones. Within the “fireshell” model, we test if this “anomalous” source can be a disguised short GRB.

22. L.J. Rangel Lemos, S. Casanova, R. Ruffini, S.S. Xue; “Fermis approach to the study of  $pp$  interactions”; in OBSERVATIONAL EVIDENCE FOR BLACK HOLES IN THE UNIVERSE: Proceedings of the 2<sup>nd</sup> Kolkata Conference, Kolkata (India), February 2008, S.K. Chakrabarti, A.S. Majumdar, Editors; AIP Conference Proceedings, 1053, 275 (2008).

The physics of hadronic interactions found much difficulties for explain the experimental data. In this work we study the approach of Fermi (1950) about the multiplicity of pions emitted in  $pp$  interactions and in follow we compare with the modern approach

23. R. Ruffini, A.G. Aksenov, M.G. Bernardini, C.L. Bianco, L. Caito, M.G. Dainotti, G. De Barros, R. Guida, G.V. Vereshchagin, S.-S. Xue; “The canonical Gamma-Ray Bursts and their ‘precursors’”; in 2008 NANJING GAMMA-RAY BURST CONFERENCE, Proceedings of the 2008 Nanjing Gamma-Ray Burst Conference, Nanjing (China), June 2008, Y.-F. Huang, Z.-G. Dai, B. Zhang, Editors; AIP Conference Proceedings, 1065, 219 (2008).

The fireshell model for Gamma-Ray Bursts (GRBs) naturally leads to a canonical GRB composed of a proper-GRB (P-GRB) and an afterglow. P-GRBs, introduced by us in 2001, are sometimes considered “precursors” of the main GRB event in the current literature. We show in this paper how the fireshell model leads to the understanding of the structure of GRBs, with precise estimates of the time sequence and intensities of the P-GRB and the of the afterglow. It leads as well to a natural classification of the canonical GRBs which overcomes the traditional one in short and long GRBs.

24. M.G. Bernardini, C.L. Bianco, L. Caito, M.G. Dainotti, R. Guida, R. Ruffini; “Preliminary analysis of GRB060607A within the fireshell model”; in 2008 NANJING GAMMA-RAY BURST CONFERENCE; Proceedings of the 2008 Nanjing Gamma-Ray Burst Conference, Nanjing (China), June 2008, Y.-F. Huang, Z.-G. Dai, B. Zhang, Editors; AIP Conference Proceedings, 1065, 227 (2008).

GRB060607A is a very distant ( $z = 3.082$ ) and energetic event ( $E_{iso} \sim 10^{53}$  erg). Its main peculiarity is that the peak of the near-infrared afterglow has been observed with the REM robotic telescope, allowing to infer the initial Lorentz gamma factor of the emitting system. We present a preliminary analysis of the spectra and light curves of GRB060607A prompt emission within the fireshell model. We show that the N(E) spectrum of the prompt emission,

whose behavior is usually described as “simple power-law”, can also be fitted in a satisfactory way by a convolution of thermal spectra as predicted by the model we applied. The theoretical time-integrated spectrum of the prompt emission as well as the light curves in the BAT and XRT energy band are in good agreement with the observations, enforcing the plausibility of our approach. Furthermore, the initial value of Lorentz gamma factor we predict is compatible with the one deduced from the REM observations.

25. C.L. Bianco, M.G. Bernardini, L. Caito, M.G. Dainotti, R. Guida, R. Ruffini; “The “fireshell” model and the “canonical GRB” scenario”; in 2008 NANJING GAMMA-RAY BURST CONFERENCE; Proceedings of the 2008 Nanjing Gamma-Ray Burst Conference, Nanjing (China), June 2008, Y.-F. Huang, Z.-G. Dai, B. Zhang, Editors; AIP Conference Proceedings, 1065, 223 (2008).

The Swift observation of GRB 060614, as well as the catalog analysis by Norris and Bonnell (2006), opened the door “on a new Gamma-Ray Bursts (GRBs) classification scheme that straddles both long and short bursts” (Gehrels et al., 2006). Within the “fireshell” model for the Gamma-Ray Bursts (GRBs) we define a “canonical GRB” light curve with two sharply different components: the Proper-GRB (P-GRB), emitted when the optically thick fireshell of electron-positron plasma originating the phenomenon reaches transparency, and the afterglow, emitted due to the collision between the remaining optically thin fireshell and the CircumBurst Medium (CBM). We here outline our “canonical GRB” scenario, which implies three different GRB classes: the “genuine” short GRBs, the “fake” or “disguised” short GRBs and the other (so-called “long”) GRBs. We also outline some implications for the theoretical interpretation of the Amati relation.

26. G. De Barros, M.G. Bernardini, C.L. Bianco, L. Caito, M.G. Dainotti, R. Guida, R. Ruffini; “Is GRB 050509b a genuine short GRB?”; in 2008 NANJING GAMMA-RAY BURST CONFERENCE; Proceedings of the 2008 Nanjing Gamma-Ray Burst Conference, Nanjing (China), June 2008, Y.-F. Huang, Z.-G. Dai, B. Zhang, Editors; AIP Conference Proceedings, 1065, 231 (2008).

Within our “fireshell” model we introduced a “canonical” GRB scenario which differentiates physically the “proper GRB” (P-GRB) emission when photons decouple, and the afterglow emission due to interaction of the accelerated baryons with the CircumBurst Medium (CBM). The ratio between energetics of the two components is ruled by the baryon loading of the fireshell. We here analyse the possibility that GRB050509b is the first case of a “genuine” short GRB the ones with smaller baryon loading. In such a case, the GRB050509b “prompt emission” would be dominated by the “proper GRB” and, moreover, the P-GRB total energy would be greater than the afterglow one. Our fit of the afterglow data and of the P-GRB energetics indicates that this source present

the smallest baryon loading we ever encountered so far, being on the order of  $10^{-4}$ .

27. G. De Barros, A.G. Aksenov, C.L. Bianco, R. Ruffini, G.V. Vereshchagin; “Fireshell versus Fireball scenarios”; in 2008 NANJING GAMMA-RAY BURST CONFERENCE; Proceedings of the 2008 Nanjing Gamma-Ray Burst Conference, Nanjing (China), June 2008, Y.-F. Huang, Z.-G. Dai, B. Zhang, Editors; AIP Conference Proceedings, 1065, 234 (2008).

We revisit Cavallo and Rees classification based on the analysis of initial conditions in electron-positron-photon plasma which appears suddenly around compact astrophysical objects and gives origin to GRBs. These initial conditions were recently studied in [1,2] by numerical integration of relativistic Boltzmann equations with collision integrals, including binary and triple interactions between particles. The main conclusion is that the pair plasma in GRB sources quickly reaches thermal equilibrium well before its expansion starts. In light of this work we comment on each of the four scenarios proposed by Cavallo and Rees and discuss their applicability to describe evolution of GRB sources.

28. M.G. Bernardini, C.L. Bianco, L. Caito, M.G. Dainotti, R. Guida, R. Ruffini; “GRB970228 as a prototype for the class of GRBs with an initial spike-like emission”; in Proceedings of the Eleventh Marcel Grossmann Meeting on General Relativity, Berlin, Germany, July 2006, H. Kleinert, R.T. Jantzen, Editors; World Scientific, (Singapore, 2008).

We interpret GRB970228 prompt emission within our “canonical” GRB scenario, identifying the initial spikelike emission with the Proper-GRB (P-GRB) and the following bumps with the afterglow peak emission. Furthermore, we emphasize the necessity to consider the “canonical” GRB as a whole due to the highly non-linear nature of the model we applied.

29. M.G. Bernardini, C.L. Bianco, L. Caito, M.G. Dainotti, R. Guida, R. Ruffini; “GRB980425 and the puzzling URCA1 emission”; in Proceedings of the Eleventh Marcel Grossmann Meeting on General Relativity, Berlin, Germany, July 2006, H. Kleinert, R.T. Jantzen, Editors; World Scientific, (Singapore, 2008).

We applied our “fireshell” model to GRB980425 observational data, reproducing very satisfactory its prompt emission. We use the results of our analysis to provide a possible interpretation for the X-ray emission of the source S1. The effect on the GRB analysis of the lack of data in the pre-Swift observations is also outlined.

30. C.L. Bianco, M.G. Bernardini, L. Caito, P. Chardonnet, M.G. Dainotti, F. Frascetti, R. Guida, R. Ruffini, S.-S. Xue; “Theoretical interpretation of ‘long’ and ‘short’ GRBs”; in Proceedings of the Eleventh Marcel

Grossmann Meeting on General Relativity, Berlin, Germany, July 2006, H. Kleinert, R.T. Jantzen, Editors; World Scientific, (Singapore, 2008).

Within the “fireshell” model we define a “canonical GRB” light curve with two sharply different components: the Proper-GRB (P-GRB), emitted when the optically thick fireshell of electron-positron plasma originating the phenomenon reaches transparency, and the afterglow, emitted due to the collision between the remaining optically thin fireshell and the CircumBurst Medium (CBM). We here present the consequences of such a scenario on the theoretical interpretation of the nature of “long” and “short” GRBs.

31. C.L. Bianco, M.G. Bernardini, P. Chardonnet, F. Fraschetti, R. Ruffini, S.-S. Xue; “Theoretical interpretation of luminosity and spectral properties of GRB 031203”; in Proceedings of the Eleventh Marcel Grossmann Meeting on General Relativity, Berlin, Germany, July 2006, H. Kleinert, R.T. Jantzen, Editors; World Scientific, (Singapore, 2008).

We show how an emission endowed with an instantaneous thermal spectrum in the co-moving frame of the expanding fireshell can reproduce the time-integrated GRB observed non-thermal spectrum. An explicit example in the case of GRB 031203 is presented.

32. C.L. Bianco, R. Ruffini; “The ‘Fireshell’ model in the Swift era”; in Proceedings of the Eleventh Marcel Grossmann Meeting on General Relativity, Berlin, Germany, July 2006, H. Kleinert, R.T. Jantzen, Editors; World Scientific, (Singapore, 2008).

We here re-examine the validity of the constant-index power-law relation between the fireshell Lorentz gamma factor and its radial coordinate, usually adopted in the current Gamma-Ray Burst (GRB) literature on the grounds of an “ultrarelativistic” approximation. Such expressions are found to be mathematically correct but only approximately valid in a very limited range of the physical and astrophysical parameters and in an asymptotic regime which is reached only for a very short time, if any.

33. L. Caito, M.G. Bernardini, C.L. Bianco, M.G. Dainotti, R. Guida, R. Ruffini; “Theoretical interpretation of GRB011121”; in Proceedings of the Eleventh Marcel Grossmann Meeting on General Relativity, Berlin, Germany, July 2006, H. Kleinert, R.T. Jantzen, Editors; World Scientific, (Singapore, 2008).

GRB 011121, detected by the BeppoSAX satellite, is studied as a prototype to understand the presence of flares observed by Swift in the afterglow of many GRB sources. Detailed theoretical analysis of the GRB 011121 light curves in selected energy bands are presented and compared with observational data. An interpretation of the flare of this source is provided by the introduction of the three-dimensional structure of the CircumBurst Medium(CBM).

34. M.G. Dainotti, M.G. Bernardini, C.L. Bianco, L. Caito, R. Guida, R. Ruffini; "On GRB 060218 and the GRBs related to Supernovae Ib/c"; in Proceedings of the Eleventh Marcel Grossmann Meeting on General Relativity, Berlin, Germany, July 2006, H. Kleinert, R.T. Jantzen, Editors; World Scientific, (Singapore, 2008).

We study the Gamma-Ray Burst (GRB) 060218: a particularly close source at  $z = 0.033$  with an extremely long duration, namely  $T_{90} \sim 2000$  s, related to SN 2006aj. This source appears to be a very soft burst, with a peak in the spectrum at 4.9 keV, therefore interpreted as an X-Ray Flash (XRF) and it obeys to the Amati relation. We fit the X- and  $\gamma$ -ray observations by Swift of GRB 060218 in the 0.1150 keV energy band during the entire time of observations from 0 all the way to 106 s within a unified theoretical model. The details of our theoretical analysis have been recently published in a series of articles. The free parameters of the theory are only three, namely the total energy  $E_{e^\pm}^{tot}$  of the  $e^\pm$  plasma, its baryon loading  $B = M_B c^2 / E_{e^\pm}^{tot}$ , as well as the CircumBurst Medium (CBM) distribution. We fit the entire light curve, including the prompt emission as an essential part of the afterglow. We recall that this value of the  $B$  parameter is the highest among the sources we have analyzed and it is very close to its absolute upper limit expected. We successfully make definite predictions about the spectral distribution in the early part of the light curve, exactly we derive the instantaneous photon number spectrum  $N(E)$  and we show that although the spectrum in the co-moving frame of the expanding pulse is thermal, the shape of the final spectrum in the laboratory frame is clearly non thermal. In fact each single instantaneous spectrum is the result of an integration of thousands of thermal spectra over the corresponding EQuiTemporal Surfaces (EQTS). By our fit we show that there is no basic differences between XRFs and more general GRBs. They all originate from the collapse process to a black hole and their difference is due to the variability of the three basic parameters within the range of full applicability of the theory.

35. R. Guida, M.G. Bernardini, C.L. Bianco, L. Caito, M.G. Dainotti, R. Ruffini; "Theoretical interpretation of GRB060124"; in Proceedings of the Eleventh Marcel Grossmann Meeting on General Relativity, Berlin, Germany, July 2006, H. Kleinert, R.T. Jantzen, Editors; World Scientific, (Singapore, 2008).

We show the preliminary results of the application of our "fireshell" model to GRB060124. This source is very peculiar because it is the first event for which both the prompt and the afterglow emission were observed simultaneously by the three Swift instruments: BAT (15 - 350 keV), XRT (0,2 - 10 keV) and UVOT (170 - 650 nm), due to the presence of a precursor  $\sim 570$  s before the main burst. We analyze GRB060124 within our "canonical" GRB scenario, identifying the precursor with the P-GRB and the prompt emission with the afterglow peak emission. In this way we reproduce correctly the energetics of both these two

components. We reproduce also the observed time delay between the precursor (P-GRB) and the main burst. The effect of such a time delay in our model will be discussed.

36. R. Ruffini, M.G. Bernardini, C.L. Bianco, L. Caito, P. Chardonnet, C. Cherubini, M.G. Dainotti, F. Frascchetti, A. Geralico, R. Guida, B. Pacelli, M. Rotondo, J. Rueda Hernandez, G. Vereshchagin, S.-S. Xue; “Gamma-Ray Bursts”; in *Proceedings of the Eleventh Marcel Grossmann Meeting on General Relativity*, Berlin, Germany, July 2006, H. Kleinert, R.T. Jantzen, Editors; World Scientific, (Singapore, 2008).

We show by example how the uncoding of Gamma-Ray Bursts (GRBs) offers unprecedented possibilities to foster new knowledge in fundamental physics and in astrophysics. After recalling some of the classic work on vacuum polarization in uniform electric fields by Klein, Sauter, Heisenberg, Euler and Schwinger, we summarize some of the efforts to observe these effects in heavy ions and high energy ion collisions. We then turn to the theory of vacuum polarization around a Kerr-Newman black hole, leading to the extraction of the blackholic energy, to the concept of dyadosphere and dyadotorus, and to the creation of an electron-positron-photon plasma. We then present a new theoretical approach encompassing the physics of neutron stars and heavy nuclei. It is shown that configurations of nuclear matter in bulk with global charge neutrality can exist on macroscopic scales and with electric fields close to the critical value near their surfaces. These configurations may represent an initial condition for the process of gravitational collapse, leading to the creation of an electron-positron-photon plasma: the basic self-accelerating system explaining both the energetics and the high energy Lorentz factor observed in GRBs. We then turn to recall the two basic interpretational paradigms of our GRB model: 1) the Relative Space-Time Transformation (RSTT) paradigm and 2) the Interpretation of the Burst Structure (IBS) paradigm. These paradigms lead to a “canonical” GRB light curve formed from two different components: a Proper-GRB (P-GRB) and an extended afterglow comprising a raising part, a peak, and a decaying tail. When the P-GRB is energetically predominant we have a “genuine” short GRB, while when the afterglow is energetically predominant we have a so-called long GRB or a “fake” short GRB. We compare and contrast the description of the relativistic expansion of the electron-positron plasma within our approach and within the other ones in the current literature. We then turn to the special role of the baryon loading in discriminating between “genuine” short and long or “fake” short GRBs and to the special role of GRB 991216 to illustrate for the first time the “canonical” GRB bolometric light curve. We then propose a spectral analysis of GRBs, and proceed to some applications: GRB 031203, the first spectral analysis, GRB 050315, the first complete light curve fitting, GRB 060218, the first evidence for a critical value of the baryon loading, GRB 970228, the appearance of “fake” short GRBs. We finally turn to the GRB-Supernova Time Sequence (GSTS) paradigm: the

concept of induced gravitational collapse. We illustrate this paradigm by the systems GRB 980425 / SN 1998bw, GRB 030329 / SN 2003dh, GRB 031203 / SN 2003lw, GRB 060218 / SN 2006aj, and we present the enigma of the URCA sources. We then present some general conclusions.

37. R. Ruffini, A.G. Aksenov, M.G. Bernardini, C.L. Bianco, L. Caito, M.G. Dainotti, G. De Barros, R. Guida, G. Vereshchagin, S.-S. Xue; "The canonical Gamma-Ray Bursts: long, 'fake'-'disguised' and 'genuine' short bursts; in PROBING STELLAR POPULATIONS OUT TO THE DISTANT UNIVERSE: CEFALU 2008, Proceedings of the International Conference; Cefal (Italy), September 2008, G. Giobbi, A. Tornambe, G. Raimondo, M. Limongi, L. A. Antonelli, N. Menci, E. Brocato, Editors; AIP Conference Proceedings, 1111, 325 (2009).

The Gamma-Ray Bursts (GRBs) offer the unprecedented opportunity to observe for the first time the blackholic energy extracted by the vacuum polarization during the process of gravitational collapse to a black hole leading to the formation of an electron-positron plasma. The uniqueness of the Kerr-Newman black hole implies that very different processes originating from the gravitational collapse a) of a single star in a binary system induced by the companion, or b) of two neutron stars, or c) of a neutron star and a white dwarf, do lead to the same structure for the observed GRB. The recent progress of the numerical integration of the relativistic Boltzmann equations with collision integrals including 2-body and 3-body interactions between the particles offer a powerful conceptual tool in order to differentiate the traditional "fireball" picture, an expanding hot cavity considered by Cavallo and Rees, as opposed to the "fireshell" model, composed of an internally cold shell of relativistically expanding electron-positron-baryon plasma. The analysis of the fireshell naturally leads to a canonical GRB composed of a proper-GRB and an extended afterglow. By recalling the three interpretational paradigms for GRBs we show how the fireshell model leads to an understanding of the GRB structure and to an alternative classification of short and long GRBs.

38. M.G. Bernardini, M.G. Dainotti, C.L. Bianco, L. Caito, R. Guida, R. Ruffini; "Prompt emission and X-ray flares: the case of GRB 060607 A"; in PROBING STELLAR POPULATIONS OUT TO THE DISTANT UNIVERSE: CEFALU 2008, Proceedings of the International Conference; Cefal (Italy), September 2008, G. Giobbi, A. Tornambe, G. Raimondo, M. Limongi, L. A. Antonelli, N. Menci, E. Brocato, Editors; AIP Conference Proceedings, 1111, 383 (2009).

GRB 060607A is a very distant and energetic event. Its main peculiarity is that the peak of the near-infrared (NIR) afterglow has been observed with the REM robotic telescope, allowing to estimate the initial Lorentz gamma factor within the fireball forward shock model. We analyze GRB 060607A within the

fireshell model. The initial Lorentz gamma factor of the fireshell can be obtained adopting the exact solutions of its equations of motion, dealing only with the BAT and XRT observations, that are the basic contribution to the afterglow emission, up to a distance from the progenitor  $r \sim 10^{18}$  cm. According to the “canonical GRB” scenario we interpret the whole prompt emission as the peak of the afterglow emission, and we show that the observed temporal variability of the prompt emission can be produced by the interaction of the fireshell with overdense CircumBurst Medium (CBM) clumps. This is indeed the case also of the X-ray flares which are present in the early phases of the afterglow light curve.

39. C.L. Bianco, M.G. Bernardini, L. Caito, M.G. Dainotti, R. Guida, R. Ruffini; “The ‘fireshell’ model and the ‘canonical GRB’ scenario. Implications for the Amati relation”; in PROBING STELLAR POPULATIONS OUT TO THE DISTANT UNIVERSE: CEFALU 2008, Proceedings of the International Conference; Cefal (Italy), September 2008, G. Giobbi, A. Torname, G. Raimondo, M. Limongi, L. A. Antonelli, N. Menci, E. Brocato, Editors; AIP Conference Proceedings, 1111, 587 (2009).

Within the “fireshell” model for GRBs we define a “canonical GRB” light curve with two sharply different components: the Proper-GRB (P-GRB), emitted when the optically thick fireshell reaches transparency, and the extended afterglow, emitted due to the collision between the remaining optically thin fireshell and the CircumBurst Medium (CBM). We here outline our “canonical GRB” scenario, which implies three different GRB classes: the “genuine” short GRBs, the “fake” or “disguised” short GRBs and the other (so-called “long”) GRBs. We will also outline the corresponding implications for the Amati relation, which are opening its use for cosmology.

40. R. Ruffini, A.G. Aksenov, M.G. Bernardini, C.L. Bianco, L. Caito, P. Chardonnet, M.G. Dainotti, G. De Barros, R. Guida, L. Izzo, B. Patricelli, L.J. Rangel Lemos, M. Rotondo, J.A. Rueda Hernandez, G. Vereshchagin, S.-S. Xue; “The Blackholic energy and the canonical Gamma-Ray Burst IV: the ‘long’, ‘genuine short’ and ‘fake disguised short’ GRBs”; in Proceedings of the XIIIth Brazilian School on Cosmology and Gravitation, Mangaratiba, Rio de Janeiro (Brazil), July-August 2008, M. Novello, S.E. Perez Bergliaffa, Editors; AIP Conference Proceedings, 1132, 199 (2009).

We report some recent developments in the understanding of GRBs based on the theoretical framework of the “fireshell” model, already presented in the last three editions of the “Brazilian School of Cosmology and Gravitation”. After recalling the basic features of the “fireshell model”, we emphasize the following novel results: 1) the interpretation of the X-ray flares in GRB afterglows as due to the interaction of the optically thin fireshell with isolated clouds in the CircumBurst Medium (CBM); 2) an interpretation as “fake - disguised”

short GRBs of the GRBs belonging to the class identified by Norris & Bonnell; we present two prototypes, GRB 970228 and GRB 060614; both these cases are consistent with an origin from the final coalescence of a binary system in the halo of their host galaxies with particularly low CBM density  $n_{cbm} \sim 10^{-3}$  particles/cm<sup>3</sup>; 3) the first attempt to study a genuine short GRB with the analysis of GRB 050509B, that reveals indeed still an open question; 4) the interpretation of the GRB-SN association in the case of GRB 060218 via the “induced gravitational collapse” process; 5) a first attempt to understand the nature of the “Amati relation”, a phenomenological correlation between the isotropic-equivalent radiated energy of the prompt emission  $E_{iso}$  with the cosmological rest-frame  $\nu F_\nu$  spectrum peak energy  $E_{p,i}$ . In addition, recent progress on the thermalization of the electron-positron plasma close to their formation phase, as well as the structure of the electrodynamics of Kerr-Newman Black Holes are presented. An outlook for possible explanation of high-energy phenomena in GRBs to be expected from the AGILE and the Fermi satellites are discussed. As an example of high energy process, the work by Enrico Fermi dealing with ultrarelativistic collisions is examined. It is clear that all the GRB physics points to the existence of overcritical electro-dynamical fields. In this sense we present some progresses on a unified approach to heavy nuclei and neutron stars cores, which leads to the existence of overcritical fields under the neutron star crust.

41. A.G. Aksenov, M.G. Bernardini, C.L. Bianco, L. Caito, C. Cherubini, G. De Barros, A. Geralico, L. Izzo, F.A. Massucci, B. Patricelli, M. Rotonondo, J.A. Rueda Hernandez, R. Ruffini, G. Vereshchagin, S.-S. Xue; “The fireshell model for Gamma-Ray Bursts”; in *The Shocking Universe, Proceedings of the conference held in Venice (Italy), September 2009*, G. Chincarini, P. D’Avanzo, R. Margutti, R. Salvaterra, Editors; SIF Conference Proceedings, 102, 451 (2010).

The fireshell model for GRBs is briefly outlined, and the currently ongoing developments are summarized.

42. M.G. Bernardini, C.L. Bianco, L. Caito, L. Izzo, B. Patricelli, R. Ruffini; “The end of the prompt emission within the fireshell model”; in *The Shocking Universe, Proceedings of the conference held in Venice (Italy), September 2009*, G. Chincarini, P. D’Avanzo, R. Margutti, R. Salvaterra, Editors; SIF Conference Proceedings, 102, 489 (2010)

The shallow decay emission, revealed by the Swift satellite in the X-ray afterglow of a good sample of bursts, is a puzzle. Within the fireshell model it has been recently proposed an alternative explanation: if we assume that after the prompt phase the system has a range of Lorentz factors, the plateau phase is simply the product of the injection of slower material into the fireshell. This injection produces a modification both in the dynamics of the fireshell and in the spectrum of the emitted radiation. We postulate that this spread in the

fireshell Lorentz factor occurs when the fireshell becomes transparent and do not depend on a prolonged activity of the central engine. The aim of this paper is to characterize dynamically the system in order to understand the nature of that material.

43. L. Izzo, M.G. Bernardini, C.L. Bianco, L. Caito, B. Patricelli, R. Ruffini; “GRB 090423 in the fireshell scenario”; in *The Shocking Universe*, Proceedings of the conference held in Venice (Italy), September 2009, G. Chincarini, P. D’Avanzo, R. Margutti, R. Salvaterra, Editors; SIF Conference Proceedings, 102, 537 (2010).

44. B. Patricelli, M.G. Bernardini, C.L. Bianco, L. Caito, L. Izzo, R. Ruffini, G. Vereshchagin; “A new spectral energy distribution of photons in the fireshell model of GRBs”; in *The Shocking Universe*, Proceedings of the conference held in Venice (Italy), September 2009, G. Chincarini, P. D’Avanzo, R. Margutti, R. Salvaterra, Editors; SIF Conference Proceedings, 102, 559 (2010).

The fireshell model of Gamma Ray Bursts (GRBs) postulates that the emission process is thermal in the comoving frame of the fireshell, but this is just a first approximation. We investigate a different spectrum of photons in the comoving frame in order to better reproduce the observed spectral properties of GRB prompt emission. We introduce a modified thermal spectrum whose low energy slope depends on an index  $\alpha$ , left as a free parameter. We test it by comparing the numerical simulations with observed BAT spectra integrated over different intervals of time. We find that the observational data can be correctly reproduced by assuming  $\alpha = -1.8$ .

45. C.L. Bianco, M.G. Bernardini, L. Caito, G. De Barros, L. Izzo, B. Patricelli, R. Ruffini; “Disguised Short Bursts and the Amati Relation”; in *Deciphering the ancient universe with Gamma-Ray Bursts*, Proceedings of the conference held in Kyoto (Japan), April 2010, N. Kawai, S. Nagataki, Editors; AIP Conference Proceedings, 1279, 299 (2010).

The class of “Disguised short” GRBs implied by the fireshell scenario is presented, with special emphasis on the implications for the Amati relation.

46. L. Izzo, M.G. Bernardini, C.L. Bianco, L. Caito, B. Patricelli, L.J. Rangel Lemos, R. Ruffini; “On GRB 080916C and GRB 090902B observed by the Fermi satellite”; in *Deciphering the ancient universe with Gamma-Ray Bursts*, Proceedings of the conference held in Kyoto (Japan), April 2010, N. Kawai, S. Nagataki, Editors; AIP Conference Proceedings, 1279, 343 (2010).

We propose a possible explanation, in the context of the Fireshell scenario, for the high-energy emission observed in GRB 080916C and GRB 090902B. The physical process underlying this emission consists mainly in the interaction

of the baryon in the Fireshell with some high-density region around the burst site. Moreover we associate the observed delay of the onset of the high-energy emission as due to the P-GRB emission.

47. B. Patricelli, M.G. Bernardini, C.L. Bianco, L. Caito, G. De Barros, L. Izzo, R. Ruffini; "Black Holes in Gamma Ray Bursts"; in Deciphering the ancient universe with Gamma-Ray Bursts, Proceedings of the conference held in Kyoto (Japan), April 2010, N. Kawai, S. Nagataki, Editors; AIP Conference Proceedings, 1279, 406 (2010).

Within the fireshell model, Gamma Ray Bursts (GRBs) originate from an optically thick  $e^\pm$  plasma created by vacuum polarization process during the formation of a Black Hole (BH). Here we briefly recall the basic features of this model, then we show how it is possible to interpret GRB observational properties within it. In particular we present, as a specific example, the analysis of GRB 050904 observations of the prompt emission light curve and spectrum in the Swift BAT energy band (15-150 keV).

48. M.G. Bernardini, C.L. Bianco, L. Caito, M.G. Dainotti, R. Guida, R. Ruffini; "The GRB classification within the "fireshell" model: short, long and "fake" short GRBs"; in Proceedings of the 3rd Stueckelberg Workshop on Relativistic Field Theories, Pescara, Italy, July 2008, N. Carlevaro, R. Ruffini, G.V. Vereshchagin, Editors; Cambridge Scientific Publishers, (UK, 2011).
49. C.L. Bianco, M.G. Bernardini, L. Caito, M.G. Dainotti, R. Guida, R. Ruffini, G.V. Vereshchagin, S.-S. Xue; "Equations of motion of the "fireshell""; in Proceedings of the 3rd Stueckelberg Workshop on Relativistic Field Theories, Pescara, Italy, July 2008, N. Carlevaro, R. Ruffini, G.V. Vereshchagin, Editors; Cambridge Scientific Publishers, (UK, 2011).
50. L. Caito, M.G. Bernardini, C.L. Bianco, M.G. Dainotti, R. Guida, R. Ruffini; "GRB 060614: another example of "fake" short burst from a merging binary system"; in Proceedings of the 3rd Stueckelberg Workshop on Relativistic Field Theories, Pescara, Italy, July 2008, N. Carlevaro, R. Ruffini, G.V. Vereshchagin, Editors; Cambridge Scientific Publishers, (UK, 2011).
51. G. De Barros, M.G. Bernardini, C.L. Bianco, L. Caito, R. Guida, R. Ruffini; "Analysis of GRB 050509b"; in Proceedings of the 3rd Stueckelberg Workshop on Relativistic Field Theories, Pescara, Italy, July 2008, N. Carlevaro, R. Ruffini, G.V. Vereshchagin, Editors; Cambridge Scientific Publishers, (UK, 2011).



## 6. Brief reminder of the fireshell model

The black hole uniqueness theorem (see Left panel in Fig. 3.4 and e.g. Ref. Ruffini and Wheeler, 1971) is at the very ground of the fact that it is possible to explain the different Gamma-Ray Burst (GRB) features with a single theoretical model, over a range of energies spanning over 6 orders of magnitude. The fundamental point is that, independently of the fact that the progenitor of the gravitational collapse is represented by merging binaries composed by neutron stars and white dwarfs in all possible combinations, or by a single process of gravitational collapse, or by the process of “induced” gravitational collapse, the formed black hole is totally independent from the initial conditions and reaches the standard configuration of a Kerr-Newman black hole (see Right panel in Fig. 3.4). It is well known that pair creation by vacuum polarization process can occur in a Kerr-Newman black hole (Damour and Ruffini, 1975; Ruffini et al., in press-).

We consequently assume, within the fireshell model, that all GRBs originate from an optically thick  $e^\pm$  plasma with total energy  $E_{tot}^{e^\pm}$  in the range  $10^{49}$ – $10^{54}$  ergs and a temperature  $T$  in the range 1–4 MeV (Preparata et al., 1998). Such an  $e^\pm$  plasma has been widely adopted in the current literature (see e.g. Refs. Piran, 2005; Meszaros, 2006, and references therein). After an early expansion, the  $e^\pm$ -photon plasma reaches thermal equilibrium with the engulfed baryonic matter  $M_B$  described by the dimensionless parameter  $B = M_B c^2 / E_{tot}^{e^\pm}$ , that must be  $B < 10^{-2}$  (Ruffini et al., 1999, 2000). As the optically thick fireshell composed by  $e^\pm$ -photon-baryon plasma self-accelerate to ultrarelativistic velocities, it finally reaches the transparency condition. A flash of radiation is then emitted. This is the P-GRB (Ruffini et al., 2001b). Different current theoretical treatments of these early expansion phases of GRBs are compared and contrasted in Bianco et al. (2006b) and Ruffini et al. (2008a). The amount of energy radiated in the P-GRB is only a fraction of the initial energy  $E_{tot}^{e^\pm}$ . The remaining energy is stored in the kinetic energy of the optically thin baryonic and leptonic matter fireshell that, by inelastic collisions with the CBM, gives rise to a multi-wavelength emission. This is the extended afterglow. It presents three different regimes: a rising part, a peak and a decaying tail. We therefore define a “canonical GRB” light curve with two sharply different components (see Fig. 6.1) (Ruffini et al., 2001b, 2007a; Bernardini et al., 2007; Bianco et al., 2008a,b): 1) the P-GRB and 2) the extended afterglow.

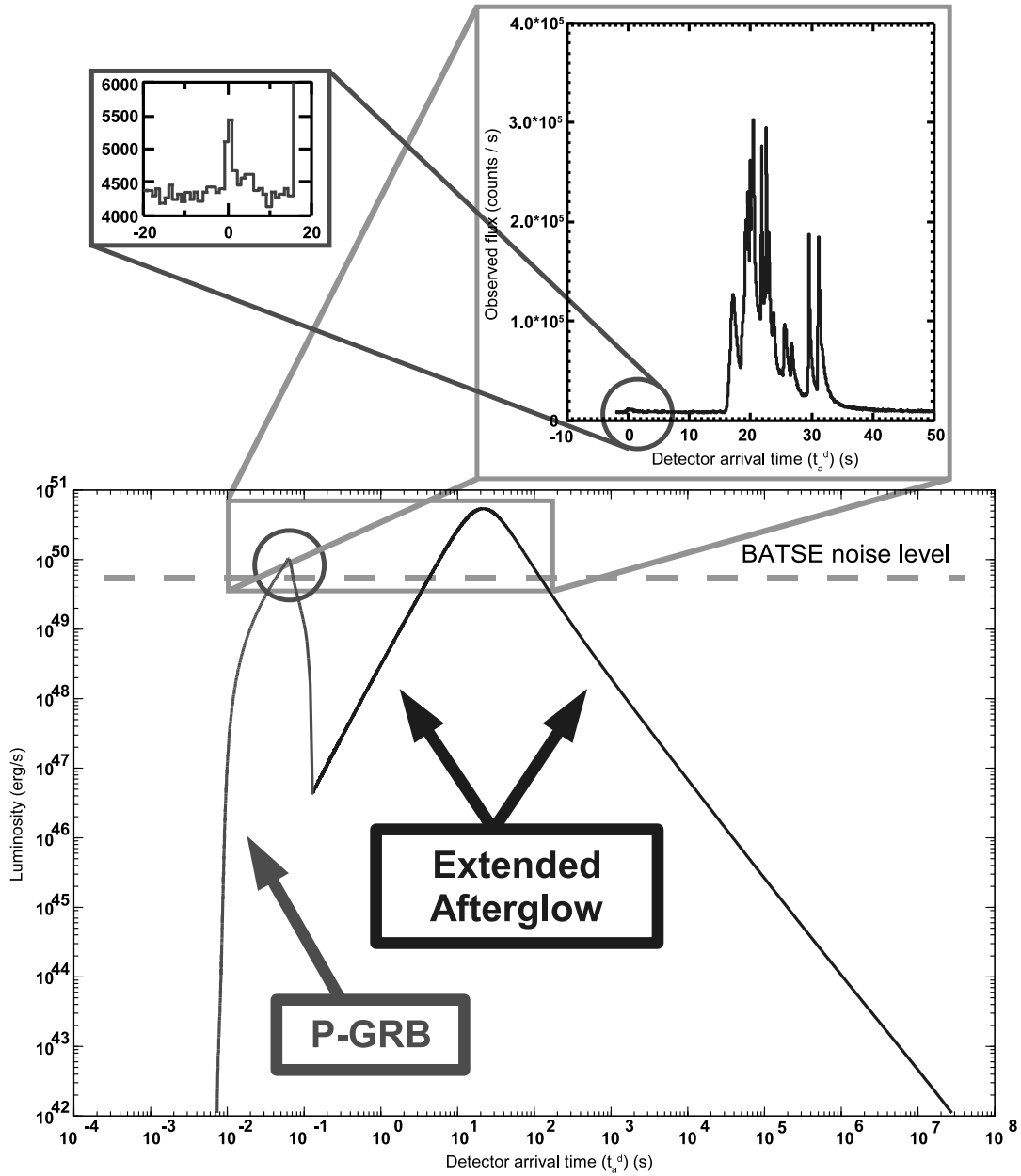


**Figure 6.1.:** The “canonical GRB” light curve theoretically computed for GRB 991216. The prompt emission observed by BATSE is identified with the peak of the extended afterglow, while the small precursor is identified with the P-GRB. For this source we have  $E_{e^{\pm}}^{tot} = 4.83 \times 10^{53}$  ergs,  $B \simeq 3.0 \times 10^{-3}$  and  $\langle n_{cbm} \rangle \sim 1.0$  particles/cm<sup>3</sup>. Details in Ruffini et al. (2001b, 2002, 2007a).

What is usually called “Prompt emission” in the current literature mixes the P-GRB with the raising part and the peak of the extended afterglow. Such an unjustified mixing of these components, originating from different physical processes, leads to difficulties in the current models of GRBs, and can as well be responsible for some of the intrinsic scatter observed in the Amati relation (Amati, 2006; Guida et al., 2008b, , see also below, section *Theoretical background for GRBs’ empirical correlations*).

## 6.1. The optically thick phase

In Fig. 6.2 we present the evolution of the optically thick fireshell Lorentz  $\gamma$  factor as a function of the external radius for 7 different values of the fireshell baryon loading  $B$  and two selected limiting values of the total energy  $E_{e^\pm}^{tot}$  of the  $e^\pm$  plasma. We can identify three different eras:

1. **Era I:** The fireshell is made only of electrons, positrons and photons in thermodynamical equilibrium (the “pair-electromagnetic pulse”, or PEM pulse for short). It self-accelerate and begins its expansion into vacuum, because the environment has been cleared by the black hole collapse. The Lorentz  $\gamma$  factor increases with radius and the dynamics can be described by the energy conservation and the condition of adiabatic expansion (Ruffini et al., 1999; Bianco et al., 2006b):

$$T^{0\nu}_{,\nu} = 0 \quad (6.1.1)$$

$$\frac{\epsilon_\circ}{\epsilon} = \left(\frac{V}{V_\circ}\right)^\Gamma = \left(\frac{\mathcal{V}\gamma}{\mathcal{V}_\circ\gamma_\circ}\right)^\Gamma \quad (6.1.2)$$

where  $T^{\mu\nu}$  is the energy-momentum tensor of the  $e^+e^-$  plasma (assumed to be a perfect fluid),  $\epsilon$  is its internal energy density,  $V$  and  $\mathcal{V}$  are its volumes in the co-moving and laboratory frames respectively,  $\Gamma$  is the thermal index and the quantities with and without the  $\circ$  subscript are measured at two different times during the expansion.

2. **Era II:** The fireshell impacts with the non-collapsed bayonic remnants and engulfs them. The Lorentz  $\gamma$  factor drops. The dynamics of this era can be described by imposing energy and momentum conservation during the fully inelastic collision between the fireshell and the baryonic remnant. For the fireshell solution to be still valid, it must be  $B \lesssim 10^{-2}$  (Ruffini et al., 2000).
3. **Era III:** The fireshell is now made of electrons, positrons, baryons and photons in thermodynamical equilibrium (the “pair-electromagnetic-

baryonic pulse”, or PEMB pulse for short). It self-accelerate again and the Lorentz  $\gamma$  factor increases again with radius up to when the transparency condition is reached, going to an asymptotic value  $\gamma_{asym} = 1/B$ . If  $B \sim 10^{-2}$  the transparency condition is reached when  $\gamma \sim \gamma_{asym}$ . On the other hand, when  $B < 10^{-2}$ , the transparency condition is reached much before  $\gamma$  reaches its asymptotic value (Ruffini et al., 2000, 2001b, , see next section for details). In this era the dynamical equations are the same of the first one, together with the baryon number conservation:

$$T^{0\nu}_{,\nu} = 0 \quad (6.1.3)$$

$$\frac{\epsilon_o}{\epsilon} = \left(\frac{V}{V_o}\right)^\Gamma = \left(\frac{\mathcal{V}\gamma}{\mathcal{V}_o\gamma_o}\right)^\Gamma \quad (6.1.4)$$

$$\frac{n_B^o}{n_B} = \frac{V}{V_o} = \frac{\mathcal{V}\gamma}{\mathcal{V}_o\gamma_o} \quad (6.1.5)$$

where  $n_B$  is the baryon number density in the fireshell. In this era it starts to be crucial the contribution of the rate equation to describe the annihilation of the  $e^+e^-$  pairs:

$$\frac{\partial}{\partial t} N_{e^\pm} = -N_{e^\pm} \frac{1}{\mathcal{V}} \frac{\partial \mathcal{V}}{\partial t} + \overline{\sigma v} \frac{1}{\gamma^2} \left( N_{e^\pm}^2(T) - N_{e^\pm}^2 \right) \quad (6.1.6)$$

where  $N_{e^\pm}$  is the number of  $e^+e^-$  pairs and  $N_{e^\pm}(T)$  is the number of  $e^+e^-$  pairs at thermal equilibrium at temperature  $T$  (Ruffini et al., 2000; Bianco et al., 2006b).

In the “fireball” model in the current literature the baryons are usually considered present in the plasma since the beginning. In other words, in the fireball dynamics there is only one era corresponding to the Era III above (Meszaros et al., 1993; Shemi and Piran, 1990; Piran et al., 1993; Bianco et al., 2006b). Moreover, the rate equation is usually neglected, and this affects the reaching of the transparency condition. A detailed comparison between the different approaches is reported in Bianco et al. (2006b).

## 6.2. The transparency point

At the transparency point, the value of the  $B$  parameter rules the ratio between the energetics of the P-GRB and the kinetic energy of the baryonic and leptonic matter giving rise to the extended afterglow. It rules as well the time separation between the corresponding peaks (Ruffini et al., 2001b, 2008a).

We have recently shown (Aksenov et al., 2009) that a thermal spectrum still occurs in presence of  $e^\pm$  pairs and baryons. By solving the rate equation we

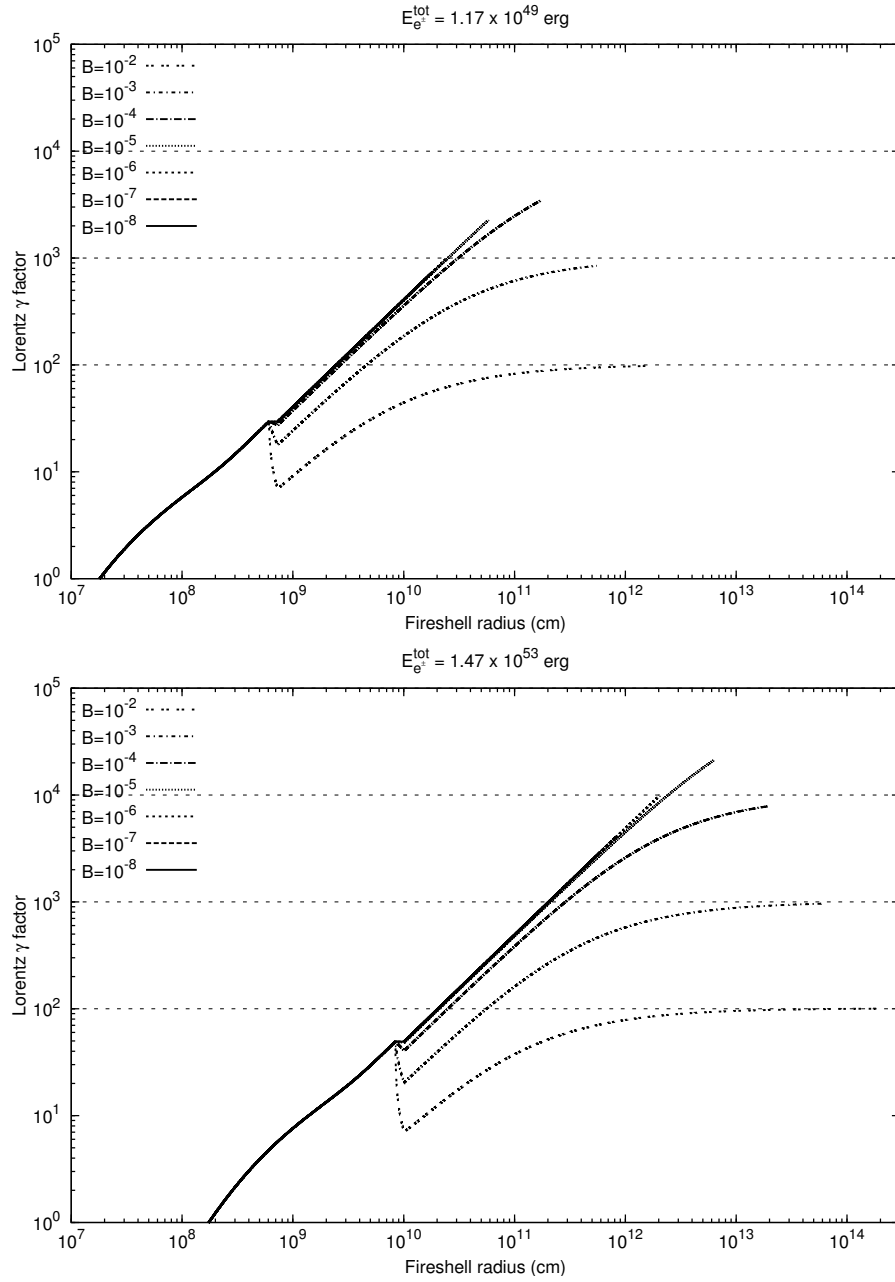


**Figure 6.2.:** The Lorentz  $\gamma$  factor of the expanding fireshell is plotted as a function of its external radius for 7 different values of the fireshell baryon loading  $B$ , ranging from  $B = 10^{-8}$  and  $B = 10^{-2}$ , and two selected limiting values of the total energy  $E_{e^\pm}^{\text{tot}}$  of the  $e^\pm$  plasma:  $E_{e^\pm}^{\text{tot}} = 1.17 \times 10^{49}$  ergs (upper panel) and  $E_{e^\pm}^{\text{tot}} = 1.47 \times 10^{53}$  ergs (lower panel). The asymptotic values  $\gamma \rightarrow 1/B$  are also plotted (dashed horizontal lines). The lines are plotted up to when the fireshell transparency is reached.

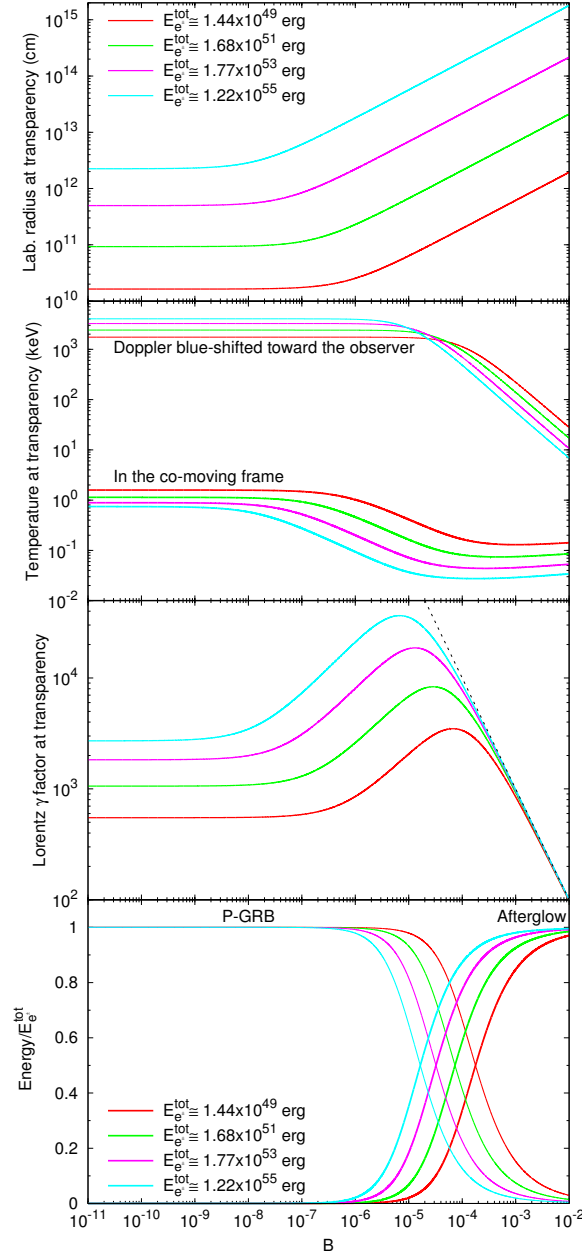


**Figure 6.3.:** At the fireshell transparency point, for 4 different values of  $E_{e^\pm}^{tot}$ , we plot as a function of  $B$ , from top panel to bottom one: The fireshell radius in the laboratory frame; the fireshell temperature in the co-moving frame  $T_{\circ}^{com}$  (thicker lines) and the one Doppler blue-shifted along the line of sight toward the observer in the source cosmological rest frame  $T_{\circ}^{obs}$  (thinner lines); The fireshell Lorentz gamma factor  $\gamma_{\circ}$  together with the asymptotic value  $\gamma_{\circ} = 1/B$ ; The energy radiated in the P-GRB (thinner lines, rising when  $B$  decreases) and the one converted into baryonic kinetic energy and later emitted in the extended afterglow (thicker lines, rising when  $B$  increases), in units of  $E_{e^\pm}^{tot}$ .

have evaluated the evolution of the temperature during the fireshell expansion, all the way up to when the transparency condition is reached (Ruffini et al., 1999, 2000). In the first panel of Fig. 6.3 we plot, as a function of  $B$ , the fireshell radius at the transparency point. The plot is drawn for four different values of  $E_{e^\pm}^{tot}$  in the interval  $[10^{49}, 10^{55}]$  ergs, well encompassing GRBs' observed isotropic energies.

In the second panel of Fig. 6.3 we plot, as a function of  $B$ , the fireshell temperature  $T_\circ$  at the transparency point, i.e. the temperature of the P-GRB radiation. The plot is drawn for the same four different values of  $E_{e^\pm}^{tot}$  of the upper panel. We plot both the value in the co-moving frame  $T_\circ^{com}$  and the one Doppler blue-shifted toward the observed  $T_\circ^{obs} = (1 + \beta_\circ)\gamma_\circ T_\circ^{com}$ , where  $\beta_\circ$  is the fireshell speed at the transparency point in units of  $c$  (Ruffini et al., 2000).

In the middle panel of Fig. 6.3 we plot, as a function of  $B$ , the fireshell Lorentz gamma factor at the transparency point  $\gamma_\circ$ . The plot is drawn for the same four different values of  $E_{e^\pm}^{tot}$  of the upper panel. Also plotted is the asymptotic value  $\gamma_\circ = 1/B$ , which corresponds to the condition when the entire initial internal energy of the plasma  $E_{e^\pm}^{tot}$  has been converted into kinetic energy of the baryons (Ruffini et al., 2000). We see that such an asymptotic value is approached for  $B \rightarrow 10^{-2}$ . We see also that, if  $E_{e^\pm}^{tot}$  increases, the maximum values of  $\gamma_\circ$  are higher and they are reached for lower values of  $B$ .

In the lower panel of Fig. 6.3 we plot, as a function of  $B$ , the total energy radiated at the transparency point in the P-GRB and the one converted into baryonic and leptonic kinetic energy and later emitted in the extended afterglow. The plot is drawn for the same four different values of  $E_{e^\pm}^{tot}$  of the upper panel and middle panels. We see that for  $B \lesssim 10^{-5}$  the total energy emitted in the P-GRB is always larger than the one emitted in the extended afterglow. In the limit  $B \rightarrow 0$  it gives rise to a "genuine" short GRB (see also Fig. 6.4). On the other hand, for  $3.0 \times 10^{-4} \lesssim B < 10^{-2}$  the total energy emitted in the P-GRB is always smaller than the one emitted in the extended afterglow. If it is not below the instrumental threshold and if  $n_{cbm} \sim 1$  particle/cm<sup>3</sup>, the P-GRB can be observed in this case as a small pulse preceding the main GRB event (which coincides with the peak of the extended afterglow), i.e. as a GRB "precursor" (Ruffini et al., 2001b, 2003; Bianco et al., 2008b; Ruffini et al., 2008a; Bernardini et al., 2007; Bianco et al., 2008c).

Particularly relevant for the new era of the *Agile* and *GLAST* satellites is that for  $B < 10^{-3}$  the P-GRB emission has an observed temperature up to  $10^3$  keV or higher. This high-energy emission has been unobservable by the *Swift* satellite.

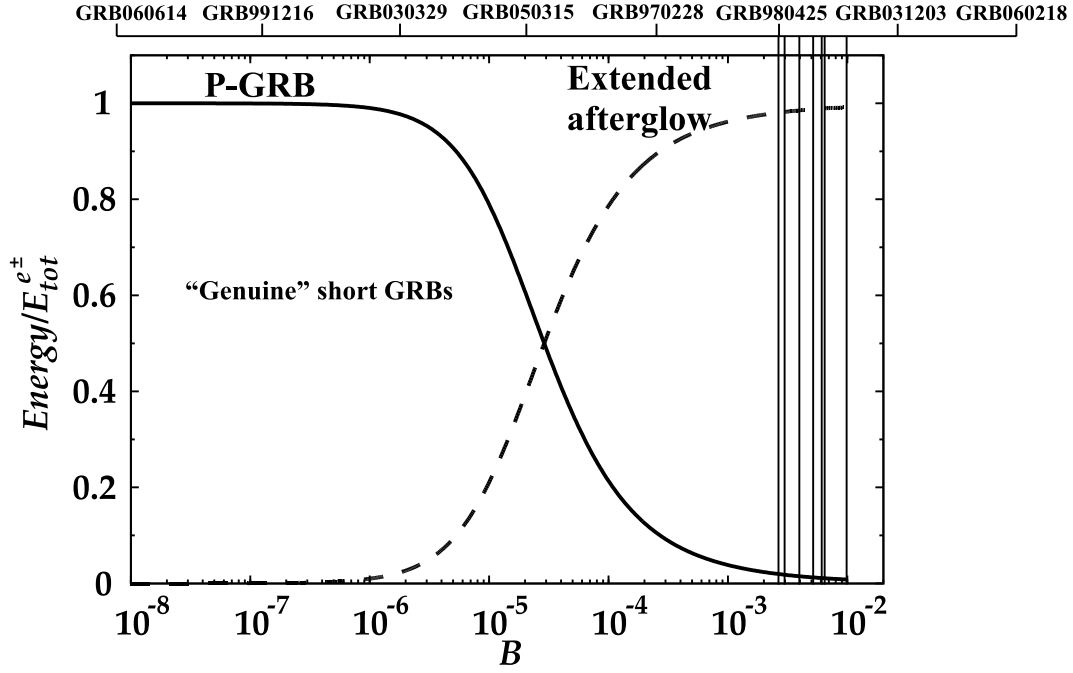


**Figure 6.4.:** Here the energies emitted in the P-GRB (solid line) and in the extended afterglow (dashed line), in units of the total energy of the plasma, are plotted as functions of the  $B$  parameter for a typical value of  $E_{e^\pm}^{\text{tot}} \sim 10^{53}$  erg (see lower panel of Fig. 6.3). When  $B \lesssim 10^{-5}$ , the P-GRB becomes predominant over the extended afterglow, giving rise to a “genuine” short GRB. In the figure are also marked the values of the  $B$  parameters corresponding to some GRBs we analyzed, all belonging to the class of long GRBs.

### 6.3. The optically thin phase

The dynamics of the optically thin fireshell of baryonic matter propagating in the CBM can be obtained from the relativistic conservation laws of energy and momentum (see e.g. Ref. Bianco and Ruffini, 2005b):

$$\left\{ \begin{array}{l} dE_{\text{int}} = (\gamma - 1) dM_{\text{cbm}} c^2 \\ d\gamma = -\frac{\gamma^2 - 1}{M} dM_{\text{cbm}} \\ dM = \frac{1 - \varepsilon}{c^2} dE_{\text{int}} + dM_{\text{cbm}} \\ dM_{\text{cbm}} = 4\pi m_p n_{\text{cbm}} r^2 dr \end{array} \right. \quad (6.3.1)$$

where  $\gamma$ ,  $E_{\text{int}}$  and  $M$  are the pulse Lorentz gamma factor, internal energy and mass-energy respectively,  $n_{\text{cbm}}$  is the CBM number density,  $m_p$  is the proton mass,  $\varepsilon$  is the emitted fraction of the energy developed in the collision with the CBM and  $M_{\text{cbm}}$  is the amount of CBM mass swept up within the radius  $r$ :  $M_{\text{cbm}} = m_p n_{\text{cbm}} (4\pi/3)(r^3 - r_o^3)$ , where  $r_o$  is the starting radius of the shock front.

In both our approach and in the other ones in the current literature (see e.g. Refs. Piran, 1999; Chiang and Dermer, 1999; Bianco and Ruffini, 2005b,a; Ruffini et al., 2007a) such conservations laws are used. The main difference is that in the current literature an ultra-relativistic approximation, following the Blandford and McKee (1976) self-similar solution, is widely adopted, leading to a simple constant-index power-law relations between the Lorentz  $\gamma$  factor of the optically thin “fireshell” and its radius:

$$\gamma \propto r^{-a}, \quad (6.3.2)$$

with  $a = 3$  in the fully radiative case and  $a = 3/2$  in the adiabatic case (Piran, 1999; Bianco and Ruffini, 2005a). On the contrary, we use the exact solutions of the equations of motion of the fireshell (Bianco and Ruffini, 2004, 2005b,a, 2006; Ruffini et al., 2007a). In the adiabatic regime ( $\varepsilon = 0$ ) we get:

$$\gamma^2 = \frac{\gamma_o^2 + 2\gamma_o (M_{\text{cbm}}/M_B) + (M_{\text{cbm}}/M_B)^2}{1 + 2\gamma_o (M_{\text{cbm}}/M_B) + (M_{\text{cbm}}/M_B)^2}, \quad (6.3.3)$$

where  $\gamma_o$  and  $M_B$  are respectively the values of the Lorentz gamma factor and of the mass of the accelerated baryons at the beginning of the afterglow phase. In the fully radiative regime ( $\varepsilon = 1$ ), instead, we have:

$$\gamma = \frac{1 + (M_{\text{cbm}}/M_B) (1 + \gamma_o^{-1}) [1 + (1/2) (M_{\text{cbm}}/M_B)]}{\gamma_o^{-1} + (M_{\text{cbm}}/M_B) (1 + \gamma_o^{-1}) [1 + (1/2) (M_{\text{cbm}}/M_B)]}. \quad (6.3.4)$$

A detailed comparison between the equations used in the two approaches has been presented by Bianco and Ruffini (2004, 2005b,a, 2006). In particular, Bianco and Ruffini (2005a) show that the regime represented in Eq.(6.3.2) is reached only asymptotically when  $\gamma_0 \gg \gamma \gg 1$  in the fully radiative regime and  $\gamma_0^2 \gg \gamma^2 \gg 1$  in the adiabatic regime, where  $\gamma_0$  the initial Lorentz gamma factor of the optically thin fireshell.

In Fig. 6.5 we show the differences between the two approaches. In the upper panel there are plotted the exact solutions for the fireshell dynamics in the fully radiative and adiabatic cases. In the lower panel we plot the corresponding “effective” power-law index  $a_{eff}$ , defined as the index of the power-law tangent to the exact solution (Bianco and Ruffini, 2005a):

$$a_{eff} = -\frac{d \ln \gamma}{d \ln r}. \quad (6.3.5)$$

Such an “effective” power-law index of the exact solution smoothly varies from 0 to a maximum value which is always smaller than 3 or 3/2, in the fully radiative and adiabatic cases respectively, and finally decreases back to 0 (see Fig. 6.5).

## 6.4. Extended afterglow luminosity and spectrum

The extended afterglow luminosity in the different energy bands is governed by two quantities associated to the environment. Within the fireshell model, these are the effective CBM density profile,  $n_{cbm,r}$ , and the ratio between the effective emitting area  $A_{eff}$  and the total area  $A_{tot}$  of the expanding baryonic and leptonic shell,  $\mathcal{R} = A_{eff}/A_{tot}$ . This last parameter takes into account the CBM filamentary structure (Ruffini et al., 2004b, 2005c) and the possible occurrence of a fragmentation in the shell (Dainotti et al., 2007).

Within the “fireshell” model, in addition to the determination of the baryon loading, it is therefore possible to infer a detailed description of the CBM, its average density and its porosity and filamentary structure, all the way from the black hole horizon to distance  $r \lesssim 10^{17}$  cm. This corresponds to the prompt emission. This description is lacking in the traditional model based on the synchrotron emission. The attempt to use the internal shock model for the prompt emission (see e.g. Refs. Rees and Meszaros, 1994; Piran, 2005; Meszaros, 2006, and references therein) only applies to regions where  $r > 10^{17}$  cm (Kumar and McMahon, 2008).

In our hypothesis, the emission from the baryonic and leptonic matter shell is spherically symmetric. This allows us to assume, in a first approximation, a modeling of thin spherical shells for the CBM distribution and consequently to consider just its radial dependence (Ruffini et al., 2002). For simplicity, and in order to have an estimate of the energetics, the emission process is

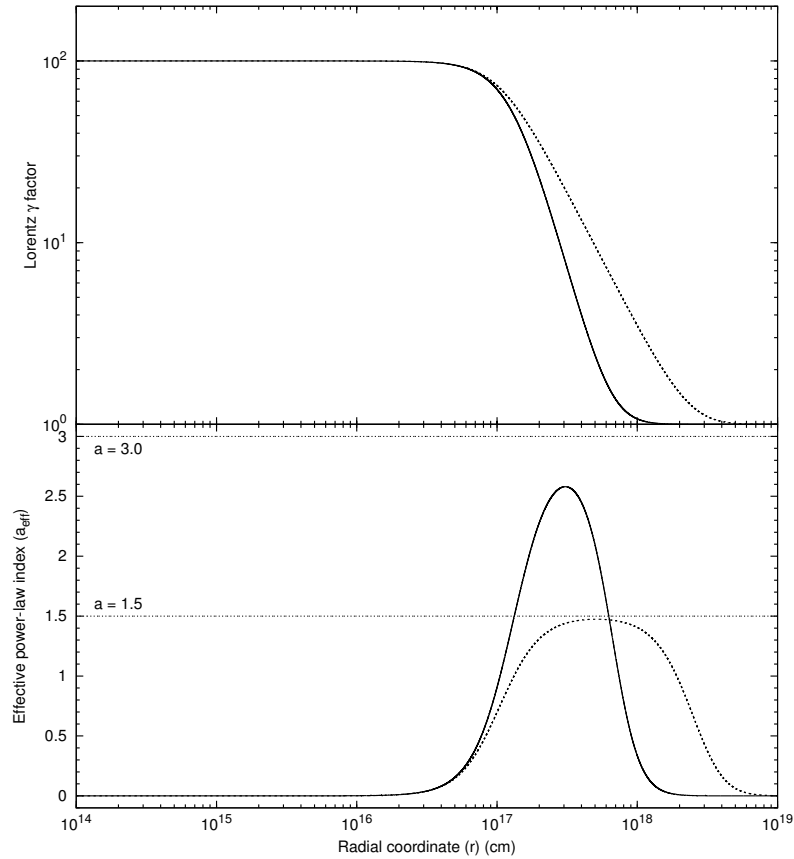


**Figure 6.5.:** In the upper panel, the analytic behavior of the Lorentz  $\gamma$  factor during the afterglow era is plotted versus the radial coordinate of the expanding optically thin fireshell in the fully radiative case (solid line) and in the adiabatic case (dotted line) starting from  $\gamma_0 = 10^2$  and the same initial conditions as GRB 991216 (Bianco and Ruffini, 2005a). In the lower panel are plotted the corresponding values of the “effective” power-law index  $a_{eff}$  (see Eq.(6.3.5)), which is clearly not constant, is highly varying and systematically lower than the constant values 3 and 3/2 purported in the current literature (horizontal thin dotted lines).

## 6. Brief reminder of the fireshell model

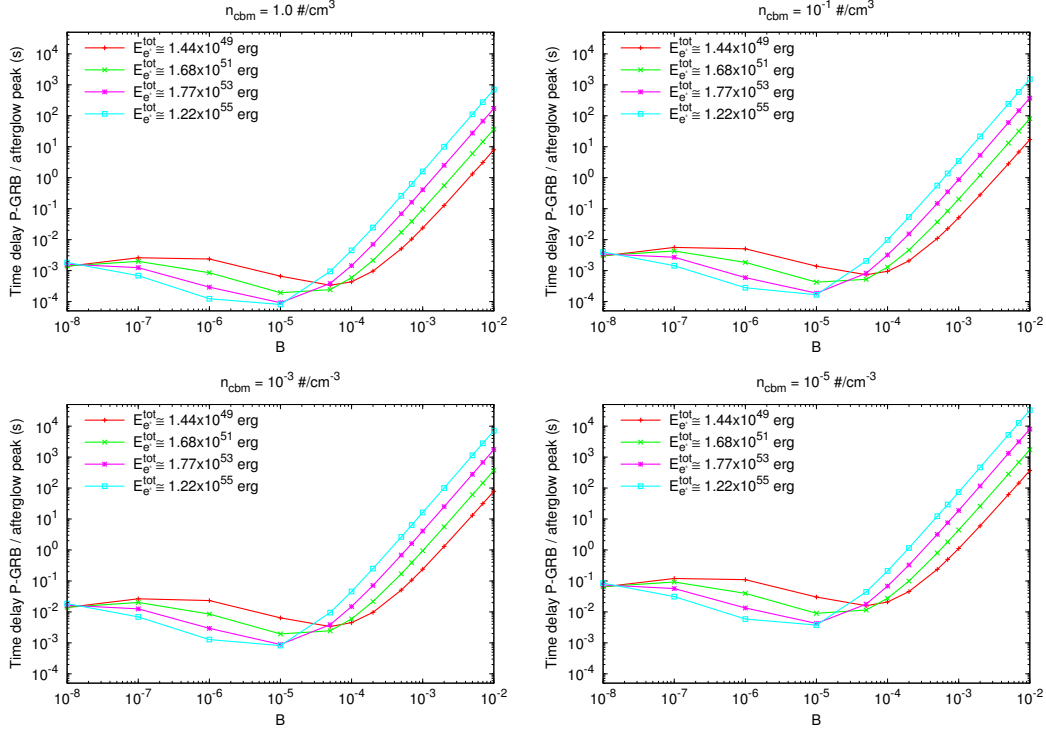


**Figure 6.6.:** For 4 different values of  $E_{e\pm}^{tot}$ , we plot as a function of  $B$  the arrival time separation  $\Delta t_a$  between the P-GRB and the peak of the extended afterglow (i.e. the “quiescent time between the “precursor” and the main GRB event), measured in the source cosmological rest frame. The computation has been performed assuming a constant value of the CBM density in four different cases:  $n_{cbm} = 1.0$  particles/cm<sup>3</sup>,  $n_{cbm} = 1.0 \times 10^{-3}$  particles/cm<sup>3</sup>,  $n_{cbm} = 1.0 \times 10^{-5}$  particles/cm<sup>3</sup>,  $n_{cbm} = 1.0 \times 10^{-7}$  particles/cm<sup>3</sup>. The points represents the actually numerically computed values, connected by straight line segments.

postulated to be thermal in the co-moving frame of the shell (Ruffini et al., 2004b). We are currently examining a departure from this basic mechanism by taking into account inverse Compton effects due to the electron collisions with the thermal photons. The observed GRB non-thermal spectral shape is due to the convolution of an infinite number of thermal spectra with different temperatures and different Lorentz and Doppler factors. Such a convolution is to be performed over the surfaces of constant arrival time of the photons at the detector (EQuiTemporal Surfaces, EQTSs; see e.g. Ref. Bianco and Ruffini, 2005b) encompassing the whole observation time (Bernardini et al., 2005a).

In Fig. 6.6 we plot, as a function of  $B$ , the arrival time separation  $\Delta t_a$  between the P-GRB and the peak of the extended afterglow measured in the cosmological rest frame of the source. Such a time separation  $\Delta t_a$  is the “quiescent time” between the precursor (i.e. the P-GRB) and the main GRB event

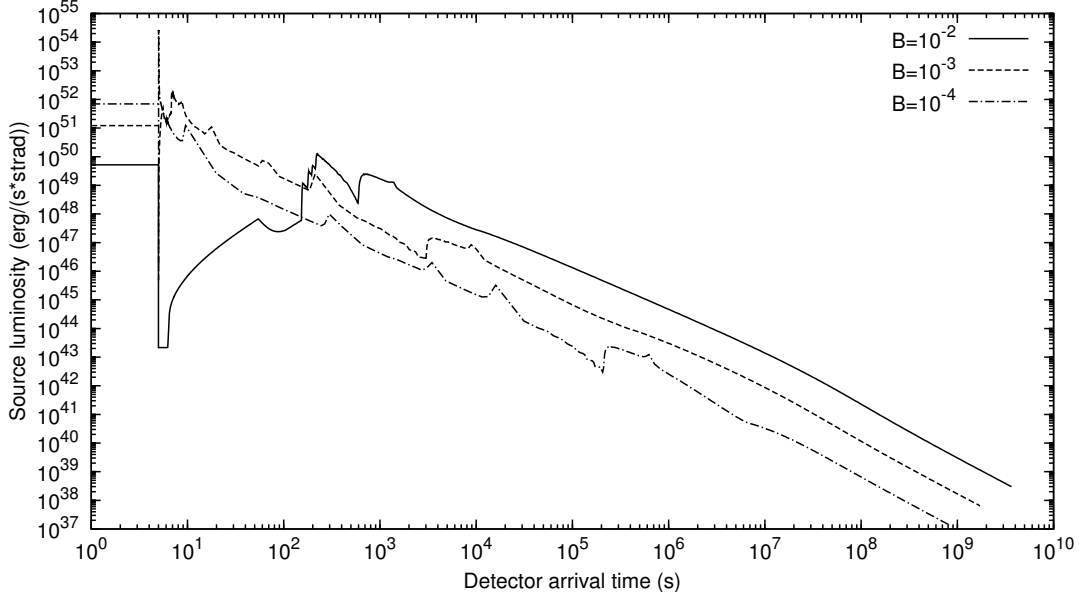


**Figure 6.7.:** We plot three theoretical extended afterglow bolometric light curves together with the corresponding P-GRB peak luminosities (the horizontal segments). The computations have been performed assuming the same  $E_{e\pm}^{tot}$  and CBM structure of GRB 991216 and three different values of  $B$ . The P-GRBs have been assumed to have the same duration in the three cases, i.e. 5 s. For  $B$  decreasing, the extended afterglow light curve squeezes itself on the P-GRB.

(i.e. the peak of the extended afterglow). The plot is drawn for the same four different values of  $E_{e\pm}^{tot}$  of Fig. 6.3. The arrival time of the peak of the extended afterglow emission depends on the detailed profile of the CBM density. In this plot it has been assumed a constant CBM density in four different cases:  $n_{cbm} = 1.0$  particles/cm<sup>3</sup>,  $n_{cbm} = 1.0 \times 10^{-3}$  particles/cm<sup>3</sup>,  $n_{cbm} = 1.0 \times 10^{-5}$  particles/cm<sup>3</sup>,  $n_{cbm} = 1.0 \times 10^{-7}$  particles/cm<sup>3</sup>. We can see that, for  $3.0 \times 10^{-4} \lesssim B < 10^{-2}$ , which is the condition for P-GRBs to be “precursors” (see above),  $\Delta t_a$  increases both with  $B$  and with  $E_{e\pm}^{tot}$ . We can have  $\Delta t_a > 10^2$  s and, in some extreme cases even  $\Delta t_a \sim 10^3$  s. For  $B \lesssim 3.0 \times 10^{-4}$ , instead,  $\Delta t_a$  presents a behavior which qualitatively follows the opposite of  $\gamma_o$  (see middle panel of Fig. 6.3).

Finally, in Fig. 6.7 we present three theoretical extended afterglow bolometric light curves together with the corresponding P-GRB peak luminosities for three different values of  $B$ . The duration of the P-GRBs has been assumed to be the same in the three cases (i.e. 5 s). The computations have been performed assuming the same  $E_{e\pm}^{tot}$  and the same detailed CBM density profile of GRB 991216 (Ruffini et al., 2003). In this picture we clearly see how, for  $B$  decreasing, the extended afterglow light curve “squeezes” itself on the P-GRB and the P-GRB peak luminosity increases.

The “prompt emission” light curves of many GRBs present a small pulse preceding the main GRB event, with a lower peak flux and separated by this last one by a quiescent time. The nature of such GRB “precursors” is one of the most debated issues in the current literature (see e.g. Refs. Burlon et al., 2008; Ruffini et al., 2008a). Already in 2001 (Ruffini et al., 2001b), within the “fireshell” model, we proposed that GRB “precursors” are the P-GRBs emitted when the fireshell becomes transparent, and we gave precise estimates of the time sequence and intensities of the P-GRB and of the extended afterglow, recalled above.

The radiation viewed in the co-moving frame of the accelerated baryonic matter is assumed to have a thermal spectrum and to be produced by the interaction of the CBM with the front of the expanding baryonic shell (Ruffini et al., 2004b). In Bernardini et al. (2005a) it is shown that, although the instantaneous spectrum in the co-moving frame of the optically thin fireshell is thermal, the shape of the final instantaneous spectrum in the laboratory frame is non-thermal. In fact, as explained in Ruffini et al. (2004b), the temperature of the fireshell is evolving with the co-moving time and, therefore, each single instantaneous spectrum is the result of an integration of hundreds of thermal spectra with different temperature over the corresponding EQTS. This calculation produces a non thermal instantaneous spectrum in the observer frame (Bernardini et al., 2005a). Another distinguishing feature of the GRBs spectra which is also present in these instantaneous spectra is the hard to soft transition during the evolution of the event (Crider et al., 1997; Piran, 1999; Frontera et al., 2000; Ghirlanda et al., 2002). In fact the peak of the energy distributions  $E_p$  drift monotonically to softer frequencies with time (Bernardini et al., 2005a). This feature explains the change in the power-law low energy spectral index (Band et al., 1993)  $\alpha$  which at the beginning of the prompt emission of the burst ( $t_a^d = 2$  s) is  $\alpha = 0.75$ , and progressively decreases for later times (Bernardini et al., 2005a). In this way the link between  $E_p$  and  $\alpha$  identified in Crider et al. (1997) is explicitly shown.

The time-integrated observed GRB spectra show a clear power-law behavior. Within a different framework (see e.g. Ref. Pozdniakov et al., 1983, and references therein) it has been argued that it is possible to obtain such power-law spectra from a convolution of many non power-law instantaneous spectra monotonically evolving in time. This result was recalled and applied to GRBs (Blinnikov et al., 1999) assuming for the instantaneous spectra a thermal shape with a temperature changing with time. It was shown that the integration of such energy distributions over the observation time gives a typical power-law shape possibly consistent with GRB spectra.

Our specific quantitative model is more complicated than the one considered by Blinnikov et al. (1999): the instantaneous spectrum here is not a black body. Each instantaneous spectrum is obtained by an integration over the corresponding EQTS: (Bianco and Ruffini, 2004, 2005b) it is itself a convolution, weighted by appropriate Lorentz and Doppler factors, of  $\sim 10^6$  thermal

spectra with variable temperature. Therefore, the time-integrated spectra are not plain convolutions of thermal spectra: they are convolutions of convolutions of thermal spectra (Ruffini et al., 2004b; Bernardini et al., 2005a). In Fig. 6.8 we present the photon number spectrum  $N(E)$  time-integrated over the 20 s of the whole duration of the prompt event of GRB 031203 observed by INTEGRAL (Sazonov et al., 2004a): in this way we obtain a typical non-thermal power-law spectrum which results to be in good agreement with the INTEGRAL data (Sazonov et al., 2004a; Bernardini et al., 2005a) and gives a clear evidence of the possibility that the observed GRBs spectra are originated from a thermal emission (Bernardini et al., 2005a)

Before closing, we like to mention that, using the diagrams represented in Figs. 6.3-6.6, in principle one can compute the two free parameters of the fireshell model, namely  $E_{e\pm}^{tot}$  and  $B$ , from the ratio between the total energies of the P-GRB and of the extended afterglow and from the temporal separation between the peaks of the corresponding bolometric light curves. None of these quantities depends on the cosmological model. Therefore, one can in principle use this method to compute the GRBs’ intrinsic luminosity and make GRBs the best cosmological distance indicators available today. The increase of the number of observed sources, as well as the more accurate knowledge of their CBM density profiles, will possibly make viable this procedure to test cosmological parameters, in addition to the Amati relation (Amati et al., 2008; Guida et al., 2008b).

## 6.5. The new class of “disguised” short GRBs

In the context of the fireshell model, we considered a new class of GRBs, pioneered by Norris and Bonnell (2006). This class is characterized by an occasional softer extended emission after an initial spike-like emission. The softer extended emission has a peak luminosity lower than the one of the initial spike-like emission. As shown in the prototypical case of GRB 970228 (Bernardini et al., 2007) and then in GRB 060614 (Caito et al., 2009), we can identify the initial spike-like emission with the P-GRB and the softer extended emission with the peak of the extended afterglow. That the time-integrated extended afterglow luminosity is much larger than the P-GRB one is crucial. This unquestionably identifies GRB 970228 and GRB 060614 as canonical GRBs with  $B > 10^{-4}$ . The consistent application of the fireshell model allows us to infer the CBM filamentary structure and average density, which, in that specific case, is  $n_{cbm} \sim 10^{-3}$  particles/cm<sup>3</sup> (Bernardini et al., 2007). This low CBM density value explains the peculiarity of the low extended afterglow peak luminosity and its more protracted time evolution. These features are not intrinsic to the progenitor, but depend uniquely on the peculiarly low value of the CBM density. This led us to expand the traditional classification of GRBs to three classes: “genuine” short GRBs, “fake” or

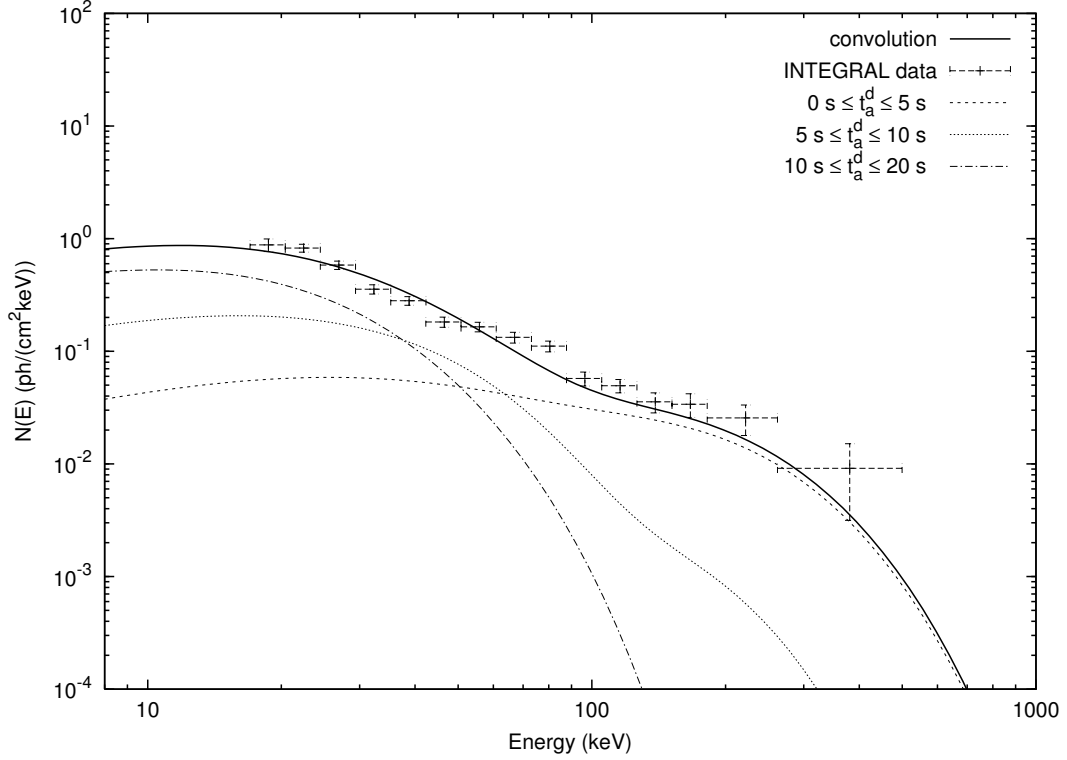


**Figure 6.8.:** Three theoretically predicted time-integrated photon number spectra  $N(E)$ , computed for GRB 031203 (Bernardini et al., 2005a), are here represented for  $0 \leq t_a^d \leq 5$  s,  $5 \leq t_a^d \leq 10$  s and  $10 \leq t_a^d \leq 20$  s (dashed and dotted curves), where  $t_a^d$  is the photon arrival time at the detector (Ruffini et al., 2001c; Bernardini et al., 2005a). The hard to soft behavior is confirmed. Moreover, the theoretically predicted time-integrated photon number spectrum  $N(E)$  corresponding to the first 20 s of the “prompt emission” (black bold curve) is compared with the data observed by INTEGRAL (Sazonov et al., 2004a). This curve is obtained as a convolution of 108 instantaneous spectra, which are enough to get a good agreement with the observed data. Details in Bernardini et al. (2005a).

“disguised” short GRBs, and the remaining “long duration” ones.

A CBM density  $n_{cbm} \sim 10^{-3}$  particles/cm<sup>3</sup> is typical of a galactic halo environment, and GRB 970228 was indeed found to be in the halo of its host galaxy (Sahu et al., 1997; van Paradijs et al., 1997). We therefore proposed that the progenitors of this new class of “disguised” short GRBs are merging binary systems, formed by neutron stars and/or white dwarfs in all possible combinations, which spiraled out from their birth place into the halo (see Bernardini et al., 2007; Caito et al., 2009; Kramer, 2008). This hypothesis can also be supported by other observations. Assuming that the soft tail peak luminosity is directly related to the CBM density, GRBs displaying a prolonged soft tail should have a systematically smaller offset from the center of their host galaxy. Some observational evidence was found in this sense (Troja et al., 2008). However, the present sample of observations does not enable us to derive any firm conclusion that short GRBs with extended emission have smaller physical offsets than those without extended emission (Fong et al., 2010; Berger, 2010).

## 6.6. The “fireshell” model and GRB progenitors

We have recalled in the introduction that “long” GRBs are traditionally related in the current literature to the idea of a single progenitor, identified as a “collapsar” (Woosley, 1993). Similarly, short GRBs are assumed to originate from binary mergers formed by white dwarfs, neutron stars, and black holes in all possible combinations. It also has been suggested that short and long GRBs originate from different galaxy types. In particular, short GRBs are proposed to be associated with galaxies with low specific star forming rate (see e.g. Berger, 2009). Some evidence against such a scenario have been advanced, due to the small sample size and the different estimates of the star forming rates (see e.g. Savaglio et al., 2009). However, the understanding of GRB structure and of its relation to the CBM distribution, within the fireshell model, leads to a more complex and interesting perspective than the one in the current literature.

The first general conclusion of the “fireshell” model (Ruffini et al., 2001b) is that, while the time scale of “short” GRBs is indeed intrinsic to the source, this does not happen for the “long” GRBs: their time scale is clearly only a function of the instrumental noise threshold. This has been dramatically confirmed by the observations of the Swift satellite (Ruffini et al., 2006a). Among the traditional classification of “long” GRBs we distinguish two different subclasses of events, neither of which originates from collapsars.

The first sub-class contains “long” GRBs that are particularly weak ( $E_{iso} \sim 10^{50}$  erg) and associated with SN Ib/c. In fact, it has been often proposed that such GRBs, only observed at smaller redshift  $0.0085 < z < 0.168$ , form a different class, less luminous and possibly much more numerous than the high

luminosity GRBs at higher redshift (Pian et al., 2006; Soderberg et al., 2004; Maeda et al., 2007; Della Valle, 2006). Therefore in the current literature they have been proposed to originate from a separate class of progenitors (Liang et al., 2007; Cobb et al., 2006). Within our “fireshell” model, they originate in a binary system formed by a neutron star, close to its critical mass, and a companion star, evolved out of the main sequence. They produce GRBs associated with SNe Ib/c, via the “induced gravitational collapse” process (Ruffini et al., 2001a). The low luminosity of these sources is explained by the formation of a black hole with the smallest possible mass: the one formed by the collapse of a just overcritical neutron star (Ruffini et al., 2007b; Dainotti et al., 2007).

A second sub-class of “long” GRBs originates from merging binary systems, formed either by two neutron stars or a neutron star and a white dwarf. A prototypical example of such systems is GRB970228. The binary nature of the source is inferred by its migration from its birth location in a star forming region to a low density region within the galactic halo, where the final merging occurs (Bernardini et al., 2007). The location of such a merging event in the galactic halo is indeed confirmed by optical observations of the GRB970228 afterglow (Sahu et al., 1997; van Paradijs et al., 1997). The crucial point is that, as recalled above, GRB970228, GRB060614, GRB071227 and GRB050509b are “canonical” GRBs with  $B > 10^{-4}$  “disguised” as short GRBs.

If the binary merging would occur in a region close to its birth place, with an average density of 1 particle/cm<sup>3</sup>, the GRB would appear as a traditional high-luminosity “long” GRB, of the kind currently observed at higher redshifts (see Fig. C.3), similar to, e.g., GRB050315 (Ruffini et al., 2006b).

Within our approach, therefore, there is the distinct possibility that all GRB progenitors are formed by binary systems, composed of neutron stars, white dwarfs, or stars evolved out of the main sequence, in different combinations.

The case of the “genuine” short GRBs is currently being examined within the “fireshell” model.

# 7. Evidence for broadening of the spectral energy distribution of GRBs within the fireshell model

## 7.1. Introduction

Thanks to the numerous missions dedicated to the detection of Gamma Ray Bursts (GRBs) such as, for example, Swift, many progresses have been made in the comprehension of these phenomena; nevertheless, there are different fundamental questions that remain unanswered, for example the mechanism for the prompt emission is still uncertain (Zou et al., 2009).

In general, the behaviour of the  $N(E)$  spectrum of the prompt emission can be phenomenologically fit by a broken power-law. To interpret this behaviour various possible physical mechanisms have been proposed, for example Synchrotron and Synchrotron Self Compton (SSC), but both of them presents various problems (Kumar and McMahon, 2008; Zou et al., 2009) and it is clear that the comprehension of the prompt emission requires the investigation of other scenarios.

A different approach to explain the properties of GRB emission is given by the Fireshell Model. The Fireshell Model postulates that the emission process is thermal in the comoving frame of the fireshell and the observed  $N(E)$  spectrum has a non thermal-shape, being the convolution of various thermal spectra having different temperatures over the Equitemporal Surfaces (EQTS, Bianco and Ruffini, 2005b) and observational time (Bernardini et al., 2005a). It was demonstrated that the assumption of thermal spectrum is a good approximation for some GRBs such as, for example, GRB 031203 (Bernardini et al., 2005a). Nevertheless, it represents just a first approximation. In particular, the discovery of very bright GRBs such as, for example, GRB 080319B, allowed to analyse in detail GRB spectra integrated just over few seconds, revealing some discrepancies between the theoretical predicted spectrum and the observed one.

The aim of this section is to investigate if a better description of GRB emission could be obtained by assuming a different spectral energy distribution of photons in the comoving frame of the fireshell; in particular, we introduce a phenomenologically modified thermal spectrum and test it by fitting the observational data of a set of GRBs.

## 7.2. The Fireshell Model

Within the Fireshell Model all GRBs are generated by the gravitational collapse of the star progenitor to a black hole (BH) (Ruffini et al., 2001b). The electron-positron plasma created in the process of BH formation, having total energy  $E_{tot}^{\pm}$ , expands as a spherically symmetric “fireshell”. After this first stage, the fireshell reaches the baryonic remnants left over from the gravitational collapse of the star progenitor, having mass  $M_B$ ; the baryon loading is measured by the dimensionless parameter  $B = \frac{M_B c^2}{E_{tot}^{\pm}}$ . After the baryonic matter loading, the fireshell expands until the transparency condition is reached and the Proper - GRB (P-GRB) is emitted. The extended afterglow emission starts due to the collision between the remaining optically thin fireshell and the CircumBurst Medium (CBM) and it depends on the parameters describing the effective CBM distribution: its density  $n_{cbm}$  and the ratio  $\mathcal{R} = A_{eff}/A_{vis}$  between the effective emitting area of the fireshell  $A_{eff}$  and its total visible area  $A_{vis}$  (Ruffini et al., 2002, 2004b, 2005c). We recall that the extended afterglow comprises both the so called “prompt” emission and the “afterglow” emission.

In general, the  $N(E)$  spectrum of the prompt emission of GRBs can be phenomenologically fit by two power laws joined smoothly at a given break energy (Band et al., 1993). The non-thermal character of the spectrum suggests Synchrotron as one possible radiation mechanism, but Kumar and McMahon (2008) have shown the inconsistency of the observational data with the overall synchrotron model: they found that for GRBs to be produced via the synchrotron process, unphysical conditions are required and the values of the various parameters are in conflict with afterglow data. Another possible mechanism is the Synchrotron self-Compton (SSC), but also in this case there are several problems. For example, Piran et al. (2009) found that SSC model cannot explain the prompt emission unless the prompt optical emission is very high ( $\lesssim 14$ th magnitude for  $z \sim 2$ ). Zou et al. (2009) applied the SSC model to GRB 080319B, that is characterized by a peak visual magnitude of 5.3 (Racusin et al., 2008), but even in this case SSC could not be responsible for the prompt  $\gamma$ -rays.

The “Fireshell” Model of GRBs has a different approach: this model assumes that radiation has a thermal spectrum in the co-moving frame of the fireshell (Ruffini et al., 2004b). The observed GRB non-thermal spectral shape is due to the convolution of various thermal spectra with different temperatures and different Lorentz and Doppler factors. Such a convolution is to be performed over the EquiTemporal Surfaces (EQTS), which are the surfaces of constant arrival time of the photons at the detector and over the observation time.

The Fireshell Model has been successfully tested on some GRBs such as, for example, GRB 031203 (Bernardini et al., 2005a), but the assumption of thermal spectrum represents just a first approximation. In fact, the discovery of very

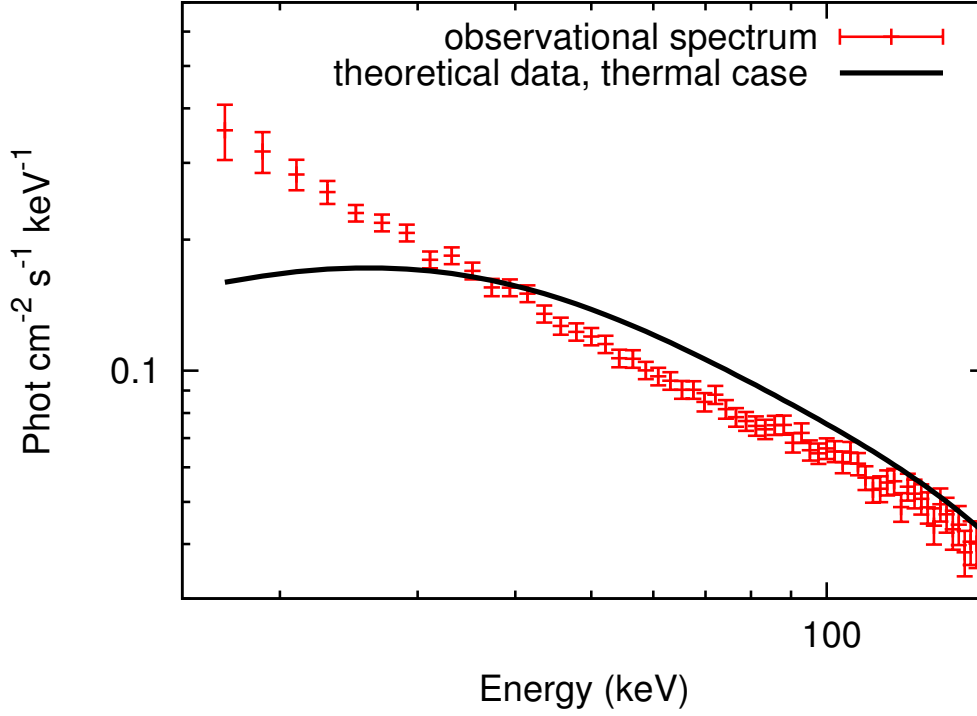


**Figure 7.1.:** Theoretically simulated time integrate spectrum of GRB 080319B for  $3s \leq t_a^d \leq 10s$  (black solid line) is compared with the observed data by BAT (red points). The theoretical data have been obtained by assuming a thermal spectrum in the comoving frame of the fireshell.

bright GRBs such as, for example, GRB 080319B, allowed to analyse in detail GRB spectra more resolved in time (integrated just over few seconds), revealing some discrepancies between the theoretical predicted spectrum and the observed one. In fig. 7.1 is shown, as an example, the fit of the BAT spectrum of this burst integrated just over 10 s: it can be seen that there are difficulties in correctly fit the observational data, especially at the lower energies. This problematic induced us to investigate the possibility of better reproducing the observed time-resolved spectra of GRBs starting from a different spectral energy distribution of photons in the comoving frame of the fireshell.

### 7.3. The source luminosity and the spectrum

Within the fireshell model, the source luminosity at the detector arrival time  $t_a^d$  per unit solid angle  $d\Omega$  and in the energy band  $[\nu_1, \nu_2]$  is given by (Ruffini

## 7. Evidence for broadening of the spectral energy distribution of GRBs within the fireshell model

---

et al., 2003)

$$\frac{dE^{[\nu_1, \nu_2]}}{dt_a^d d\Omega} = \int_{EQTS} \frac{\Delta\epsilon}{4\pi} v \cos\theta \Lambda^{-4} \frac{dt}{dt_a^d} W(\nu_1, \nu_2, T_{arr}) d\Sigma, \quad (7.3.1)$$

where  $\Delta\epsilon = \frac{\Delta E_{int}}{V}$  is the emitted energy density released in the interaction of the accelerated baryons with the ISM measured in the comoving frame,  $\Lambda = \gamma[1 - (v/c)\cos\theta]$  is the Doppler factor,  $W(\nu_1, \nu_2, T_{arr})$  is an “effective weight” required to evaluate only the contributions in the energy band  $[\nu_1, \nu_2]$ ,  $d\Sigma$  is the surface element of the EQTS at detector arrival time  $t_a^d$  on which the integration is performed and  $T_{arr}$  is the observed temperature of the radiation emitted from  $d\Sigma$ . In eq. (7.3.1), there is only one term depending on the spectral energy distribution of photons: the “effective weight”  $W(\nu_1, \nu_2, T_{arr})$ , defined as ratio between the energy density emitted in a given energy band  $[\nu_1, \nu_2]$  and the bolometric energy density:

$$W(\nu_1, \nu_2, T_{arr}) = \frac{\int_{\epsilon_1}^{\epsilon_2} \left( \frac{dN_\gamma}{dVd\epsilon} \right) \epsilon d\epsilon}{\int_0^\infty \left( \frac{dN_\gamma}{dVd\epsilon} \right) \epsilon d\epsilon}, \quad (7.3.2)$$

where  $\frac{dN_\gamma}{dVd\epsilon}$  is the number density of photons per unit of energy.

### 7.3.1. Thermal case

With the assumption of thermal spectrum in the comoving frame of the fireshell

$$\frac{dN_\gamma}{dVd\epsilon} = \left( \frac{8\pi}{h^3 c^3} \right) \frac{\epsilon^2}{\exp\left(\frac{\epsilon}{k_B T}\right) - 1} \quad (7.3.3)$$

we have

$$W(\nu_1, \nu_2, T_{arr}) = \frac{\int_{\epsilon_1}^{\epsilon_2} \left( \frac{dN_\gamma}{dVd\epsilon} \right) \epsilon d\epsilon}{aT^4}, \quad (7.3.4)$$

where  $a$  is the radiation constant and  $T$  is the temperature in the comoving frame.

In general, the temperature in the comoving frame can be evaluated starting from the following relation:

$$\frac{\Delta E_{int}}{\Delta\tau} = \pi r^2 c \mathcal{R} \int_0^\infty \left( \frac{dN_\gamma}{dVd\epsilon} \right) \epsilon d\epsilon, \quad (7.3.5)$$

where  $\Delta\tau$  is the time interval in which the energy  $\Delta E_{int}$  is developed and  $\mathcal{R}$  is the surface filling factor. By inserting eq. (7.3.3) in eq. (7.3.5) we obtain

$$T = \left( \frac{\Delta E_{int}}{4\pi r^2 \sigma \mathcal{R}} \right)^{1/4}, \quad (7.3.6)$$

with  $\sigma$  the Stefan-Boltzmann constant.

### 7.3.2. The “modified” thermal spectrum

We introduce the new spectral energy distribution for the radiation emitted in the comoving frame of the fireshell: we assume that it is a “modified” thermal spectrum, with the number density of photons per unit of energy given by

$$\frac{dN_\gamma}{dV d\epsilon} = \left( \frac{8\pi}{h^3 c^3} \right) \frac{1}{(k_B T)^\alpha} \frac{\epsilon^{\alpha+2}}{\exp\left(\frac{\epsilon}{k_B T}\right) - 1}, \quad (7.3.7)$$

where  $k_B$  is the Boltzmann constant. The index  $\alpha$  is a free parameter; the case  $\alpha = 0$  corresponds to the thermal spectrum case.

By using the eq. (7.3.7) and introducing the variable  $y = \frac{\epsilon}{k_B T}$ , we obtain the following expression for the “effective weight”:

$$W(\nu_1, \nu_2, T_{arr}) = \frac{\int_{y_1}^{y_2} \frac{y^{\alpha+3}}{\exp(y)-1} dy}{\Gamma(4+\alpha) Li_{4+\alpha}(1)} \quad (7.3.8)$$

where  $\Gamma(z) = \int_0^\infty t^{z-1} e^{-t} dt$  is the Gamma function and  $Li_n(z) = \sum_{k=1}^\infty \frac{z^k}{k^n}$  is the Jonquière’s function.

By inserting eq. 7.3.7 in eq. 7.3.5 we obtain the expression for the temperature:

$$T = \left[ \left( \frac{\Delta E_{int}}{\Delta\tau} \right) \frac{h^3 c^2}{(4\pi r^2) 2\pi \mathcal{R} \Gamma(4+\alpha) Li_{4+\alpha}(1)} \right]^{1/4}. \quad (7.3.9)$$

It can be easily seen that, for  $\alpha = 0$ , we obtain eq. (7.3.6).

In fig. 7.2 are shown several theoretically predicted instantaneous spectra characterized by the same temperature and different values of the index  $\alpha$ . It can be seen that the main effect of varying the value of  $\alpha$  is a change in the low energy slope of the spectral energy distribution. In particular, by decreasing  $\alpha$  the low energy emission increases.

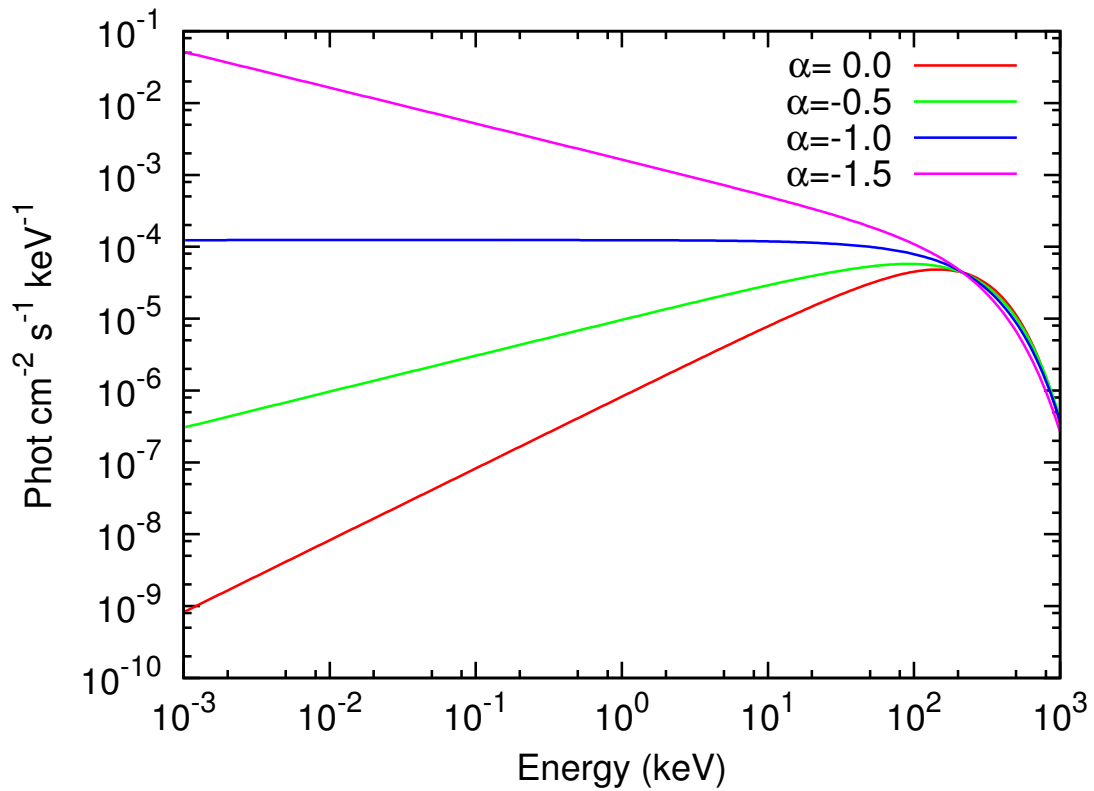


**Figure 7.2.:** Theoretically predicted instantaneous modified thermal spectra for  $t_a^d = 5s$  characterized by the same temperature and different values of the index  $\alpha$ . The curve with  $\alpha = 0.0$  corresponds to the pure thermal spectrum case.

## 7.4. Comparison with observational data

We apply the “modified” thermal spectrum to fit the observed BAT light curves and spectra of GRBs. In particular here we present, as specific examples, the analysis of the prompt emission spectrum of GRB 080319B and GRB 050904. For a complete analysis of these bursts see Patricelli et al., in preparation.

### 7.4.1. GRB 080319B

GRB 080319B is a very bright burst: it is characterized by a redshift  $z = 0.937$  (Vreeswijk et al., 2008) and an isotropic energy release of  $E_\gamma = 1.32 \times 10^{54}$  ergs (Golenetskii et al., 2008). We analysed the spectrum of the prompt emission within the Fireshell Model, using the “modified” thermal spectrum. According to the canonical GRB scenario, we identify the first 8 s of emission with the P-GRB. Concerning the remaining part of the BAT data, there is clear evidence that the emission can be separated into two main episodes, partitioned at about 28 s (Stamatikos et al., 2009; Margutti et al., 2008). We interpret the first episode with the peak of the extended afterglow. In particular, we obtain the best fit of the spectrum (fig. 7.3) of this first episode ( $3s \leq t_a^d \leq 28s$ ) with the following parameters:  $E_{e^+e^-}^{tot} = 1.0 \times 10^{54}$  ergs,  $B = 2.5 \times 10^{-3}$  and  $\alpha = -1.8$ ; we also consider a mean number density  $\langle n_{cbm} \rangle \sim 6$  particles  $\text{cm}^{-3}$  and  $\mathcal{R} = 3.5 \times 10^{-10}$ . This burst is very bright, so it was possible to analyse also spectra more resolved in time. In fig 7.4 is shown, as an example, the spectrum for  $3s \leq t_a^d \leq 13s$ : it can be seen that with the modified thermal spectrum we can correctly reproduce the observational data; on the contrary, by assuming a thermal spectrum there are several discrepancies between the theoretical prediction and the observational data, especially at the lower energies.

Concerning the second episode, we propose that it is due to a different physical mechanism; details about this interpretation will be presented elsewhere.

### 7.4.2. GRB 050904

GRB 050904 is a very long burst, with  $T_{90} = 225 \pm 10$  s (Sakamoto et al., 2005); it is characterized by a very high redshift:  $z = 6.29$  (Kawai et al., 2005) and an isotropic energy release of  $E_{iso} = 1.04 \times 10^{54}$  ergs (Sugita et al., 2009). We analysed the spectrum of the prompt emission within the Fireshell Model, applying the “modified” thermal spectrum. We identify this emission with the peak of the extended afterglow. In this case we don’t see the P-GRB, as its energetics is under the BAT threshold ( $E_{P-GRB}^{iso} = 2.1\% E_{e^+e^-}^{tot} = 1.47 \times 10^{52}$  ergs). The best fit of the spectrum (see fig. 7.5) is obtained with  $E_{e^+e^-}^{tot}$  and  $B$  found for GRB 080319B  $E_{e^+e^-}^{tot} = 1.0 \times 10^{54}$  ergs and  $B = 2.5 \times 10^{-3}$  and,

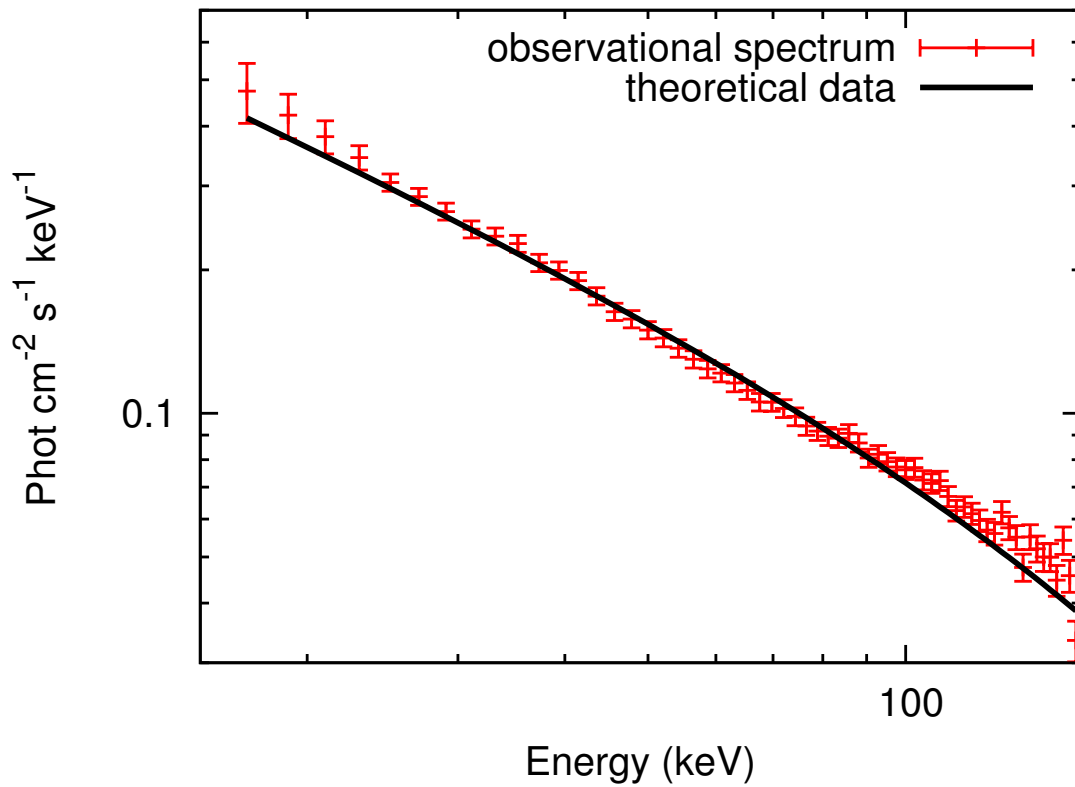


**Figure 7.3.:** Theoretically simulated time integrate spectrum of GRB 080319B for  $3s \leq t_a^d \leq 28s$  (black solid line) is compared with the observed data by BAT (red points).

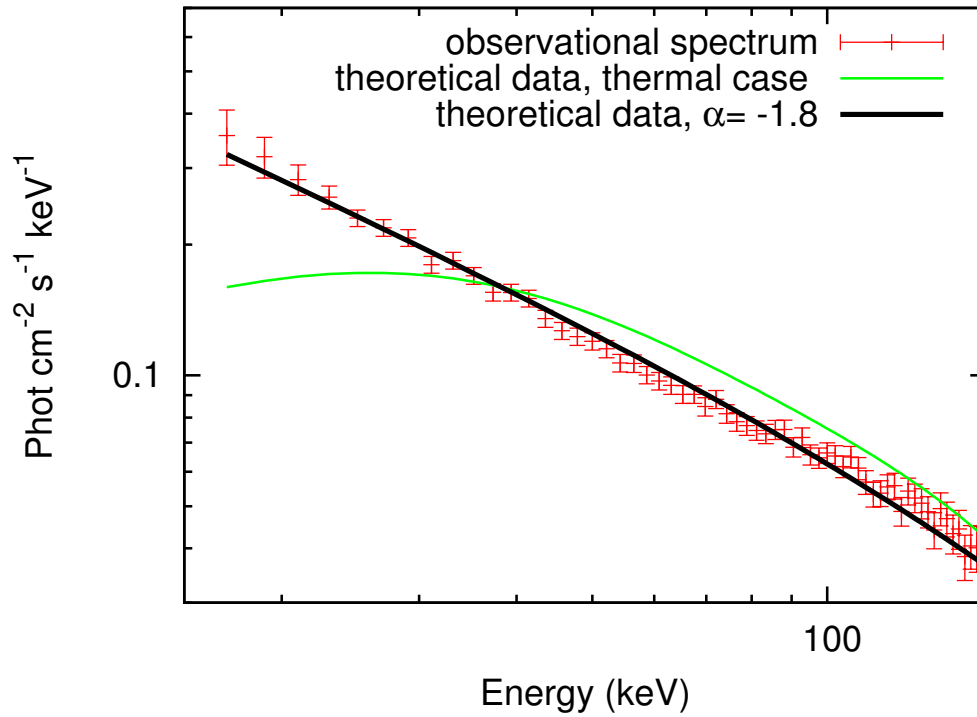


**Figure 7.4.:** Theoretically simulated time integrate spectrum of GRB 080319B for  $3s \leq t_a^d \leq 13s$  with  $\alpha = -1.8$  (black solid line) and  $\alpha = 0.0$  (thermal case, green solid line) are compared with the observed data by BAT (red points). It can be seen that with the “modified” thermal spectrum we can correctly fit the observed spectrum, contrarily to what happens with the thermal spectrum.

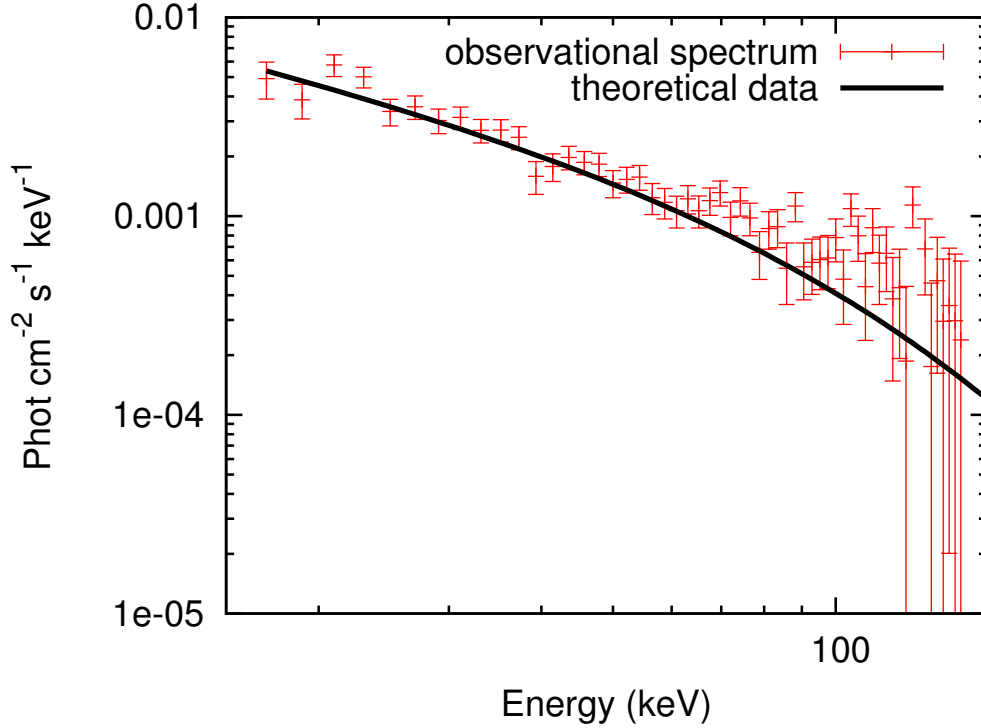


**Figure 7.5.:** Theoretically simulated time integrate spectrum of GRB 050904 for  $0 \leq t_a^d \leq 225s$  (black solid line) is compared with the observed data by BAT (red points).

also in this case,  $\alpha = -1.8$ . In the fit we considered a mean number density  $\langle n_{cbm} \rangle \sim 10^{-1}$  particles  $\text{cm}^{-3}$  and  $\mathcal{R} = 2 \times 10^{-11}$ .

Also for this burst we analyse also spectra integrated over intervals of time smaller than the entire duration of the prompt emission. In fig. 7.6 is shown, as an example, the spectrum for  $0s \leq t_a^d \leq 50s$ : it can be seen that by assuming a modified thermal spectrum with  $\alpha = -1.8$  we can correctly reproduce also these data.

## 7.5. Conclusions

The analysis of various GRBs has shown how the  $N(E)$  spectrum of their prompt emission, whose behaviour is usually represented by a “power-law”, can also be fitted in a satisfactory way by a convolution of thermal spectra as predicted by the Fireshell model. Nevertheless, this description can be considered just a first approximation. In particular, the observation of very bright GRBs such as, for example, GRB 080319B, allowed to analyse in detail GRB spectra integrated just over few seconds, revealing some discrepancies

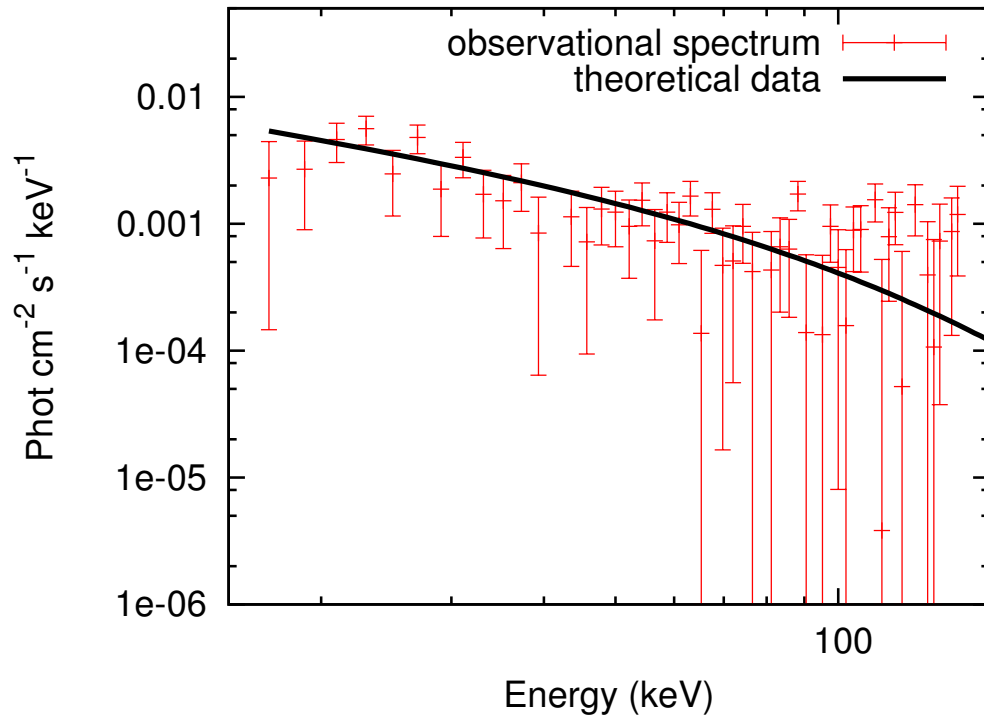


**Figure 7.6.:** Theoretically simulated time integrate spectrum of GRB 050904 for  $0 \leq t_a^d \leq 50s$  (black solid line) is compared with the observed data by BAT (red points).

between the theoretical predicted spectrum and the observed one.

To better explain the  $N(E)$  spectrum of the prompt emission we have introduced a phenomenologically modified thermal spectrum for photons in the comoving frame of the fireshell. We have obtained all the equations to determine the source luminosity, then we have applied the new model to fit the spectrum of the prompt emission of GRBs. In particular we have shown, as an example, the comparison between the theoretical simulations and the observational data of GRB 080319B and GRB 050904. From this analysis we have found some very interesting results: applying the modified thermal spectrum with  $\alpha = -1.8$  we can successfully reproduce the observational spectra integrated over intervals of time from few seconds up to the entire prompt duration. It's important to point out that from the integration of the modified thermal spectrum over the EQTS and observational time we obtain a phenomenological fit as the "Band relation" does; but our approach is different: we made an assumption about the shape of the spectrum for photons, but in the co-moving frame; the final spectrum is the result of the convolution over EQTS and observational time. This may allow to put some constraints about the microphysics underlying the emission processes.

# 8. On the nature of GRB 050509b: a disguised short GRB

## 8.1. Introduction

The traditional classification of gamma ray bursts (GRBs) is based on the observed time duration of the prompt emission measured with the criterion of “ $T_{90}$ ”, which is the time duration in which the cumulative counts increase from 5% to 95% above the background, encompassing 90% of the total GRB counts. This parameter shows that there are two groups of GRBs, the short ones with  $T_{90} < 2$  s, and the long ones with  $T_{90} > 2$  s. This analysis motivated the standard classification in the literature of short and long GRBs (Klebesadel, 1992; Dezalay et al., 1992; Kouveliotou et al., 1993).

The observations of GRB 050509b by BAT and XRT on board the *Swift* satellite (see Gehrels et al., 2004; Burrows et al., 2005a) represent a new challenge to the classification of GRBs as long and short, since it is the first short GRB associated with an afterglow (Gehrels et al., 2005). Its prompt emission observed by BAT lasts 40 milliseconds, but it also has an afterglow in the X-ray band observed by XRT, which begins 100 seconds after the BAT trigger (time needed to point XRT to the position of the burst) and lasts until  $\approx 1000$  seconds. It is located 40 kpc away from the center of its host galaxy (Bloom et al., 2006, , see Fig. 8.1), which is a luminous, non-star-forming elliptical galaxy with redshift  $z = 0.225$  (Gehrels et al., 2005). Although an extensive observational campaign has been performed using many different instruments, no convincing optical-IR candidate afterglow nor any trace of any supernova has been found associated with GRB 050509b (see Cenko et al., 2005; Bersier et al., 2005; Hjorth et al., 2005; Castro-Tirado et al., 2005; Bloom et al., 2005a,b, 2006). An upper limit in the *R*-band 18.5 days after the event onset imply that the peak flux of any underlying supernova should have been  $\sim 3$  mag fainter than the one observed for the type Ib/c supernova SN 1998bw associated with GRB 980425, and 2.3 mag fainter than a typical type Ia supernova (Castro-Tirado et al., 2005, see also Hjorth et al., 2005). An upper limit to the brightening caused by a supernova or supernova-like emission has also been established at 8.17 days after the GRB:  $R_c \sim 25.0$  mag (Bloom et al., 2006). While some core-collapse supernovae might be as faint as (or fainter than) this limit (Pastorello et al., 2007), the presence of this supernova in the outskirts of an elliptical galaxy would be truly extraordinary (Mannucci et al.,

2005; van den Bergh et al., 2005).

Unfortunately, we cannot obtain exhaustive observational constraints for this GRB because XRT data are missing in-between the first 40 milliseconds and 100 seconds. However, this makes the theoretical work particularly interesting, because we can infer from first principles some characteristics of the missing data, which are inferred by our model, and consequently reach a definite understanding of the source. This is indeed the case, specifically, for the verification of the Amati relation (Amati et al., 2002; Amati, 2006; Amati et al., 2009) for these sources as we see in section 8.4.

GRB 050509b is an example that the usual classification is at least incomplete. Within the fireshell model, we propose three classes of GRBs: long, genuine short and disguised short (Ruffini et al., 2009, and references therein). We have a well-defined way of differentiating between the classes, which is based on two parameters, the baryon loading parameter  $B$  and the Circum-Burst Medium (CBM) number density  $n_{CBM}$  (see next section), that help to make the classification clearer. In this paper, we analyze GRB 050509b within the fireshell model. We proceed with the identification of the two basic parameters,  $B$  and  $n_{CBM}$ , within two different scenarios. We first investigate the “ansatz” that this GRB is the first example of a “genuine” short bursts. After disproving this possibility, we show that this GRB is indeed another example of a disguised short burst.

In the next section, we briefly introduce the fireshell model and explain the classification, in section 8.3 we show the analysis of the data, in section 8.4 we present the theoretical spectrum and the study of the fulfillment of the Amati relation, in section 8.5 we comment on the results, and in section 8.6 we finally present our conclusions.

## 8.2. Fireshell model

Within the fireshell model (Ruffini et al., 2002, 2004b, 2005c, 2009; Bianco and Ruffini, 2005b,a), all GRBs originate from an optically thick  $e^\pm$  plasma of total energy  $E_{tot}^{e^\pm}$  in the range  $10^{49}$ – $10^{54}$  ergs and a temperature  $T$  in the range 1–4 MeV. After an early expansion, the  $e^\pm$ -photon plasma reaches thermal equilibrium with the engulfed baryonic matter  $M_B$  described by the dimensionless parameter  $B = M_B c^2 / E_{tot}^{e^\pm}$ , which must be  $B < 10^{-2}$  to allow the fireshell to expand further. As the optically thick fireshell composed of  $e^\pm$ -photon-baryon plasma self-accelerates to ultrarelativistic velocities, it finally reaches the transparency condition. A flash of radiation is then emitted. This represents the proper-GRB (P-GRB). The amount of energy radiated in the P-GRB is only a fraction of the initial energy  $E_{tot}^{e^\pm}$ . The remaining energy is stored in the kinetic energy of the optically thin baryonic and leptonic matter fireshell that, by inelastic collisions with the CBM, gives rise to multiwave-

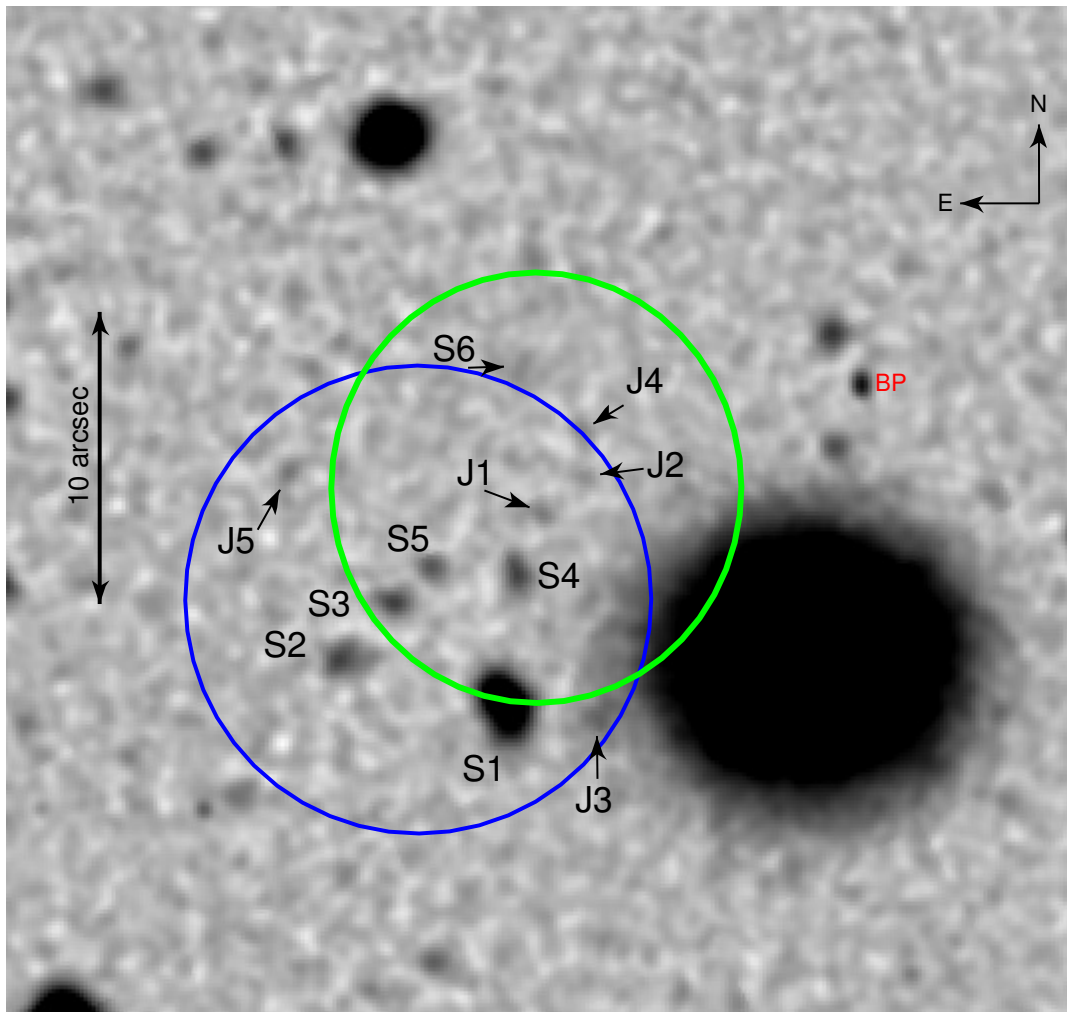


**Figure 8.1.:** Keck LRIS G-band image, zoomed to show the XRT error circle. The larger, blue circle is the revised XRT position from Rol et al. (2005); the smaller, green circle to the west and north of that is the  $2\sigma$  confidence region of the XRT position computed in Bloom et al. (2006). The 11 sources consistent with the Rol et al. (2005) X-ray afterglow localization are labeled in the image. North is up and east is to the left. G1 is the large galaxy to the west and south of the XRT. Bad pixel locations are denoted with “BP”. Figure reproduced from Bloom et al. (2006) with the kind permission of J. Bloom and of the AAS.

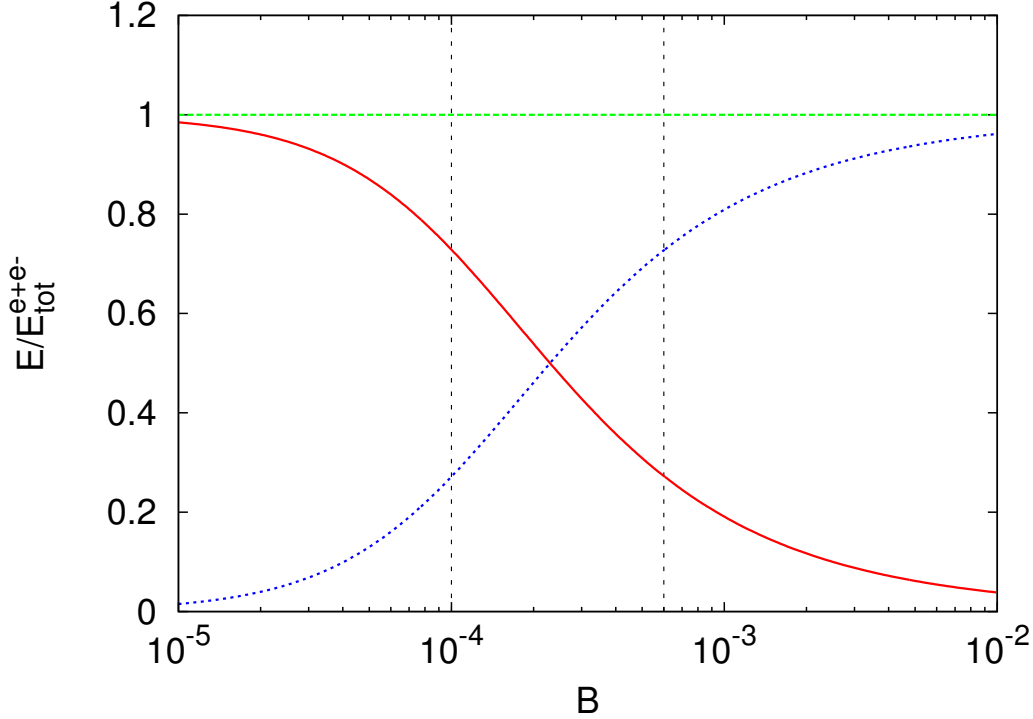


**Figure 8.2.:** The dashed (blue) curve is the energy emitted in the extended afterglow, the solid (red) curve is the energy emitted in the P-GRB, their sum is  $E_{tot}^{e\pm}$ . From left to right, the first vertical line corresponds to the value of  $B = 1.0 \times 10^{-4}$  of scenario 1, the second to the value of  $B = 6.0 \times 10^{-4}$  of scenario 2 (see Sec. 8.3).

length emission. This is the extended afterglow.

Within this model, the value of  $B$  strongly affects the ratio of the energetics of the P-GRB to the kinetic energy of the baryonic and leptonic matter within the extended afterglow phase. It also affects the time separation between the corresponding peaks (Ruffini et al., 2009). For baryon loading  $B \lesssim 10^{-5}$ , the P-GRB component is always energetically dominant over the extended afterglow (see Fig. 8.2). In the limit  $B \rightarrow 0$ , it gives rise to a “genuine” short GRB. Otherwise, when  $3.0 \times 10^{-4} \lesssim B \leq 10^{-2}$ , the kinetic energy of the baryonic and leptonic matter, and consequently the extended afterglow emission, predominates with respect to the P-GRB (Ruffini et al., 2002; Bernardini et al., 2007). Since the “critical” value of  $B$  corresponding to the crossing point in Fig. 8.2 is a slowly varying function of the total energy  $E_{tot}^{e\pm}$ , for  $10^{-5} \lesssim B \lesssim 3.0 \times 10^{-4}$  the ratio of the total energies of the P-GRB and the extended afterglow is also a function of  $E_{tot}^{e\pm}$ .

The extended afterglow luminosity in the different energy bands is governed by two quantities associated with the environment: the CBM density

profile,  $n_{CBM}$ , and the ratio of the effective emitting area  $A_{eff}$  to the total area  $A_{tot}$  of the expanding baryonic shell,  $\mathcal{R} = A_{eff} / A_{tot}$ . This second parameter takes into account the CBM filamentary structure (Ruffini et al., 2004b). Typical values of  $\mathcal{R}$  ranges between  $10^{-10}$  and  $10^{-6}$  (see e.g. Bernardini et al., 2007, 2005a; Caito et al., 2009, 2010; Dainotti et al., 2007; Ruffini et al., 2006b).

The emission from the baryonic matter shell is spherically symmetric. This allows us to assume, to a first approximation, a modeling of thin spherical shells for the CBM distribution and consequently only consider their radial dependence (Ruffini et al., 2002). The emission process is assumed to be thermal in the comoving frame of the shell (Ruffini et al., 2004b). The observed GRB non-thermal spectral shape is produced by the convolution of a very large number of thermal spectra with different temperatures and different Lorentz and Doppler factors. This convolution is performed over the surfaces of constant arrival times for the photons at the detector (EQuiTemporal Surfaces, EQTSs; Bianco and Ruffini, 2005b,a) encompassing the total observation time. The fireshell model does not address the plateau phase described by Nousek et al. (2006), which may not be related to the interaction of the single baryonic shell with the CBM (Bernardini et al., 2010).

In the context of the fireshell model, we considered a new class of GRBs, pioneered by Norris and Bonnell (2006). This class is characterized by an occasional softer extended emission after an initial spike-like emission. The softer extended emission has a peak luminosity lower than the one of the initial spike-like emission. As shown in the prototypical case of GRB 970228 (Bernardini et al., 2007) and then in both GRB 060614 (Caito et al., 2009) and GRB 071227 (Caito et al., 2010), we can identify the initial spike-like emission with the P-GRB and the softer extended emission with the peak of the extended afterglow. A crucial point is that the time-integrated extended afterglow luminosity (i.e. its total radiated energy) is much higher than the P-GRB one. This unquestionably identifies GRB 970228 and GRB 060614 as canonical GRBs with  $B > 10^{-4}$ . The consistent application of the fireshell model allows us to infer the CBM filamentary structure and average density, which, in that specific case, is  $n_{CBM} \sim 10^{-3}$  particles/cm<sup>3</sup>, typical of a galactic halo environment (Bernardini et al., 2007). This low CBM density value explains the peculiarity of the low extended afterglow peak luminosity and its more protracted time evolution. These features are not intrinsic to the progenitor, but depend uniquely on the peculiarly low value of the CBM density. This led us to expand the traditional classification of GRBs to three classes: “genuine” short GRBs, “fake” or “disguised” short GRBs, and the remaining “long duration” ones.

A CBM density  $n_{CBM} \sim 10^{-3}$  particles/cm<sup>3</sup> is typical of a galactic halo environment, and GRB 970228 was indeed found to be in the halo of its host galaxy (Sahu et al., 1997; van Paradijs et al., 1997). We therefore proposed that the progenitors of this new class of disguised short GRBs are merging binary systems, formed by neutron stars and/or white dwarfs in all possi-

ble combinations, which spiraled out from their birth place into the halo (see Bernardini et al., 2007; Caito et al., 2009; Kramer, 2008). This hypothesis can also be supported by other observations. Assuming that the soft-tail peak luminosity is directly related to the CBM density, short GRBs displaying a prolonged soft tail should have a systematically smaller offset from the center of their host galaxy. Some observational evidence was found in this sense (Troja et al., 2008). However, the present sample of observations does not enable us to derive any firm conclusion that short GRBs with extended emission have smaller physical offsets than those without extended emission (Fong et al., 2010; Berger, 2011).

### 8.3. Data analysis of GRB 050509b

#### 8.3.1. Scenario 1

We first attempt to analyze GRB 050509b under the scenario that assumes it is a “genuine” short GRB, namely a GRB in which more than 50% of the total energy is emitted in the P-GRB. This would be the first example of an identified “genuine” short GRB.

Within our model, the only consistent solution that does not contradict this assumption leads to the interpretation that all the data belongs to the extended afterglow phase; the BAT data of the prompt emission (see figure 2 in Gehrels et al., 2005) are then the peak of the extended afterglow, and the XRT data represents the decaying phase of the extended afterglow (which in the literature is simply called “the afterglow”, see section 8.2).

In figure 8.3, we show the result of this analysis. We obtained the following set of parameters:  $E_{tot}^{e^\pm} = 2.8 \times 10^{49}$  erg,  $B = 1.0 \times 10^{-4}$ , and  $n_{CBM} = 1.0 \times 10^{-3}$  particles/cm<sup>3</sup>. These parameters would imply, however, that the energy emitted in the P-GRB should be almost 72% of the total value. This P-GRB should have been clearly observable, and has not been detected. Consequently, this scenario is ruled out and we conclude that GRB 050509b cannot be interpreted as a “genuine” short GRB.

#### 8.3.2. Scenario 2

We now analyze GRB 050509b under the alternative scenario that assumes the energy of the extended afterglow is higher than the P-GRB one. Within our model, the only consistent solution that does not contradict this assumption leads to the prompt emission observed by BAT (see Fig. 2 in Gehrels et al., 2005) being interpreted as the P-GRB, and the X-ray decaying afterglow data observed by XRT being interpreted as the extended afterglow.

In Fig. 8.4, we show the result of this analysis. We obtained the parameters  $E_{tot}^{e^\pm} = 5.52 \times 10^{48}$  erg,  $B = 6 \times 10^{-4}$ , and an almost constant CBM density

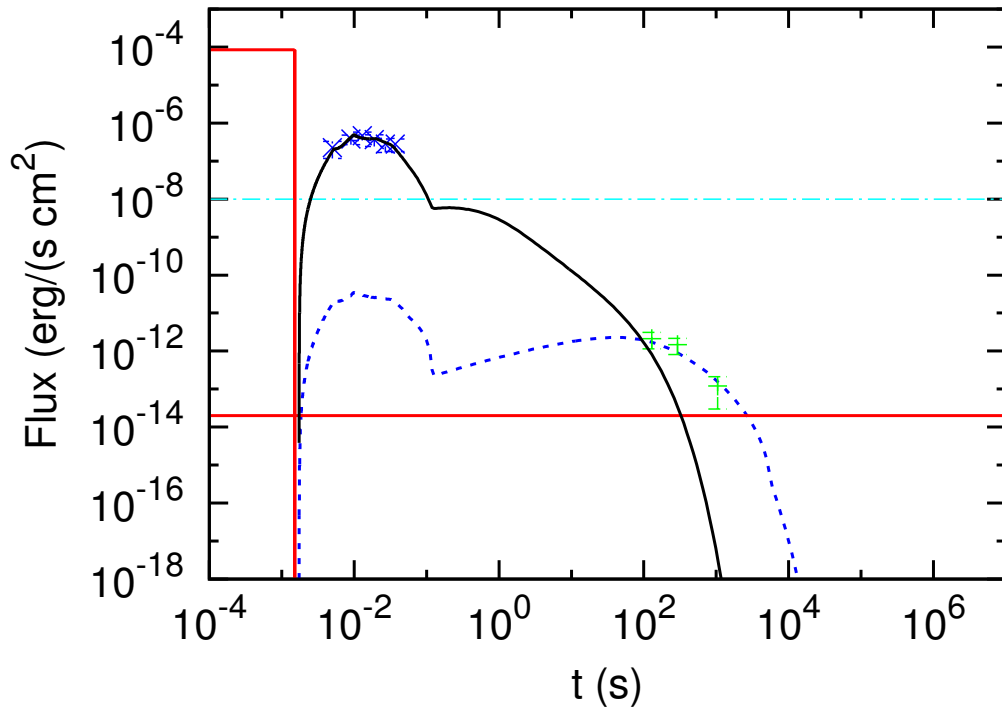


**Figure 8.3.:** Our numerical simulation within scenario 1, assuming that GRB 050509b is a “genuine” short GRB, i.e. that the P-GRB is energetically predominant over the extended afterglow. The BAT data (crosses) are interpreted as the peak of the extended afterglow. In this case, the predicted P-GRB (solid rectangle) total energy is more than twice the extended afterglow one. The solid line is the theoretical light curve in the 15-150 keV energy band, and the dashed one is the theoretical light curve in the 0.3-10 keV energy band. The dot-dashed horizontal line represents the BAT threshold and the solid horizontal one represents the XRT threshold.

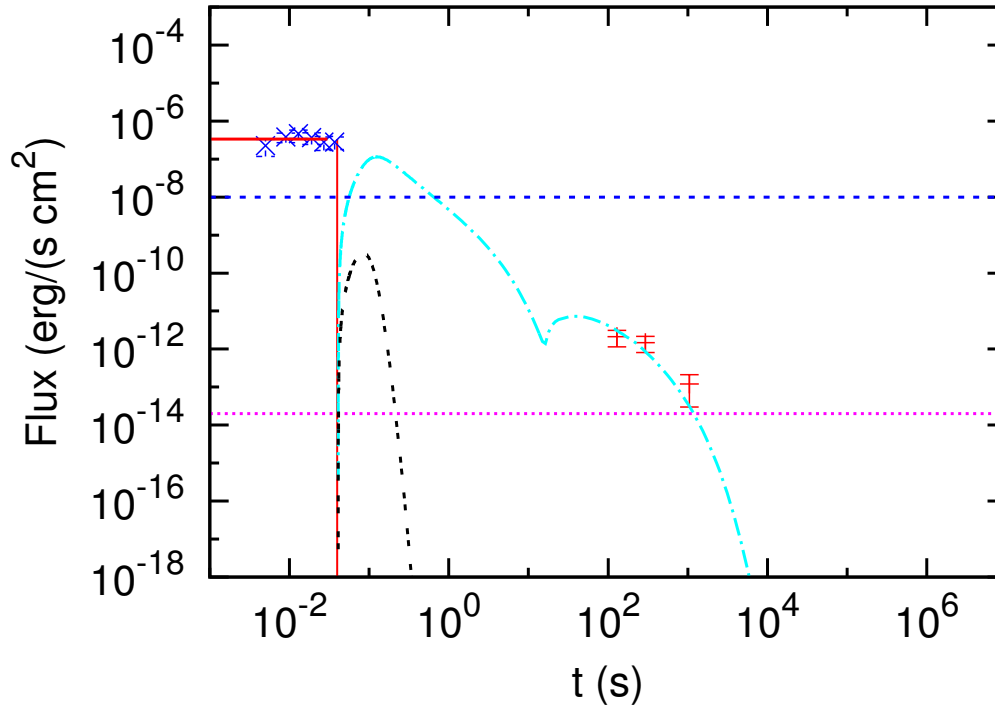


**Figure 8.4.:** Our numerical simulation within scenario 2, assuming that the extended afterglow is energetically predominant over the P-GRB. In this case, the predicted P-GRB (solid rectangle) is less than twice the extended afterglow. We interpret the BAT data (crosses) as the P-GRB and the XRT data as the extended afterglow. The P-GRB has just 28% of the total energy. The double-dashed line is the theoretical light curve in the band 15–150 keV, and the dot-dashed line is the theoretical light curve in the band 0.3–10 keV. The two horizontal lines are from above to below: the BAT threshold and the XRT threshold.

$n_{CBM} = 1.0 \times 10^{-3}$  particles/cm<sup>3</sup>. The low value of the number density is justified by the GRB being located 40 kpc away from the center of the host galaxy (Bloom et al., 2006, , see Fig. 8.1). The initial value of  $\mathcal{R}$  is quite large,  $\mathcal{R} = 1.2 \times 10^{-1}$ , which indicates that there is a very homogeneous CBM in the region close to the progenitor system. However, at  $t \approx 10$  seconds, corresponding to a fireshell radius of  $\sim 2 \times 10^{16}$  cm, the effective area of interaction between the expanding plasma and the CBM drops six orders of magnitude and we have  $\mathcal{R} = 3 \times 10^{-7}$ , a value pointing to the typical CBM filamentary structure also encountered in other sources (see Sec. 8.2). The P-GRB has an estimated energy of  $E_{P-GRB} = 28\% E_{tot}^{\pm}$ , which means that 72% of the energy is released in the extended afterglow. The peak of the extended afterglow, theoretically predicted by our model in figure 8.4, was not observed by BAT, since the energy was below its threshold, and also not observed by XRT, since unfortunately its data collection started only 100 seconds after the BAT trigger.

Following our classification, therefore, due to the values of the baryon loading and of the CBM density, as well as due to the offset with respect to the host galaxy, GRB 050509b is consistent with being another example of a disguised short GRB. This follows the previous identification of GRB 970228 (Bernardini et al., 2007) GRB 060614 (Caito et al., 2009) and GRB 071227 (Caito et al., 2010).

## 8.4. The theoretical spectrum and Amati relation

We turn now to the most interesting aspects of our theoretical work, namely the possibility of inferring some characteristics of the missing data and finally the nature of the burst from first principles. The most effective tool for determining the nature and, then, interpreting the different classes of GRBs, is the Amati relation (Amati et al., 2002; Amati, 2006; Amati et al., 2009). This empirical spectrum-energy correlation states that the isotropic-equivalent radiated energy of the prompt emission  $E_{iso}$  is correlated with the cosmological rest-frame  $\nu F_{\nu}$  spectrum peak energy  $E_{p,i}$ :  $E_{p,i} \propto (E_{iso})^a$ , where  $a \approx 0.5$  and a dispersion  $\sigma(\log_{E_p}) \sim 0.2$ . The Amati relation holds only for long duration bursts, while short ones, as it has been possible to prove after the “afterglow revolution” and the measurement of their redshift, are inconsistent with it (Amati, 2006; Amati et al., 2009).

This dichotomy can naturally be explained by the fireshell model. As recalled in Sect. 8.2, within this theoretical framework the prompt emission of long GRBs is dominated by the peak of the extended afterglow, while that of the short GRBs is dominated by the P-GRB. Only the extended afterglow emission follows the Amati relation (see Guida et al., 2008b; Caito et al., 2010). Therefore, all GRBs in which the P-GRB provides a negligible contribution to the prompt emission (namely the long ones, where the P-GRB is at most a

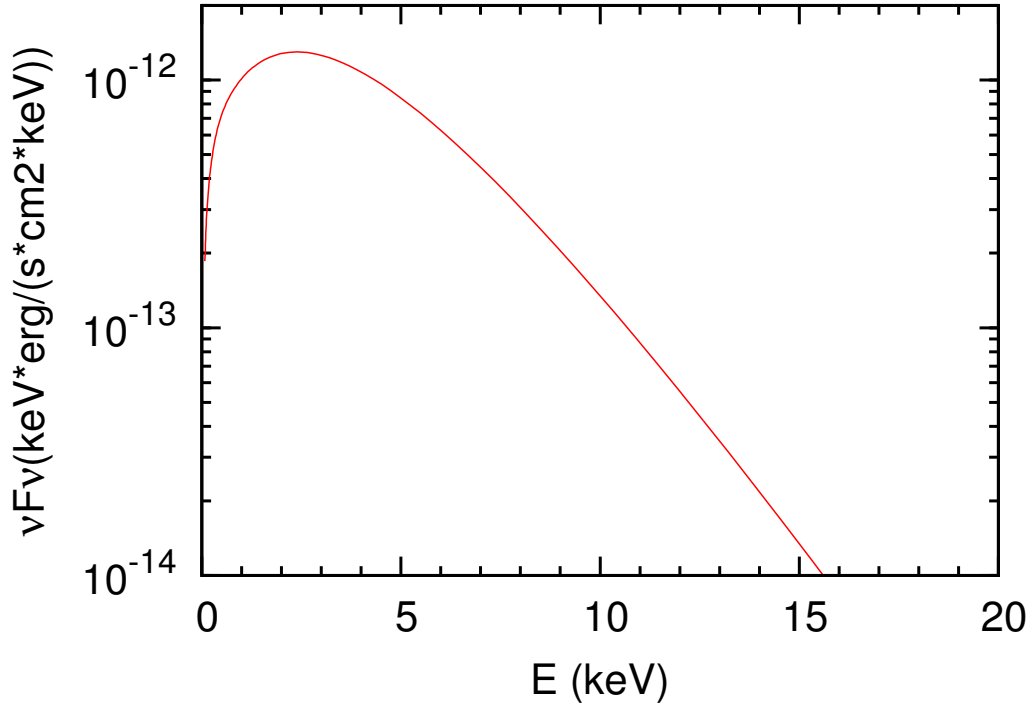


**Figure 8.5.:** Our theoretical spectrum in the observer frame integrated over the entire extended afterglow up to  $10^4$  s, see also Guida et al. (2008b).

small precursor) fulfill the Amati relation, while all GRBs in which the extended afterglow provides a negligible contribution to the prompt emission (namely the short ones) do not (see Bernardini et al., 2007, 2008; Guida et al., 2008b; Caito et al., 2009, 2010). As a consequence, for disguised short bursts the two components of the prompt emission must be analyzed separately. The first spikelike emission alone, which is identified with the P-GRB, should not follow the Amati relation; the prolonged soft tail, which is identified with the peak of the extended afterglow, should instead follow the Amati relation. This has been confirmed in the cases of GRB 060614 and GRB 071227 (Caito et al., 2010).

Owing to the lack of extended afterglow observational data before 100 seconds, there is no way to confirm whether this source follows the Amati relation on an observational ground. To verify whether GRB 050509b follows the Amati relation, and so clarify its nature, we simulated a theoretical spectrum (see figure 8.5), following scenario 2, to verify a posteriori the consistency of this source with the Amati relation.

We first calculate  $E_{iso}$ , which, as mentioned above, in our case is not the total energy of the GRB but the total energy of the extended afterglow,  $E_{iso} \equiv E_{after} = 72\%E_{tot}^{\pm} = 4 \times 10^{48}$  erg. To calculate  $E_{p,i}$ , we simulated the  $\nu F\nu$  theoretical spectrum integrated over the entire extended afterglow up to  $10^4$

s, as described in Guida et al. (2008b). The theoretical  $\nu F_\nu$  spectrum in the observer frame is shown in figure 8.5: it peaks at  $E_p \sim 2.3$  keV, which implies that  $E_{p,i} = (1+z)E_p \sim 2.8$  keV.

We also checked the position of GRB 050509b in the  $E_{p,i}/E_{iso}$  plane considering only the short hard spikelike emission observed by BAT, which is identified with the P-GRB. In this case, only a lower limit to  $E_{p,i}$  can be established from the observational data. The  $\nu F_\nu$  observed spectrum in the BAT 15–150 keV energy range indeed increase with energy and does not exhibit any peak (Bloom et al., 2006). Therefore, a first estimate would lead us to conclude that  $E_p > 150$  keV and then that  $E_{p,i} > 184$  keV. The corresponding value of the isotropic equivalent energy emitted in the BAT 15–150 keV energy range is  $E_{iso,15-150} = (2.7 \pm 1) \times 10^{48}$  ergs (Bloom et al., 2006). Bloom et al. (2006) conclude that the total isotropic equivalent energy emitted can be  $E_{iso} \gtrsim 3E_{iso,15-150}$  if  $E_p \gtrsim 1-2$  MeV. A more conservative estimate of  $E_{p,i}$  and  $E_{iso}$  can be found by fitting the observed BAT spectrum with a Band model where  $\alpha$  and  $\beta$  indices are fixed to typical values ( $\alpha = -1$  and  $\beta = -2.3$ ). This leads to the following lower limit to  $E_p$  at 90% c.l. of  $E_p > 55$  keV, which corresponds to  $E_{p,i} > 67$  keV. To compute the corresponding total isotropic equivalent energy  $E_{iso}$ , we must integrate this Band spectrum from 1 keV to 10000 keV. Since the exact value of  $E_p$  is not known, but we have only a lower limit, the result of this integration, and therefore  $E_{iso}$ , will depend on  $E_p$ . We find that  $E_{iso}$  can range from  $5 \times 10^{48}$  erg, if  $E_p$  is equal to its lower limit (i.e.  $E_p = 55$  keV), all the way up to  $3 \times 10^{49}$  erg, if  $E_p$  is as high as the upper limit of the integration (i.e.  $E_p = 10000$  keV).

In Fig. 8.6, the result of this analysis are shown. When considering both the upper limit following Bloom et al. (2006), namely  $E_{p,i} > 184$  keV and  $2.6 \times 10^{48} < E_{iso} \lesssim 7.8 \times 10^{48}$  erg, and the more conservative upper limit computed above, namely  $E_{p,i} > 67$  keV and  $5 \times 10^{48} < E_{iso} < 3 \times 10^{49}$  erg, we find that the short hard spikelike emission observed by BAT, which is identified with the P-GRB, does not fulfill the Amati relation. When, instead, we consider the peak of the extended afterglow alone ( $E_{p,i} \sim 2.8$  keV,  $E_{iso} \sim 4 \times 10^{48}$  erg, see above), as should be done according to the fireshell scenario (Guida et al., 2008b; Caito et al., 2010), GRB 050509b is fully consistent with the Amati relation.

This result allows us to conclude that, within the theoretical fireshell model, GRB 050509b is consistent with the Amati relation. It implies that this is not a genuine short burst, but instead a long burst disguised as a short one, confirming our hypothesis.

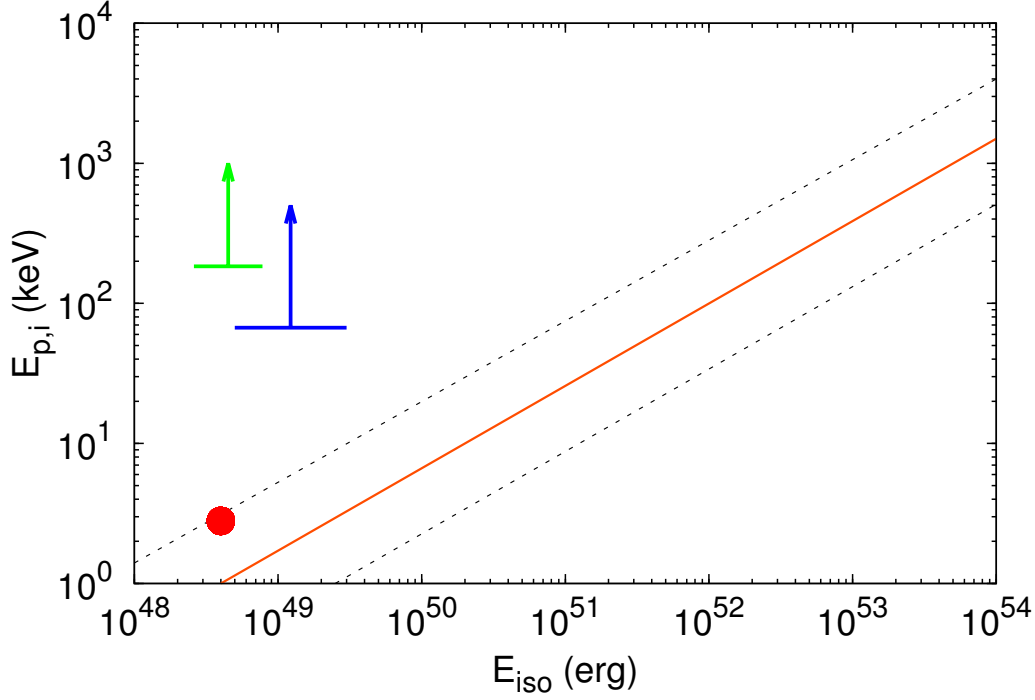


**Figure 8.6.:** GRB 050509b position in the  $E_{p,i}/E_{iso}$  plane. The continuous orange lines show the best-fit power law of the  $E_{p,i} - E_{iso}$  correlation and the dotted gray ones are the  $2\sigma$  confidence region, as determined by Amati et al. (2009). The green lower limit ( $2.6 \times 10^{48} < E_{iso} \lesssim 7.8 \times 10^{48}$  erg and  $E_{p,i} > 184$  keV, computed following Bloom et al., 2006) and the blue lower limit ( $5 \times 10^{48} < E_{iso} < 3 \times 10^{49}$  erg and  $E_{p,i} > 67$  keV, computed following the more conservative approach described in this paper) correspond to the short hard spikelike emission observed by BAT. The red dot ( $E_{iso} \sim 4 \times 10^{48}$  erg,  $E_{p,i} \sim 2.8$  keV) corresponds to the unobserved peak of the extended afterglow theoretically computed within the fireshell model.

## 8.5. Discussion

In a set of papers based on the fireshell model, it has been introduced a new class of GRBs, called “disguised” short GRBs (see Bernardini et al., 2007, 2008; Caito et al., 2009, 2010; Ruffini et al., 2009, and references therein). These are canonical long GRBs with an extended afterglow that is energetically predominant with respect to the P-GRB (see Fig. 8.2). Their main characteristic is that the emission of the afterglow occurs in an environment characterized by a peculiarly low value of the average CBM density ( $n_{CBM} = 1.0 \times 10^{-3}$  particles/cm<sup>3</sup>), which is a value typical of a galactic halo environment. Under this condition, the extended afterglow peak luminosity is much lower than the one expected for a canonical value of the average CBM density inside the galaxy ( $n_{CBM} = 1.0$  particle/cm<sup>3</sup>). Consequently, the extended afterglow peak luminosity is “deflated” and the energy of the extended afterglow is released on a much longer timescale. The energetic predominance of the afterglow with respect to the P-GRB is quantified by the value of the baryon loading  $B$  (see Fig. 8.2) and can be verified by integrating over time the luminosity of the extended afterglow. Examples of this class are GRB 970228 (Bernardini et al., 2007), GRB 060614 (Caito et al., 2009), and GRB 071227 (Caito et al., 2010).

We have shown that GRB 050509b cannot be considered a “genuine” short GRB and proposed that it be classified as a disguised short GRB. We have tested two alternative scenarios for this GRB, one assuming it is a “genuine” short GRB and an alternative one assuming it is a disguised short GRB. We have demonstrated that the only interpretation of the data compatible with the first scenario would lead to an extremely intense P-GRB that is not observed (see Fig. 8.3); therefore this scenario should be discarded and GRB 050509b cannot be interpreted as a “genuine” short GRB. We have instead obtained a reasonable interpretation within the second scenario for  $B = 6.0 \times 10^{-4}$ , corresponding to a long GRB, and an average CBM density of  $n_{CBM} = 1.0 \times 10^{-3}$  particles/cm<sup>3</sup>, which clearly implies that GRB 050509b is a disguised short GRB (see Fig. 8.4).

GRB 050509b does not have XRT data before 100 s. The BAT light curve went beneath its threshold at  $\sim 40$  ms. All the data about the peak of the extended afterglow is therefore missing, which is the relevant part for the calculation of the energy peak  $E_{p,i}$  of the  $\nu F\nu$  spectrum for the Amati relation. Despite this lack of data, it has been possible, from our theoretical simulation, to infer both the spectrum of the extended afterglow peak emission and a value of  $E_{p,i}$ , and to check a posteriori whether GRB 050509b fulfills the Amati relation. This has been done, as already shown in previous papers (Guida et al., 2008b; Caito et al., 2010), by duly neglecting the contribution of the P-GRB, assuming that the Amati relation is connected only to the extended afterglow emission process. It has been proven indeed (see Fig. 8.6) that GRB 050509b, when the P-GRB contribution is neglected, is in perfect agreement

with the Amati relation. This interpretation is also supported by the P-GRB alone being inconsistent with the Amati relation (see also Fig. 8.6, Sec. 8.4 and e.g. Bloom et al., 2006, and references therein).

The understanding reached for this source and others of the same class points also to a difficulty in identifying a “genuine” short GRB. A selection effect is at work: a genuine short GRB must have a very weak extended afterglow (see Fig. 8.2); consequently, it is very difficult to determine its redshift.

## 8.6. Conclusion

It has been shown that GRB 050509b originates from the gravitational collapse to a black hole of a merging binary system consisting of two degenerate stars according to three different and complementary considerations:

1. Very stringent upper limits on an associated supernova event have been established (see Cenko et al., 2005; Bersier et al., 2005; Hjorth et al., 2005; Castro-Tirado et al., 2005; Bloom et al., 2005a,b, 2006);
2. The host galaxy has been identified with a luminous, non-star-forming elliptical galaxy (Prochaska et al., 2005; Gehrels et al., 2005; Bloom et al., 2005a, 2006);
3. The GRB exploded in the halo of the host galaxy (Bloom et al., 2006), because the binary system spiraled out before merging.

From an astrophysical point of view, there are three possible cases of merging binary systems that must be considered:

1. Neutron star / neutron star: unlike the case of GRB 970228 (Bernardini et al., 2007), the low energetics of GRB 050509b disfavor this hypothesis;
2. Neutron star / white dwarf: this appears to be the most likely case for GRB 050509b, as in GRB 060614 (Caito et al., 2009) and in GRB 071227 (Caito et al., 2010);
3. White dwarf / white dwarf: this case is viable only for two very massive white dwarfs, allowing the critical mass of neutron stars against gravitational collapse to a black hole to be overcome in the merging process; that low massive white dwarf / white dwarf merging binary systems may lead to low energetics events has been widely expressed in the literature (see e.g. Iben and Tutukov, 1984; Paczynski, 1985; Pakmor et al., 2010).

From the point of view of GRB classification, we conclude that:

1. GRB 050509b is a disguised short GRB occurring in a low CBM density environment ( $n_{CBM} < 10^{-3}$  particles/cm<sup>3</sup>), typical of a galactic halo;

2. The baryon loading of GRB 050509b, and consequently the ratio of the P-GRB to the extended afterglow energetics, is typical of canonical long-duration GRBs;
3. The possible origin of a genuine short GRB from a merging binary system, as often purported in the literature (see e.g. Meszaros, 2006 but also Gehrels et al., 2009), still remains an open issue both from an observational and a theoretical point of view; in theory, this will crucially depend on the amount of baryonic matter left over in the process of gravitational collapse originating the fireshell baryon loading, which must be  $B \lesssim 10^{-5}$ .

From all the above considerations, it also follows that a binary system merging in a higher density region (i.e.  $n_{CBM} \sim 1$  particles/cm<sup>3</sup>) would give rise to a canonical long-duration GRB without an associated supernova (see also Bernardini et al., 2007; Caito et al., 2009).



# 9. A new class of very energetic GRBs within the fireshell model

Here we present a detailed analysis of two very interesting GRBs: GRB 080319B and GRB 050904. There are two sources with very different redshifts:  $z \sim 1$  and  $z \sim 6.3$  respectively, but present many similarities. In fact, both of them are very energetic sources, with an isotropic energy of the order of  $10^{54}$  ergs and show a very intense optical emission; furthermore, their light curves present a similar structure: both of them have a strong temporal variability.

## 9.1. GRB 080319B

GRB 080319B was discovered by the Burst Alert Telescope (BAT) on board of the Swift satellite on March 19, 2008 (Racusin et al., 2008). It is a very peculiar burst: it is the most luminous GRB observed in the optical energy band and one of the brightest in  $\gamma$  and X. It is characterized by a redshift  $z = 0.937$  (Vreeswijk et al., 2008) and an isotropic energy release of  $E_\gamma = 1.32 \times 10^{54}$  ergs (Golenetskii et al., 2008). Furthermore, there is clear evidence that the prompt emission can be separated into two main episodes, partitioned at about 28 s (Stamatikos et al., 2009; Margutti et al., 2008).

We analysed the prompt emission light curve and spectrum of this burst within the Fireshell Model, using the “modified” thermal spectrum. According to the canonical GRB scenario, we identify the first 8 s of emission with the P-GRB and the remaining part of the first episode (ending at about 28 s) with the peak of the extended afterglow, whose temporal variability is produced by the interaction with the Circumburst Medium (CBM). We obtain the best fit of the light curve (fig. 9.1) and the spectrum (fig. 9.2) of this first episode ( $3s \leq t_a^d \leq 28s$ ) with the following parameters:  $E_{e^+e^-}^{tot} = 1.0 \times 10^{54}$  ergs,  $B = 2.5 \times 10^{-3}$  and  $\alpha = -1.8$ ; the Lorentz gamma factor at the transparency point, occurring at  $r_0 = 2.6 \times 10^{14}$  cm, is  $\gamma_0 = 394$ . We also consider a mean number density  $\langle n_{cbm} \rangle \sim 6$  particles  $\text{cm}^{-3}$  and  $\mathcal{R} = 3.5 \times 10^{-10}$ .

Thanks to the high energetics of the burst, it was possible to analyse also spectra more resolved in time. In fig 9.3 is shown, as an example, the spectrum for  $3s \leq t_a^d \leq 13s$ : it can be seen that with the modified thermal spectrum we can correctly reproduce the observational data.

Concerning the second episode, lasting from 28 s to the end of the prompt emission, we propose that it is a “gamma-ray plateau” that originates from

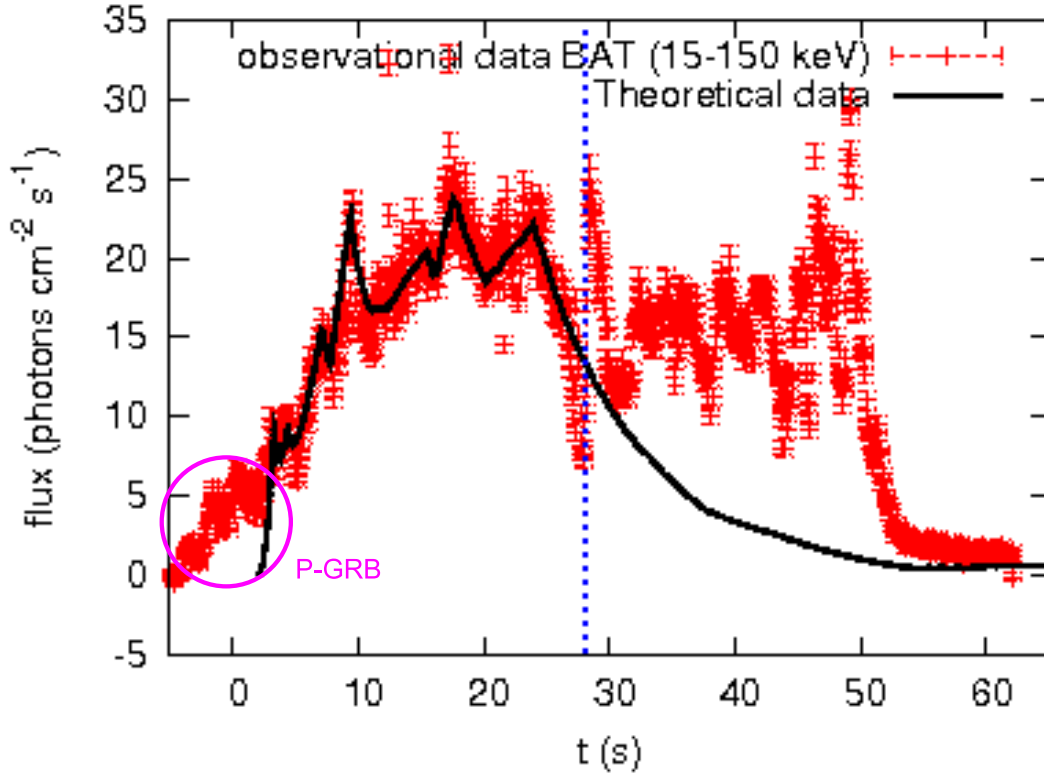


**Figure 9.1.:** Theoretically simulated light curve of GRB 080319B prompt emission in the 15-150 keV energy band (black solid curve) is compared with the observed data (red points); the P-GRB is marked with a magenta circle. The blue vertical dotted line marks the begin of the second part of the prompt emission.

a delayed emission produced by a “second component” of the fireshell, as explained in Sec. 7.2; this interpretation is supported by the correlation between the the Lorentz factor of the second shell and the maximum Lorentz factor of the fireshell (see Bernardini et al., in prep.).

After the prompt emission, GRB 080319B shows also an X-ray afterglow which decays as a simple power-law (Racusin et al., 2008); here we don’t present the study of this component, after the onset of the “gamma-ray plateau”, the dynamics of the fireshell as well as the spectrum of the emitted radiation are different and another treatment is needed.

## 9.2. GRB 050904

GRB 050904 was discovered by BAT on September 4, 2005 (Cummings et al., 2005). This burst is characterized by a very high redshift:  $z = 6.29$  (Kawai et al., 2005) and an isotropic energy release of  $E_{iso} = 1.04 \times 10^{54}$  ergs (Sugita

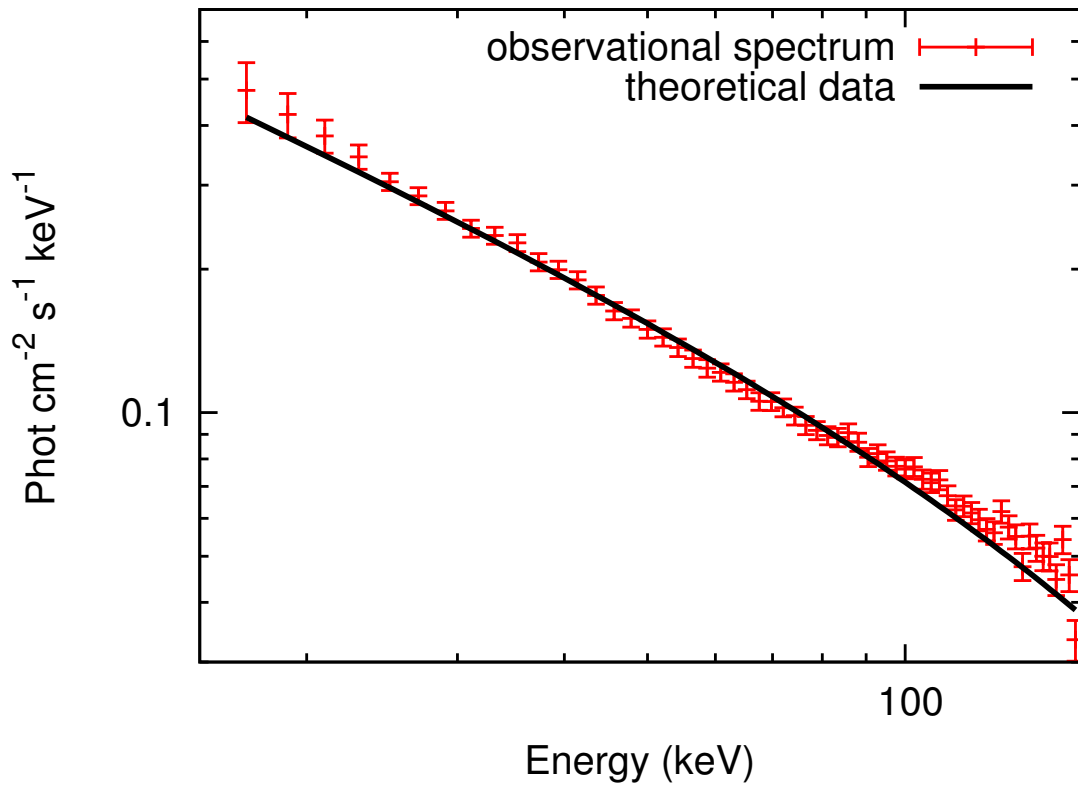


**Figure 9.2.:** Theoretically simulated time integrate spectrum of GRB 080319B for  $3s \leq t_a^d \leq 28s$  (black solid line) is compared with the observed data by BAT (red points).

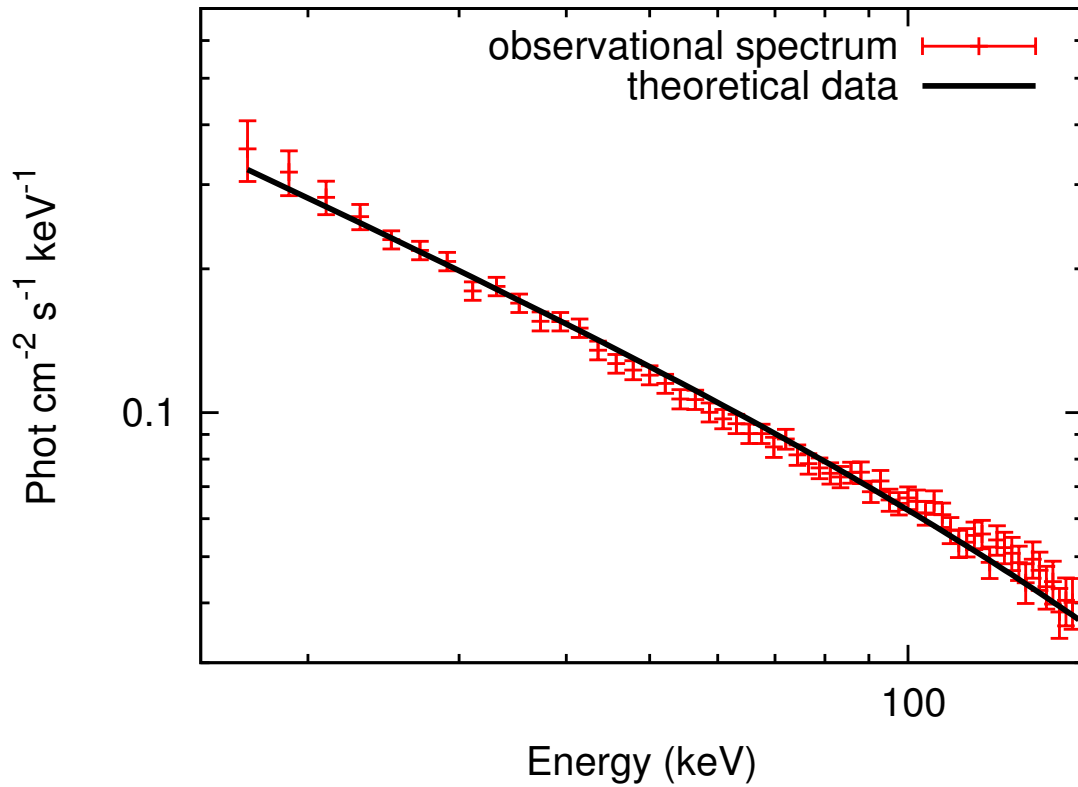


**Figure 9.3.:** Theoretically simulated time integrate spectrum of GRB 080319B for  $3s \leq t_a^d \leq 13s$  with  $\alpha = -1.8$  (black solid line) is compared with the observed data by BAT (red points).

et al., 2009). Furthermore, a bright optical flare was detected by TAROT near the end of the prompt emission (Boër et al., 2006). Another interesting feature of this burst is a long-lasting variability of the X-ray emission, showing several X-ray flares (Watson et al., 2006b; Cusumano et al., 2007). In particular, the light curve shows a bright flare at  $443 \pm 3$  s; this flaring is similar to the one observed in other GRBs at early times (Burrows et al., 2005b), but the light curve does not settle into a power-law decay, continuing to be dominated by large variability (Watson et al., 2006b). We analysed the light curve (fig. 9.4) and the spectrum (fig. 9.5) of the prompt emission within the Fireshell Model, applying the “modified” thermal spectrum. We identify this emission with the peak of the extended afterglow. In this case we don’t see the P-GRB, as its energetics is under the BAT threshold ( $E_{P-GRB}^{iso} = 2.1\%E_{e^+e^-}^{tot} = 1.47 \times 10^{52}$  ergs). The best fit of the light curve (see fig. 9.4) and spectrum (see fig. 9.5) is obtained with the same values of  $E_{e^+e^-}^{tot}$  and  $B$  found for GRB 080319B:  $E_{e^+e^-}^{tot} = 1.0 \times 10^{54}$  ergs,  $B = 2.5 \times 10^{-3}$ ; this is an indication of a similar progenitor for the two sources. Furthermore, also in this case we obtain  $\alpha = -1.8$  and  $\gamma_0 = 394$ . We also considered a mean number density  $\langle n_{cbm} \rangle \sim 10^{-1}$  particles  $\text{cm}^{-3}$  and  $\mathcal{R} = 2 \times 10^{-11}$ ; these values are different from the ones obtained for GRB 080319B and this indicates that, although the two sources have a similar progenitor, the bursts occurred in different environments. Thanks to the high energetics of the burst, it was possible to analyse spectra more resolved in time. In fig. 9.6 is shown, as an example, the spectrum for  $0\text{s} \leq t_a^d \leq 50\text{s}$ : it can be seen that with the modified thermal spectrum we can correctly reproduce the observational data.

We also analysed the XRT observed light curve within the Fireshell Model. In particular, we separate it into two different episodes: a first one, lasting up to  $t_a^d \sim 10^3\text{s}$  and a second one, characterized by a strong flaring activity. We propose that the first episode contributes to the extended afterglow emission, while the second one originates from a delayed emission produced by a “second component” of the fireshell, like the second component identified in the prompt emission of GRB 080319B. This interpretation is supported by the correlation between the the Lorentz factor of the second shell and the maximum Lorentz factor of the fireshell (see Bernardini et al., in prep.).

Concerning the first episode, we can correctly fit the first part of the XRT emission, but there are difficulties in reproducing the steep decay of the flare (see fig. 9.8 and 9.9). Within the fireshell model, flares have the same origin of the prompt emission: they are the result of the interaction of the fireshell with the CBM. The observed discrepancies between the theoretical and the observational data are due to the “radial approximation” adopted in the Fireshell Model: the CBM is arranged in spherical shells (Ruffini et al., 2002). This approximation is valid when the fireshell visible area is larger than the typical size of the CBM clump, but fails when it becomes comparable to the dimension of the clump: this is the case of the X-ray flares, since at those time

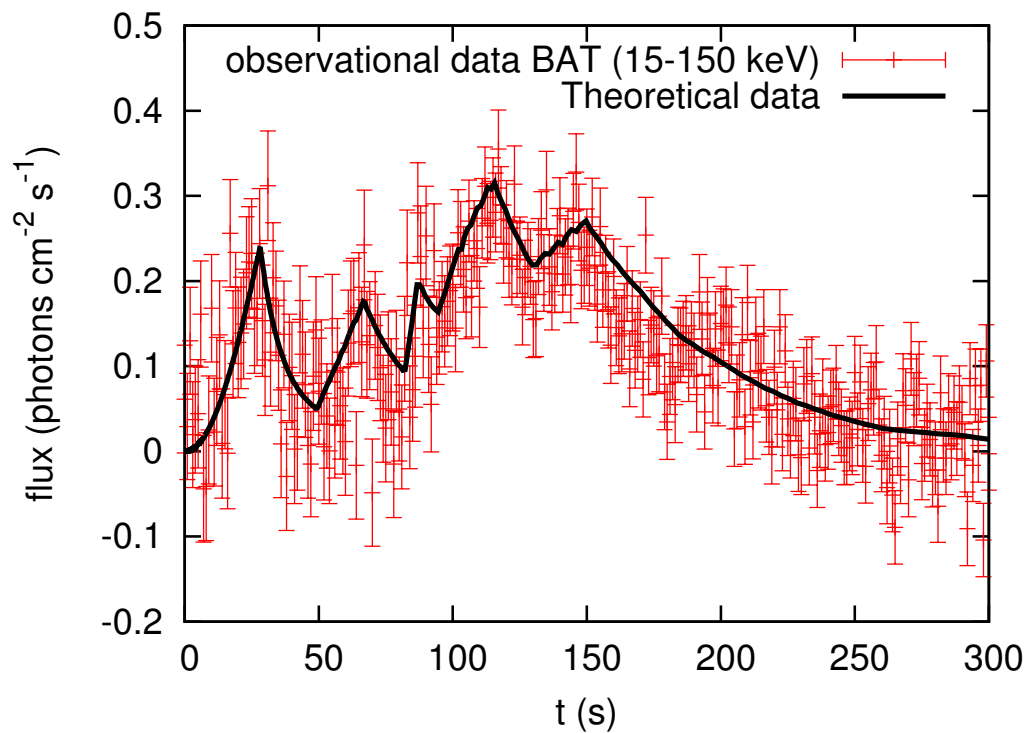


**Figure 9.4.:** Theoretically simulated light curve of GRB 050904 prompt emission in the 15-150 keV energy band (black solid curve) is compared with the observed data (red points).

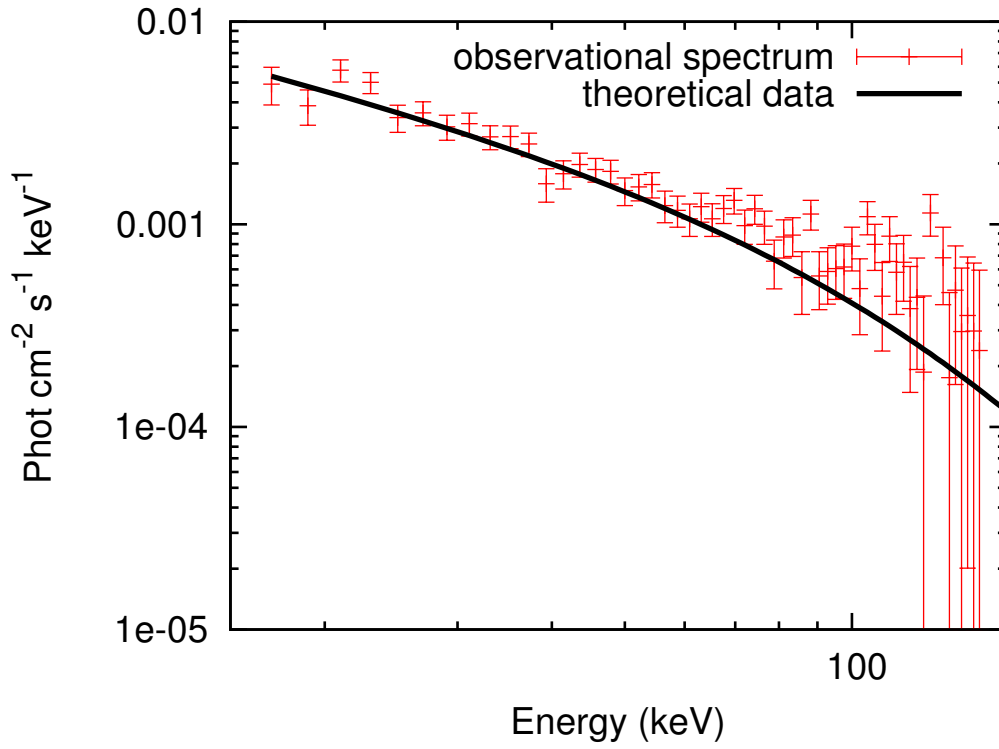


**Figure 9.5.:** Theoretically simulated time integrate spectrum of GRB 050904 for  $0 \leq t_a^d \leq 225s$  (black solid line) is compared with the observed data by BAT (red points).

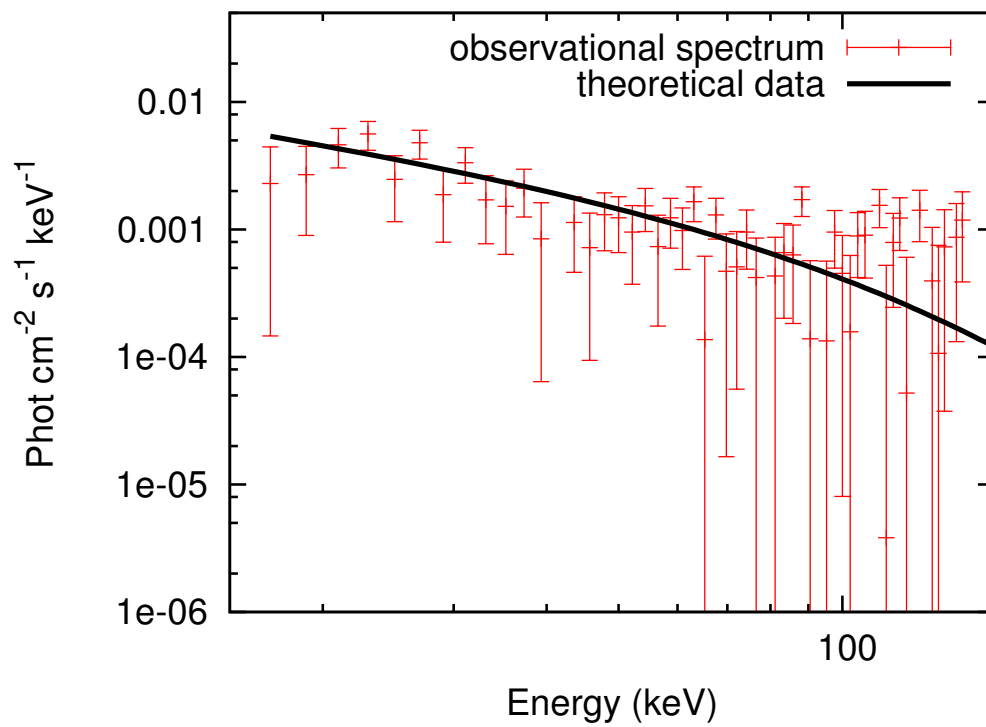


**Figure 9.6.:** Theoretically simulated time integrate spectrum of GRB 050904 for  $0 \leq t_a^d \leq 50s$  (black solid line) is compared with the observed data by BAT (red points).

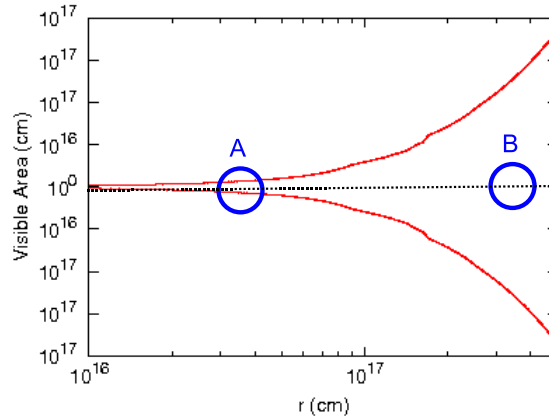


**Figure 9.7.:** Boundaries of the fireshell visible area (red solid lines) compared with the dimensions of two CBM clumps, corresponding to the first spike of the prompt emission (A) and the flare (B).

the fireshell visible area is much larger than during the prompt phase (see fig. 9.7). To solve this problem, following Bernardini et al., we simulate the flare light curve accounting for the three dimensional structure of the CBM clumps: we integrate over the emitting surface only up to a certain angle  $\theta_c$  from the line of sight, corresponding to the transverse dimension of the CBM clump. In this way it is possible to correctly reproduce the observed flare (see fig. 9.10).

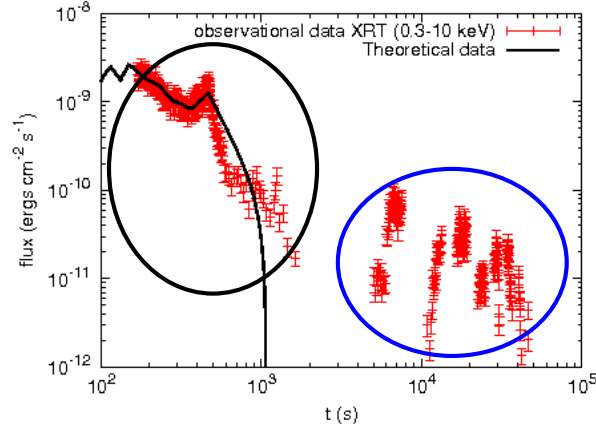


**Figure 9.8.:** Theoretically simulated light curve of GRB 050904 afterglow emission in the Swift XRT energy band (0.2-10 keV) (black solid curve) is compared with the observed data (red points). The black circle marks the first episode, the blue circle the second one.

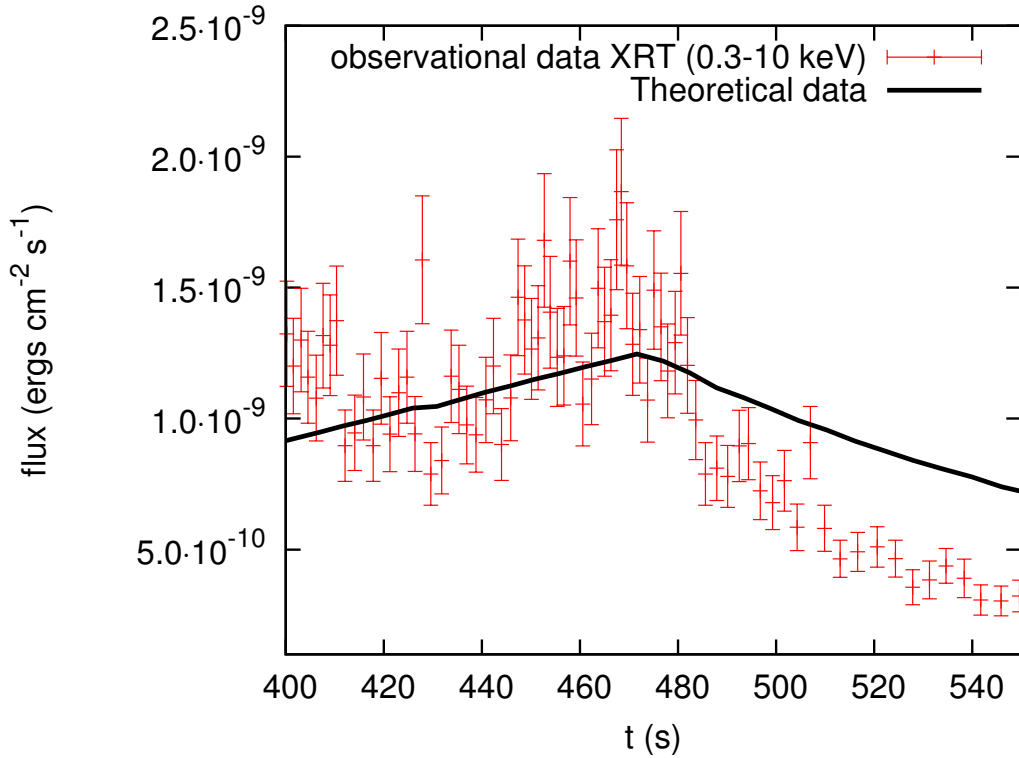


**Figure 9.9.:** Theoretically simulated light curve of GRB 050904 afterglow emission in the Swift XRT energy band obtained under the “radial approximation” (black solid curve) is compared with the observed data (red points).

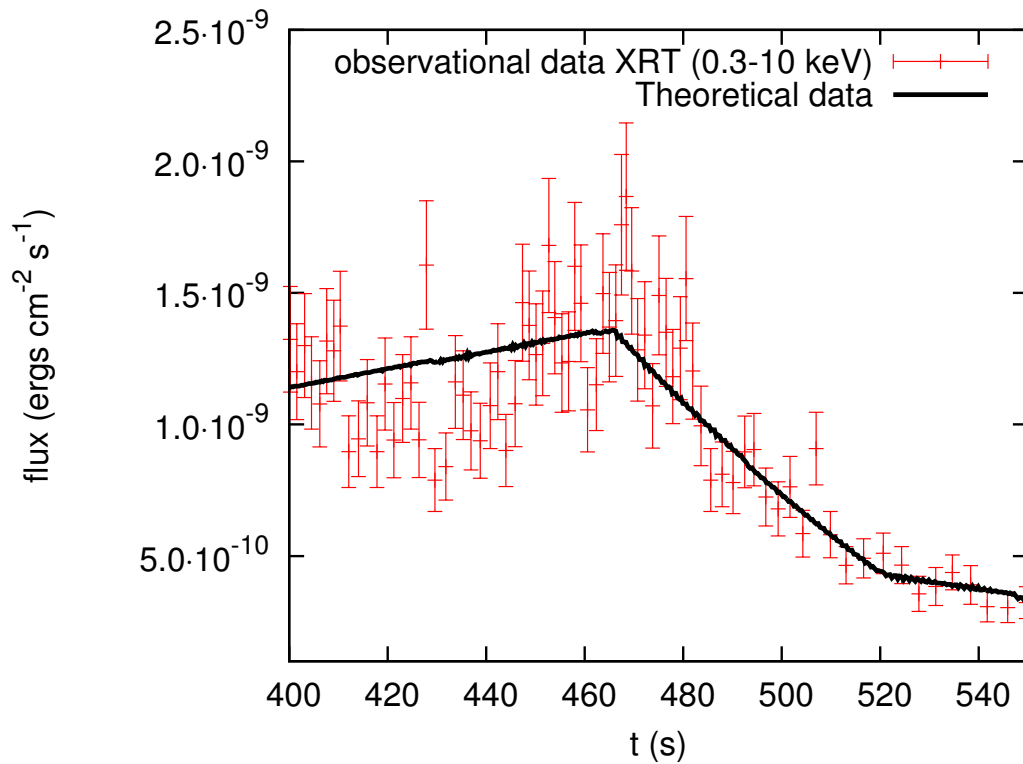


**Figure 9.10.:** Theoretically simulated light curve of GRB 050904 afterglow emission in the Swift XRT obtained by imposing a finite transverse dimension for the CBM clump (black solid curve) is compared with the observed data (red points).



# 10. GRB 090423 : a canonical GRB at redshift 8.1

GRB 090423 is the most distant GRB known to-date, with a spectroscopically determined redshift of  $z \simeq 8.1$ , (Tanvir et al. 2009), that was confirmed with an in-depth analysis of the TNG spectrum of GRB 090423 taken on Apr 23 at 22:16 UT using the Italian TNG 3.6m telescope located in the Canary Islands (Spain), (Guidorzi et al. 2009). The Swift satellite triggered GRB 090423 on April 09, 2009 at 07:55:19 UT, (Krimm et al. 2009). At almost the same instant also the Fermi Gamma Ray Burst Monitor (GBM) triggered on GRB 090423. The two light curves show a structured single peak lasting  $\sim 19$  seconds, while the T-90, in the Swift (15-150 keV) band, is equal to  $12 \pm 1.4$  s. This measure, and the estimate of the redshift, suggests that this GRB is intrinsically a short-GRB. Nevertheless GRB 090423 is fully consistent with the Amati relation, (Amati et al. 2009), so that it is considered as a long-GRB. Moreover if we consider the Swift-BAT sensitivity of  $\sim 10^{-8}$  ergs  $\text{cm}^{-2}$   $\text{s}^{-1}$ , and considering the redshift of  $\sim 8.1$ , it is likely that part of the emission of gamma-rays from GRB 090423 has not been detected because it was below the threshold of Swift-BAT. This evidence is supported by observations of Swift-XRT, which started to observe GRB 090423  $\sim 72$  seconds after the BAT trigger time. The XRT light curve of GRB 090423 is a classical 3-steps X-ray light curve, showing in particular a flare just before the start of the plateau phase. This flare is a signature of a prolonged activity of the peak of the afterglow up to  $\sim 400$  seconds, so when the flare stops then it starts the plateau component.

This second phase in the X-ray afterglow was discovered with the launch of the Swift satellite, which was the first instrument to obtain early X-ray light curves immediately following GRBs. In literature there are several possible explanation for this second component, (Butler & Kovevski 2007, Nousek et al. 2006, Zhang et al. 2006). In the standard model it was attributed to the outflow, being jet-like, and the break in the X-ray light curve occurs when the edge of the jet becomes visible, as the jet slows down, (Meszaros & Rees 2009, Roads 1997, Roads 1999, Sari et al. 1999), while the other models, which exclude a jet-emission model, need a mechanism that allows a prolonged injection of energy, (Kumar & Piran 2000, O'Brien et al. 2006). Here we consider the application of the fireshell model, (Ruffini et al. 2001, Ruffini et al. 2001b, Ruffini 2007a), to GRB 090423, in which a possible alternative to the existing models to explain this second component is the following : we

**Table 10.1.:** Starting parameters for the fireshell fit of GRB 090423

Parameter	Starting value
$E_{dya}$	$1.00 \times 10^{53} \text{ ergs}$
$M_{BH}$	$10 M_{\odot}$
$B$	$\sim 10^{-3}$

consider the shell, which expands in the medium surrounding the burst, as a shell structured, which consists of the classical compact front, but ending more smoothly with a tail of the matter distribution less energetic. As the forward shell collides with the circumburst medium (CBM), it loses energy and velocity while the tail moves forward undisturbed by the collision with the CBM. At a certain time,  $t_r$ , the forward shell, which continues to lose energy and slow down, reaching a Lorentz Gamma factor,  $\Gamma_2$ , value such that it is caught up by the delayed shells, which constitute the tail of the total fireshell. This second shell does not interact with the CBM, since the first one, after its passage, cleaned up most of the interstellar medium near the GRB site, leaving this second shell in a quasi empty space. It's important to note the existence of a correlation between the value of the bulk Lorentz Gamma factor at the transparency,  $\Gamma_0$ , and at the collision of these two shells,  $\Gamma_2$ . This fact is known only for a tens of GRBs, (Bernardini in preparation), and it could be interesting for constraining better the fireshell dynamics.

At this moment it starts the second component, the plateau, which lasts  $10^2 - 10^4$  seconds until a break occurs in the light curve at a time  $t_b$ , where the radiation flow begins to decline steadily. The physical origin of this second component is to seek in the collision of the shell which occurs at  $t_r$ . The collision would generate a sort of refreshed shock, whose following dominant radiation emission process is due to magnetohydrodynamics of electrons accelerated in the shell's collisions.

In the literature there are several indications, see for example (Butler & Kocevski 2007), that the late afterglows is due to a synchrotron-like emission scenario, whose radiation emission theory is well known in the case, (Sari et al. 1998, Granot & Sari 2002). For this reason we strongly believe that the plateau phase and the following X-ray emission is due to another emission process and for the first time we do not expect the equations of motion to hold.

## 10.1. GRB 090423 in the fireshell model

We start the fit of the *Swift*-BAT light curve and the spectrum of GRB 090423 considering as starting parameters the values indicated in the Table 10.2.

In Fig. 10.1 we report the theoretical fit of *Swift*-BAT (15-150 keV) light

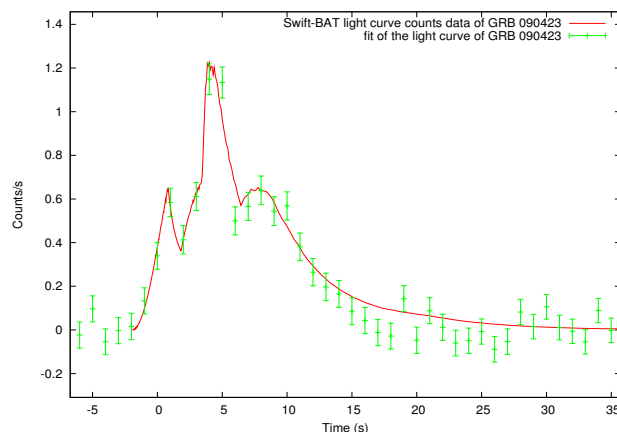


**Figure 10.1.:** *Swift*-BAT (15-150 keV) light curve (green bars) compared with the theoretical fit (red lines).

curve of GRB 090423 prompt emission. As said before, we find the P-GRB below the detector threshold, so we identify all of the gamma-pulses with the afterglow peak emission, in the context of the “fireshell” scenario. These pulses have been reproduced in our simulations assuming a spherical distribution of the density of the CBM. In particular each pulse corresponds to an overdense shell of matter around the site of the burst. On average, we find that during the prompt emission we have for the CBM density the value of  $\langle n \rangle = 5 \times 10^{-2}$  particles/cm<sup>3</sup>. Nevertheless after the prompt emission, when it starts the X-afterglow, the density decreases abruptly up to the lower value of  $10^{-7}$  at the onset of the plateau. In particular the big X-flare, starting at  $T_0 + 170$  s is fitted considering a density shell of  $10^{-5}$ . This value is quite low, but it could be reconsidered in light of the possible shell’s fragmentations, e.g. (Dainotti et al. 2008), as we can see in the next subsection.

Last we obtain for the two parameters characterizing the source in the Fireshell model the value of  $E_{dya} = 1.20 \times 10^{53}$  ergs, and  $B = 8 \times 10^{-4}$ . With these values we obtain an initial plasma created between the radii  $r_1 = 2.93 \times 10^6$  cm and  $r_2 = 1.39 \times 10^8$  cm, with a total number of pairs  $N_{e\pm} = 4.10 \times 10^{57}$  and an initial temperature of about 2.3 MeV. So we can estimate the energy emitted in the P-GRB, which turns out to be  $E_{P-GRB} = 4.5\% E_{dya} = 5.4 \times 10^{51}$  ergs. Immediately we note that, at that redshift and with the energy given by  $E_{P-GRB}$ , the P-GRB should not be visible, as we verify in the observations. The transparency point happens to the radius of  $r_0 = 5.03 \times 10^{13}$  cm, when the fireshell has a Lorentz Gamma factor of about 1100.

For the fit of the energy spectrum we assume that the spectral energy distribution of photons emitted in the co-moving frame of the fireshell is:

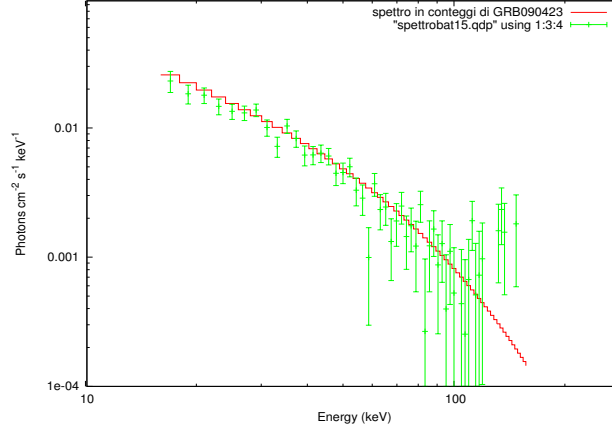


**Figure 10.2.:** *Swift*-BAT (15-150 keV) energy spectrum (green bars) compared with the theoretical fit (red lines).

$$\frac{dE}{dAd\Omega dv dt} = \frac{2hv^3}{c^2} \left( \frac{hv}{k_B T} \right)^\alpha \frac{1}{\exp\left(\frac{hv}{k_B T}\right) - 1} \quad (10.1.1)$$

which is characterized by the parameter  $\alpha$ . The spectrum in the observer's frame is obtained by the convolution over the EquiTemporal Surfaces (EQTS, (Bianco et al. 2001)) and the observational time, (Patricelli et al. in preparation). Here we show the application of this spectral model, for which we find for the  $\alpha$ -index in Eq.(10.1.1) the value of  $\alpha = -1.8$ . The fit of the energy spectrum is plotted in Fig.10.2.

### 10.1.1. The fragmentation of the fireshell

The fit of the X-afterglow of GRB 090423 appears to have a significant lower effective CBM density. This fact could be due to the possible fragmentation of the incoming baryon fireshell. One of the possible causes of the fireshell fragmentation is attributable to the interaction of the same shell with the CBM. In particular at a certain radius the surface of the fireshell, responsible for the radiation emission, does not increase as  $r^2$ , but as  $r^\beta$ , with  $\beta < 2$ , (Ruffini et al. 2007). So the effective CBM density  $n$  is linked to the actual one  $n_{act}$  by the following relation:

$$n = \mathcal{R} n_{act} \quad (10.1.2)$$

where  $\mathcal{R} = (r^*/r)^\delta$ , with  $r^*$  the starting radius at which the fragmentation occurs and  $\delta = 2 - \beta$ . Considering a constant density of the CBM, exactly  $n_{act} = 10^{-2}$  particles/cm<sup>3</sup> at  $r^* = 6 \times 10^{16}$  cm, we obtain from the fit of the late-prompt light curve, the value of  $\beta = -3$ .

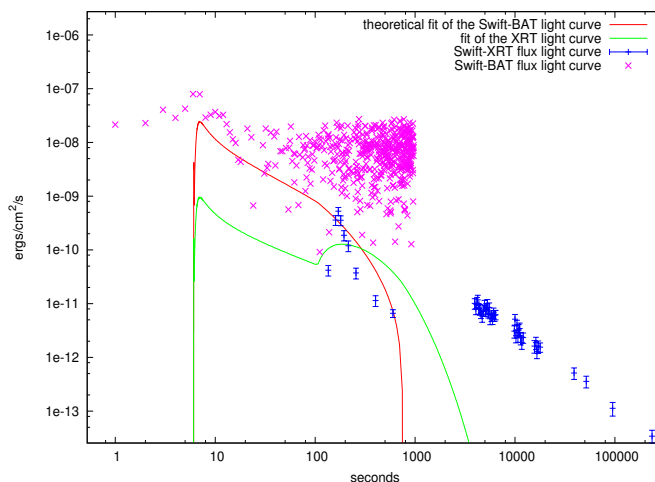


**Figure 10.3.:** The fit of the Swift BAT and XRT light curve of 090423, obtained considering the prompt emission as due to the P-GRB. Note the lack of efficiency for the simulation of the x-ray flare.

### 10.1.2. GRB 090423 considered as a disguised short GRB

In light of the new results from the disguised short GRBs, see Secs. C.3, C.1 and C.2 an intriguing possible explanation for the emission observed in GRB 090423 could be that this GRB is a disguised short GRB. We tried to simulate the emission observed considering the prompt light curve, and of consequence the most energetic part of the GRB, as due to the P-GRB emission, and an intermediate case, where we considered both the contributes, the P-GRB and the extended afterglow, in the GRB prompt light curve.

In the first case, see Fig. 10.3, we don't see the peak of the afterglow and, more important, we are not able to simulate the x-ray flare observed in the XRT light curve. Moreover we don't have in this case enough energy to model the following x-ray emission (the plateau and the late decay), which we consider as due to a different emission mechanism, see next section. In the latter case the simulation of the light curve is in good agreement with the observed data, see Fig. 10.4, but in order to simulate it we must take into account a strong variation of the emitting fireshell area.

In all cases the CBM average density exhibits a sharp variation at a certain radius. This fact seems in agreement with an initial wind density of the CBM,  $\rho \propto r^{-2}$ , and a subsequent high-density cloud,  $\rho \sim 10$  particles/cm<sup>3</sup>.

The work about this source is still in progress, and it would be very interesting in particular to take some other similar results from other high-redshift sources as, for example, GRB 080913.

Finally we note that these two extra possibilities can be discarded by the fact that, at that redshift, the detector threshold act as a sort of selection effect for the GRB emission. In particular there could be a hidden emission that

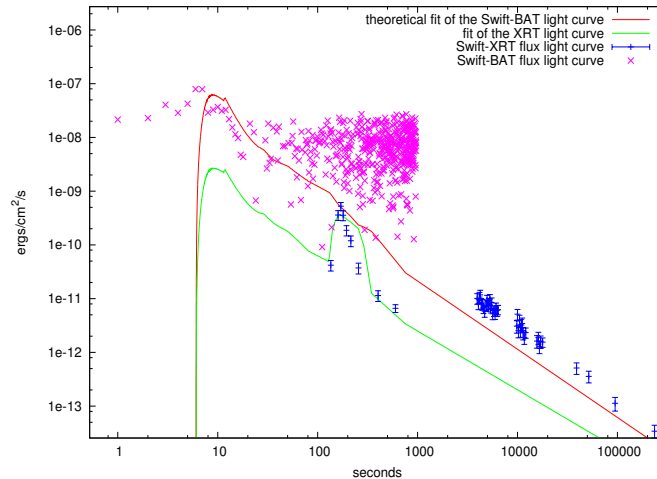


**Figure 10.4.:** The fit of the Swift BAT and XRT light curve of 090423, obtained considering the first 4 seconds of the prompt light curve as due to the P-GRB emission.

was not detected by Swift BAT, and it can be happened both before and after the observed prompt light curve. However we cannot speculate more on this argument, but there is the possibility that the prompt emission is due to the most energetic pulse of the intrinsic hard x-ray emission of the GRB.

## 10.2. A new component in the afterglow scenario

This GRB was first detected in the X-ray by Swift-XRT, which began observing the region of the explosion 72.5 s after the Swift-BAT trigger. The analysis of the first 8.4 ks in the 0.3-10 keV band, (Stratta et al. 2009), reveals a classical 3-steps X-ray trend. In the first steep phase, at T0+170 s, there is a big flare, ending at about T0+260 s when immediately the plateau component starts. At about T0+3.9ks the light curve is well-described by a power-law model with index  $\alpha = -1.30 \pm 0.10$ .

Then we consider the time integrated and time resolved spectral analysis, in particular analyzing the spectrum emitted during each of the X-ray phase. All of these spectrum are well fit by an absorbed power-law spectral model whose energy indexes  $\beta$  are shown in the second column of the Table 10.2. For these spectrum we impose as the Galactic column density the value of  $6.9 \times 10^{22} \text{cm}^{-2}$ , which was found for the fit of the total spectrum, while as intrinsic column density we obtain the value of  $2.9 \times 10^{20} \text{cm}^{-2}$ .

As a result of the previous analysis we report an evident spectral variation in the respective energy index between the first phase and the remaining ones of the X-ray light curve. Nevertheless we note that a similar spectral variation was also noted in the past, (Butler). In that work the authors describe this

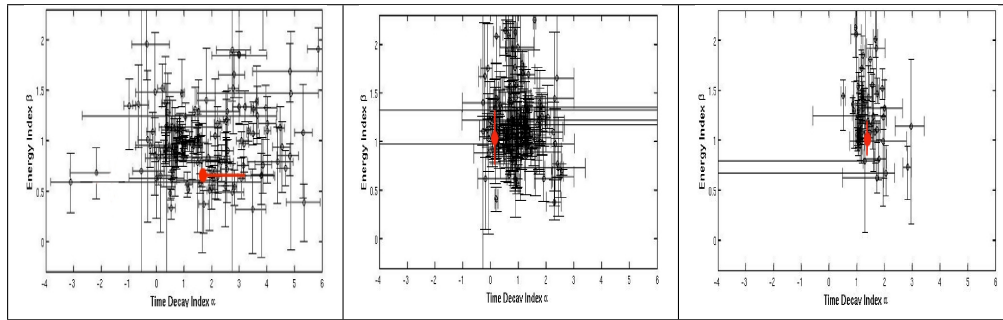


**Figure 10.5.:** Time decay index  $\alpha$  versus Energy index  $\beta$  for the X-ray afterglows for each of the three afterglow phases described in the text. We consider a sample of 133 GRBs with time decay  $\alpha$  and energy index  $\beta$  taken in (Evans2). In particular we consider only energy spectra taken by the Swift-XRT satellite in Photon Counting mode for at least the first two afterglow phases. Note the data sample clustering in the second and the third phase, as delineated in (Butler & Kocevski 2007).

variation as the signature of a second component in the afterglow of GRBs, (Nousek). In particular a detailed spectral analysis of a sample of GRBs, that we reproduce in Fig. 10.5, where the red dot represents GRB090423, led the authors to state that this second component has all of the observational characteristics of an adiabatic external shock synchrotron radiation, e.g. see (Sari). In this work we don't tackle directly this argument, but we assert that after a certain time, the fireshell emission drops down so that the following dominant radiation emission process is due to the magnetohydrodynamics of electrons accelerated in the previous shell's collision. A complete analysis and explanation of these considerations will be explained in a forthcoming paper.

In this way we stop our analysis of GRB 090423 at the start of the plateau component. As delineated previously, the plateau component starts after a big flare lasting about 150 s. It is also the presence of this flare which bring us to the conclusion that 090423 is a long GRB. Indeed it is seen in the X-ray part of the e.m. spectrum, but if we consider the correction for the redshift of the GRB, we obtain that this emission should be stay in the  $\gamma$ -ray part of the e.m. spectrum. Moreover the flare is the signature of a prolonged activity of the shell with the CBM. From our analysis we preliminarily obtain that this flare is due to some blob of interstellar matter located at  $\approx 0.5$  l. y. along the line of sight from the Black Hole formed. At these high distances from the progenitor we have that the fireshell visible area (defined by the condition  $\cos \theta = v/c$ , where  $\theta$  is the angle between the emitted photon and the line of sight, and  $v$  is the fireshell velocity, (Bernardini et al. 2009), is wider than that at short distances, see Fig. , and this fact translates in the fit with a different treatment for the flare: we consider a bidimensional structure

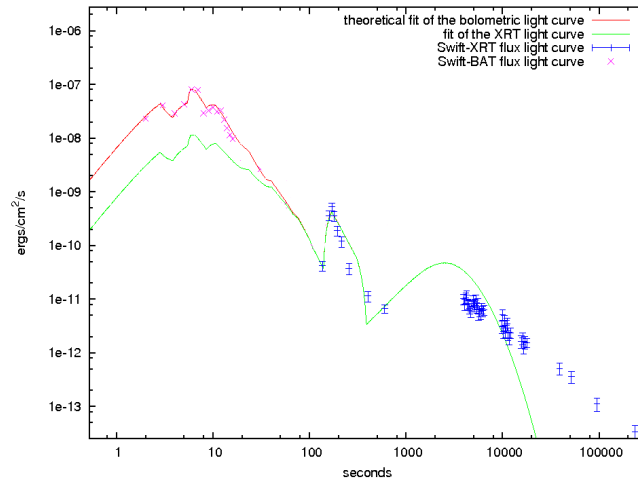


**Figure 10.6.:** The fit of the X-ray light curve of 090423. Note the end-point  $t$  the start of the plateau and the fit of the BAT light curve (in purple).

**Table 10.2.:** Time-resolved X-light curve analysis. The light curve index for the plateau and late decay phase are taken from the XRT refined analysis, (Stratta et a. 2009)

Phase	$\beta$	$\alpha$	$C - STAT$
Total	$0.825 \pm 0.09$	$xxx$	308.11(345)
Flare	$0.44 \pm 0.20$	$< -1.4$	152.65(168)
Plateau	$1.01 \pm 0.33$	$0.13 \pm 0.11$	109.19(118)
Late	$0.901 \pm 0.15$	$-1.30 \pm 0.10$	238.63(271)
Plateau + Late	$0.93 \pm 0.14$	$xxx$	279.81(301)

of the CBM clump along the line of sight, as already done for GRB 011121, (Caito et al. 2009). For this reason we integrate up to a well-defined angle  $\theta_c$  from the line of sight, corresponding to the transverse dimension of the CBM clump which in this case is given by  $d_c = 2r_c \sin \theta_c$ , where  $r_c$  is the distance of the clump from the formed black hole. We obtain a good fit for the flare considering a cut at 170 s after the initial emission, which corresponds to a distance from the black hole formed of  $r_{cut} = 3.25 \times 10^{17}$  cm. The final fit of the flare is shown in Fig.10.8 while a graphical explanation of our flare analysis is shown in Fig.10.9. Even if the fireshell emission after the cut is different from that simulated, our procedure confirms the fact that we can obtain a good representations of the flares in the context of the interactions of the fireshell with the CircumBurst medium. However, in order to simulate the effective emission after a cut to the fireshell visible area, it is required a net improvement of the code, also for a fully treatment in a three-dimensional context of the CBM clump responsible for the flare.

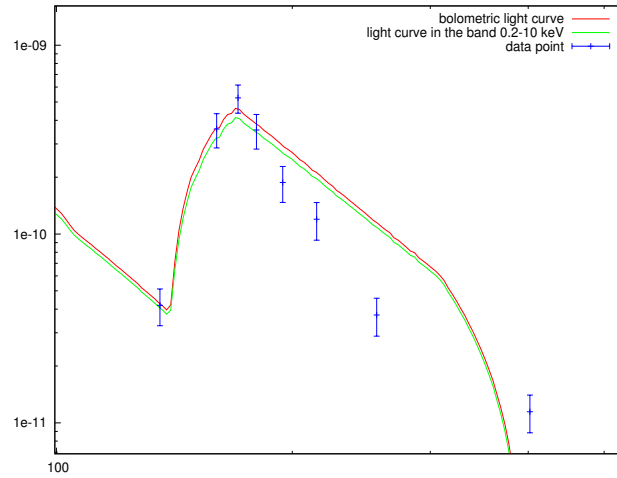


**Figure 10.7.:** The fit of the X-ray flare of 090423 considering that all of the emission from the fireshell contributes to it.

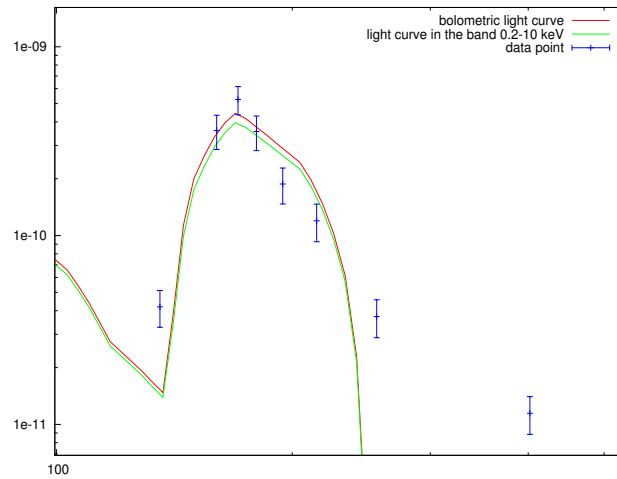


**Figure 10.8.:** The fit of the X-ray flare of 090423. In order to obtain a good fit, we consider a cut to the fireshell visible area corresponding to the total emission up to 170 s after the initial emission.

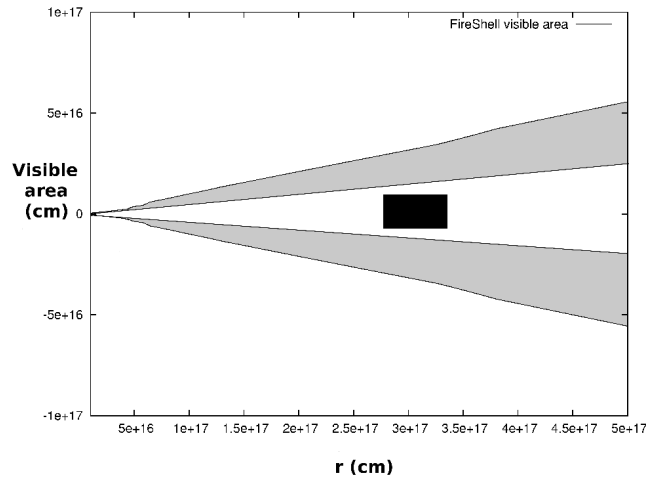


**Figure 10.9.:** A graphical explanation for the cut to the fireshell visible area explaining the flare in the X-ray light curve.

### 10.3. Discussions and conclusions

GRB 090423 is the most distant GRB up to date, with a redshift of about  $z = 8.1$ . In the cosmological  $\Lambda$ CDM standard model this means that 090423 bursted about 700.000 years after the Big Bang. For this reason we argue that 090423 originated from the collapse of a massive star, generating a Black Hole with a minimum mass of 10 solar masses. A binary merging origin is rejected since the time for the formation and the merging of two compact binary stars is supposed greater than 700.000 years.

The fit in the fireshell scenario suggests that 090423 is a canonical Gamma Ray Burst. We obtain a CBM average density of about  $10^{-2} \text{ \#}/\text{cm}^3$ , and a high value of the Lorentz Gamma factor at the transparency  $\Gamma \approx 10^3$ . The presence of a big flare in the X-ray light curve is a signature of the late interaction of the fireshell with the CBM and, more important, is the confirmation that 090423 is a long GRB. This fact is supported also by the fact that this GRB satisfies the Amati relation.

The X-ray light curve consists of 3 distinct power-law segments. The first one consists of a rapid flux decay (if we do not consider the flare) and it represents the residual emission of the fireshell. In the second phase the flux is approximately constant so the light curve become shallower than the previous phase, while in the last one we have another flux decay but with a different time decay index  $\alpha$  than the first phase. Nevertheless we note a variation in the power-law spectral index  $\beta$  between the first and the remaining 2 X-ray light curve phases. This fact is more evident in the diagram shown in Fig.10.5, where is reported the same analysis but considering a sample of 133 GRBs.

In particular it is clearly evident a clustering of the data sample in the second and the third phases. This fact suggests the presence of a second component in the GRB scenario. We are studying this possibility in the FireShell scenario and in particular we believe that this second component is due to the structure of the FireShell, (De Barros et al. 2009). In particular the ejecta should have a range of bulk Lorentz factor  $\Gamma$ , interacting with each other when the outer shells slow down due to the interaction with the CBM. This interaction should generate some bumps, turning off the FireShell emission and highlighting sub-process of emission due to the magnetohydrodynamics of the electrons accelerated in the previous shell's collisions. One of the possible evolutions of the model will be the explanation of this second component in terms of this electron-generated emission.



# 11. The high-energy emission in the fireshell scenario

The launch of the *Fermi* satellite opened a new window on the GRB science. Thanks to the Large Area Telescope (LAT) (Atwood et al., 2009) on-board the *Fermi* spacecraft, we can detect very high energy photons ( $> 100$  MeV) from GRBs. The first result we obtained from *Fermi* is that not all GRBs own this high energy component, but just a fraction of them: currently LAT has detected energetic photons from  $\sim 20$  GRBs upon the whole set of  $\sim 480$  GRBs detected by the *Fermi* Gamma-ray Burst Monitor (GBM) (Meegan et al., 2009). However this last evidence has been already noticed by the EGRET detector on board the Compton Gamma-Ray Observer satellite, which detected high energy photons just from few GRBs.

The other very interesting discovery of the *Fermi* LAT was that this high energy component is delayed compared to the emission observed by the GBM detector. Moreover when the GBM signal fades in the canonical way, the high energy one is prolonged and can last for hundreds of seconds. The case of GRB 080916c (Abdo et al., 2009b) is remarkable: it is currently the most energetic GRB to date, with an estimated isotropic energy of  $E_{iso} = 8.8 \times 10^{54}$  ergs. A significant contribution to this value was provided by the high-energy gamma-rays ( $> 100$  MeV) emitted by this GRB. Moreover this high energy emission started  $\sim 3.6$  s after the GBM trigger and persisted up to 1400 s after the GBM trigger. The spectral energy distribution of these high energy photons is best represented by a power-law function, whose photon index was found to be the same of the harder component of the GBM Band spectrum. This observed feature suggested the possibility that the origin of the high energy component can be the same of the GRB emission in the "canonical" electromagnetic energy range. The case of GRB 090902b on the contrary is quite different. Its energy distribution shows a deviation from the Band function obtained from fitting GBM data between 50 keV and 40 MeV (Bissaldi and Connaughton, 2009). This deviation is apparent both below 50 keV in the GBM and above 100 MeV in the LAT. It is well-fit by a single power-law, with a well-constrained index that is retrieved from a fit of the GBM data alone, the LAT data alone, and when jointly fitting the entire data set, see Fig. 11.1. Moreover the time-resolved spectral analysis shows an evolution with the time for the peak energy  $E_p$ , (Abdo et al., 2009a).

In the case of the fireshell scenario, since the adopted modified black-body spectrum can never produce large MeV and GeV photons, a new mechanism

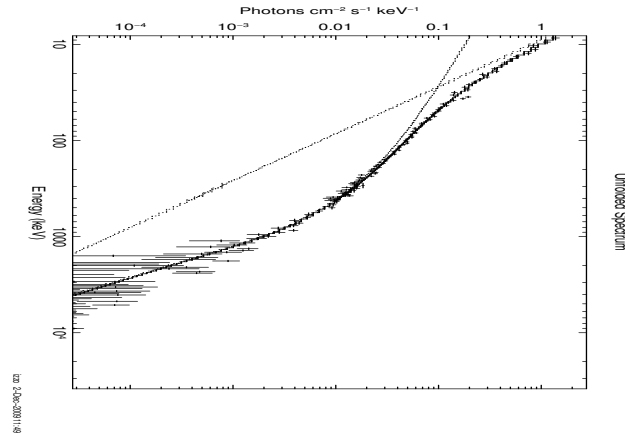


**Figure 11.1.:** The fit of the spectrum of 090902B considering as spectral model a Band model plus a power-law component.

is needed in the fireshell to explain the high energy component. Following an idea first formulated by Katz (1994), we propose that the GeV emission is originated by the collision between relativistic baryons in the fireshell after the transparency and the nucleons located in some giant molecular clouds (GMC) near the burst site. This collision should give rise pion production, whose immediate decay provides high energy photons, neutrinos and leptons. In these GMCs, there are structures composed mainly of molecules and nucleons, so that the interaction of relativistic nucleons of the Fireshell and the nucleons at rest in the GMC could happen. For this reason we consider the proton-proton interaction as responsible for the high energy emission in GRBs. So we have that the interaction of the fireshell with these GMCs will happen at a certain radius  $R_{ext} \sim 10^{16-17}$  cm. If the radius of these GMCs is of the same order, from the fact that the mean free path in p-p collisions is  $l = (n\sigma_{pp})^{-1}$ , with  $\sigma_{pp} \simeq 30$  mbarn the cross section in the case of a pp interaction, we obtain an average density  $n$  of the cloud of about  $10^9-10^{10}$  particles/cm<sup>3</sup> if  $l$  and the GMC radius are similar. However from the IR and radio observations of GMCs, we know that the particle density in these regions reaches high values ( $10^3-4$  particles/cm<sup>3</sup>) but there are substructures in these clouds, in the forms of filaments, bubbles and clumps, in which the density reaches very high values ( $10^4-6$  particles/cm<sup>3</sup>) (Williams et al., 2000). Moreover, if we consider a magnetic field of the cloud such that the respective gyroradius is of the order of the cloud size, the relativistic protons could spend a greater time inside the cloud, giving a possible explanation for the prolonged emission in the MeV-GeV energy range. We have that for a gyroradius of the order of  $10^{16}$  cm, and for a proton energy of 3 TeV, the average magnetic field should be of  $\sim 10^{-7}-10^{-6}$  G, a value in agreement with the magnetic field of interstellar medium (Beck, 2005). Nevertheless a very detailed dimensional

---

analysis is needed, in order to constraining better the physics underlying the p-p process in the fireshell.

Our scope consists in determining the spectral shape of the pp fireshell process, or at least some estimates which connect the canonical GRB fireshell emission with this latter one. The interaction of the ABM-pulse with the CBM, including the GMC, will generate the extended afterglow emission, which is simulated using the GRBsim code (Bianco and Ruffini, 2005b), whose results (light curve and spectrum) are shown in Figs. 11.3, 11.4. In our simulation we consider as dyadosphere energy the value  $E_{dya} = 8.8 \times 10^{54}$  ergs, but the fraction of this energy going in the extended afterglow emission is the 75 % of the totality. In this picture, the onset of the high energy emission allow us to distinguish the P-GRB emission from the extended afterglow. In fact, since the P-GRB is the emission at the transparency of the original fireball, there should be no signatures of particle interaction in its spectrum. So we have a powerful tool for identify the P-GRB emission in a GRB.

In GRB 080916c the P-GRB should correspond with the first pulse visible in the Fermi-GBM light curve, see Fig 11.3. From the observed flux, we have estimated the energy emitted in the P-GRB,  $E_{P-GRB} = 2.8 \times 10^{53}$  ergs, in order to compute the baryon loading of the GRB (Ruffini et al., 2001a), which results to be  $B = 3.3 \times 10^{-4}$ . From the simulation we have obtained an average CBM density of  $\langle n \rangle = 2.2 \times 10^{-3}$  particles/cm<sup>-3</sup>, which seems to be inconsistent with the predicted value of the GMC responsible for the pp interaction. However, we note that this value correspond to an ISM in a volume spherically-distributed around the burst site, while the GMC should occupy only a tiny fraction of the entire solid angle so that the real density is larger. The first important result that we obtain from the simulation is that the Lorentz  $\gamma$  factor at the transparency is very high,  $\gamma = 3170$ . We found very high value for the Lorentz factor also for the other GRBs with high energy emission, so that it is possible to conclude that a requirement for the presence of high energy in GRBs is a very large value for  $\gamma$ . Moreover, the very large energy emitted in these GRBs reflects in the number of baryons located in the incoming fireshell, so that in these GRBs there will be a large number of pp collisions and of consequence a large probability to observe very high energy photons incoming from them.

Likewise, in GRB 090902b the P-GRB should correspond with the first 6 s and its energy emitted is constrained to be  $\sim 5-6\%$  of the dyadosphere, which in this case is  $E_{dya} = 3.63 \times 10^{54}$  ergs. With a baryon loading of  $3 \times 10^{-4}$ , the Lorentz  $\gamma$  factor at the transparency also in this case is very high,  $\gamma = 2386$ . This fact seems to suggest a sort of energy threshold for the high energy component in the GRBs.

We tried to model this high energy emission considering the pp interaction in the center of mass (c.m.) frame. We note that the threshold for the creation of pion is relatively low: the Lorentz  $\gamma$  value of the incident proton can be  $\sim$

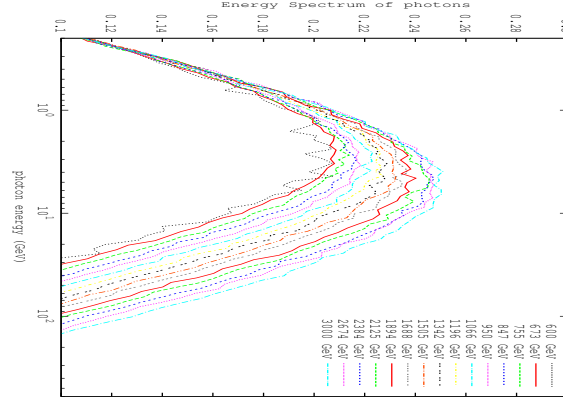


**Figure 11.2.:** Energy spectrum of photons obtained from our simulations of proton-proton interactions, with different values for the energy of the relativistic proton incoming.

2.2. From the previous analysis, we have obtained a very high value for the Lorentz  $\gamma$  of the incoming baryons so their energy in the interaction is very large  $E_p = (\gamma 1)m_p c^2$ , that for  $\gamma \propto 10^3$  is of the order of some TeV.

In order to obtain an energy distribution of the high energy photons obtained from the pion decay, we used the Monte Carlo code SIBYLL (Fletcher et al., 1994) to reproduce the spectra of the collisions for different energies of the incident protons. Using the SIBYLL code, we could note that  $\sim 83\%$  of the radiation produced is from the decay of the neutral pion  $\pi^0$ , where the decay  $\pi^0 \rightarrow 2\gamma$  is by 98.8 %. In the Fig. 11.2 it is shown the count spectrum of emission for fifteen different energies of the incident protons, so that we can note how the most part of the emitted photons increases from 2 to 5 GeV while the incident proton energy increase from 600 to 3000 GeV. In the case of incident protons with the highest energy, the production of photons with 300 MeV and 100 GeV is the half of the peak production (5 GeV).

Note that for the data of GRB 080916c we consider the Fermi GBM observations (8 keV - 5000 MeV), reduced with the standard FTOOLS package for the Fermi satellite <sup>1</sup>.

## 11.1. Spectral analysis of the P-GRB candidates

According to the Fireshell scenario, the main emission in a GRB, the extended afterglow, is due to the interaction of the baryonic and leptonic shell with the interstellar medium surrounding the GRB. Before the extended afterglow,

<sup>1</sup>[http://heasarc.gsfc.nasa.gov/ftools/ftools\\_menu.html](http://heasarc.gsfc.nasa.gov/ftools/ftools_menu.html)

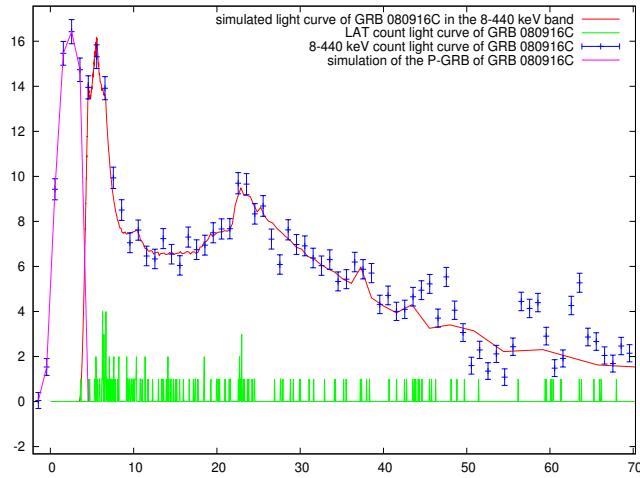


**Figure 11.3.:** Fermi-GBM (8-440 keV) light curve (blue points) compared with the results of our simulation of the light curve of GRB 080916C (red lines) and the P-GRB emission (pink line). The green bars correspond to the LAT (> 100 MeV) count light curve. Note the P-GRB emission starting before the LAT data.

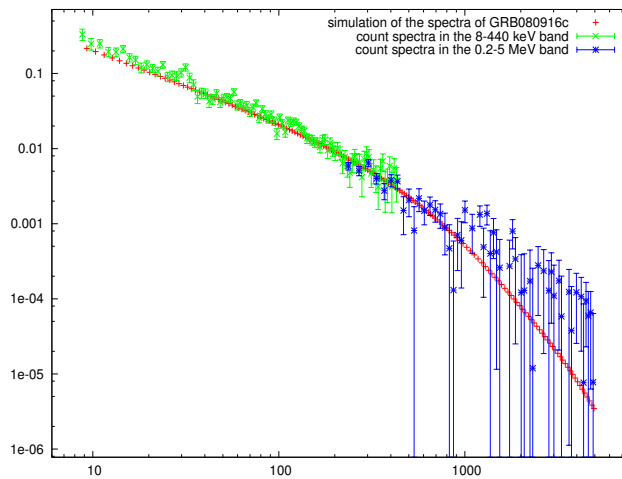


**Figure 11.4.:** Fermi-GBM (8-440 keV - green bars) and Fermi-BGO (260-5000 keV - blue bars) energy spectrum compared with the results of our simulation for the energy spectrum of GRB 080916C (red lines).

**Table 11.1.:** Time-resolved spectral analysis in the range (8 keV - 5 MeV) for the first pulse of GRB 080916C using a blackbody spectral model with an extra power-law  $kE^{-\gamma}$  component, a classical Band function and a modified blackbody spectral model.

GRB 080916C			
BB+po	$kT = 56.91 \pm 2.49$	$-1.26 \pm 0.03$	
Band	$\alpha = -0.33 \pm 0.08$	$\beta = -2.11 \pm 0.18$	$E_0 = 209.98 \pm 30.83$
ModifiedBB	$kT = 199.74 \pm 17.99$	$-0.52 \pm 0.05$	

we should see a flash of X and gamma radiation, the P-GRB, due to the initial plasma composed of  $e^{\pm}$ -pairs and photons, that reaches the condition of transparency. This relativistic plasma thermalizes before the transparency, so the energy spectrum of the P-GRB should have the characteristics of a blackbody spectrum. However, as it is well known, the spectrum of a GRB, and of a typical pulse observed in a burst, is not thermal. This seems could have interesting consequences for the Fireshell model. The possibilities are different: among the many ones considered are those that 1) in addition to a thermal emission there is another dominant process together the P-GRB emission, 2) the spectrum is purely thermal, but not of the type described above, i.e. a convolution of one or more black-body with the EQTS, 3) what is observed is not the P-GRB.

Since in GRB 080916c we the delayed onset of the high-energy emission could be due to the interaction of the fireshell with the CBM, and the emission previously observed in the lower energy bands associated with another phenomenon, as the P-GRB, we made a spectral analysis of this emission, in order to find some signatures of the P-GRB thermal emission. We note that the duration of this first pulse in GRB 080916c is comparable with what is expected for a P-GRB, e.g. of the order of few seconds (Ruffini et al., 1999). Moreover a time-resolved analysis of the different pulses seen in all GRBs shows a soft-to-hard trend for the first two pulses, becoming the canonical hard-to-soft one for the following emission. We consider three different spectral models in our analysis: 1) a classical Band model, represented by two broken power-laws smoothly connected at a given energy  $E_0$ ; 2) a black-body model with an extra power-law component; 3) the modified black-body spectral model described in a previous section. A simple black-body model didn't explain the observed energy distribution. All of these spectral models are in agreement with the observed Fermi-GBM spectrum (8 - 5000 keV), and the final results are shown in Table 11.1 and in Figs. 11.5.

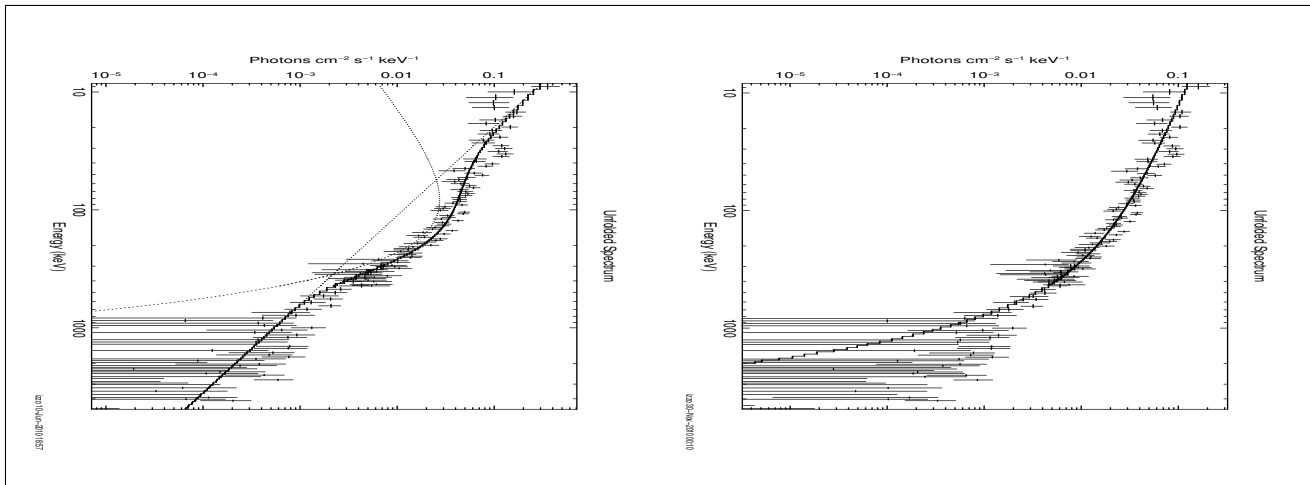


**Figure 11.5.:** Spectral fits of the Fermi GBM and BGO count spectra of the P-GRBs of GRB 080916C in the range (8 keV - 5 MeV). We consider in these cases a blackbody spectral model with an extra power-law component and a modified blackbody spectral model respectively.



# 12. A double component in the prompt emission of GRB 090618

## 12.1. Introduction

We have studied the emission in the fireshell model of GRB 090618, which is one of the closest ( $z = 0.54$ ) and the most energetic ( $E_{iso} = 2.4 \times 10^{54}$  erg) GRBs. It has been observed by many satellites, namely Fermi, Swift, Konus-WIND, AGILE, RT-2 and Suzaku. We have analyzed the emission of this GRB first identifying the transparency emission, the P-GRB, and then using different spectral models with XSPEC. The fundamental parameters to be determined in the fireshell model, (Ruffini et al., 2009), in order to obtain information on the spectral energy emission, are the dyadosphere energy, the baryon loading and the density and porosity of the CBM. We found that in this GRB there exists two different components. The first component lasts 50 s with a spectrum showing a very clear thermal component evolving, between  $kT = 60$  keV and  $kT = 14$  keV, and a radius increasing between 9000 km and 50000 km, with an estimate mass of  $\sim 10 M_{\odot}$ . The second component is a canonical long GRB with a Lorentz gamma factor at the transparency of  $\Gamma = 490$ , a temperature at transparency of 25.48 keV and with a characteristic size of the CBM cloud of  $R_{cl} \approx 10^{15}$  cm which generated the observed luminosity. We confirm that the second episode corresponds to a canonical GRB, while the first episode do not. Indeed, it appears to be related to the progenitor of the collapsing bare core – defined by us as the “proto black hole” (Izzo et al. A&A submitted) – leading to the black hole formation.

### 12.1.1. A brief description of the fireshell scenario

Within the fireshell scenario, all GRBs originate from an optically thick  $e^+e^-$  plasma in thermal equilibrium, as a result of a gravitational collapse to form a black hole. This plasma has a total energy of  $E_{tot}^{e^+e^-}$ . The annihilation of  $e^+e^-$  pairs occurs gradually and is confined in an expanding shell called “fireshell”. This plasma engulfs the baryonic material (of mass  $M_B$ ) left over in the process of gravitational collapse. The baryon loading is measured by the dimensionless parameter  $B = M_B c^2 / E_{tot}^{e^+e^-}$ . The fireshell self-accelerates

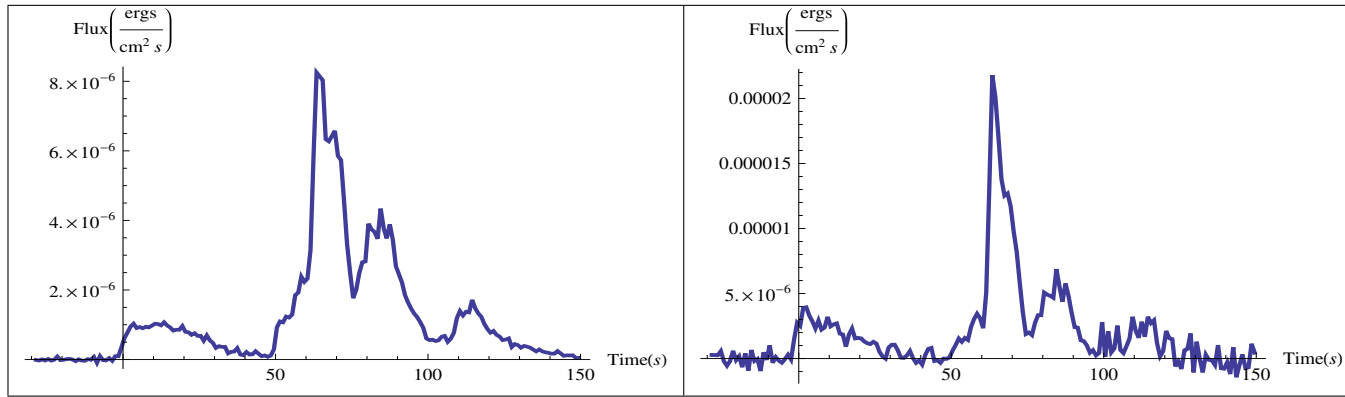


**Figure 12.1.:** Fermi-GBM flux light curve of GRB 090618 referring to the NaI (8-440 keV, *left panel*) and BGO (260 keV - 40 MeV, *right panel*) detectors.

to ultra-relativistic velocities until it reaches the transparency, when all the photons are emitted in what is called the P-GRB. The remaining accelerated baryonic matter starts then to slow down due to the collisions with the Circum Burst Medium (CBM), of average density  $n_{CBM}$ . This collision between baryons and the CBM will give rise to the extended afterglow emission, which represents the residual high-energy emission observed in GRBs.

## 12.2. Data analysis

### 12.2.1. Data reduction and light curve

We made use of Swift-BAT and XRT (Gehrels et al., 2004; Burrows et al., 2005a) data, together with the Fermi-GBM (Meegan et al., 2009) and Coronas PHOTON-RT2 (Rao et al., 2011) ones. The data reduction was done using the Heasoft packages <sup>1</sup> for BAT and XRT, plus the Fermi-Science tools for GBM. The Swift-BAT light curve was obtained in the band (15- 150 keV) using the standard procedure. The Fermi-GBM light curves are shown in Fig. 12.1.

### 12.2.2. Spectral analysis: identification of the P-GRB

The identification of the P-GRB emission is fundamental since it allows us to determine the value of the Baryon Loading and other physical properties of the fireshell plasma at the initial stage, such as the temperature and the Lorentz gamma factor at the transparency and the lab radius when the P-GRB emission would happen. From the observations we obtain the the

<sup>1</sup><http://heasarc.gsfc.nasa.gov/lheasoft>

**Table 12.1.:** Time-resolved spectral analysis of GRB 090618.

Time Interval	$\alpha$	$\beta$	$E_0^{BAND}$ (keV)	conv. factor (ergs/cm <sup>2</sup> /ctg)	$\tilde{\chi}^2$
0 - 50	$-0.86 \pm 0.10$	$-2.30 \pm 0.10$	$152.4 \pm 37.4$	$1.50 \times 10^{-9}$	1.1
	$-1.48 \pm 0.10$	$-2.86 \pm 0.86$	$227.6 \pm 50$	$9.03 \times 10^{-9}$	1.0
50 - 57	$-1.10 \pm 0.10$	$-3.23 \pm 6.33$	$174.0 \pm 51.8$	$1.32 \times 10^{-9}$	1.2
	$-3.03 \pm 1.57$	$-2.30 \pm 0.10$	$701.7 \pm 50$	$5.94 \times 10^{-9}$	1.1
57 - 68	$-0.84 \pm 0.03$	$-2.44 \pm 0.37$	$198.5 \pm 17.0$	$1.64 \times 10^{-9}$	1.8
	$-1.34 \pm 0.40$	$-3.78 \pm 1.21$	$565.4 \pm 132.16$	$7.22 \times 10^{-9}$	1.1
68 - 76	$-1.03 \pm 0.03$	$-2.30 \pm 0.10$	$175.7 \pm 16.6$	$1.41 \times 10^{-9}$	1.6
	$-1.75 \pm 0.71$	$-4.50 \pm 6.99$	$548.9 \pm 415.5$	$6.67 \times 10^{-9}$	0.9
76 - 103	$-1.06 \pm 0.03$	$-2.90 \pm 0.28$	$124.4 \pm 7.67$	$1.23 \times 10^{-9}$	1.2
	$-2.25 \pm 1.77$	$-2.30 \pm 0.10$	$520.1 \pm 50$	$6.97 \times 10^{-9}$	0.8
103 - 150	$-2.56 \pm 0.10$	$-2.03 \pm 0.02$	$< 100$	$1.17 \times 10^{-9}$	2.2
	$-0.84 \pm 1.00$	$-0.57 \pm 1.39$	$< 100$	$1.79 \times 10^{-8}$	1.0

P-GRB energy and the temperature of the black body due to the P-GRB emission (Ruffini et al., 2000). For this reason we proceeded with the time resolved spectral analysis of GRB 090618 dividing the emission in several time intervals. We then made a data fitting procedure with XSPEC [3] using two spectral models: a Band function and black body plus a power-law component (bb+po). The results are shown in table 12.1.

## 12.3. Results

### 12.3.1. From 0 to 50s

The results of this analysis showed the presence of a possible single black body component in the first two intervals considered in the Table 12.1. The former one corresponds to a long precursor, lasting  $\sim 50$  s, which is characterized by a single fast rise and exponential decay (FRED) pulse.

For this reason, we divided the emission into two main episodes – the first one lasting from 0 to 50s, and the second one from 50 to 150s. The first episode is well-fitted by a BB+po model of temperature  $kT = 29.84 \pm 1.38$  keV (which in principle is a distinctive feature of a P-GRB) and a photon index  $\gamma = -1.67 \pm 0.03$ . We know that the isotropic energy of the GRB is  $E_{iso} = 2.8 \times 10^{53}$  erg, while the energy emitted by the sole black body component in this first 50 s emission is  $E_{BB,1st} = 8.88 \times 10^{51}$  erg (the 3.2% of the total energy emitted). This implies a baryon loading  $B = 10^{-4}$ . From the fireshell equations of motion we derived a theoretically predicted temperature at the transparency which, when corrected for the cosmological redshift

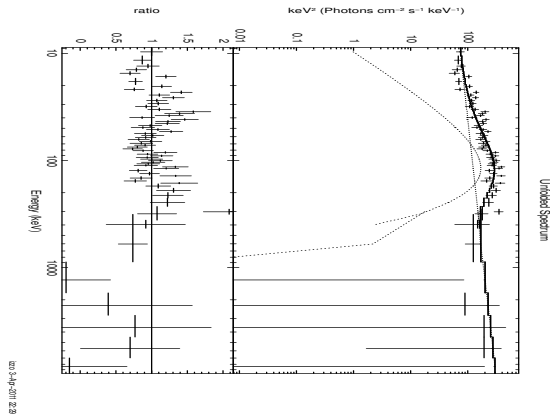


**Figure 12.2.:** Time-integrated spectra of the P-GRB of the second episode (from 50 to 54 s after the trigger time) of GRB 090618 fitted with the black-body + power-law model,  $\chi^2 = 1.52$ .

of the source, gives  $kT = 425$  keV. This value is in clear disagreement with the observed temperature which led us to conclude that the first episode cannot be considered as the transparency emission, or the P-GRB. Another peculiar feature is that the duration of this episode is much longer than the typical one considered for P-GRBs, which is at the most 10s, see e.g. (Ruffini et al., 2009).

### 12.3.2. The second episode as an independent GRB

We tried to identify the P-GRB within the thermal emission observed in the interval B, so from 50s to 59s after the GBM trigger time. A detailed analysis allowed us to consider the first 4 s as due to the P-GRB emission. The P-GRB spectrum is well-fitted by a black body plus a power-law extra component, see Fig. 12.2 with temperature  $kT = 25.48 \pm 2.04$  keV and a photon index  $\gamma = 1.85 \pm 0.06$ . The integrated spectrum of the remaining part is best fitted with a Band model (see Table 12.1). The isotropic energy of the second episode is  $E_{iso,2nd} = 2.37 \times 10^{53}$  erg. If we assume the equality  $E_{iso} = E_{tot}^{e^+e^-}$  and a baryon loading  $B = 2 \times 10^{-3}$ , we find that the P-GRB energy should correspond to the 2% of the total energy of the GRB. Since from the fireshell equations we obtain a Lorentz gamma factor at the transparency of  $\Gamma_0 = 490$ , the corresponding theoretical, and cosmologically corrected, temperature at transparency should be  $kT = 24.48$  keV, in agreement with the observations. So as a final result, this second episode can be considered as a canonical GRB in the fireshell scenario. We have simulated in this model the GRB 090618 light curve and spectrum, that are shown in Fig.12.3.

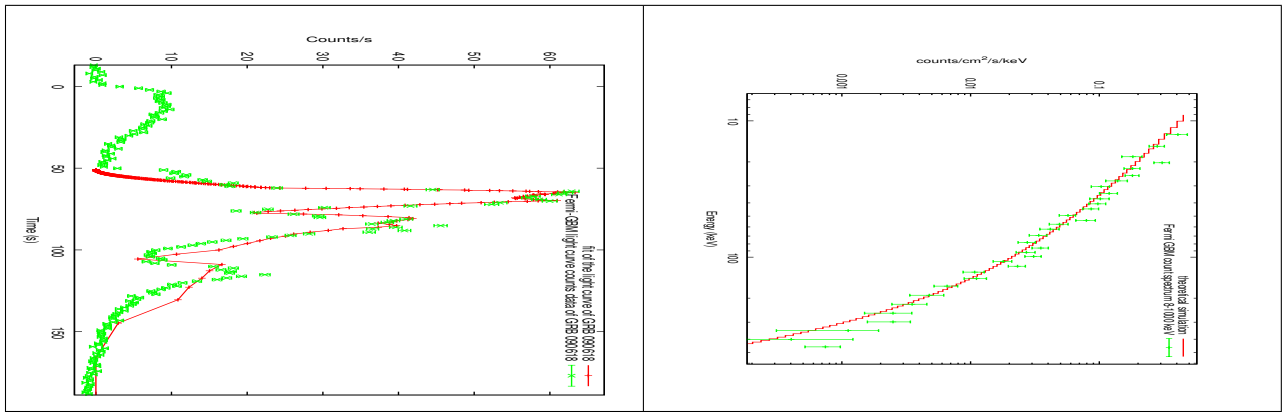


**Figure 12.3.:** Simulated light curve (left) and time integrated ( $t_0+58$ ,  $t_0+150$  s) spectrum (8-440 keV, on the right) of the extended afterglow of GRB 090618.

### 12.3.3. The first 50 s emission is not a GRB

We then have checked if the first 50s emission could be considered to be an independent GRB. We attempted a first interpretation by assuming the first 6 s as the P-GRB component, as opposed to the remaining 44 s as the possible extended afterglow. A possible combination of values is given by  $E_{tot}^{e^+e^-} = 3.87 \times 10^{52}$  erg and  $B = 1.5 \times 10^{-4}$ , but this would imply a very high value for the Lorentz factor at the transparency of  $\sim 5000$ . In turn, this value would imply a thermal spectrum of the P-GRB peaking at around 300 keV, which is in contrast with the observed temperature of  $kT_{1st} = 58$  keV.

Anyway, if we consider all the 50s emission as the extended afterglow, and assuming a “virtual” P-GRB lasting 10s and below the nominal Fermi detector threshold, we conclude that this P-GRB should have been detected by Fermi (Ruffini et al., Adv. Space Res. submitted). We can then conclude that in no way we can interpret this episode either as a P-GRB of the second episode or, as proved here, as a separate GRB.

## 12.4. A different emission process

A detailed spectral analysis of the first episode showed a strong spectral evolution, see Table 12.2, where we have taken into account two different models, a Band model and a blackbody plus an extra power-law component, in order to explain this first emission episode. We have seen, in the case of the black body plus power-law, that the temperature varies from the initial value of 54 keV to 14 keV, where the extra power-law non-thermal component is assumed to be related to the blackbody by some process which will be studied in the future. Assuming a non-relativistic expansion for this first episode, we computed the evolution of the blackbody radius just from the luminosity

**Table 12.2.:** Time-resolved spectral analysis of the first episode in GRB 090618. We have considered seven time intervals, as described in the text, and we used two spectral models, whose best-fit parameters are shown here.

Time	$\alpha$	$\beta$	$E_0$ (keV)	$\tilde{\chi}_{BAND}^2$	$kT$ (keV)	$\gamma$	$\tilde{\chi}_{BB+p}^2$
0 - 5	$-0.45 \pm 0.11$	$-2.89 \pm 0.78$	$208.9 \pm 36.13$	0.93	$59.86 \pm 2.72$	$1.62 \pm 0.07$	1.07
5 - 10	$-0.16 \pm 0.17$	$-2.34 \pm 0.18$	$89.84 \pm 17.69$	1.14	$37.57 \pm 1.76$	$1.56 \pm 0.05$	1.36
10 - 17	$-0.74 \pm 0.08$	$-3.36 \pm 1.34$	$149.7 \pm 21.1$	0.98	$34.90 \pm 1.63$	$1.72 \pm 0.05$	1.20
17 - 23	$-0.51 \pm 0.17$	$-2.56 \pm 0.26$	$75.57 \pm 16.35$	1.11	$25.47 \pm 1.38$	$1.75 \pm 0.06$	1.19
23 - 31	$-0.93 \pm 0.13$	unconstr.	$104.7 \pm 21.29$	1.08	$23.75 \pm 1.68$	$1.93 \pm 0.10$	1.13
31 - 39	$-1.27 \pm 0.28$	$-3.20 \pm 1.00$	$113.28 \pm 64.7$	1.17	$18.44 \pm 1.46$	$2.77 \pm 0.83$	1.10
39 - 49	$-3.62 \pm 1.00$	$-2.19 \pm 0.17$	$57.48 \pm 50.0$	1.15	$14.03 \pm 2.35$	$3.20 \pm 1.38$	1.10

observed:

$$r_{em} = \frac{[\phi_{obs}/(\sigma T_{obs}^4)]^{1/2} D}{(1+z)^2}. \quad (12.4.1)$$

, where  $\phi_{obs}$  is the observed thermal flux,  $\sigma$  the Stefan constant and  $D$  the luminosity distance. We have also obtained a lower limit estimate of the mass of the proto-black hole by considering the sole blackbody energy emitted in the first episode, given by the thermal luminosity times the emission time, and its origin as due to the gravitational energy:

$$E_{iso} = 4\pi r_{em}^2 \sigma T^4 \Delta t = \frac{3}{5} \frac{GM_{pbh}^2}{r_{em}} \quad (12.4.2)$$

where  $E_{iso}$  is the total isotropic energy of the event,  $\Delta t$  is the time duration of the first episode in the rest frame and  $M_{pbh}$  denotes the proto-black hole mass. We then obtained

$$M_{pbh} \gtrsim \sqrt{\frac{20\pi r_{em}^3 \sigma T^4 \Delta t}{3G}} \sim 4M_{\odot}. \quad (12.4.3)$$

as a lower limit for proto-black hole mass. The physical explanation for the proto-black hole emission is to be attributed to the processes of shells' mixing that happen in the last stages of the final collapse of a very massive star (Arnett and Meakin, 2011). Full details on the observational and theoretical evidences of the double episodes nature of GRB 090618 can be found in Izzo et al., A&A submitted.

# 13. Evidences for a double component in GRB 101023

## 13.1. Introduction

GRB 101023 has been observed by many satellites, as Konus Wind, Swift BAT and Fermi in gamma rays, Swift XRT in X-rays and Swift UVOT, Gemini and GROND in the optical band. Its redshift cannot be determined due to the lack of data, but we tried to infer it by using different methods. The source appears to be morphologically very similar to GRB 090618, with a total energy of  $E_{iso} = 2.7 \times 10^{53}$  erg. The aim is to compare and contrast these two sources; to identify from this comparison the redshift of GRB 101023, and to consequently determine all the physical parameters. In this work we present the method we used to constrain the redshift. Then we proceed to examine episode 1 and episode 2 of this GRB, building its light curve and spectrum. We identify episode 2 with a canonical GRB, identifying also the P-GRB. We simulate the light curve and spectrum of this second episode with a numerical code called GRBsim. Afterwards, we go into further detail in the analysis of the first episode, making clear the evolution of the thermal component and the radius of the outermost shell, establishing the complete correspondence with GRB 090618. Finally, we present the conclusions.

### 13.1.1. Fireshell Scenario

In the fireshell scenario, the GRB emission originates from a process of vacuum polarization, resulting in pair creation in the so-called dyadosphere. In the process of gravitational collapse to a black hole, there forms an  $e^\pm$  plasma in thermal equilibrium, with total energy  $E_{tot}^{e^\pm}$ . The annihilation of these pairs occurs gradually and is confined in a shell, called "fireshell. This shell self-accelerates to relativistic velocities, engulfing the baryonic matter (of mass  $M_B$ ) left over in the process of collapsing and reaching a thermal equilibrium with it. The baryon load is measured by the dimensionless parameter  $B = M_B c^2 / E_{e^\pm}$ . The fireshell continues to self-accelerate up to relativistic velocities until it reaches the transparency condition. At this time we have a first flash of radiation, the Proper-GRB (P-GRB). The energy released in the P-GRB is a fraction of the initial energy of the dyadosphere  $E_{dya}$ . The residual plasma of leptons and baryons interacts with the circumburst medium (CBM)

as it expands, giving rise to a multi-wavelength emission, the extended afterglow. The structures observed in the prompt emission of a GRB are due to the inhomogeneities in this CBM. In this way we need few parameters for a complete description of a GRB: the dyadosphere energy  $E_{dya}$ , the baryon load  $B$  and the CBM density distribution,  $n_{CBM}$ .

## 13.2. Data analysis

### 13.2.1. Data reduction

To obtain the Fermi GBM light-curve and spectra in the band (8 - 440) KeV (see Fig. 13.1) we made use of the standard headas procedure. We downloaded the data from the gsfsc website<sup>1</sup> and constructed the count light curve with `gtbindef` and `gtbin` tools, to obtain a GTI file for the energy distribution and the light curve, respectively. We fixed the time binning in 1s. We used the data from the second INa detector in the range 8- 440 KeV. Once the light curve was created, we subtracted the background and made the starting time coincide with the trigger time, of 309567006.72 in MET seconds. After the reduction of data was complete, we proceeded with its time resolved spectral analysis with the program XSPEC.

### 13.2.2. light curve

The GBM light curve (Fig. 13.1) shows two major pulses. The first one starts at the trigger time and lasts 25 s. It consists of a small peak that lasts about 10s, followed by a higher emission that decays slowly with time. The duration, as well as the topology of this curve, lead to think that this may not be the case of a canonical GRB, but its origin may lie on another kind of source, which remains still unidentified. The second pulse starts at 45s after the trigger time and lasts 44s. It presents a peaky structure, composed by a short and weak peak at the beginning, followed by several bumps, big not only in magnitude but also in duration. This second emission, on the contrary, does have all the characteristics which describe a canonical GRB.

## 13.3. Redshift determination

The redshift of this source is unknown, due to the lack of data in the optical band. However, we can infer a value of  $z=0.9$  under the hypothesis that, as every long GRB, it should follow the Amati relation (Amati, 2006). This relates the isotropic energy  $E_{iso}$  emitted by a GRB to the peak energy in the rest frame  $E_{p,i}$  of its  $\nu F\nu$  electromagnetic spectrum.  $E_{iso}$  is the isotropic equivalent

---

<sup>1</sup><http://heasarc.gsfsc.nasa.gov/heasoft>

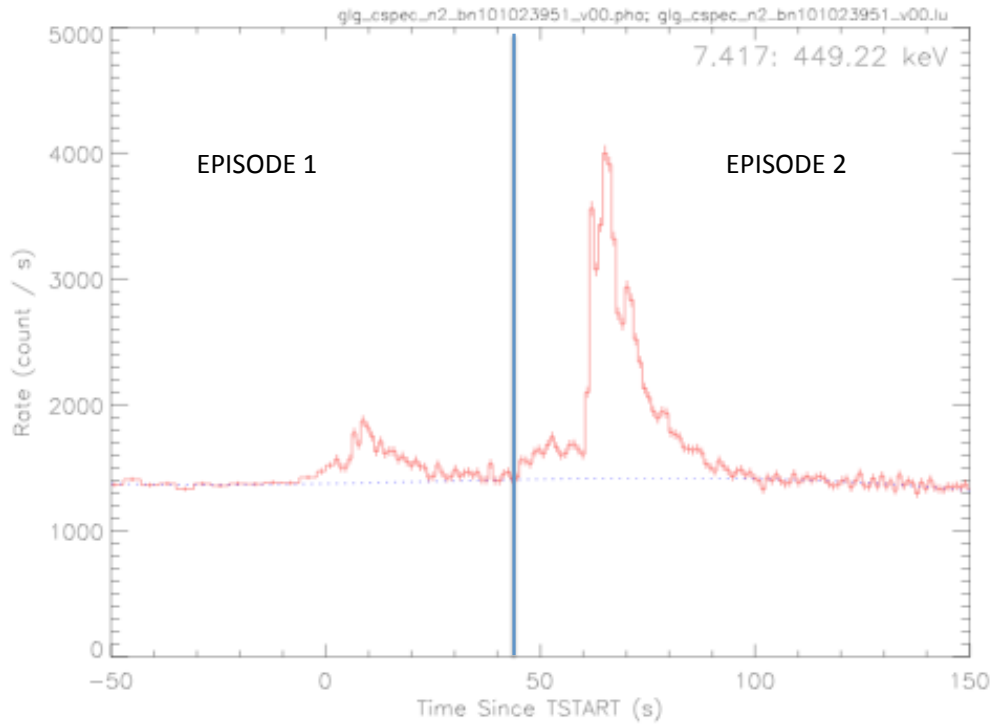


**Figure 13.1.:** Count light curve of GRB 101023 obtained from Fermi GBM detector, with a bin time of 1 s. The time is given with respect to the GBM trigger time of 22:50:04.73 UT, 23 October, 2010. The plot was obtained with the RM-FIT program. The two-episode nature of the GRB is evidenced in analogy with GRB 090618.

radiated energy, while  $E_{p,i}$  is the photon energy at which the time averaged  $\nu F\nu$  spectrum peaks.  $E_{iso}$  is given by:

$$E_{iso} = \frac{4\pi d_l^2}{(1+z)} S_{bol}, \quad (13.3.1)$$

where  $d_l^2$  is the luminosity distance,  $z$  is the redshift and  $S_{bol}$  is the bolometric fluence (estimated between 1 keV and 10 MeV), related to the observed fluence in a given detection band ( $E_{min}$ ,  $E_{max}$ ) by

$$S_{bol} = S_{obs} \frac{\int_{1keV/(1+z)}^{10MeV/(1+z)} E\phi(E)dE}{\int_{E_{min}}^{E_{max}} E\phi(E)dE}, \quad (13.3.2)$$

with  $\phi$  the spectral model considered for the spectral data fit.  $E_{p,i}$  is related to the peak energy  $E_p$  in the observer frame by

$$E_{p,i} = E_p(1+z) \quad (13.3.3)$$

We started our analysis under the hypothesis that episode 2 is a long GRB. We computed the values of  $E_{p,i}$  and  $E_{iso}$  for different given values of  $z$  and plotted them in Fig 13.2. We found that the Amati relation is fulfilled by episode 2 for  $0.3 < z < 1.0$ . This interval has been calculated at  $1\sigma$  from the best fit from the Amati relation. We chose  $z = 0.9$  because for this value of the redshift the energetics of this source are very similar to those of GRB 090618, whose redshift is known to be  $z=0.54$ . This is, the isotropic energy of events 1 and 2 in GRB 090618 are exactly the same as the isotropic energy of GRB1 and GRB2 in GRB 101023, respectively.

## 13.4. Spectral analysis

To proceed with the fitting of the spectra, we defined first of all the time intervals we wanted to analyze making use of the `gtbindef` tool. We obtained a GTI file for the energy distribution. Secondly, we used `gtbin` to obtain the spectrum and in that way be able to fit the data with different models, via XSPEC. We used a Black body plus a power-law model and a Band model. The results are shown in Table 13.1.

We can see that the second emission can be very well fitted by a Black body plus a power-law model. In particular, we find for the P-GRB an observed temperature of  $kT = 13.5 \pm 2.8$  keV, a photon index of  $\gamma = 2.5 \pm 0.7$  and a  $\chi^2 = 0.91$ . From these values we can infer a P-GRB energy  $E_{P-GRB} = 1.32 \times 10^{51}$  erg and a total energy of  $E_{iso} = 1.65 \times 10^{53}$  erg, i.e. the P-GRB energy release is the 0.7% of the total. We introduced these results in a numerical code to simulate the light curve (see Fig. 13.3) and we found the following

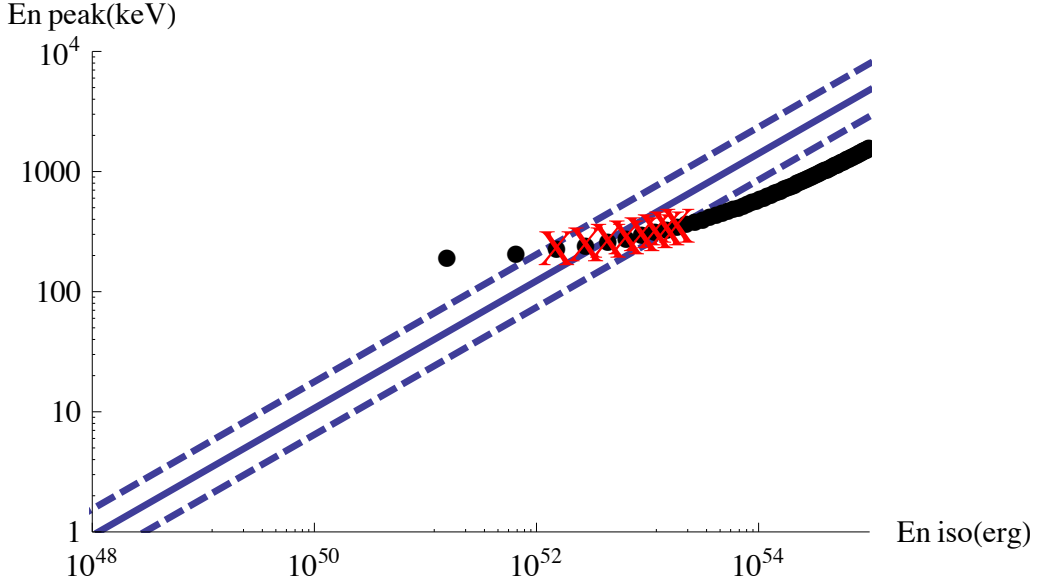


**Figure 13.2.:** Plot of the relation between  $E_{p,i}$  and  $E_{iso}$  for the second episode of GRB 101023, considering different values of the redshift. It can be seen that the plot lies within  $1\sigma$  for the range  $z=0.3 - z=1.0$ .

**Table 13.1.:** Time-resolved spectral analysis of GRB 101023. We have considered two main time intervals, corresponding to episode 1 and episode 2 in the light curve. We have proposed for each time interval a Band spectral model (Band et al., 1993) and a Black body plus a power-law model.

Time [s]	$\alpha$	$\beta$	$E_0^{BAND}$ [keV]	$\chi^2$	Norm	$kT$ [keV]	$\gamma$	$\lambda$
0-44	$-1.3 \pm 0.8$	$-1.9 \pm 0.2$	$87 \pm 147$	0.98	$0.006 \pm 0.01$	$14 \pm 6$	$-1.7 \pm 0.1$	0.
45-89	$-0.9 \pm 0.1$	$-2.02 \pm 0.1$	$151 \pm 24$	1.09	$0.043 \pm 0.008$	$26 \pm 1$	$-1.58 \pm 0.03$	1.

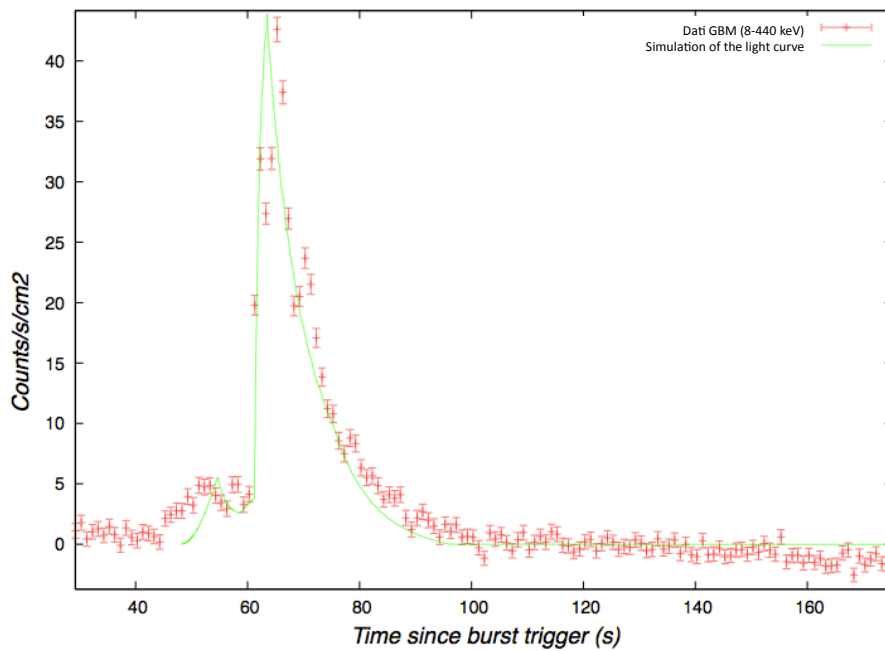


**Figure 13.3.:** Fit of the second major pulse of the light curve of GRB 101023.

values for the parameters in the fireshell model:  $B = 4.8 \times 10^{-3}$ ,  $kT_{th} = 20.83$  keV,  $\Gamma = 206.81$ , and a Laboratory radius of  $1.44 \times 10^{14}$  cm. We also simulated the spectrum of episode 2, shown in Fig. 13.4.

### 13.4.1. Episode 1: Temperature and radius evolution

To analyze episode 1 more into detail, in order to identify the nature of this phenomenon, we plotted the temperature of the Black body component as a function of time, for the first 20 s of emission (see Fig. 13.5). We note a strong evolution in the first 20 s of emission which, according to Ryde (2004) can be reproduced by a broken power-law behavior, with  $\alpha = -0.47 \pm 0.34$  and  $\beta = -1.48 \pm 1.13$  being the indices of the first and second power-law, respectively. We also plotted the radius of the most external shell with time (see Fig. 13.6). Following sec. 12, the radius can be written as

$$r_{em} = \frac{\hat{R}D}{(1+z)^2}, \quad (13.4.1)$$

where  $\hat{R} = \phi_{obs}/(4\pi\sigma T_{obs}^4)$  is a parameter,  $D$  is the luminosity distance,  $\Gamma$  is the Lorentz factor and  $\phi_{obs}$  is the observed flux. We can see that the radius remains almost constant (in fact it increases, but only slightly). From this it is possible to see that the plasma is expanding at non-relativistic velocities.

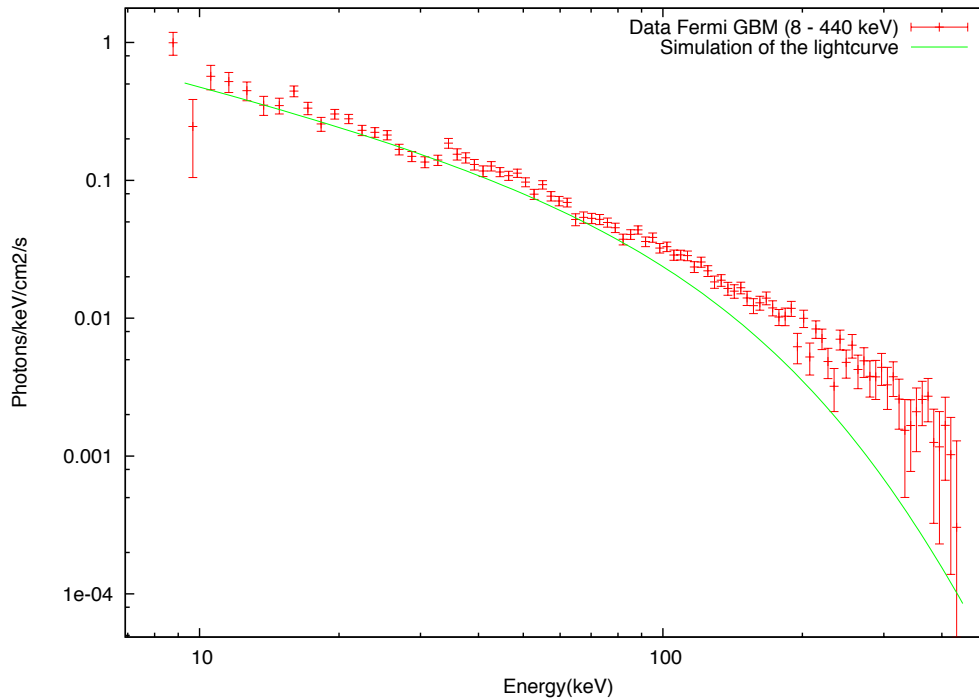


**Figure 13.4.:** Fit of the spectrum of Episode 2.

According to the work of Arnett and Meakin (2011), there is an expansion phase of the boundary layers, while the iron core suffers a contraction. This is due to the presence of strong waves originated while the different shells of the progenitor mix during the collapse phase. This fact confirms the non-GRB nature for the first episode.

## 13.5. Conclusions

GRB 101023 is a very interesting source for the following reasons:

1) It has been observed by many satellites in different energy bands. Despite the wide energy range coverage, there is no redshift determination for this source, which complicates the determination of its characteristic parameters. This has challenged the indirect inference of its cosmological redshift.

2) Morphologically, there is a striking similarity between GRB 101023 and GRB 090618, as can be seen from the light curves. Following the study of GRB 090618, we have divided the emission into two episodes: Episode 1, that lasts 45 s, presents a smooth emission, without spikes, that decays slowly with time. Episode 2, of 44 s of duration, presents a spiky structure, composed of a short and small peak at the beginning, followed by several intense bumps, after which there is a fast decay with time. Episode 2 has all the characteristics of a canonical long GRB.

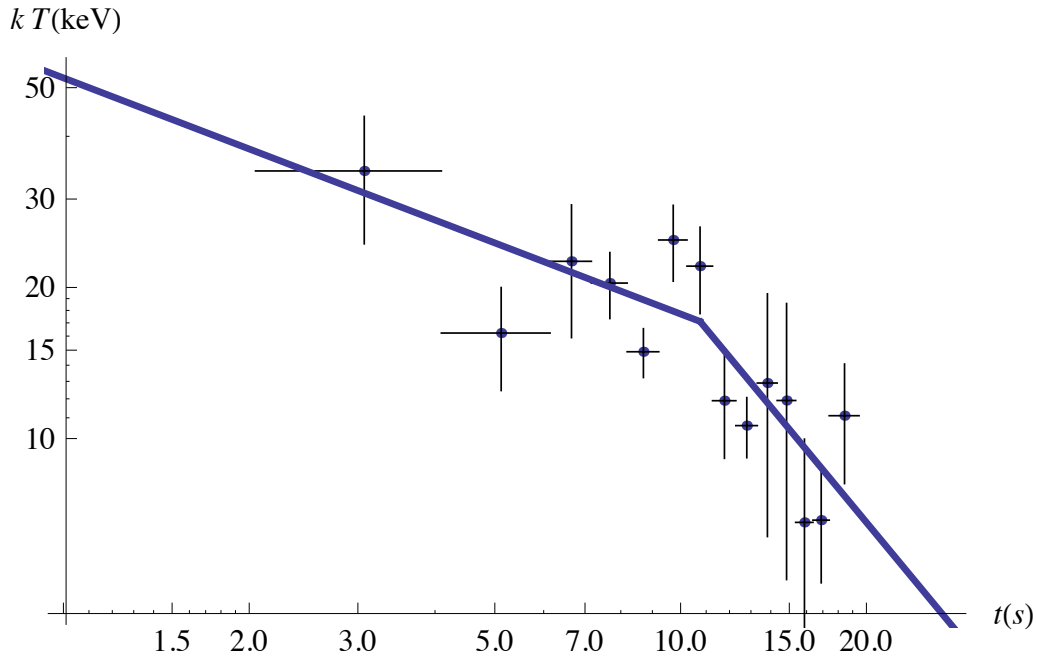


**Figure 13.5.:** Evolution of the observed temperature  $kT$  of the BB component. The blue line corresponds to a broken power-law fit. The indices of the first and second power-law are  $\alpha = -0.47 \pm 0.34$  and  $\beta = -1.48 \pm 1.13$ , respectively. The break occurs at 11 s after the trigger time.

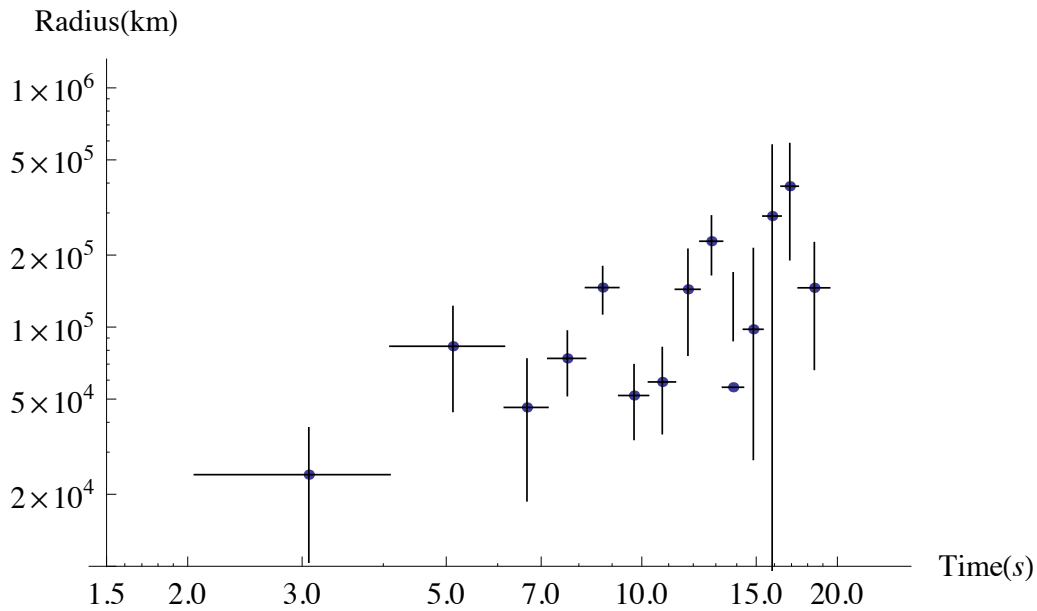


**Figure 13.6.:** Evolution of the radius of the first episode progenitor.

3) Since we do not know the redshift, we cannot infer the total energy of the source,  $E_{iso}$ . We have attempted to infer the cosmological redshift of the source from the peak energy  $E_{peak}$ , using the Amati relation under the hypothesis that Episode 2 is a canonical long GRB. We constrain the value of the redshift to be between 0.3 and 1.0. We assumed for the redshift of this source  $z = 0.9$ .

4) We performed a time-resolved analysis of Episode 1. We fitted a Black body plus a power law model and plotted the evolution of the black body component with time. The observed temperature decreases during the first 20 s following a broken power-law: the first with index  $\alpha = -0.47 \pm 0.34$  and the second with index  $\beta = -1.48 \pm 1.13$ . From the observed Black body temperature, we infer the radius of the Black body emitter and its variation with time, see Fig. 13.5. We have seen that it increases slightly during the first 20 s of emission. In analogy with GRB 090618, we conclude that Episode 1 originates from the last phases of gravitational collapse of a stellar core, just prior to the collapse to a black hole. We call this core a “proto-black hole” (Ruffini et al., 2011, 2010). Immediately after, the collapse occurs and the GRB is emitted (Ep. 2).

5) From the knowledge of the redshift of the source, we have analyzed Episode 2 within the fireshell model. We determined a total energy  $E_{iso} = 1.79 \times 10^{53}$  erg and a P-GRB energy of  $2.51 \times 10^{51}$  erg, which we used to simulate the light curve and spectrum with the numerical code GRBsim. We find a baryon load  $B = 3.8 \times 10^{-3}$  and, at the transparency point, a value of the laboratory radius of  $1.34 \times 10^{14}$  cm, a theoretically predicted temperature of  $kT_{th} = 13.26$  keV (after cosmological correction) and a Lorentz Gamma factor of  $\Gamma = 260.48$ , confirming that Episode 2 is indeed a canonical GRB.

We conclude that GRB 101023 and GRB 090618 have striking analogies and are members of a specific new family of GRBs originating from a single core collapse. The existence of precise scaling laws between these two sources opens a new window on the use of GRBs as distance indicators. We are planning further identifications of additional sources belonging to this family at higher redshifts.

Full details on the analysis of GRB 101023 can be found in Penacchioni et al., submitted to A&A.



## A. On the GRB-SN association

Models of GRBs based on a single source (the “collapsar”) generating both the SN and the GRB abounds in the literature (see e.g. Woosley and Bloom, 2006). Since the two phenomena are qualitatively very different, in our approach we have emphasized the concept of induced gravitational collapse, which occurs strictly in a binary system. The SN originates from a star evolved out of the main sequence and the GRB from the collapse to a black hole. The concept of induced collapse implies at least two alternative scenarios. In the first, the GRB triggers a SN explosion in the very last phase of the thermonuclear evolution of a companion star (Ruffini et al., 2001a). In the second, the early phases of the SN induce gravitational collapse of a companion neutron star to a black hole (Ruffini, 2006). Of course, in absence of SN, there is also the possibility that the collapse to a black hole, generating the GRB, occurs in a single star system or in the final collapse of a binary neutron star system. Still, in such a case there is also the possibility that the black hole progenitor is represented by a binary system composed by a white dwarf and/or a neutron star and/or a black hole in various combinations. What is most remarkable is that, following the “uniqueness of the black hole” (see Ruffini, 2009), all these collapses lead to a common GRB independently of the nature of their progenitors.

Having obtained success in the fit of GRB 991216, as well as of GRB 031203 and GRB 050315 (see sections C.5 and C.6), we turn to the application of our theoretical analysis to the GRBs associated with SNe. We start with GRB 980425 / SN 1998bw. We have however to caution about the validity of this fit. From the available data of BeppoSAX, BATSE, XMM and Chandra, only the data of the prompt emission ( $t_a^d < 10^2$  s) and of the latest afterglow phases ( $t_a^d > 10^5$  s all the way to more than  $10^8$  s!) were available. Our fit refers only to the prompt emission, as usually interpreted as the peak of the afterglow. The fit, therefore, represents an underestimate of the GRB 980425 total energy and in this sense it is not surprising that it does not fit the Amati et al. (2002) relation. The latest afterglow emission, the URCA-1 emission, presents a different problematic which we will shortly address (see below).

### A.1. GRB 980425 / SN 1998bw / URCA-1

The best fit of the observational data of GRB 980425 (Pian et al., 2000; Frontera et al., 2000) leads to  $E_{e^\pm}^{tot} = 1.2 \times 10^{48}$  erg and  $B = 7.7 \times 10^{-3}$ . This implies

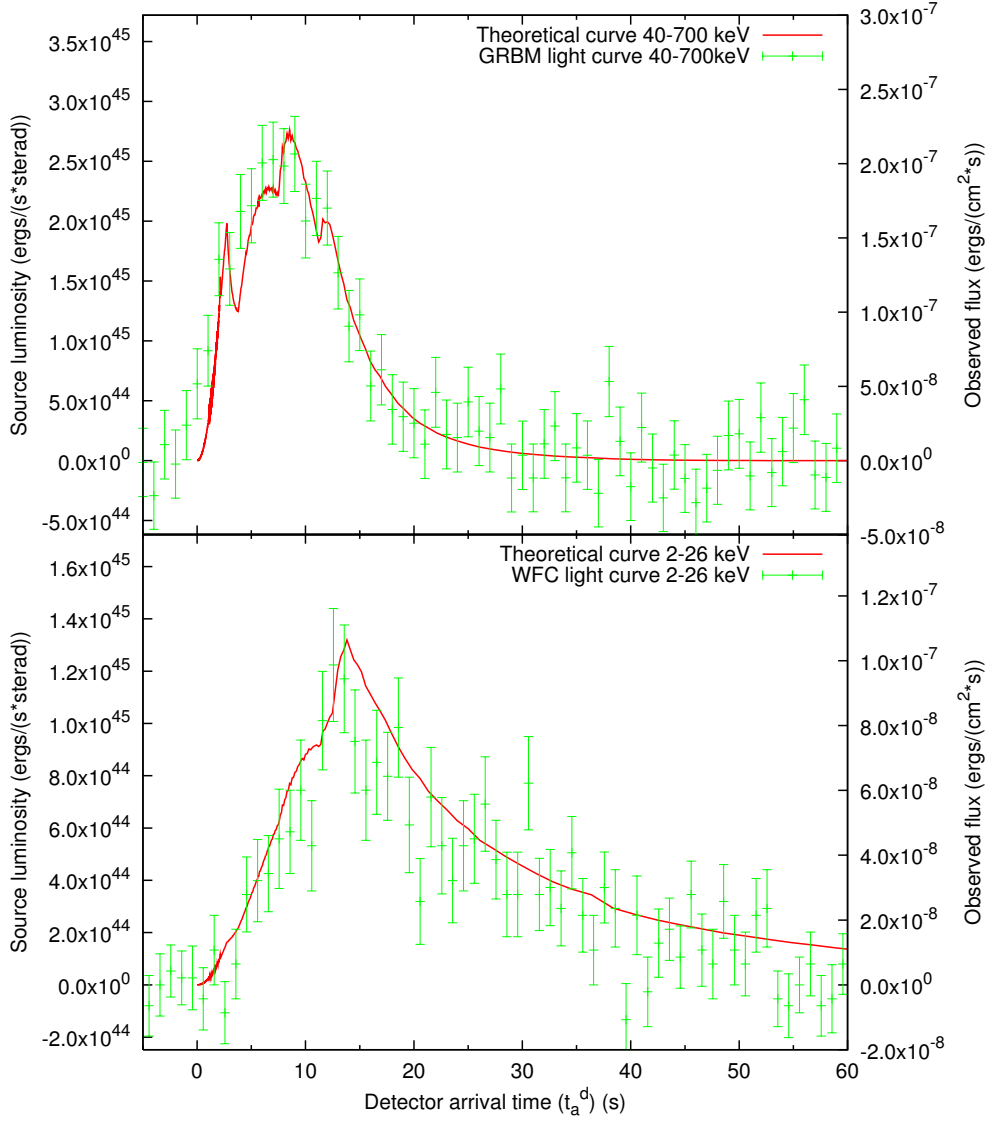


**Figure A.1.:** Theoretical light curves of GRB 980425 prompt emission in the 40–700 keV and 2–26 keV energy bands (red line), compared with the observed data respectively from Beppo-SAX GRBM and WFC (see Pian et al., 2000; Frontera et al., 2000).

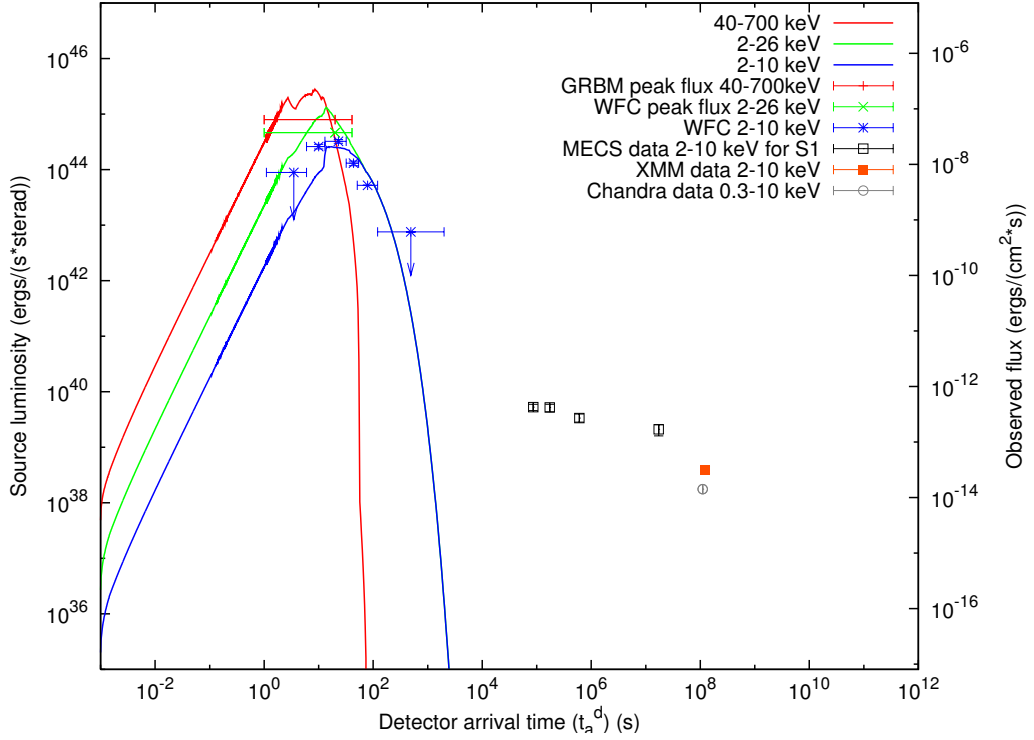


**Figure A.2.:** Theoretical light curves of GRB 980425 in the 40–700 keV (red line), 2–26 keV (green line), 2–10 keV (blue line) energy bands, represented together with URCA-1 observational data. All observations are by BeppoSAX (Pian et al., 2000), with the exception of the last two URCA-1 points, which is observed by XMM and Chandra (Pian et al., 2004; Kouveliotou et al., 2004).

an initial  $e^\pm$  plasma with  $N_{e^+e^-} = 3.6 \times 10^{53}$  and with an initial temperature  $T = 1.2$  MeV. After the transparency point, the initial Lorentz gamma factor of the accelerated baryons is  $\gamma_o = 124$ . The variability of the luminosity, due to the inhomogeneities of the CBM, is characterized by a density contrast  $\delta n/n \sim 10^{-1}$  on a length scale of  $\Delta \sim 10^{14}$  cm. We determine the effective CBM parameters to be:  $\langle n_{cbm} \rangle = 2.5 \times 10^{-2}$  particle/cm<sup>3</sup> and  $\langle \mathcal{R} \rangle = 1.2 \times 10^{-8}$ .

In Fig. A.1 we test our specific theoretical assumptions comparing our theoretically computed light curves in the 40–700 and 2–26 keV energy bands with the observations by the BeppoSAX GRBM and WFC during the first 60 s of data (see Pian et al., 2000; Frontera et al., 2000). The agreement between observations and theoretical predictions in Fig. A.1 is very satisfactory.

In Fig. A.2 we summarize some of the problematic implicit in the old *pre-Swift* era: data are missing in the crucial time interval between 60 s and  $10^5$  s, when the BeppoSAX NFI starts to point the GRB 980425 location. In this region we have assumed, for the effective CBM parameters, constant values inferred by the last observational data. Currently we are relaxing this condition, also in view of the interesting paper by Ghisellini et al. (2006).

The follow-up of GRB980425 with BeppoSAX NFI 10 hours, one week and 6 months after the event revealed the presence of an X-ray source consistent with SN1998bw (Pian et al., 2000), confirmed also by observations by XMM (Pian et al., 2004) and Chandra (Kouveliotou et al., 2004). The S1 X-ray light curve shows a decay much slower than usual X-ray GRB afterglows (Pian et al., 2000). We then address to this peculiar X-ray emission as “URCA-1” (see the following sections). In Fig. A.3A we represent the URCA-1 observations (Pian et al., 2000, 2004; Kouveliotou et al., 2004). The separation between the light curves of GRB 980425 in the 2–700 keV energy band, of SN 1998bw in the optical band (Nomoto et al., 2007; Pian et al., 2006), and of the above mentioned URCA-1 observations is evident.

## A.2. GRB 030329 / SN 2003dh / URCA-2

For GRB 030329 we have obtained (see Bernardini et al., 2004, 2005b; Ruffini et al., 2007b) a total energy  $E_{e^\pm}^{tot} = 2.12 \times 10^{52}$  erg and a baryon loading  $B = 4.8 \times 10^{-3}$ . This implies an initial  $e^\pm$  plasma with  $N_{e^+e^-} = 1.1 \times 10^{57}$  and with an initial temperature  $T = 2.1$  MeV. After the transparency point, the initial Lorentz gamma factor of the accelerated baryons is  $\gamma_o = 206$ . The effective CBM parameters are  $\langle n_{cbm} \rangle = 2.0$  particle/cm<sup>3</sup> and  $\langle \mathcal{R} \rangle = 2.8 \times 10^{-9}$ , with a density contrast  $\delta n/n \sim 10$  on a length scale of  $\Delta \sim 10^{14}$  cm. The resulting fit of the observations, both of the prompt phase and of the afterglow have been presented in Bernardini et al. (2004, 2005b). We compare in Fig. A.3B the light curves of GRB 030329 in the 2–400 keV energy band, of SN 2003dh in the optical band (Nomoto et al., 2007; Pian et al., 2006) and of the possible

**Table A.1.:** a) see Kaneko et al. (2007); b) Mazzali, P., private communication at MG11 meeting in Berlin, July 2006; c) evaluated fitting the URCAs with a power law followed by an exponentially decaying part; d) evaluated assuming a mass of the neutron star  $M = 1.5M_{\odot}$  and  $T \sim 5\text{--}7$  keV in the source rest frame; e) see Galama et al. (1998); Greiner et al. (2003); Prochaska et al. (2004); Mirabal et al. (2006).

GRB	$E_{e^{\pm}}^{tot}$ (erg)	$B$	$\gamma_0$	$E_{SN}^{bolom}$ (erg) <sup>a</sup>	$E_{SN}^{kin}$ (erg) <sup>b</sup>	$E_{URCA}$ (erg) <sup>c</sup>	$\frac{E_{e^{\pm}}^{tot}}{E_{URCA}}$	$\frac{E_{SN}^{kin}}{E_{URCA}}$	$R_{NS}$ (km) <sup>d</sup>	$z^e$
980425	$1.2 \times 10^{48}$	$7.7 \times 10^{-3}$	124	$2.3 \times 10^{49}$	$1.0 \times 10^{52}$	$3 \times 10^{48}$	0.4	$1.7 \times 10^4$	8	0.0085
030329	$2.1 \times 10^{52}$	$4.8 \times 10^{-3}$	206	$1.8 \times 10^{49}$	$8.0 \times 10^{51}$	$3 \times 10^{49}$	$6 \times 10^2$	$1.2 \times 10^3$	14	0.1685
031203	$1.8 \times 10^{50}$	$7.4 \times 10^{-3}$	133	$3.1 \times 10^{49}$	$1.5 \times 10^{52}$	$2 \times 10^{49}$	8.2	$3.0 \times 10^3$	20	0.105
060218	$1.8 \times 10^{50}$	$1.0 \times 10^{-2}$	99	$9.2 \times 10^{48}$	$2.0 \times 10^{51}$	?	?	?	?	0.033

URCA-2 emission observed by XMM-EPIC in 2–10 keV energy band (Tiengo et al., 2003, 2004).

### A.3. GRB 031203 / SN 2003lw / URCA-3

We will show in section C.5 the detailed analysis of GRB 031203 which leads to a total energy  $E_{e^{\pm}}^{tot} = 1.85 \times 10^{50}$  erg and to a baryon loading  $B = 7.4 \times 10^{-3}$ . This implies an initial  $e^{\pm}$  plasma with  $N_{e^+e^-} = 3.0 \times 10^{55}$  and with an initial temperature  $T = 1.5$  MeV. After the transparency point, the initial Lorentz gamma factor of the accelerated baryons is  $\gamma_0 = 132$ . The effective CBM parameters are  $\langle n_{cbm} \rangle = 1.6 \times 10^{-1}$  particle/cm<sup>3</sup> and  $\langle \mathcal{R} \rangle = 3.7 \times 10^{-9}$ , with a density contrast  $\delta n/n \sim 10$  on a length scale of  $\Delta \sim 10^{15}$  cm. In Fig. A.3C we compare the light curves of GRB 031203 in the 2–200 keV energy band, of SN 2003lw in the optical band (Nomoto et al., 2007; Pian et al., 2006) and of the possible URCA-3 emission observed by XMM-EPIC in the 0.2–10 keV energy band (Watson et al., 2004) and by Chandra in the 2–10 keV energy band (Soderberg et al., 2004).

### A.4. The GRB / SN / URCA connection

In Tab. A.1 we summarize the representative parameters of the above three GRB-SN systems together with GRB 060218-SN 2006aj which will be presented in section C.7, including the very large kinetic energy observed in all SNe (Mazzali, 2006). Some general conclusions on these weak GRBs at low redshift, associated to SN Ib/c, can be established on the ground of our analysis:

1) From the detailed fit of their light curves, as well as their accurate spectral analysis, it follows that all the above GRB sources originate consistently from the formation of a black hole. This result extends to this low-energy GRB class at small cosmological redshift the applicability of our model, which now

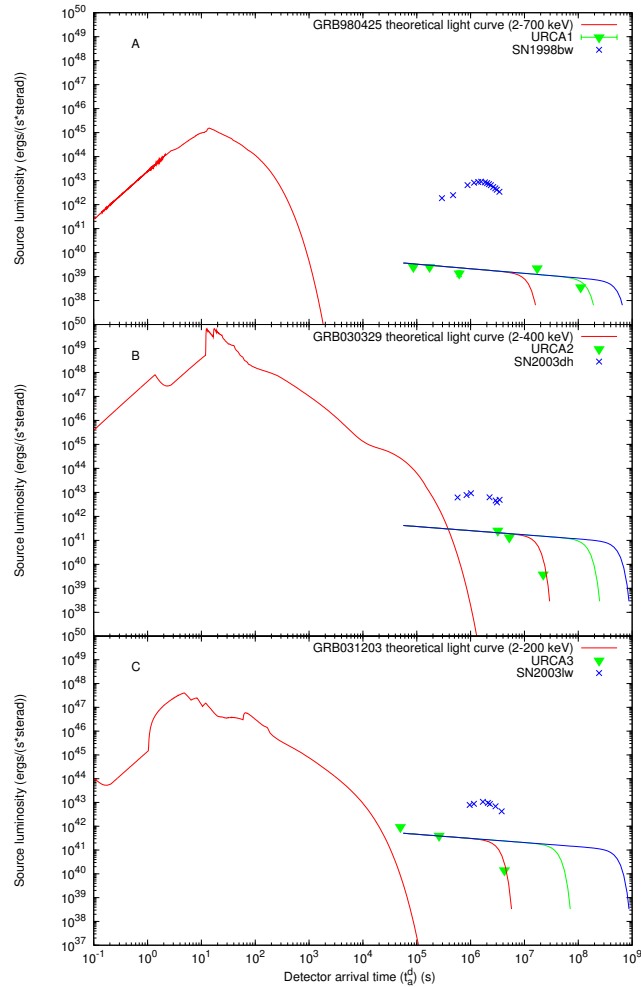


**Figure A.3.:** Theoretically computed light curves of GRB 980425 in the 2–700 keV band (A), of GRB 030329 in the 2–400 keV band (B) and of GRB 031203 in the 2–200 keV band (C) are represented, together with the URCA observational data and qualitative representative curves for their emission, fitted with a power law followed by an exponentially decaying part. The luminosity of the SNe in the 3000 – 24000 Å are also represented (Nomoto et al., 2007; Pian et al., 2006).

spans over a range of energy of six orders of magnitude from  $10^{48}$  to  $10^{54}$  ergs (Ruffini et al., 2003, 2004a, 2007b; Bernardini et al., 2004, 2005b,a; Ruffini et al., 2006b). Distinctive of this class is the very high value of the baryon loading which in one case (GRB 060218, see section C.7 and Dainotti et al., 2007) is very close to the maximum limit compatible with the dynamical stability of the adiabatic optically thick acceleration phase of the GRBs (Ruffini et al., 2000). Correspondingly, the maximum Lorentz gamma factors are systematically smaller than the ones of the more energetic GRBs at large cosmological distances. This in turn implies the smoothness of the observed light curves in the so-called “prompt phase”. The only exception to this is the case of GRB 030329.

2) The accurate fits of the GRBs allow us to infer also some general properties of the CBM. While the size of the clumps of the inhomogeneities is  $\Delta \approx 10^{14}$  cm, the effective CBM average density is consistently smaller than in the case of more energetic GRBs: we have in fact  $\langle n_{cbm} \rangle$  in the range between  $\sim 10^{-6}$  particle/cm<sup>3</sup> (GRB 060218) and  $\sim 10^{-1}$  particle/cm<sup>3</sup> (GRB 031203), while only in the case of GRB 030329 it is  $\sim 2$  particle/cm<sup>3</sup>. We are also currently studying a characteristic trend in the variability of  $\mathcal{R}$  during some specific bursts as well as the physical origin of the consistently smaller effective CBM density  $\langle n_{cbm} \rangle$  values observed in these sources (see Dainotti et al., 2007).

3) Still within their weakness these four GRB sources present a large variability in their total energy: a factor  $10^4$  between GRB 980425 and GRB 030329. Remarkably, the SNe emission both in their very high kinetic energy and in their bolometric energy appear to be almost constant respectively  $10^{52}$  erg and  $10^{49}$  erg. The URCA sources present also a remarkably steady behavior around a “standard luminosity” and a typical temporal evolution. The weakness in the energetics of GRB 980425 and GRB 031203, and the sizes of their dyadospheres, suggest that they originate from the formation of the smallest possible black hole, just over the critical mass of the neutron star (see Fig. A.4 and Ruffini, 2006).

## A.5. URCA-1, URCA-2 and URCA-3

We turn to the search for the nature of URCA-1, URCA-2 and URCA-3. These systems are not yet understood and may have an important role in the comprehension of the astrophysical scenario of GRB sources. It is important to perform additional observations in order to verify if the URCA sources are related to the black hole originating the GRB phenomenon or to the SN. Even a single observation of an URCA source with a GRB in absence of a SN would prove their relation with the black hole formation. Such a result is today theoretically unexpected and would open new problematics in relativistic astrophysics and in the physics of black holes. Alternatively, even a single observation of an URCA source during the early expansion phase of a Type Ib/c

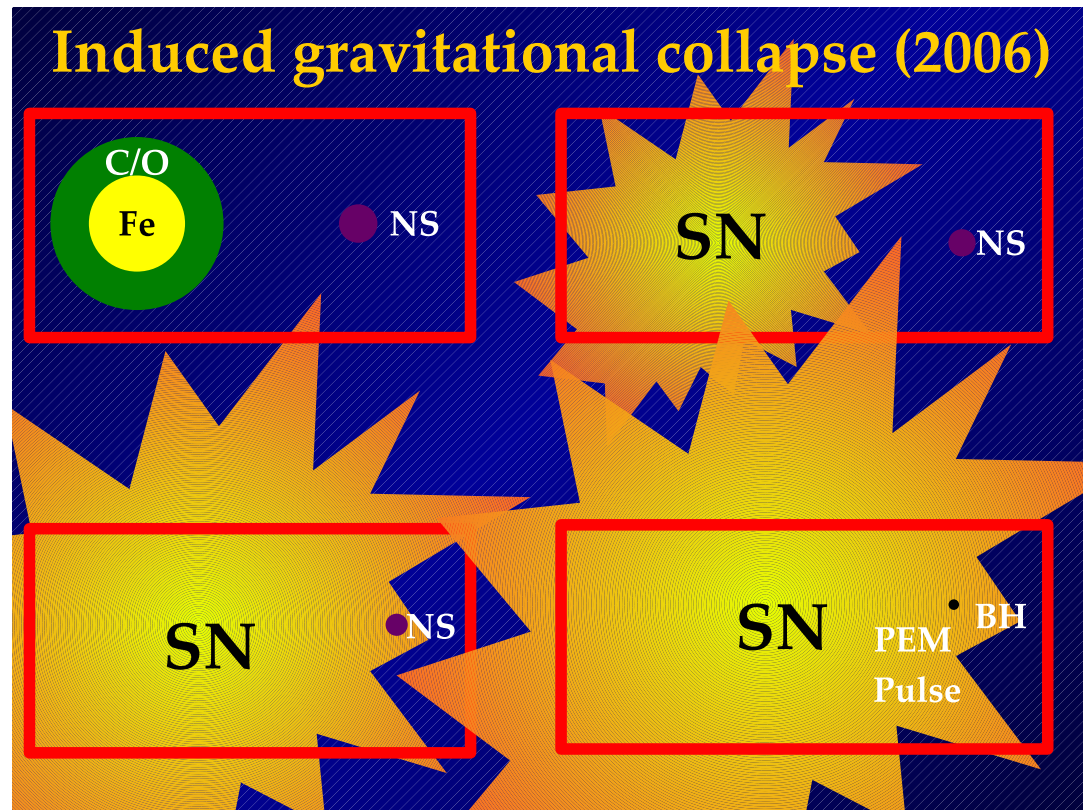


**Figure A.4.:** A possible process of gravitational collapse to a black hole “induced” by the Ib/c SN on a companion neutron star in a close binary system. Details in Ruffini (2006).

SN in absence of a GRB would prove the early expansion phases of the SN remnants. In the case that none of such two conditions are fulfilled, then the URCA sources must be related to the GRBs occurring in presence of a SN. In such a case, one of the possibilities would be that for the first time we are observing a newly born neutron star out of the supernova phenomenon unveiled by the GRB. This last possibility would offer new fundamental information about the outcome of the gravitational collapse, and especially about the equations of state at supranuclear densities and about a variety of fundamental issues of relativistic astrophysics of neutron stars.

The names of “URCA-1” and “URCA-2” for the peculiar late X-ray emission of GRB 980425 and GRB 030329 were given in the occasion of the Tenth Marcel Grossmann meeting held in Rio de Janeiro (Brazil) in the Village of Urca (see Ruffini et al., 2005b). Their identification was made at that time and presented at that meeting. However, there are additional reasons for the choice of these names. Another important physical phenomenon was indeed introduced in 1941 in the same Village of Urca by George Gamow and Mario Schoenberg (see Gamow and Schoenberg, 1941). The need for a rapid cooling process due to neutrino anti-neutrino emission in the process of gravitational collapse leading to the formation of a neutron star was there considered for the first time. It was Gamow who named this cooling as “Urca process” (see Gamow, 1970). Since then, a systematic analysis of the theory of neutron star cooling was advanced by Tsuruta (1964, 1979); Tsuruta and Cameron (1966); Tsuruta et al. (2002); Canuto (1978). The coming of age of X-ray observatories such as Einstein (1978-1981), EXOSAT (1983-1986), ROSAT (1990-1998), and the contemporary missions of Chandra and XMM-Newton since 1999 dramatically presented an observational situation establishing very embarrassing and stringent upper limits to the surface temperature of neutron stars in well known historical supernova remnants (see e.g. Romani, 1987). It was so that, for some remnants, notably SN 1006 and the Tycho supernova, the upper limits to the surface temperatures were significantly lower than the temperatures given by standard cooling times (see e.g. Romani, 1987). Much of the theoretical works has been mainly directed, therefore, to find theoretical arguments in order to explain such low surface temperature  $T_s \sim 0.5\text{--}1.0 \times 10^6$  K — embarrassingly low, when compared to the initial hot ( $\sim 10^{11}$  K) birth of a neutron star in a supernova explosion (see e.g. Romani, 1987). Some important contributions in this researches have been presented by van Riper (1988, 1991); Burrows and Lattimer (1986); Lattimer et al. (1994); Yakovlev and Pethick (2004). The youngest neutron star to be searched for thermal emission has been the pulsar PSR J0205+6449 in 3C 58 (see e.g. Yakovlev and Pethick, 2004), which is 820 years old! Trümper (2005) reported evidence for the detection of thermal emission from the crab nebula pulsar which is, again, 951 years old.

URCA-1, URCA-2 and URCA-3 may explore a totally different regime: the X-ray emission possibly from a recently born neutron star in the first days –

months of its existence. The thermal emission from the young neutron star surface would in principle give information on the equations of state in the core at supranuclear densities and on the detailed mechanism of the formation of the neutron star itself with the related neutrino emission. It is also possible that the neutron star is initially fast rotating and its early emission could be dominated by the magnetospheric emission or by accretion processes from the remnant which would overshadow the thermal emission. A periodic signal related to the neutron star rotational period should in principle be observable in a close enough GRB-SN system. In order to attract attention to this problematic, we have given in Tab. A.1 an estimate of the corresponding neutron star radius for URCA-1, URCA-2 and URCA-3. It has been pointed out (see e.g. Pian et al., 2000) the different spectral properties between the GRBs and the URCAs. It would be also interesting to compare and contrast the spectra of all URCAs in order to evidence any analogy among them. Observations of a powerful URCA source on time scales of 0.1–10 seconds would be highly desirable.

## B. Collisions in the slowing down phase of the prompt emission

One of the main results of the *Swift* satellite was to unveil the unknown window time of the early afterglow ( $10^2 - 10^4$  s) with multiwavelength observations, in order to answer some questions concerning in particular the possibility that the prompt emission and the afterglow originate from the same physical process (Meszaros and Rees, 1993; Rees and Meszaros, 1994; Ruffini et al., 2001b). These observations allowed the identification in a good sample of bursts of a so-called canonical behavior (Nousek et al., 2006; Evans et al., 2009): a steep decay followed by a shallow decline, the “plateau phase”, followed then by a more conventional decay.

The origin of this “plateau phase” is a puzzle. Within the standard fireball model, a variety of explanations have been advanced. In particular, Zhang et al. (2006) summarizes three possible physical origins: **1)** the central engine itself is long lasting, behaving like  $L(t) \propto t^{-q}$  (Dai and Lu, 1998; Zhang and Mészáros, 2001); **2)** the central engine activity may be brief but at the end of the prompt phase the ejecta have a range of Lorentz factors such that the amount of mass with Lorentz factor greater than  $\gamma$  is  $M(> \gamma) \propto \gamma^{-5}$  (Rees and Meszaros, 1998; Panaitescu et al., 1998; Sari and Mészáros, 2000); **3)** the energy injection is also brief but the outflow has a significant fraction of Poynting flux (Usov, 1992; Thompson, 1994; Meszaros and Rees, 1997b; Lyutikov and Blandford, 2003). In this case the energy transfer to the ambient medium can be delayed with respect to the standard case (Zhang and Kobayashi, 2005).

In this Letter we consider one of these possibilities within the fireshell model. Following the Rees and Meszaros (1998) proposal, we consider the material stored inside the fireshell not as a unique shell, instead it moves with a range of Lorentz factors. During the prompt emission phase, the fastest material that is in front is slowed by the interaction of the CircumBurst Medium (CBM) so that at the end of the prompt emission the slower material will catch up with it. Therefore, the plateau phase is the result of this injection, that produces a modification both in the dynamics of the fireshell and in the spectrum of the emitted radiation.

We postulate that this spread in the fireshell Lorentz factor occurs when the fireshell becomes transparent, and some hints on this directions have been provided by studies of the Proper-GRB (P-GRB) structure with different baryon loadings (see De Barros et al, in preparation). This hypothesis is

compatible with the basic idea of the fireshell model that all GRBs originate from the gravitational collapse to a black hole that provides the initial energy of the system, but all the following evolution is unconnected from the progenitor's details and do not depend on a prolonged activity of the central engine. The novelty in this approach is that while the prompt phase has an "external" origin, being the result of the interaction of the fireshell with the CBM, the shallow decaying phase paradoxically has an "internal" origin.

The aim of this section is to characterize dynamically the system in order to understand the nature of that material. In doing so, we schematically represent the outflow as two shells: one is the main fireshell that moves with an initial Lorentz factor  $\gamma_0$  that decreases due to the interaction with the CBM and the other represent the trailing slow material that expands ballistically with constant speed. We examine the several GRBs for which we have all details of the parameters characterizing the dynamics of the system. The aim is to see if we can find a quantitative correlation between the two Lorentz gamma factors considered in this process.

## **B.1. Dynamics of the Collision and determination of $\gamma_2$**

Suppose that the fireshell moves with an initial Lorentz factor  $\gamma_0$  that decreases due to the interaction with the CBM, and that the injecting material is contained in a second shell with constant Lorentz factor  $\gamma_2 \leq \gamma_0$  (see Fig. B.1). The second shell will catch up with the fireshell at a certain radius  $r^*$  and laboratory time  $t^*$  such that:

$$r^* = \beta_2 c t^*, \quad (\text{B.1.1})$$

where  $\beta_2 = \sqrt{1 - 1/\gamma_2^2}$  is the velocity of the second shell, and  $r^*$  and  $t^*$  are fixed by the dynamics of the fireshell.

If we assume that the X-ray plateau is the result of the collision between the fireshell and the second shell, we can identify its onset with the moment at which the collision occurs. We determine this time in the observer frame  $t_{ob}^*$  by fitting the X-ray afterglow with a broken power law:

$$F(t_{ob}) = N \left( \left( \frac{t_{ob}}{t_{ob}^*} \right)^a + \left( \frac{t_{ob}}{t_{ob}^*} \right)^b \right). \quad (\text{B.1.2})$$

Since the second shell expands with constant velocity, the corresponding laboratory time at which a photon is emitted along the line of sight is (neglecting the initial time that corresponds to the time at which the transparency occurs

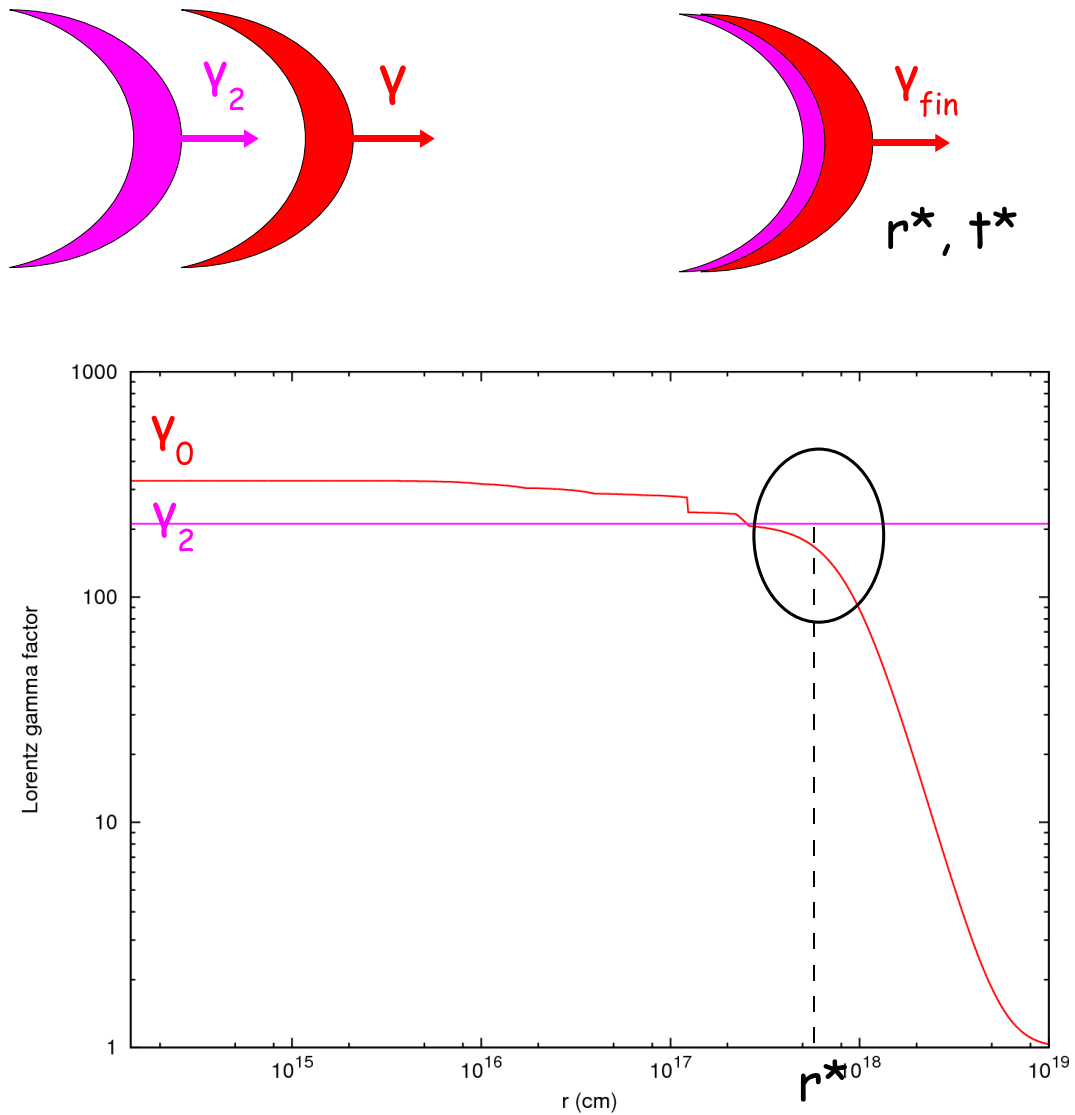


**Figure B.1.:** The fireshell (red shell) moves with an initial Lorentz factor  $\gamma_0$  that decreases due to the interaction with the CBM, and the injecting material, represented by the second shell (pink shell), moves with constant Lorentz factor  $\gamma_2 \leq \gamma_0$ . The second shell will catch up with the fireshell at a certain radius  $r^*$ .

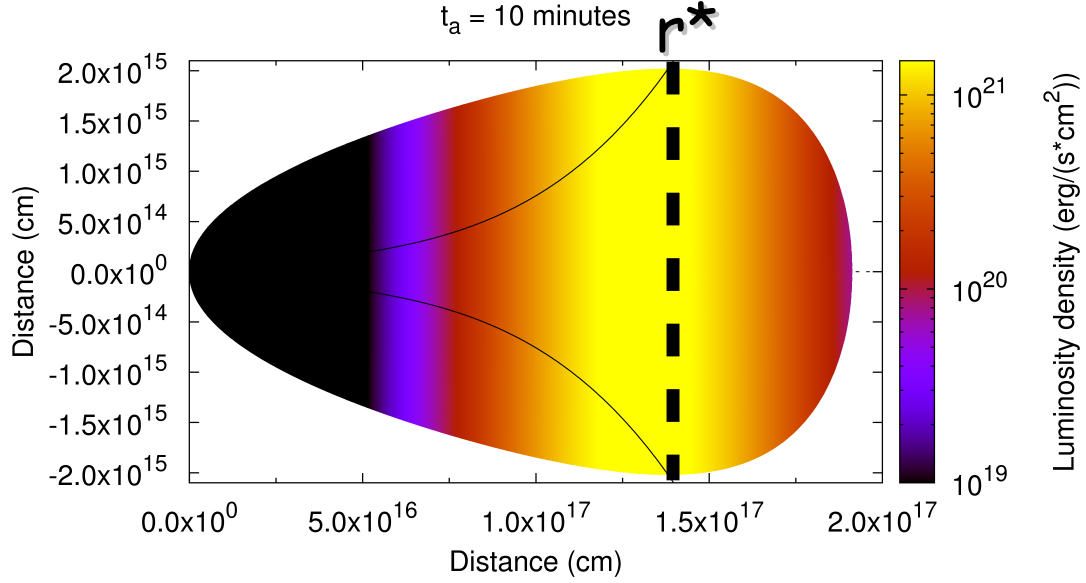


**Figure B.2.:** Emitted bolometric luminosity on an EQTS corresponding to an observed time of 10 minutes. It is manifest how the most luminous emitting region corresponds to the boundary of the visible region (solid line). The dashed line therefore traces the radius that we assume to be the collision radius  $r^*$ .

$t_o \ll t^*$ ):

$$t^* = 2\gamma^2 \frac{t_{ob}^*}{1+z}, \quad (\text{B.1.3})$$

where we accounted also for the cosmological redshift of the source  $z$ .

The second step is to identify the radius  $r^*$ . For relativistic extended emitters, the photons observed at the same time are emitted by the source at different radii, and they describe a surface called EQuiTemporal Surface (EQTS, see Fig. B.2 and Bianco and Ruffini, 2005b). Therefore, it is not obvious to establish in the evolution of the fireshell which is the collision radius, i.e. which radius corresponds to the  $t_{ob}^*$  determined above. From the analysis of the luminosity emitted by a fixed EQTS (see Section ...Carlo..EQTS...) it results that at observed times corresponding to the onset of the plateau the most luminous region is the boundary of the visible region,  $\theta_{max} \sim 1/\gamma$ , where  $\gamma$  is the Lorentz factor of the fireshell at the moment of the collision and depends strongly on the details of the CircumBurst Medium (CBM) adopted. The most reasonable choice is to estimate tentatively  $r^*$  as the radius corresponding to the boundary of the EQTS visible area associated to  $t_{ob}^*$  (dashed line in Fig. B.2), which is approximately smaller than the head on radius by a factor 2 for a constant speed motion.

We can now evaluate the Lorentz factor that the second shell should have

in order to produce a collision observed at  $t_{ob}^*$  with the fireshell:

$$\gamma_2 \simeq \sqrt{\frac{r^*(1+z)}{ct_{ob}^*} + \frac{1}{2}}. \quad (\text{B.1.4})$$

We select 6 GRBs among those examined within the fireshell model that show in the X-ray afterglow a behavior compatible with the X-ray plateau. In Table B.1 the results obtained for the GRBs of the sample are reported.

**Table B.1.:** Table of the GRBs of our sample including also GRB080319B (see Sec. B.2). For these GRBs there are reported the observed time with error and radius of the collision ( $t_{ob}^*$  and  $r^*$ ), the Lorentz gamma factor of the fireshell at  $r^*$  ( $\gamma_1$ ) and at the transparency ( $\gamma_\circ$ ), the redshift  $z$ , the value adopted for the free parameters of the fireshell model ( $E_{tot}^{e\pm}$  and  $B$ ) and the Lorentz gamma factor of the second shell derived  $\gamma_2$  with error.

GRB	$t_{ob}^*$ (s)	$\Delta t_{ob}^*$ (s)	$r^*$ (cm)	$\gamma_1$	$\gamma_\circ$	$z$	$E_{tot}^{e\pm}$ (erg)	$B$
<b>060218</b>	$1.05 \times 10^4$	$1.57 \times 10^3$	$1.12 \times 10^{18}$	53.6	99.3	0.03	$2.32 \times 10^{50}$	$1.00 \times 10$
<b>050315</b>	$4.64 \times 10^2$	$2.98 \times 10^1$	$7.30 \times 10^{16}$	102.0	220.0	1.95	$1.46 \times 10^{53}$	$4.55 \times 10$
<b>060607A</b>	$1.18 \times 10^3$	$5.41 \times 10^2$	$3.87 \times 10^{17}$	196.0	328.0	3.08	$2.50 \times 10^{53}$	$3.00 \times 10$
<b>060614</b>	$1.20 \times 10^3$	$4.60 \times 10^1$	$9.40 \times 10^{17}$	146.0	345.0	0.13	$2.94 \times 10^{51}$	$2.80 \times 10$
<b>080319B</b>	$3.00 \times 10^1$	$2.00 \times 10^1$	$5.65 \times 10^{16}$	335.0	394.0	0.94	$1.00 \times 10^{54}$	$2.50 \times 10$
<b>090423</b>	$3.94 \times 10^2$	$5.13 \times 10^1$	$4.26 \times 10^{17}$	548.0	1190.0	8.1	$1.20 \times 10^{53}$	$8.00 \times 10$
<b>050904</b>	$6.46 \times 10^2$	$4.54 \times 10^1$	$1.68 \times 10^{17}$	201.0	489.0	6.29	$5.00 \times 10^{53}$	$2.00 \times 10$

## B.2. $\gamma_2$ - $\gamma_\circ$ correlation

The result of this analysis reveals (see Fig. B.3) the existence of a correlation between the Lorentz factor of the second shell  $\gamma_2$  and the maximum Lorentz factor of the fireshell  $\gamma_\circ$ ,  $\gamma_2 \propto \gamma_\circ^{0.9}$ , with  $\chi^2/dof = 0.67$  and a Spearman rank coefficient  $r_s = 0.91$  (null hypothesis probability  $nhp = 0.0083$ ).

This correlation is not trivial since the dynamics of the fireshell after the transparency is determined uniquely by the CBM distribution that is different for each GRB. It reveals indeed that the second shell is not erratic, emitted in a second episode of the engine activity, but it is intertwined with the main fireshell until the transparency. Therefore, the correlation provides some hints on the origin of the second shell (see e.g. De Barros et al., in preparation).

The correlation between  $\gamma_2$  and  $\gamma_\circ$  can also be used to “predict” the X-ray

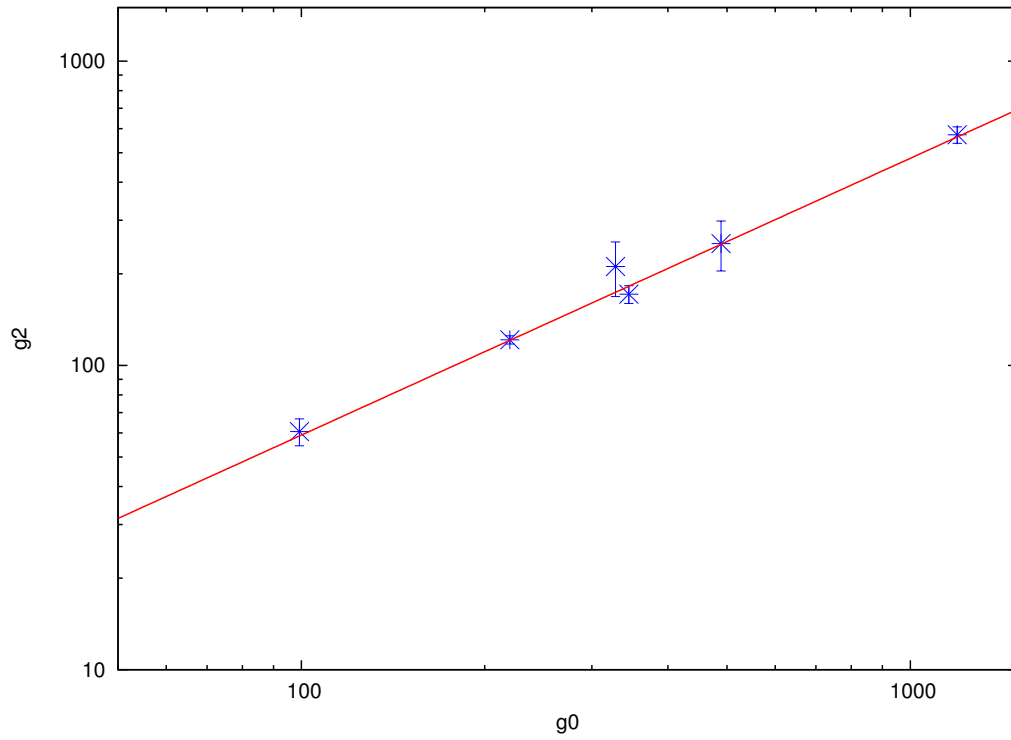


**Figure B.3.:** Lorentz gamma factor of the second shell  $\gamma_2$  versus the maximum Lorentz factor of the fireshell  $\gamma_0$  for the 6 GRBs of the sample. The correlation between the two quantities is manifest.

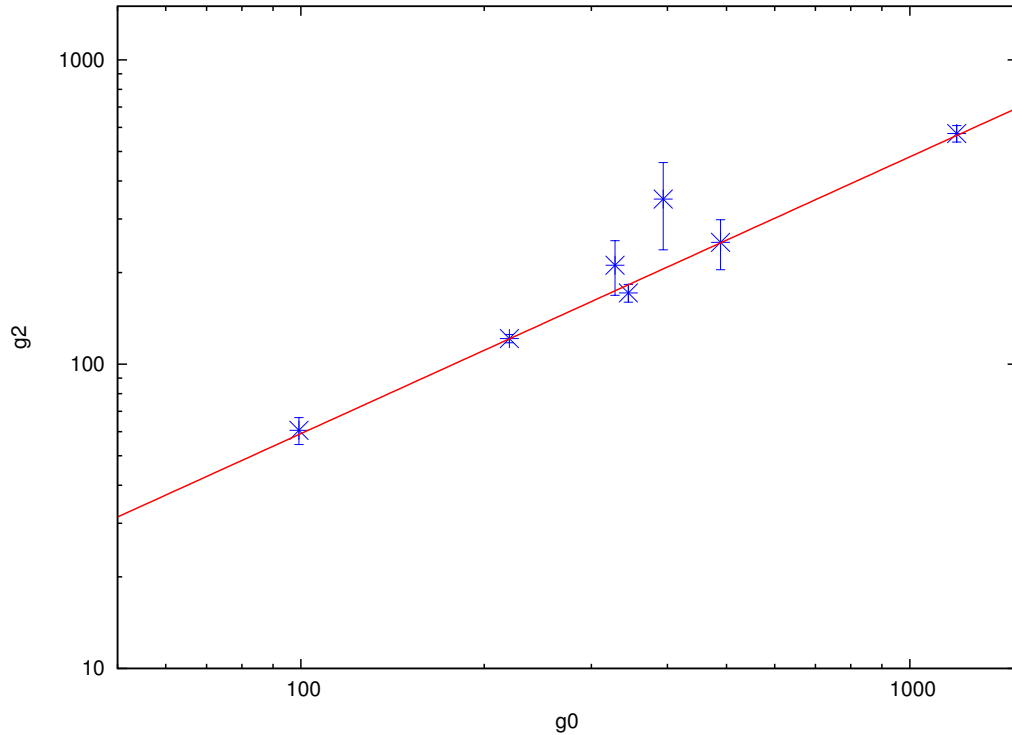


**Figure B.4.:** Same as Fig. B.3 with in addition the values for GRB080319B, assuming that the plateau phase occurs during the prompt emission. A correlation is still present.

plateau when it is not observed. We use as an example GRB080319B (Racusin et al., 2008, , Patricelli et al., in preparation). This GRB exhibits an X-ray afterglow well monitored from 51 s (Racusin et al., 2008) that decays as a simple power-law. Moreover, it has been pointed out (Margutti et al., 2008; Stamatikos et al., 2009) that the prompt emission can be divided in two different episodes on the basis of different properties of the temporal variability. We guessed therefore that the plateau phase could be occurred during the prompt emission as a “ $\gamma$ -ray plateau”, coincident with the second episode. With this assumption we performed the analysis described before and we found that the  $\gamma_2$  obtained is only marginally correlated with  $\gamma_0$ , thus neither confirming nor excluding this possibility (see Fig. B.4).



## C. Applications to various sources from previous year report

### C.1. Application to GRB 970228

GRB 970228 was detected by the Gamma-Ray Burst Monitor (GRBM, 40–700 keV) and Wide Field Cameras (WFC, 2–26 keV) on board BeppoSAX on February 28.123620 UT (Frontera et al., 1998). The burst prompt emission is characterized by an initial 5 s strong pulse followed, after 30 s, by a set of three additional pulses of decreasing intensity (Frontera et al., 1998). Eight hours after the initial detection, the NFIs on board BeppoSAX were pointed at the burst location for a first target of opportunity observation and a new X-ray source was detected in the GRB error box: this is the first “afterglow” ever detected (Costa et al., 1997). A fading optical transient has been identified in a position consistent with the X-ray transient (van Paradijs et al., 1997), coincident with a faint galaxy with redshift  $z = 0.695$  (Bloom et al., 2001). Further observations by the Hubble Space Telescope clearly showed that the optical counterpart was located in the outskirts of a late-type galaxy with an irregular morphology (Sahu et al., 1997).

The BeppoSAX observations of GRB 970228 prompt emission revealed a discontinuity in the spectral index between the end of the first pulse and the beginning of the three additional ones (Costa et al., 1997; Frontera et al., 1998, 2000). The spectrum during the first 3 s of the second pulse is significantly harder than during the last part of the first pulse (Frontera et al., 1998, 2000), while the spectrum of the last three pulses appear to be consistent with the late X-ray afterglow (Frontera et al., 1998, 2000). This was soon recognized by Frontera et al. (1998, 2000) as pointing to an emission mechanism producing the X-ray afterglow already taking place after the first pulse.

As recalled above, the simultaneous occurrence of an afterglow with total time-integrated luminosity larger than the P-GRB one, but with a smaller peak luminosity, is indeed explainable in terms of a peculiarly small average value of the CBM density and not due to the intrinsic nature of the source. In this sense, GRBs belonging to this class are only “fake” short GRBs. We show that GRB 970228 is a very clear example of this situation. We identify the initial spikelike emission with the P-GRB, and the late soft bump with the peak of the afterglow. GRB 970228 shares the same morphology and observational features with the sources analyzed by Norris and Bonnell (2006) as well as

with e.g. GRB 050709 (Villasenor et al., 2005), GRB 050724 (Campana et al., 2006b) and GRB 060614 (see appendix C.2 and Gehrels et al., 2006). Therefore, we propose GRB 970228 as a prototype for this new GRB class.

### C.1.1. The analysis of GRB 970228 prompt emission

In Fig. C.1 we present the theoretical fit of BeppoSAX GRBM (40–700 keV) and WFC (2–26 keV) light curves of GRB 970228 prompt emission (Frontera et al., 1998). Within our “canonical GRB” scenario we identify the first main pulse with the P-GRB and the three additional pulses with the afterglow peak emission, consistently with the above mentioned observations by Costa et al. (1997) and Frontera et al. (1998). Such last three pulses have been reproduced assuming three overdense spherical CBM regions (see Fig. C.2) with a very good agreement (see Fig. C.1).

We therefore obtain for the two parameters characterizing the source in our model  $E_{e^\pm}^{tot} = 1.45 \times 10^{54}$  erg and  $B = 5.0 \times 10^{-3}$ . This implies an initial  $e^\pm$  plasma created between the radii  $r_1 = 3.52 \times 10^7$  cm and  $r_2 = 4.87 \times 10^8$  cm with a total number of  $e^\pm$  pairs  $N_{e^\pm} = 1.6 \times 10^{59}$  and an initial temperature  $T = 1.7$  MeV. The theoretically estimated total isotropic energy emitted in the P-GRB is  $E_{P-GRB} = 1.1\% E_{e^\pm}^{tot} = 1.54 \times 10^{52}$  erg, in excellent agreement with the one observed in the first main pulse ( $E_{P-GRB}^{obs} \sim 1.5 \times 10^{52}$  erg in 2 – 700 keV energy band, see Fig. C.1), as expected due to their identification. After the transparency point at  $r_0 = 4.37 \times 10^{14}$  cm from the progenitor, the initial Lorentz gamma factor of the fireshell is  $\gamma_0 = 199$ . On average, during the afterglow peak emission phase we have for the CBM  $\langle \mathcal{R} \rangle = 1.5 \times 10^{-7}$  and  $\langle n_{cbm} \rangle = 9.5 \times 10^{-4}$  particles/cm<sup>3</sup>. This very low average value for the CBM density is compatible with the observed occurrence of GRB 970228 in its host galaxy’s halo (Sahu et al., 1997; van Paradijs et al., 1997; Panaitescu, 2006) and it is crucial in explaining the light curve behavior.

The values of  $E_{e^\pm}^{tot}$  and  $B$  we determined are univocally fixed by two tight constraints. The first one is the total energy emitted by the source all the way up to the latest afterglow phases (i.e. up to  $\sim 10^6$  s). The second one is the ratio between the total time-integrated luminosity of the P-GRB and the corresponding one of the whole afterglow (i.e. up to  $\sim 10^6$  s). In particular, in GRB 970228 such a ratio results to be  $\sim 1.1\%$  (see Fig. 3.8). However, the P-GRB peak luminosity actually results to be much more intense than the afterglow one (see Fig. C.1). This is due to the very low average value of the CBM density  $\langle n_{cbm} \rangle = 9.5 \times 10^{-4}$  particles/cm<sup>3</sup>, which produces a less intense afterglow emission. Since the afterglow total time-integrated luminosity is fixed, such a less intense emission lasts longer than what we would expect for an average density  $\langle n_{cbm} \rangle \sim 1$  particles/cm<sup>3</sup>.

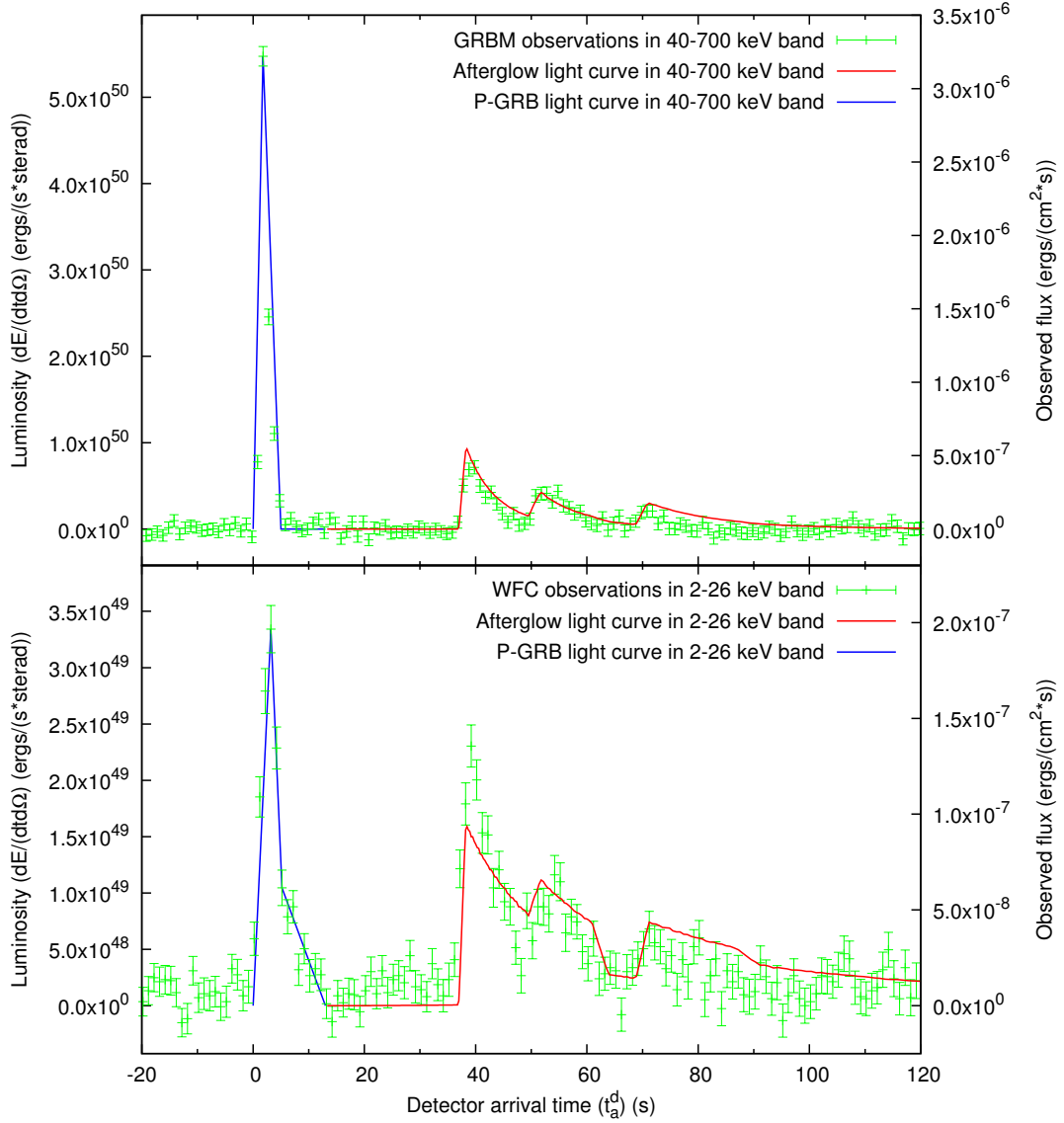


**Figure C.1.:** The “canonical GRB” light curve theoretically computed for the prompt emission of GRB 970228. BeppoSAX GRBM (40–700 keV, above) and WFC (2–26 keV, below) light curves (data points) are compared with the afterglow peak theoretical ones (solid lines). The onset of the afterglow coincides with the end of the P-GRB (represented qualitatively by the dotted lines). For this source we have  $B \simeq 5.0 \times 10^{-3}$  and  $\langle n_{cbm} \rangle \sim 10^{-3}$  particles/cm<sup>3</sup>.

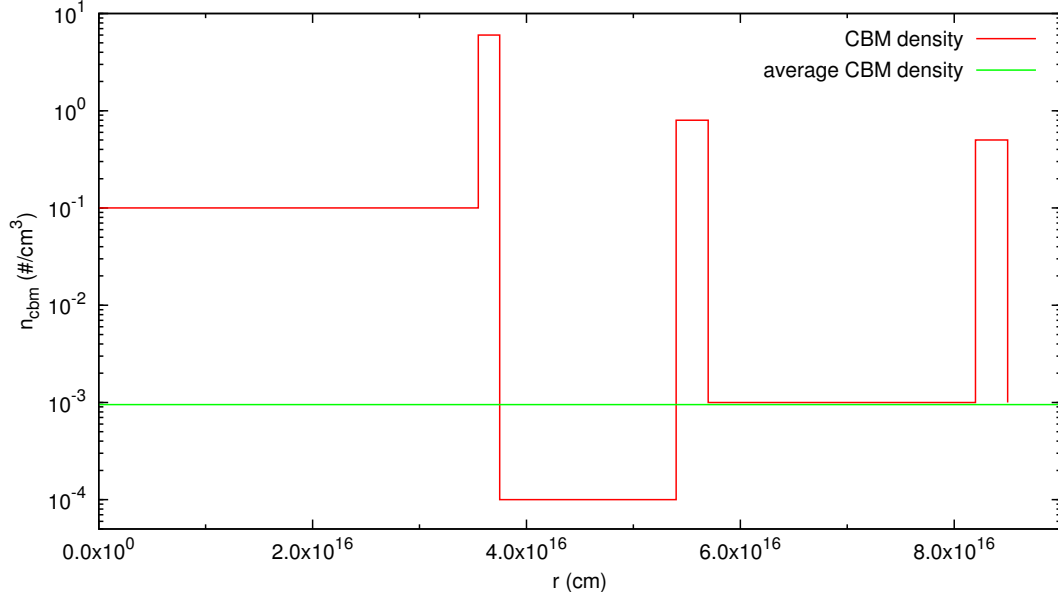


**Figure C.2.:** The CBM density profile we assumed to reproduce the last three pulses of the GRB 970228 prompt emission (red line), together with its average value  $\langle n_{cbm} \rangle = 9.5 \times 10^{-4}$  particles/cm<sup>3</sup> (green line).

### C.1.2. Rescaling the CBM density

We present now an explicit example in order to probe the crucial role of the average CBM density in explaining the relative intensities of the P-GRB and of the afterglow peak in GRB 970228. We keep fixed the basic parameters of the source, namely the total energy  $E_{e^\pm}^{tot}$  and the baryon loading  $B$ , therefore keeping fixed the P-GRB and the afterglow total time-integrated luminosities. Then we rescale the CBM density profile given in Fig. C.2 by a constant numerical factor in order to raise its average value to the standard one  $\langle n_{ism} \rangle = 1$  particle/cm<sup>3</sup>. We then compute the corresponding light curve, shown in Fig. C.3.

We notice a clear enhancement of the afterglow peak luminosity with respect to the P-GRB one in comparison with the fit of the observational data presented in Fig. C.1. The two light curves actually crosses at  $t_a^d \simeq 1.8 \times 10^4$  s since their total time-integrated luminosities must be the same. The GRB “rescaled” to  $\langle n_{ism} \rangle = 1$  particle/cm<sup>3</sup> appears to be totally similar to, e.g., GRB 050315 (Ruffini et al., 2006b) and GRB 991216 (Ruffini et al., 2003, 2004b, 2005a).

It is appropriate to emphasize that, although the two underlying CBM density profiles differ by a constant numerical factor, the two afterglow light curves in Fig. C.3 do not. This is because the absolute value of the CBM density at each point affects in a non-linear way all the following evolution of the fireshell due to the feedback on its dynamics (Bianco and Ruffini, 2005a).

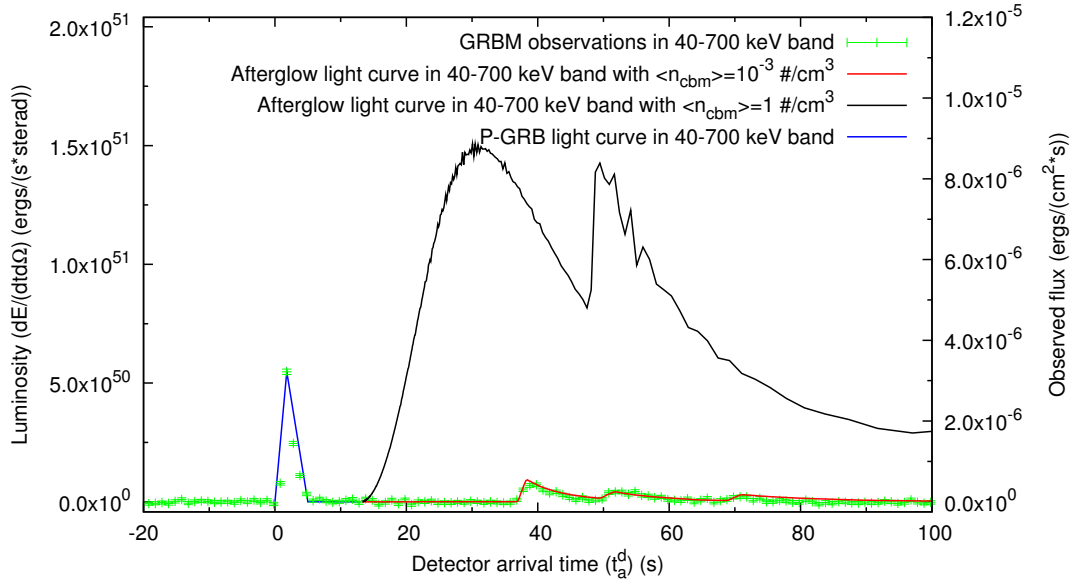


**Figure C.3.:** The theoretical fit of the BeppoSAX GRBM observations (red line, see Fig. C.1) is compared with the afterglow light curve in the 40–700 keV energy band obtained rescaling the CBM density to  $\langle n_{cbm} \rangle = 1$  particle/cm<sup>3</sup> keeping constant its shape and the values of the fundamental parameters of the theory  $E_{e\pm}^{tot}$  and  $B$  (black line). The P-GRB duration and luminosity (blue line), depending only on  $E_{e\pm}^{tot}$  and  $B$ , are not affected by this process of rescaling the CBM density.

Moreover, the shape of the surfaces of equal arrival time of the photons at the detector (EQTS) is strongly elongated along the line of sight (Bianco and Ruffini, 2005b). Therefore photons coming from the same CBM density region are observed over a very long arrival time interval.

### C.1.3. GRB 970228 and the Amati relation

We turn now to the “Amati relation” (Amati et al., 2002; Amati, 2006) between the isotropic equivalent energy emitted in the prompt emission  $E_{iso}$  and the peak energy of the corresponding time-integrated spectrum  $E_{p,i}$  in the source rest frame. It has been shown by Amati et al. (2002); Amati (2006) that this correlation holds for almost all the “long” GRBs which have a redshift and an  $E_{p,i}$  measured, but not for the ones classified as “short” (Amati, 2006). If we focus on the “fake” short GRBs, namely the GRBs belonging to this new class, at least in one case (GRB 050724 Campana et al., 2006b) it has been shown that the correlation is recovered if also the extended emission is considered (Amati, 2007).

It clearly follows from our treatment that for the “canonical GRBs” with large values of the baryon loading and high  $\langle n_{cbm} \rangle$ , which presumably are most of the GRBs for which the correlation holds, the leading contribution to the prompt emission is the afterglow peak emission. The case of the “fake” short GRBs is completely different: it is crucial to consider separately the two components since the P-GRB contribution to the prompt emission in this case is significant.

To test this scenario, we evaluated from our fit of GRB 970228  $E_{iso}$  and  $E_{p,i}$  only for the afterglow peak emission component, i.e. from  $t_a^d = 37$  s to  $t_a^d = 81.6$  s. We found an isotropic energy emitted in the 2–400 keV energy band  $E_{iso} = 1.5 \times 10^{52}$  erg, and  $E_{p,i} = 90.3$  keV. As it is clearly shown in Fig. C.4, the sole afterglow component of GRB 970228 prompt emission is in perfect agreement with the Amati relation. If this behavior is confirmed for other GRBs belonging to this new class, this will enforce our identification of the “fake” short GRBs. This result will also provide a theoretical explanation for the the apparent absence of such correlation for the initial spikelike component in the different nature of the P-GRB.

### C.1.4. Conclusions

We conclude that GRB 970228 is a “canonical GRB” with a large value of the baryon loading quite near to the maximum  $B \sim 10^{-2}$  (see Fig. 3.8). The difference with e.g. GRB 050315 (Ruffini et al., 2006b) or GRB 991216 (Ruffini et al., 2003, 2004b, 2005a) is the low average value of the CBM density  $\langle n_{cbm} \rangle \sim 10^{-3}$  particles/cm<sup>3</sup> which deflates the afterglow peak luminosity. Hence, the predominance of the P-GRB, coincident with the initial

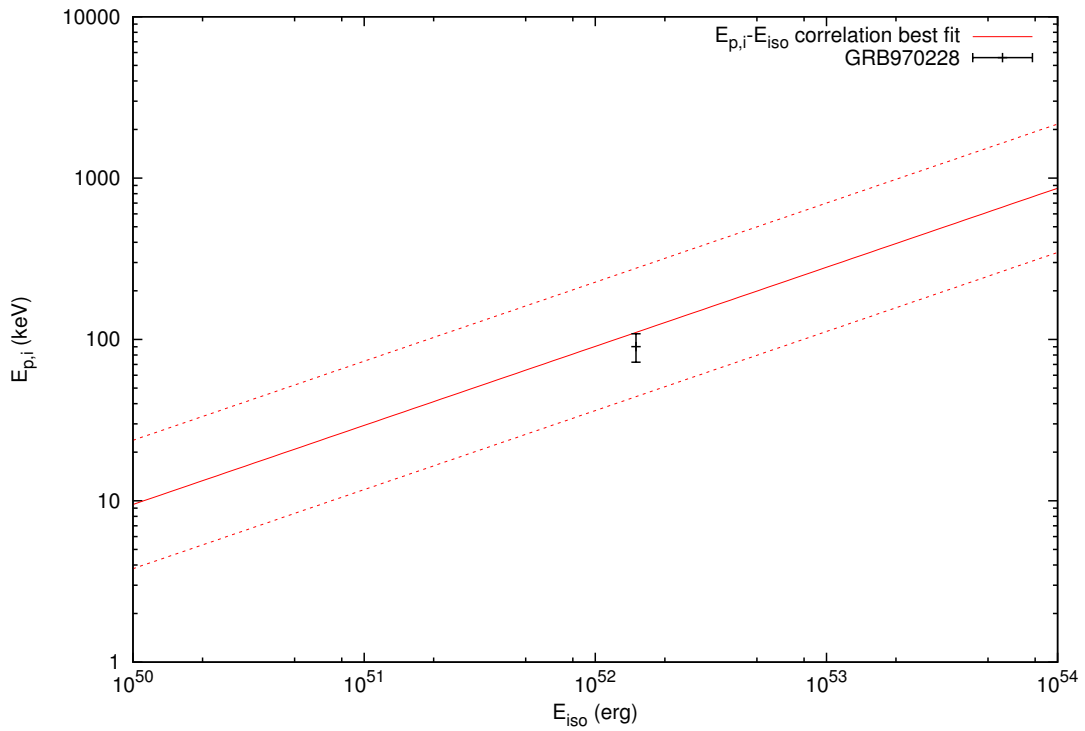


**Figure C.4.:** The estimated values for  $E_{p,i}$  and  $E_{iso}$  obtained by our analysis (black dot) compared with the “Amati relation” (Amati et al., 2002): the solid line is the best fitting power law (Amati, 2006) and the dashed lines delimit the region corresponding to a vertical logarithmic deviation of 0.4 (Amati, 2006). The uncertainty in the theoretical estimated value for  $E_{p,i}$  has been assumed conservatively as 20%.

spikelike emission, over the afterglow is just apparent: 98.9% of the total time-integrated luminosity is indeed in the afterglow component. Such a low average CBM density is consistent with the occurrence of GRB 970228 in the galactic halo of its host galaxy (Sahu et al., 1997; van Paradijs et al., 1997), where lower CBM densities have to be expected (Panaitescu, 2006).

We propose GRB 970228 as the prototype for the new class of GRBs comprising GRB 060614 and the GRBs analyzed by Norris and Bonnell (2006). We naturally explain the hardness and the absence of spectral lag in the initial spikelike emission with the physics of the P-GRB originating from the gravitational collapse leading to the black hole formation. The hard-to-soft behavior in the afterglow is also naturally explained by the physics of the relativistic fireshell interacting with the CBM, clearly evidenced in GRB 031203 (Bernardini et al., 2005a) and in GRB 050315 (Ruffini et al., 2006b). Also justified is the applicability of the Amati relation to the sole afterglow component (see Amati, 2006, 2007).

This class of GRBs with  $z \sim 0.4$  appears to be nearer than the other GRBs detected by *Swift* ( $z \sim 2.3$ , see Guetta, 2006). This may be explained by the afterglow peak luminosity deflation. The absence of a jet break in those afterglows has been pointed out (Campana et al., 2006b; Watson et al., 2006a), consistently with our spherically symmetric approach. Their association with non-star-forming host galaxies appears to be consistent with the merging of a compact object binary (Barthelmy et al., 2005b; Fox et al., 2005). It is here appropriate, however, to caution on this conclusion, since the association of GRB 060614 and GRB 970228 with the explosion of massive stars is not excluded (Della Valle et al., 2006; Galama et al., 2000).

Most of the sources of this class appear indeed not to be related to bright “Hypernovae”, to be in the outskirts of their host galaxies (Fox et al., 2005, see above) and a consistent fraction of them are in galaxy clusters with CBM densities  $\langle n_{cbm} \rangle \sim 10^{-3}$  particles/cm<sup>3</sup> (see e.g. Lewis et al., 2003; Berger et al., 2007). This suggests a spiraling out binary nature of their progenitor systems (Kramer, 2008) made of neutron stars and/or white dwarfs leading to a black hole formation.

Moreover, we verified the applicability of the Amati relation to the sole afterglow component in GRB 970228 prompt emission, in analogy with what happens for some of the GRBs belonging to this new class. In fact it has been shown by Amati (2006, 2007) that the “fake” short GRBs do not fulfill the  $E_{p,i} - E_{iso}$  correlation when the sole spikelike emission is considered, while they do if the long soft bump is included. Since the spikelike emission and the soft bump contributions are comparable, it is natural to expect that the soft bump alone will fulfill the correlation as well.

Within our “canonical GRB” scenario the sharp distinction between the P-GRB and the afterglow provide a natural explanation for the observational features of the two contributions. We naturally explain the hardness and the absence of spectral lag in the initial spikelike emission with the physics of the

P-GRB originating from the gravitational collapse leading to the black hole formation. The hard-to-soft behavior in the afterglow is also naturally explained by the physics of the relativistic fireshell interacting with the CBM, clearly evidenced in GRB 031203 (Bernardini et al., 2005a) and in GRB 050315 (Ruffini et al., 2006b). Therefore, we expect naturally that the  $E_{p,i}-E_{iso}$  correlation holds only for the afterglow component and not for the P-GRB. Actually we find that the correlation is recovered for the afterglow peak emission of GRB 970228.

In the original work by Amati et al. (2002); Amati (2006) only the prompt emission is considered and not the late afterglow one. In our theoretical approach the afterglow peak emission contributes to the prompt emission and continues up to the latest GRB emission. Hence, the meaningful procedure within our model to recover the Amati relation is to look at a correlation between the total isotropic energy and the peak of the time-integrated spectrum of the whole afterglow. A first attempt to obtain such a correlation has already been performed using GRB 050315 as a template, giving very satisfactory results (Guida et al., 2008b).

## C.2. Application to GRB 060614

GRB060614 (Gehrels et al., 2006; Mangano et al., 2007) has drawn the general attention of the gamma-ray burst's (GRB) scientific community because it is the first clear example of a nearby ( $z = 0.125$ ), long GRB not associated with a bright Ib/c supernova (SN) (Della Valle et al., 2006; Gal-Yam et al., 2006). It has been estimated that, if present, the SN-component should be about 200 times fainter than the archetypal SN 1998bw associated with GRB980425; moreover, it would also be fainter (at least 30 times) than any stripped-envelope SN ever observed (Richardson et al., 2006).

Within the standard scenario, long duration GRBs ( $T_{90} > 2$  s) are thought to be produced by SN events during the collapse of massive stars in star forming regions ("collapsar", see Woosley, 1993). The observations of broad-lined and bright type Ib/c SNe associated with GRBs are often reported to favor this scenario (Woosley and Bloom, 2006, and references therein). The *ansatz* has been advanced that every long GRB should have a SN associated with it (Zhang et al., 2007). Consequently, in all nearby long GRBs ( $z \leq 1$ ), SN emission should be observed.

For these reasons the case of GRB060614 is unusual. Some obvious hypotheses have been proposed and ruled out: the chance superposition with a galaxy at low redshift (Gal-Yam et al., 2006) and strong dust obscuration and extinction (Fynbo et al., 2006). Appeal has been made to the possible occurrence of an unusually low luminosity stripped-envelope core-collapse SN (Della Valle et al., 2006).

The second novelty of GRB060614 is that it challenges the traditional sepa-

ration between Long Soft GRBs and Short Hard GRBs. Traditionally (Klebesadel, 1992; Dezalay et al., 1992), the “short” GRBs have  $T_{90} < 2$  s, present an harder spectrum and negligible spectral lag, and are assumed to originate from the merging of two compact objects, i.e. two neutron stars or a neutron star and a black hole (see e.g. Blinnikov et al., 1984; Paczynski, 1986; Goodman, 1986; Eichler et al., 1989; Piran, 2005; Meszaros, 2006, and references therein). GRB060614 lasts about one hundred seconds ( $T_{90} = (102 \pm 5)$  s; Gehrels et al., 2006), it fulfills the  $E_p^{rest} - E_{iso}$  correlation (Amati et al., 2007), and therefore traditionally it should be classified as a “long” GRB. However, its morphology is different from typical long GRBs, being similar to the one of GRB050724, traditionally classified as a short GRB (Zhang et al., 2007; Piro, 2005). Its optical afterglow luminosity is intermediate between the traditional long and short ones (Kann et al., 2008). Its host galaxy has a moderate specific star formation rate ( $R_{Host} \approx 2M_{\odot}y^{-1}(L^*)^{-1}$ ,  $M_{vHost} \approx -15.5$ ; Fynbo et al., 2006; Della Valle et al., 2006). The spectral lag in its light curves is very small or absent (Gehrels et al., 2006). All these features are typical of short GRBs.

A third peculiarity of GRB060614 is that its 15–150 keV light curve presents a short, hard and multi-peaked episode (about 5 s). The episode is followed by a softer, prolonged emission that manifests a strong hard to soft evolution in the first 400 s of data (Mangano et al., 2007). The total fluence in the 15–150 keV energy band is  $F = (2.17 \pm 0.04) \times 10^{-5}$  erg/cm<sup>2</sup>, the 20% emitted during the initial spikelike emission, where the peak luminosity reaches the value of 300 keV before decreasing to 8 keV during the BAT-XRT overlap time (about 80 s).

These apparent contradictions find a natural explanation in the framework of the “fireshell” model<sup>1</sup>. Within the fireshell model, the occurrence of a GRB-SN is not a necessity. The origin of all GRBs is traced back to the formation of a black hole, either occurring in a single process of gravitational collapse, or in a binary system composed of a neutron star and a companion star evolved out of the main sequence, or in a merging binary system composed of neutron stars and/or white dwarfs in all possible combinations. The occurrence of a GRB-SN is indeed only one of the possibilities, linked, for example, to the process of “induced gravitational collapse” (Ruffini et al., 2001a, 2007b; Dainotti et al., 2007).

Within the “fireshell” model, the difference between the “short” and “long” GRBs does not rely uniquely on the time scale of the event, as in the traditional classification. It is theoretically explained by the fireshell baryon loading affecting the structure of the “canonical” GRB light curve. The “canonical” GRB light curve is indeed composed of a proper-GRB (P-GRB, often la-

---

<sup>1</sup>We indicate here and in the following by the “fireshell” model the one we have consistently developed encompassing the three basic paradigms presented in Ruffini et al. (2001c,b,a) as well as all the technical developments in the emission process, in the equations of motion and in the relativistic treatment of the extended afterglow as summarized in Ruffini et al. (2007a).

beled as “precursor”), emitted at the fireshell transparency, and an extended afterglow. The peak of such an extended afterglow is traditionally included in the prompt emission. The relative energetics of two such components and the temporal separation of the corresponding peaks are ruled by the fireshell baryon loading. In the limit of vanishing baryon loading, all the GRB energy is emitted in the P-GRB: these are the “genuine” short GRBs (Ruffini et al., 2001b, 2008a; Bernardini et al., 2007; Bianco et al., 2008a,b).

Within the “fireshell” model, in addition to the determination of the baryon loading, it is possible to infer a detailed description of the circumburst medium (CBM), its average density and its porosity and filamentary structure, all the way from the black hole horizon to a distance  $r \lesssim 10^{17}$  cm. This corresponds to the prompt emission. This description is lacking in the traditional model based on the synchrotron emission. The attempt to use the internal shock model for the prompt emission (see e.g. Rees and Meszaros, 1994; Piran, 2005; Meszaros, 2006, and references therein) only applies to regions where  $r > 10^{17}$  cm (Kumar and McMahon, 2008).

Our aim is to show how the “fireshell” model can explain all the abovementioned GRB060614 peculiarities and solve the apparent contradictions. In doing so, we also infer constraints on the astrophysical nature of the GRB060614 progenitors. In turn, these conclusions lead to a new scenario for all GRBs. We can confirm a classification of GRBs as “genuine” short, “fake” or “disguised” short, and all the remaining “canonical” GRBs. The connection between this new classification and the nature of GRB progenitors is quite different from the traditional one in the current literature.

### C.2.1. The fit of the observed luminosity

In this scenario, GRB060614 is naturally interpreted as a “disguised” short GRB. We have performed the analysis of the observed light curves in the 15–150 keV energy band, corresponding to the  $\gamma$ -ray emission observed by the BAT instrument on the Swift satellite, and in the 0.2–10 keV energy band, corresponding to the X-ray component from the XRT instrument on Swift satellite. We do not address in this paper the issue of the optical emission, which represent less than 10% of the total energy of the GRB. From this fit (see Figs. C.5, C.7) we have derived the total initial energy  $E_{tot}^{e^\pm}$ , the value of  $B$  as well as the effective CBM distribution (see Fig. C.6). We find  $E_{tot}^{e^\pm} = 2.94 \times 10^{51}$  erg, that accounts for the bolometric emission of both the P-GRB and the extended afterglow. Such a value is compatible with the observed  $E_{iso} \simeq 2.5 \times 10^{51}$  erg (Gehrels et al., 2006). The value of  $B$  is  $B = 2.8 \times 10^{-3}$ , which corresponds to the lowest one of all the GRBs we have examined (see Fig. 6.4). It corresponds to a canonical GRB with a very clear extended afterglow predominance over the P-GRB. From the model, having determined  $E_{tot}^{e^\pm}$  and  $B$ , we can compute the theoretical expected P-GRB energetics  $E_{P-GRB}$  (Ruffini

et al., 2001b). We obtain  $E_{P-GRB} \simeq 1.15 \times 10^{50}$  erg, that is in good agreement with the observed  $E_{iso,1p} \simeq 1.18 \times 10^{50}$  erg (Gehrels et al., 2006). The Lorentz Gamma Factor at the transparency is  $\gamma_o = 346$ , one of the highest of all the GRBs we have examined.

In Fig. C.5 we plot the comparison between the BAT observational data of the GRB0606014 prompt emission in the 15–150 keV energy range and the P-GRB and extended afterglow light curves computed within our model. The temporal variability of the extended afterglow peak emission is due to the inhomogeneities in the effective CBM density (see Figs. C.5, C.6). Toward the end of the BAT light curve, the good agreement between the observations and the fit is affected by the Lorentz gamma factor decrease and the corresponding increase of the maximum viewing angle. The source visible area becomes larger than the typical size of the filaments. This invalidates the radial approximation we use for the CBM description. To overcome this problem it is necessary to introduce a more detailed three-dimensional CBM description, in order to avoid an over-estimated area of emission and, correspondingly, to describe the sharpness of some observed light curves. We are still working on this issue (Ruffini et al., 2002; Caito et al., 2008; Bianco et al., 2006a; Guida et al., 2008a).

We turn now to the crucial determination of the CBM density, which is derived from the fit. At the transparency point it was  $n_{cbm} = 4.8 \times 10^{-3}$  particles/cm<sup>3</sup> (see Fig. C.6). This density is compatible with the typical values of the galactic halos. During the peak of the extended afterglow emission the effective average CBM density decreases reaching  $\langle n_{cbm} \rangle = 2.25 \times 10^{-5}$  particles/cm<sup>3</sup>, possibly due to an occurring fragmentation of the shell (Dainotti et al., 2007) or due to a fractal structure in the CBM. The  $\mathcal{R}$  value on average was  $\langle \mathcal{R} \rangle = 1.72 \times 10^{-8}$ . Note the striking analogy of the numerical value and the overall radial dependence of the CBM density in the present case of GRB060614 when compared and contrasted with the ones of GRB970228 (Bernardini et al., 2007).

Concerning the 0.2–10 keV light curve of the decaying phase of the afterglow observed with the XRT instrument, we have also reproduced very satisfactorily both the hard decrease in the slope and the plateau of the light curve, keeping constant the effective CBM density and changing only  $\mathcal{R}$ . The result of this analysis is reported in Fig. C.7. We assume in this phase  $n_{cbm} = 4.70 \times 10^{-6}$  particles/cm<sup>3</sup>. The average value of the  $\mathcal{R}$  parameter is  $\langle \mathcal{R} \rangle = 1.27 \times 10^{-2}$ . The drastic enhancement in the  $\mathcal{R}$  parameter with respect to the values at the peak of the extended afterglow is consistent with similar features encountered in other sources we have studied: GRB060218 presents an enhancement of five orders of magnitude (Dainotti et al., 2007), in GRB060710 the enhancement is of about four orders of magnitude (see Izzo et al., in preparation) while in GRB050315 there is a three orders of magnitude enhancement (Ruffini et al., 2006b). In these last two cases, we find the enhancement of  $\mathcal{R}$  between  $r=2 \times 10^{17}$  cm and  $r=3 \times 10^{17}$  cm, just as for

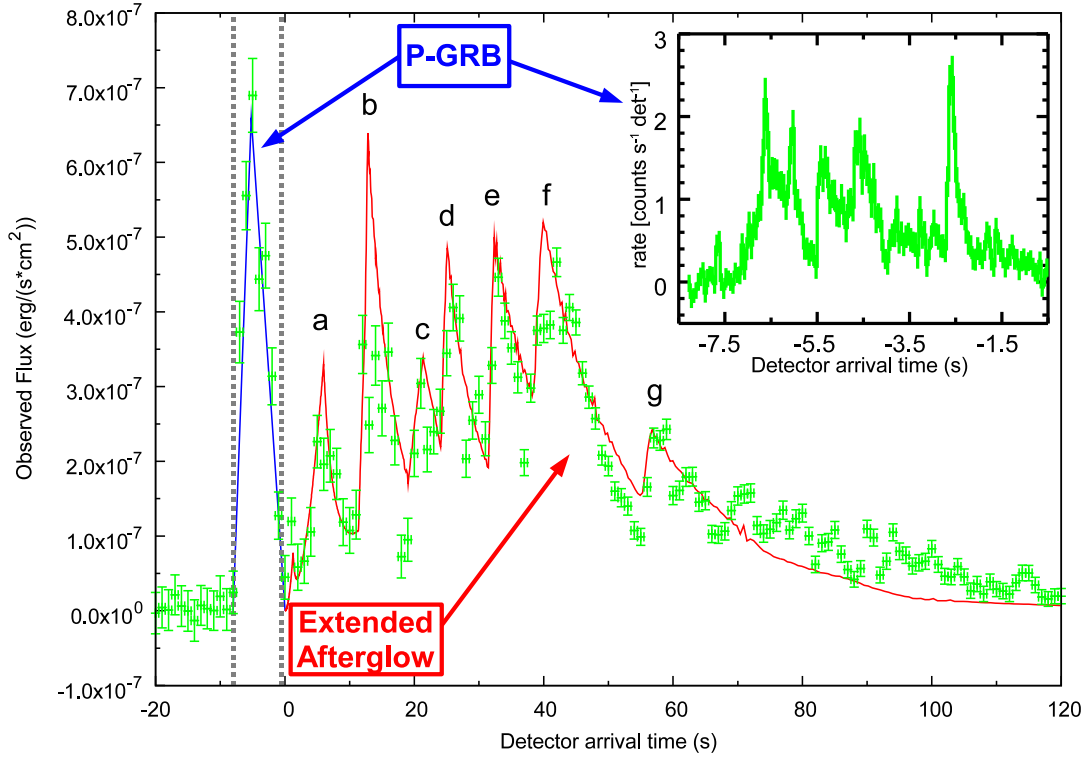


**Figure C.5.:** The BAT 15–150 keV light curve (green points) at 1 s time resolution compared with the corresponding theoretical extended afterglow light curve we compute (red line). The onset of the extended afterglow is at the end of the P-GRB (qualitatively sketched in blue lines and delimited by dashed gray vertical lines). Therefore the zero of the temporal axis is shifted by 5.5 s with respect to the BAT trigger time. The peaks of the extended afterglow light curves are labeled to match them with the corresponding CBM density peak in Fig. C.6. In the upper right corner there is an enlargement of the P-GRB at 50ms time resolution (reproduced from Mangano et al., 2007), showing its structure.

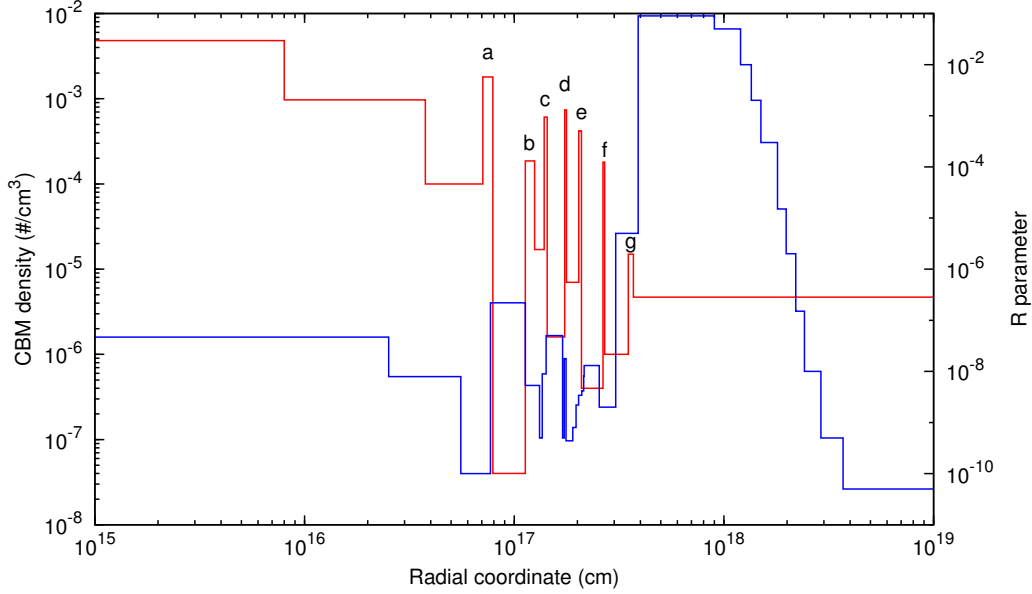


**Figure C.6.:** The effective CBM density (red line) and the  $\mathcal{R}$  parameter (blue line) versus the radial coordinate of the shell. The CBM density peaks are labeled to match them with the corresponding extended afterglow light curve peaks in Fig. C.5. They correspond to filaments of characteristic size  $\Delta r \sim 10^{15}$  cm and density contrast  $\Delta n_{cbm} / \langle n_{cbm} \rangle \sim 20$  particles/cm<sup>3</sup>.

GRB060614, for which we have the enhancement at  $r=3.5 \times 10^{17}$  cm. The time of the bump approximately corresponds to the appearance of the optical emission observed in GRB060614 and, more in general, to the onset of the second component of the Willingale et al. (2007) scheme for GRBs.

### C.2.2. Open issues in current theoretical models

The “fireshell” model addresses mainly the  $\gamma$  and X-ray emission, which are energetically the most relevant part of the GRB phenomenon. The model allows a detailed identification of the fundamental three parameters of the GRB source: the total energy, the baryon loading, as well as the CBM density, filamentary structure and porosity. Knowledge of these phenomena characterizes the region surrounding the black hole up to a distance which in this source reaches  $\sim 10^{17}$ – $10^{18}$  cm. When applied, however, to larger distances, which correspond to the latest phases of the X-ray afterglow, since the beginning of the “plateau” phase, the model reveals a different regime which has not yet been fully interpreted in its astrophysical implications. To fit the light curve in the soft X-ray regime for  $r > 4 \times 10^{17}$  cm, we require an enhancement of about six orders of magnitude in the  $\mathcal{R}$  factor (see Fig. C.6). This would correspond to a more diffuse CBM structure, with a smaller porosity, interacting with the fireshell. This implies a different main physical process

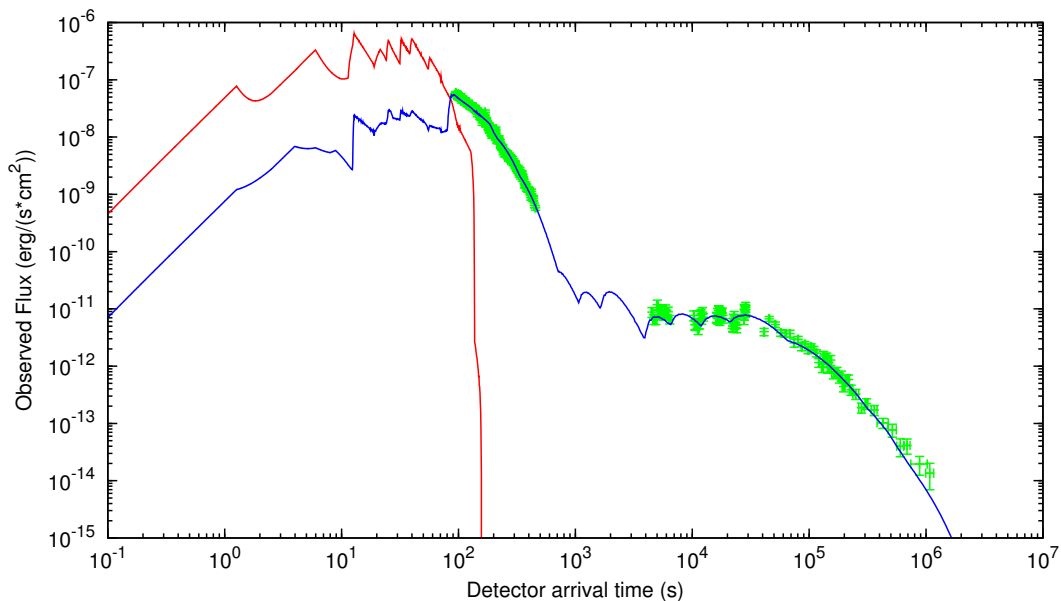


**Figure C.7.:** The XRT 0.2–10 keV light curve (green points) compared with the corresponding theoretical extended afterglow light curve we compute (blue line). In this case also we have a good correspondence between data and theoretical results. For completeness, the red line shows the theoretical extended afterglow light curve in the 15–150 keV energy range presented in Fig. C.5.

during the latest X-ray afterglow phases. For the optical, IR and radio emission, the fireshell model leads to a much lower flux than the observed one, especially for  $r \sim 10^{17}$ – $10^{18}$  cm. Although the optical, IR, and radio luminosities have a minor energetic role, they may lead to the identification of crucial parameters and new phenomena occurring in the source, and they deserve careful attention.

In these late phases for  $r \geq 10^{17}$  cm the treatment based on synchrotron emission, pioneered by Meszaros and Rees (1997a) even before the discovery of the afterglow (Costa et al., 1997), is currently applied. Such a model has been further developed (see Sari et al., 1998; Piran, 2005; Meszaros, 2006, and references therein). Also in this case, however, some difficulties remain since it is necessary to invoke the presence of an unidentified energy injection mechanism (Zhang et al., 2006). Such a model appears to be quite successful in explaining the late phases of the X-ray emission of GRB060614, as well as the corresponding optical emission, in terms of different power-law indexes for the different parts of the afterglow light curves (Mangano et al., 2007; Xu et al., 2008). However, also in this case an unidentified energy injection mechanism between  $\sim 0.01$  days and  $\sim 0.26$  days appears to be necessary (Xu et al., 2008).

The attempt to describe the prompt emission via the synchrotron process by the internal shock scenario (see e.g. Rees and Meszaros, 1994; Piran, 2005;

Meszaros, 2006, and references therein) also encounters difficulties: Kumar and McMahon (2008) have shown that the traditional synchrotron model can be applied to the prompt emission only if it occurs at  $r > 10^{17}$  cm. A proposed solution to this problem, via the inverse Compton process, suffers from an “energy crisis” (see e.g. Piran et al., 2008).

Interestingly, the declared region of validity of the traditional synchrotron model ( $r > 10^{17}$  cm) is complementary to the one successfully described by our model ( $r < 10^{17}$ – $10^{18}$  cm). Astrophysically, Xu et al. (2008) have reached, within the framework of the traditional synchrotron model, two conclusions which are consistent with the results of our analysis. First, they also infer from their numerical fit a very low density environment, namely  $n_{cbm} \sim 0.04$  particles/cm<sup>3</sup>. Second, they also mention the possibility that the progenitor of GRB0606014 is a merging binary system formed by two compact objects.

### C.2.3. Conclusions

As recalled in the introduction, GRB060614 presents three major novelties, which challenge the most widespread theoretical models and which are strongly debated in the current literature. The first one is that it challenges the traditional separation between long soft GRBs and short hard GRBs (Gehrels et al., 2006). The second one is that it presents a short, hard and multi-peaked episode, followed by a softer, prolonged emission with a strong hard to soft evolution (Gehrels et al., 2006; Mangano et al., 2007). The third one is that it is the first clear example of a nearby, long GRB not associated with a bright SN Ib/c (Della Valle et al., 2006; Gal-Yam et al., 2006). All these three issues are naturally explained within our “fireshell” model, which allows a detailed analysis of the temporal behavior of the signal originating up to a distance  $r \sim 10^{17}$ – $10^{18}$  cm from the black hole, and relates, with all the relativistic transformation, the arrival time to the CBM structure and the relativistic parameters of the fireshell.

One of the major outcomes of the Swift observation of, e.g., GRB050315 (Vaughan et al., 2006; Ruffini et al., 2006b) has been the confirmation that long GRB duration is not intrinsic to the source but it is merely a function of the instrumental noise threshold (Ruffini et al., 2006a). GRB060614 represents an additional fundamental progress in clarifying the role of the CBM density in determining the GRB morphology. It confirms the results presented in GRB970228 (Bernardini et al., 2007), that is the prototype of the new class of “fake” short GRBs, or, better, of canonical GRBs “disguised” as short ones. They correspond to canonical GRBs with an extended afterglow emission energetically predominant relative to the P-GRB one and a baryon loading  $B > 10^{-4}$ . The sharp spiky emission corresponds to the P-GRB. As recalled before, a comparison of the luminosities of the P-GRB and of the extended afterglow is indeed misleading: it follows from the low average CBM den-

sity inferred from the fit of the fireshell model, which leads to  $n_{cbm} \sim 10^{-3}$  particles/cm<sup>3</sup>. Therefore such a feature is neither intrinsic to the progenitor nor to the black hole, but it is only indicative of the CBM density at the location where the final merging occurs. GRB060614 is a canonical GRB and it is what would be traditionally called a “long” GRB if it had not exploded in an especially low CBM density environment. GRB060614 must necessarily fulfill, and indeed it does, the Amati relation. This happens even taking into account the entire prompt emission mixing together the P-GRB and the extended afterglow (Amati et al., 2007), due to the energetic predominance of the extended afterglow discussed above (see also Guida et al., 2008b). These results justify the occurrence of the abovementioned first two novelties.

The low value of the CBM density is compatible with a galactic halo environment. This result points to an old binary system as the progenitor of GRB060614 and it justifies the abovementioned third novelty: the absence of an associated SN Ib/c (see also Davies et al., 2007). Such a binary system departed from its original location in a star-forming region and spiraled out in a low density region of the galactic halo (see e.g. Kramer, 2008). The energetics of this GRB is about two orders of magnitude lower than the one of GRB970228 (Bernardini et al., 2007). A natural possible explanation is that instead of a neutron star - neutron star merging binary system we are in the presence of a white dwarf - neutron star binary. We therefore agree, for different reasons, with the identification proposed by Davies et al. (2007) for the GRB060614 progenitor. In principle, the nature of the white dwarf, with a typical radius of the order of  $10^3$  km, as opposed to the one of the neutron star, typically of the order of 10 km, may manifest itself in characteristic signatures in the structure of the P-GRB (see Fig. C.5).

It is interesting that these results lead also to three major new possibilities:

- The majority of GRBs declared as shorts (see e.g. Piro, 2005) are likely “disguised” short GRBs, in which the extended afterglow is below the instrumental threshold.
- The observations of GRB060614 offer the opportunity, for the first time, to analyze in detail the structure of a P-GRB lasting 5 s. This feature is directly linked to the physics of the gravitational collapse that generated the GRB. Recently, there has been a crucial theoretical physics result showing that the characteristic time constant for the thermalization of an  $e^\pm$  plasma is of the order of  $10^{-13}$  s (Aksenov et al., 2007). Such a time scale still applies for an  $e^\pm$  plasma with a baryon loading of the order of the one observed in GRBs (Aksenov et al., 2008). The shortness of such a time scale, as well as the knowledge of the dynamical equations of the optically thick phase preceding the P-GRB emission (Bianco et al., 2006b), implies that the structure of the P-GRB is a faithful representation of the gravitational collapse process leading to the formation

of the black hole (Ruffini et al., 2005d). In this respect, it is indeed crucial that the Swift data on the P-GRB observed in GRB060614 (see Fig. C.5) appear to be highly structured all the way to a time scale of 0.1 s. This opens a new field of research: the study of the P-GRB structure in relation to the process of gravitational collapse leading to the GRB.

- If indeed the binary nature of the progenitor system and the peculiarly low CBM density  $n_{cbm} \sim 10^{-3}$  particles/cm<sup>3</sup> will be confirmed for all “fake” or “disguised” GRBs, then it is very likely that the traditionally “long” high luminosity GRBs at higher redshift also originates in the merging of binary systems formed by neutron stars and/or white dwarfs occurring close to their birth location in star-forming regions with  $n_{cbm} \sim 1$  particle/cm<sup>3</sup> (see Fig. C.3).

### C.3. Application to GRB 071227: an additional case of a disguised short burst

GRB 071227 presents some intriguing anomalies. As for the “Norris and Bonnell” GRBs, its BAT light curve shows in the 15–150 keV range a multi-peaked structure lasting  $T_{90} = (1.8 \pm 0.4)$  s, followed by an extended but much softer emission up to  $t_0 + 100$  s (D’Avanzo et al., 2009). A fading X-ray (0.3–10 keV) and a faint optical afterglow have also been identified. The optical afterglow emission allowed to measure its redshift,  $z = 0.383$ , and therefore its isotropic equivalent energy,  $E_{iso} = 5.8 \times 10^{50}$  erg in 20–1300 keV (D’Avanzo et al., 2009). The observed X-ray and optical afterglow is superimposed on the plane of the host galaxy, at  $(15.0 \pm 2.2)$  kpc from its center.

On the basis of these characteristics, GRB 071227 has been classified as a short burst. This statement is supported by other main features: **1)** If we consider the first and apparently predominant short-duration episode, it does not fulfill the Amati relation between the isotropic equivalent radiated energy of the prompt emission  $E_{iso}$  and the cosmological rest-frame  $\nu F_\nu$  spectrum peak energy  $E_{p,i}$  (Amati et al., 2002; Amati, 2006; Amati et al., 2007, 2009). **2)** The spectral lag of the first spike-like emission in 25–50 keV to 100–350 keV bands is consistent with zero (Sakamoto et al., 2007). **3)** Multiwavelength observations performed over many days have displayed that there is no association with a Ib/c hypernova, the type of SN generally observed with GRBs, even if it is a nearby burst and its isotropic energy is compatible with that of other GRBs associated with them (D’Avanzo et al., 2009), although the upper limits are not deep enough to rule out a low-energetic core-collapse event. Nevertheless, the explosion of this burst in a star-forming region of a spiral galaxy, and its prolonged tail of emission, makes it most likely to be a long burst.

In this paper, we show that all these ambiguities and peculiarities can be explained in the framework of the fireshell model if we assume GRB 071227 to be a *disguised* short burst, in which the first spike-like emission coincides with the P-GRB and the prolonged softer tail with the peak of the extended afterglow emitted in a low CircumBurst Medium (CBM) density region. We show, moreover, that this tail satisfies the Amati relation, and this is consistent with our interpretation.

### C.3.1. The interpretation of GRB 071227 light curves

We examine the possibility that GRB 071227 can also be classified as a “disguised” burst. We analyzed the observed light curves of this burst in the 15–50 keV bandpass, corresponding to the lowest band of the  $\gamma$ -ray emission, detected by the BAT instrument on the *Swift* satellite, and in the 0.3–10 keV energy band, corresponding to the X-ray component from the XRT instrument. To model the CBM structure, we assume that  $n_{cbm}$  is a function of only the radial coordinate,  $n_{cbm} = n_{cbm}(r)$  (radial approximation). The CBM is arranged in spherical shells of width  $\sim 10^{15} - 10^{16}$  cm arranged in such a way that the corresponding modulation of the emitted flux closely resembles the observed shape. We assumed that the first short spike-like emission represents the P-GRB and the  $\gamma$ -ray tail is the peak of the extended afterglow. We therefore began the simulation in such a way that the extended afterglow light curve begins in coincidence with the peak of the P-GRB (about 1s), as shown in Fig. C.8. To reproduce the observational data and the energetics observed for the P-GRB emission ( $E_{iso} \sim 1.0 \times 10^{51}$  erg), we require the initial conditions  $E_{tot}^{e^{\pm}} = 5.04 \times 10^{51}$  erg and  $B = 2.0 \times 10^{-4}$ . In Figs. C.8 and C.9 we plot the comparison of the GRB 071227 BAT and XRT data with the theoretical extended afterglow light curves. We obtained a good result in the prompt emission for the 15–50 keV bandpass (see Fig. C.8), while, for 0.3–10 keV, we only succeeded in reproducing the first decaying part of the XRT light curve (see Fig. C.9). We assumed this to correspond to the possible onset of the “plateau” phase of the extended afterglow (Nousek et al., 2006).

From our simulation, the amount of energy stored in the P-GRB is found to be about 20% of the total energetics of the explosion. Hence, this burst cannot be a short burst within the fireshell scenario. The baryon loading obtained ( $B = 2.0 \times 10^{-4}$ ) remains in the range of long duration GRBs. This is a very critical value, because it is very close to the crossing point of the plot of the energetics of GRBs as a function of  $B$  (see above). This is the lowest baryon loading that we have ever found in our analysis within the fireshell scenario. From our analysis, we found a peculiar result for the average CBM density. We obtained a density of  $n_{cbm} = 1.0 \times 10^{-2}$  particles/cm<sup>3</sup> at the beginning of the process, later decreasing to  $n_{cbm} = 1.0 \times 10^{-4}$  particles/cm<sup>3</sup>. This low average density, inferred from the analysis, is responsible for the strong de-

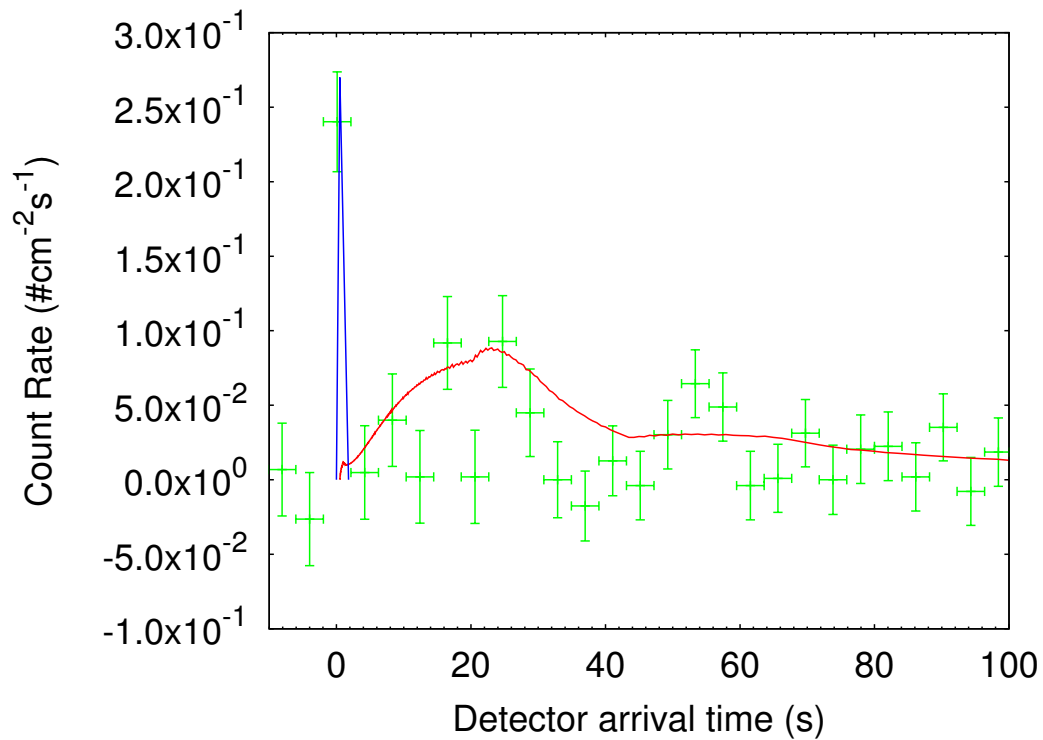


**Figure C.8.:** The BAT 15–50 keV light curve (green points) compared with the corresponding theoretical extended afterglow light curve (red line). The P-GRB is qualitatively sketched by the blue line.

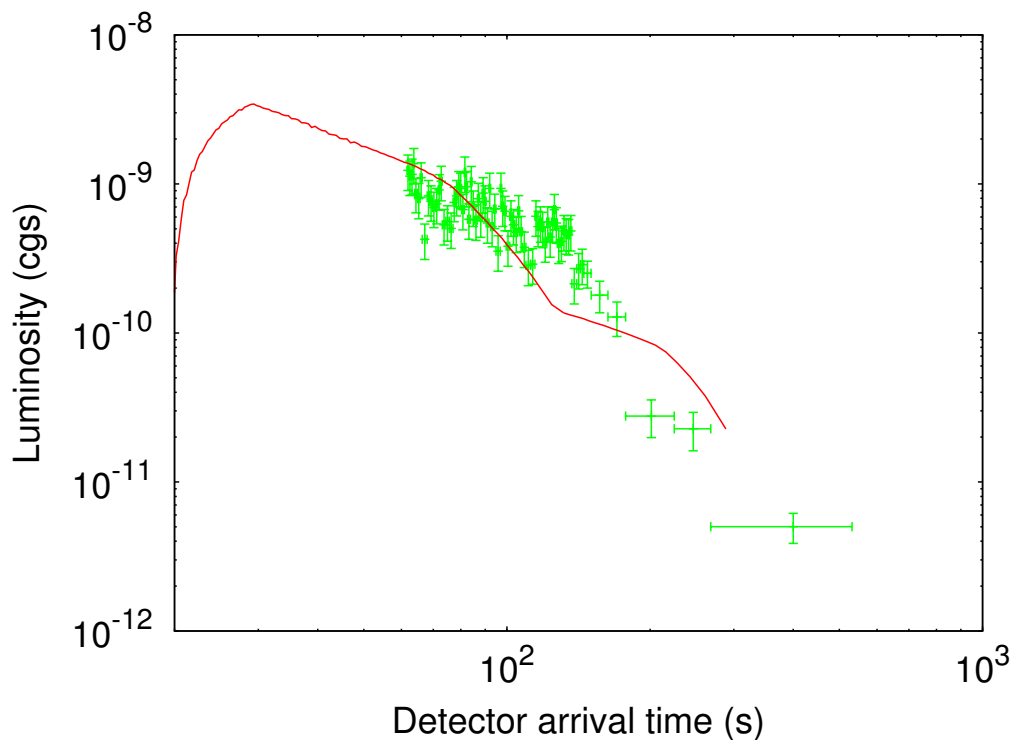


**Figure C.9.:** The XRT 0.3–10 keV light curve (green points) compared with the corresponding theoretical extended afterglow light curve we obtain (red line). The X-ray data corresponding to the first 60 seconds are not available since XRT starts to observe only 60 seconds after the BAT trigger. We stop our analysis at  $\gamma \sim 5$  when our relativistic dynamical model can no longer be applied

flation of the  $\gamma$ -ray tail. However, at the radius of about  $2.0 \times 10^{17}$  cm, the density becomes higher and reaches the value of  $n_{cbm} = 10$  particles/cm<sup>3</sup> (the complete profiles of  $n_{cbm}$  and  $\mathcal{R}$  as functions of the radial coordinate are reported in Fig. C.10). This is compatible with the observations. The observed X-ray and optical afterglow of GRB 071227 is indeed superimposed on the plane of the host galaxy, at  $(15.0 \pm 2.2)$  kpc from its center (D’Avanzo et al., 2009). An interesting possibility observed by D. Arnett (private communication) is that this very low density “cavity” could be formed in the coalescing phase of a binary formed by a neutron star and a white dwarf. Accurate studies on compact object mergers have shown the distribution of merger locations for different host galaxies (Belczynski et al., 2006; Berger, 2010). In starburst galaxies, most of the mergers are expected to be found within hosts, while in elliptical galaxies a substantial fraction of mergers take place outside hosts. Spiral galaxies, hosting both young and old stellar populations, represent the intermediate case between the preceding two. This result is therefore compatible with our hypothesis about the binary nature of the progenitor of GRB 071227. Although they did not consider the case of binary systems formed by a neutron star and a white dwarf, the progenitor of GRB 071227 would fit into the tight binary scenario described by Belczynski et al. (2006).

These results clearly imply that GRB 071227 is another example of a disguised burst.

### C.3.2. GRB 071227 within the Amati relation

One of the most effective tools for discriminating between “short” and “long” bursts, and possibly clarifying the interpretation of these different classes of events, is the Amati relation (Amati et al., 2002; Amati, 2006; Amati et al., 2007, 2009).

This empirical spectrum-energy correlation states that the isotropic-equivalent radiated energy of the prompt emission  $E_{iso}$  is correlated with the cosmological rest-frame  $\nu F_\nu$  spectrum peak energy  $E_{p,i}$ :  $E_{p,i} \propto (E_{iso})^a$ , with  $a \approx 0.5$  (Amati et al., 2002). The existence of the Amati relation, discovered when analyzing the *BeppoSAX* long duration bursts, has been confirmed by studying a sample of GRBs observed by *Swift*, intense or soft, with available measurements of redshift and spectral parameters, and also by *HETE-2* and *Konus/WIND*. When the “afterglow revolution” allowed the redshift estimation of also some short GRBs, it was found that these bursts are inconsistent with the Amati relation, holding instead for long GRBs (Amati, 2006, 2010; Antonelli et al., 2009). The most recent updating of the correlation (95 GRBs with the data available up to April 2009) also includes two high-energetic events detected by *Fermi* (GRB 090323 and GRB 080916C), which are fully consistent with the  $E_{p,i}-E_{iso}$  relation (Amati et al., 2009). We also note that the short event

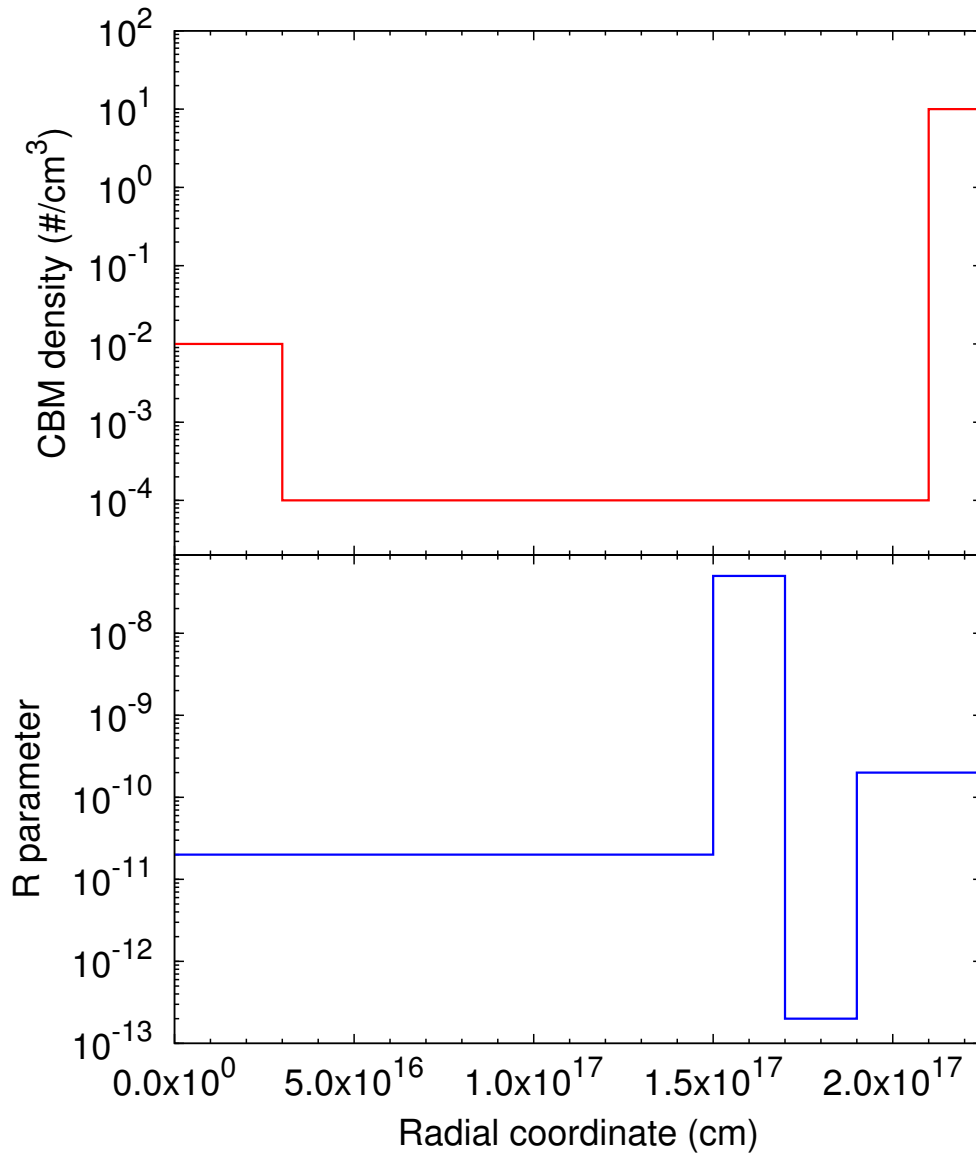


**Figure C.10.:** The CBM particle number density  $n_{cbm}$  (upper panel, red line) and the  $\mathcal{R}$  parameter (lower panel, blue line) as functions of the radial coordinate

GRB 090510, observed by the same satellite, is an outlier of the relation, as expected for short bursts. This dichotomy finds a natural explanation within the fireshell model. As recalled above, within this theoretical framework the prompt emission of long GRBs is dominated by the peak of the extended afterglow, while the one of the short GRBs is dominated by the P-GRB. Only the extended afterglow emission follows the Amati relation (see Guida et al., 2008b, for details). Therefore, all GRBs in which the P-GRB provides a negligible contribution to the prompt emission (namely the long ones, where the P-GRB is at most a small precursor) fulfill the Amati relation, while all GRBs in which the extended afterglow provides a negligible contribution to the prompt emission (namely the short ones) do not.

Apart from this general feature, there are peculiar cases. One of these is GRB 050724, a short burst followed by a long, softer tail in the  $\gamma$ -ray energy band. While the first short emission is inconsistent with the Amati relation, the soft tail is again consistent with it. Another one, the intriguing case of GRB 060614, a *disguised* short burst within the fireshell scenario (Caito et al., 2009), shows similar behavior: the first hard episode does not fulfill the Amati relation, while the whole event is fully consistent with it (Amati et al., 2007). This is again fully consistent with the predictions of the fireshell model for the disguised GRB class. Since the first short and hard episode is the P-GRB and the prolonged softer tail is the peak of the extended afterglow, the Amati relation must be fulfilled only when the softer tail is considered alone, or considered together with the first episode if this episode provides a negligible contribution (see Bernardini et al., 2008, for details). Thus, to discriminate its nature, we studied the position of GRB 071227 in the  $E_{p,i}$ - $E_{iso}$  plane. At the observed redshift, we assumed a “flat  $\Lambda$ -CDM model” with  $H_0 = 70 \text{ Km/s/Mpc}$  and  $\Omega_\Lambda = 0.73$ . For the first, hard spike, lasting about 1.8s, using *Konus/WIND* data (Golenetskii et al., 2007), and integrating between 1 and 10 000 keV, we found that  $E_{p,i} = (1384 \pm 277) \text{ keV}$  and  $E_{iso} = (1.0 \pm 0.2) \times 10^{51} \text{ erg}$ . As shown in Fig. C.11, this is inconsistent with the  $E_{p,i}$ - $E_{iso}$  relation, and instead occupies the short-populated region of the plane. For the long tail, lasting about 100s, we used a Band model with  $\alpha = -1.5$  and  $\beta = -3$ , which are typical of soft events. These values are compatible with the low quality statistics of this event. We found that  $E_{p,i} = 20_{-11}^{+19} \text{ keV}$  and  $E_{iso} = (2.2 \pm 0.1) \times 10^{51} \text{ erg}$ . With these values, the tail of emission is fully consistent with the Amati relation, as for any long GRB (see Fig. C.11). This clearly supports our hypothesis about the nature of GRB 071227.

### C.3.3. Conclusions

GRB 071227 has been classified in the current literature as a short GRB not fulfilling the Amati relation. By analyzing it using the fireshell model, we have

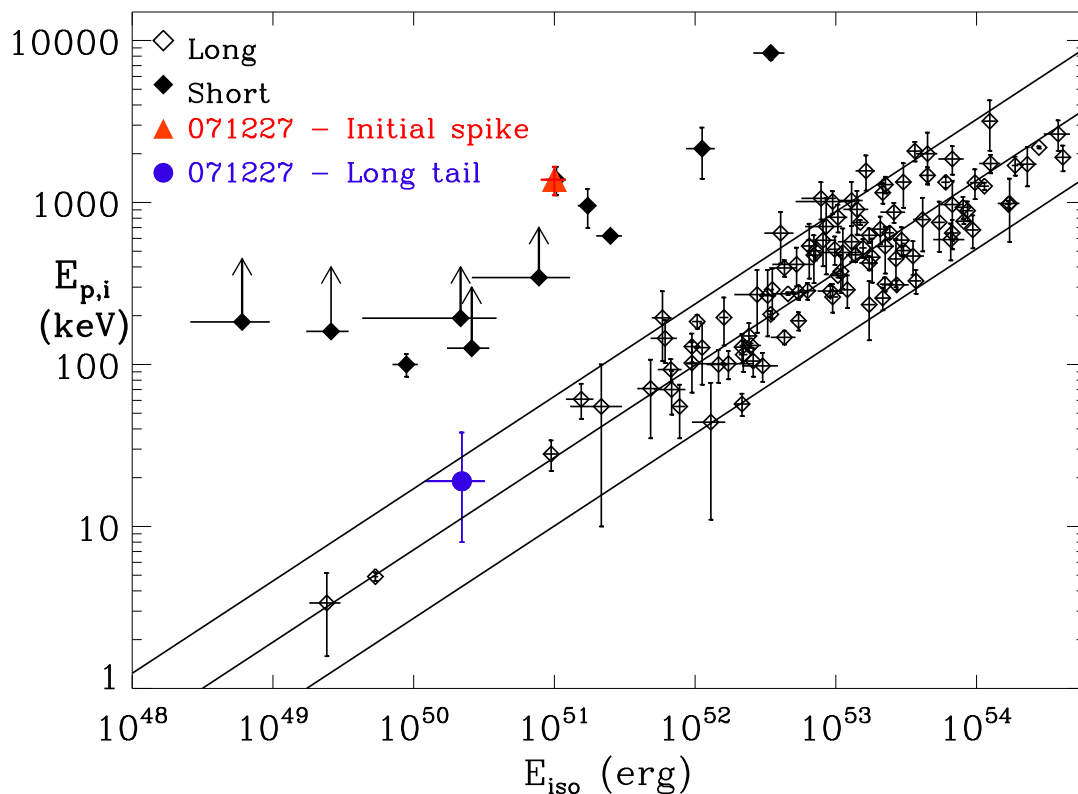


**Figure C.11.:** Location of the initial short spike and soft long tail of GRB 071227 in the  $E_{p,i} - E_{iso}$  plane. The data points of long GRBs are from Amati et al. (2008, 2009), the data points and limits of short GRBs are from Amati (2006); Amati et al. (2009); Piranomonte et al. (2008). The continuous lines show the best-fit power law and the  $2\sigma$  confidence region of the correlation, as determined by Amati et al. (2008).

identified the first spike-like emission with the P-GRB and consequently the prolonged softer tail with the peak of the extended afterglow. We have shown that this tail indeed fulfills the Amati relation. We have shown that the Amati relation is a characteristic of the extended afterglow phase of GRBs and does not occur during the P-GRB emission. As presented above, the relative energy of the P-GRB with respect to the extended afterglow is a strong function of the baryon loading. For  $B \rightarrow 10^{-2}$ , the energetic relevance of the P-GRB decreases and its contribution to the total GRB energetics can be neglected with respect to the extended afterglow: in this limit, the Amati relation always applies. In the present case, we have  $B = 2.0 \times 10^{-4}$  and the exclusion of the P-GRB from the total energetics of the GRB is indeed essential to fulfill the Amati relation. This is similar to the case of GRB 050724. With the considerations given above, it is appropriate to consider GRB 071227 to be another “Norris and Bonnell” kind of burst. It is quite similar to the bright GRB 060614, which we have previously analyzed (Caito et al., 2009), although underluminous. The value of  $B = 2.0 \times 10^{-4}$  that we obtained appears to be the smallest of all GRBs we examined. It is particularly interesting that the CBM distribution is given by  $\langle n_{cbm} \rangle < 10^{-2}$  particles/cm<sup>3</sup> to a radius of the order of  $\sim 2.1 \times 10^{17}$  cm and then monotonically rises to a value of  $\langle n_{cbm} \rangle = 10$  particles/cm<sup>3</sup>. While this last value is expected in the region where the GRB occurred, at  $(15.0 \pm 2.2)$  kpc from the center of its host galaxy, the existence of a very low density “cavity” appears to be of great interest. On the other side, as for GRB 060614, the energetics of GRB 071227 is compatible with the progenitor being the merging of a binary system of a neutron-star and a white-dwarf. This binary system, during the long-lasting merging process, may have swept the CBM around by means of the pulsar radiation emission (D. Arnett, private communication). This remains under investigation and may be an additional factor affecting the analogous low density observed in GRB 060614. In that burst, the progenitor was also consistent with a binary system formed by a white dwarf and a neutron star.

## C.4. Application to GRB 011121

### C.4.1. A widely debated issue: the interpretation of flares

A flare is a large scale activity in excess on the underlying light curve that manifests as a bump in luminosity rather intense and sharp in the decaying phase of the X-Ray afterglow.

When the first flare was detected by BeppoSAX, on the X-Ray light curve of GRB 011121, it was assumed as an extremely peculiar phenomenon. However, by the advent of the Swift Mission, many flares have been discovered in the light curves of about the 50% of the total amount of X-Ray afterglows observed: it was clear that flares are a very typical feature of GRBs phenomenon.

The many observations collected until today show that flares are random events that manifest in different shapes and in all sizes, in each kind of burst (both long and short) and at each measure of redshift. X-Ray flares have been observed in all phases of the X-Ray light curve, the peak time ranges between 95 s and 75 ks. There are light curves with more than one flare, although the more frequent case exhibits one single pulse on the Gamma-Ray peak followed by one or two flares. They are often characterized by large flux variations, can be strongly energetics and in some cases flares have surpassed the original GRB (ex. GRB 060526). This extreme variability and, in particular, the smallness of the time interval in which these big variation of flux happens, makes hard to give reason of such a phenomenon.

As discussed in the previous sections, in our theory the multiwavelength emission is entirely due to the fully inelastic collisions of the baryonic remnants of the fireshell with the CBM. Flares also, as characteristic parts of the afterglow, can be naturally explained in this context. The most relevant results of recent data analysis made on big samples (Chincarini et al., 2007b; Falcone et al., 2007a) are consistent with our hypothesis of inelastic collisions as the origin of flares. In fact, first of all, flares manifest until very late times and follow the typical hard to soft evolution; then, bumps become broader as the time increases, consistently with a general trend of GRB light curves. Moreover, the distribution of intensity ratios between successive Gamma-Ray pulses and that between successive X-Ray flares is the same, while there is no correlation between the number of pulses of the Gamma-Ray emission and the number of X-Ray flares. These last features seem to establish a common origin of Gamma-Ray bumps and X-Ray flares, and this is consistent with our hypothesis concerning to which the entire emission (from the Gamma 'Prompt emission' to the late Afterglow phase) is generated by the same inelastic collisions process.

On the other hand, it is difficult to conciliate all these aspects within the standard model or any other model founded on an internal shock process (eventually followed by an external shock phase). In particular, is hardly explained the presence of flares at very late times and their strong, rapid variation of flux. As already said, this is one of the most debated peculiarity of the appearing flares. It has been found that  $\langle dt/t \rangle = 0.13 \pm 0.10$ , corresponding to variations of flux of one or also two orders of magnitude. It's a shared opinion that an external shock scenario can't reproduce a similar range of variability, but we are able to show that this is consistent with our fully inelastic collision hypothesis. This assumption implies just the consideration of the three-dimensional structure of the CBM, until now neglected for the radial approximation modeling for the CBM profile. We realized a first attempt to check this idea by its application on the burst with the first flare observed, GRB 011121.

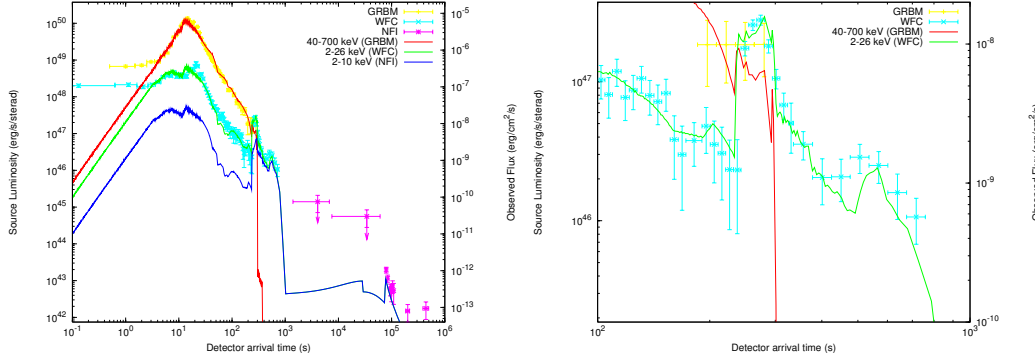


**Figure C.12.:** **Left:** Theoretical fit of the GRB 01121 light curves in the 40 – 700 keV (BeppoSAX GRBM), 2 – 26 keV (BeppoSAX WFC), 2/10 keV (BeppoSAX NFI). **Right:** Enlargement of the Flare.

### C.4.2. The first step on the first flare: analysis of GRB 01121

GRB 01121 is a near, long burst with  $T_{90} = 28$  s and redshift  $z = 0.36$  (Infante et al., 2001). Its fluence (Price et al., 2002) is  $2.4 \times 10^{-5}$  erg/cm<sup>2</sup> that corresponds, in the hypothesis of isotropic emission at the observed redshift, to an energy in the band 2 – 700 keV of  $2.8 \times 10^{52}$  erg. This is the second brightest source detected by BeppoSAX in  $\gamma$ -rays and X-rays. At the time  $t = 240$  s, in the X-ray 2 – 26 keV energy band, there is a big flare (Piro et al., 2005; Greiner et al., 2003). It lasts about seventy seconds ( $dt/t \sim 0.29$ ) and corresponds to a bump of an order of magnitude in luminosity. It is however very soft, since its energy is about 3% of the total amount of the prompt emission (Piro et al., 2005).

In figure C.12 we present the observed GRB 01121 light curves in the three different energy bands we analyzed, together with their theoretical fit in the framework of our model: 40 – 700 keV, 2 – 26 keV, 2 – 10 keV. Looking at the observational data we can see that the 40 – 700 keV energy band light curve presents a temporal profile particularly regular, smooth and homogeneous, while the 2 – 26 keV light curve has a remarkably irregular profile. This is quite anomalous, in fact generally the light curves in these energy bands presents just the opposite trend.

In figure C.12 there is also an enlargement of the flare of this source that shows in detail the comparison between the theoretical light curve and the observational data.

In the computation of the theoretical light curve for the flare we reproduce it as due to a spherical cloud of CBM along the line of sight introducing, in this way, a three-dimensional structure for the Circum Burst Medium. In fact, in the first approximation, we assume a modeling of thin spherical shells for the distribution of the CBM. This allows us to consider a purely radial profile

in the expansion (Ruffini et al., 2002, 2003). This radial approximation is valid until the visible area of emission of photons is sufficiently small with respect to the characteristic size of the CBM shell. The visible area of emission is defined by the maximum value of the viewing angle; it varies with time and is inversely proportional to the Lorentz Gamma Factor (see the previous). So it happens that, at the beginning of the expansion, when the Gamma Factor is big (about  $10^2$ ), the effective distribution of the CBM doesn't matter for the narrowness of the viewing angle but, at the end of the expansion, the remarkable lessening of the Gamma Factor produces a strong increase of the viewing angle and a correct estimation of the CBM by the introduction of the angular coordinate distribution becomes necessary.

We can see that our results are in very good agreement with the observational data, also in the late tail of the flare. In particular, the short time variability has been successfully reproduced.

Here we performed just a first attempt of application of our interpretation of flares and we found an encouraging result. Now we plan to verify our hypothesis by its application to other sources and to produce a detailed cinematic and dynamic theory concerning this fundamental features of Gamma-Ray Burst.

## C.5. Application to GRB 031203

GRB 031203 was observed by IBIS, on board of the INTEGRAL satellite (see Mereghetti and Gotz, 2003), as well as by XMM (Watson et al., 2004) and Chandra (Soderberg et al., 2004) in the 2 – 10 keV band, and by VLT (Soderberg et al., 2004) in the radio band. It appears as a typical long burst (Sazonov et al., 2004a), with a simple profile and a duration of  $\approx 40$  s. The burst fluence in the 20 – 200 keV band is  $(2.0 \pm 0.4) \times 10^{-6}$  erg/cm<sup>2</sup> (Sazonov et al., 2004a), and the measured redshift is  $z = 0.106$  (Prochaska et al., 2004). We analyze in the following the gamma-ray signal received by INTEGRAL. The observations in other wavelengths, in analogy with the case of GRB 980425 (Pian et al., 2000; Ruffini et al., 2004a, 2007b), could be related to the supernova event, as also suggested by Soderberg et al. (2004), and they will be examined elsewhere.

The INTEGRAL observations find a direct explanation in our theoretical model. We reproduce correctly the observed time variability of the prompt emission (see Fig. C.13 and Bernardini et al., 2005a). The radiation produced by the interaction of the optically thin fireshell with the CBM agrees with observations both for intensity and time structure.

The progress in reproducing the X and  $\gamma$ -ray emission as originating from a thermal spectrum in the comoving frame of the burst (Ruffini et al., 2004b) leads to the characterization of the instantaneous spectral properties which are shown to drift from hard to soft during the evolution of the system. The

convolution of these instantaneous spectra over the observational time scale is in very good agreement with the observed power-law spectral shape.

### C.5.1. The initial conditions

The best fit of the observational data leads to a total energy of the electron-positron plasma  $E_{e^\pm}^{tot} = 1.85 \times 10^{50}$  erg. Assuming a black hole mass  $M = 10M_\odot$ , we then have a black hole charge to mass ratio  $\xi = 6.8 \times 10^{-3}$ ; the plasma is created between the radii  $r_1 = 2.95 \times 10^6$  cm and  $r_2 = 2.81 \times 10^7$  cm with an initial temperature  $T = 1.52$  MeV and a total number of pairs  $N_{e^\pm} = 2.98 \times 10^{55}$ . The amount of baryonic matter in the remnant is  $B = 7.4 \times 10^{-3}$ .

After the transparency point and the P-GRB emission, the initial Lorentz gamma factor of the accelerated baryons is  $\gamma_\circ = 132.8$  at an arrival time at the detector  $t_a^d = 8.14 \times 10^{-3}$  s and a distance from the Black Hole  $r_\circ = 6.02 \times 10^{12}$  cm. The CBM parameters are:  $\langle n_{cbm} \rangle = 0.3$  particle/cm<sup>3</sup> and  $\langle \mathcal{R} \rangle = 7.81 \times 10^{-9}$ .

### C.5.2. The GRB luminosity in fixed energy bands

The aim of our model is to derive from first principles both the luminosity in selected energy bands and the time resolved/integrated spectra. We recall that the luminosity in selected energy bands is evaluated integrating over the EQTSs (see Ruffini et al., 2004b) the energy density released in the interaction of the accelerated baryons with the CBM measured in the co-moving frame, duly boosted in the observer frame. The radiation viewed in the comoving frame of the accelerated baryonic matter is assumed to have a thermal spectrum and to be produced by the interaction of the CBM with the front of the expanding baryonic shell.

In order to evaluate the contributions in the band  $[\nu_1, \nu_2]$  we have to multiply the bolometric luminosity with an “effective weight”  $W(\nu_1, \nu_2, T_{arr})$ , where  $T_{arr}$  is the observed temperature.  $W(\nu_1, \nu_2, T_{arr})$  is given by the ratio of the integral over the given energy band of a Planckian distribution at temperature  $T_{arr}$  to the total integral  $aT_{arr}^4$  (Ruffini et al., 2004b). The resulting expression for the emitted luminosity is Eq.(7.3.1).

### C.5.3. The “prompt emission”

In order to compare our theoretical prediction with the observations, it is important to notice that there is a shift between the initial time of the GRB event and the moment in which the satellite instrument has been triggered. In fact, in our model the GRB emission starts at the transparency point when the P-GRB is emitted. If the P-GRB is under the threshold of the instrument,

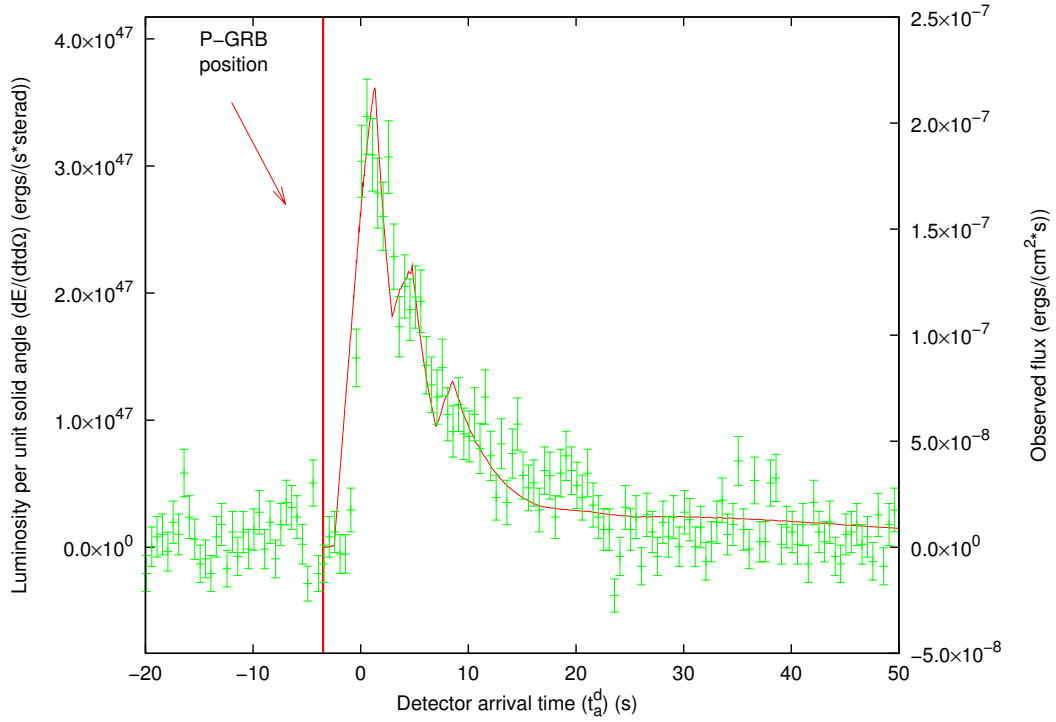


**Figure C.13.:** Theoretically simulated light curve of the GRB 031203 prompt emission in the 20 – 200 keV energy band (solid red line) is compared with the observed data (green points) from Sazonov et al. (2004a). The vertical bold red line indicates the time position of P-GRB.

the trigger starts a few seconds later with respect to the real beginning of the event. Therefore it is crucial, in the theoretical analysis, to estimate and take into due account this time delay. In the present case it results in  $\Delta t_a^d = 3.5$  s (see the bold red line in Fig. C.13). In what follows, the detector arrival time is referred to the onset of the instrument.

The structure of the prompt emission of GRB 031203, which is a single peak with a slow decay, is reproduced assuming an CBM which has not a constant density but presents several density spikes with  $\langle n_{cbm} \rangle = 0.16$  particle/cm<sup>3</sup>. Such density spikes corresponding to the main peak are modeled as three spherical shells with width  $\Delta$  and density contrast  $\Delta n/n$ : we adopted for the first peak  $\Delta = 3.0 \times 10^{15}$  cm and  $\Delta n/n = 8$ , for the second peak  $\Delta = 1.0 \times 10^{15}$  cm and  $\Delta n/n = 1.5$  and for the third one  $\Delta = 7.0 \times 10^{14}$  cm and  $\Delta n/n = 1$ . To describe the details of the CBM filamentary structure we would require an intensity vs. time information with an arbitrarily high resolving power. With the finite resolution of the INTEGRAL instrument, we can only describe the average density distribution compatible with the given accuracy. Only structures at scales of  $10^{15}$  cm can be identified. Smaller structures would need a stronger signal and/or a smaller time resolution of the detector. The three clouds here considered are necessary and sufficient to reproduce the observed light curve: a smaller number would not fit the data, while a larger number is unnecessary and would be indeterminable.

The result (see Fig. C.13) shows a good agreement with the light curve reported by Sazonov et al. (2004a), and it provides a further evidence for the possibility of reproducing light curves with a complex time variability through CBM inhomogeneities (Ruffini et al., 2002, 2003, 2005a).

#### C.5.4. The instantaneous spectrum

As outlined in previous sections, in addition to the the luminosity in fixed energy bands we can derive also the instantaneous photon number spectrum  $N(E)$ . In Fig. C.14 are shown samples of time-resolved spectra for five different values of the arrival time which cover the whole duration of the event.

It is manifest from this picture that, although the spectrum in the comoving frame of the expanding pulse is thermal, the shape of the final spectrum in the laboratory frame is clearly non thermal. In fact, as explained in Ruffini et al. (2004b), each single instantaneous spectrum is the result of an integration of hundreds of thermal spectra over the corresponding EQTS. This calculation produces a non thermal instantaneous spectrum in the observer frame (see Fig. C.14).

Another distinguishing feature of the GRBs spectra which is also present in these instantaneous spectra, as shown in Fig. C.14, is the hard to soft transition during the evolution of the event (Crider et al., 1997; Piran, 1999; Frontera et al., 2000; Ghirlanda et al., 2002). In fact the peak of the energy distributions

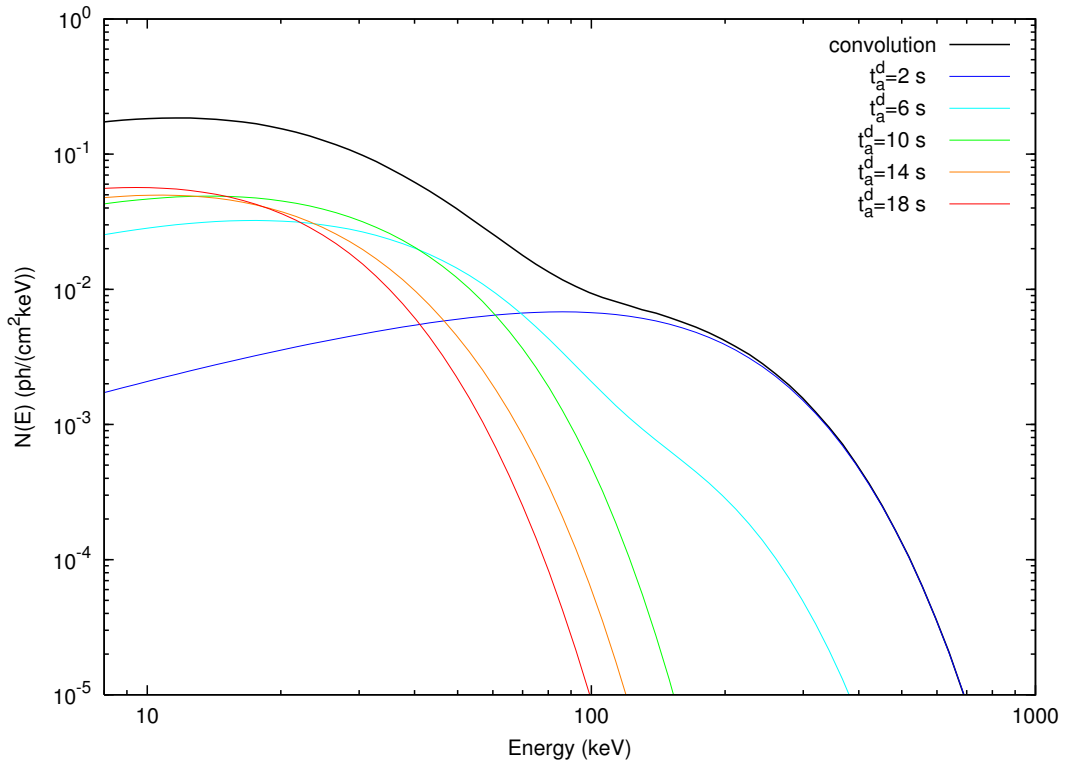


**Figure C.14.:** Five different theoretically predicted instantaneous photon number spectrum  $N(E)$  for  $t_a^d = 2, 6, 10, 14, 18$  s are here represented (colored curves) together with their own temporal convolution (black bold curve). The shapes of the instantaneous spectra are not blackbodies due to the spatial convolution over the EQTS (see text).

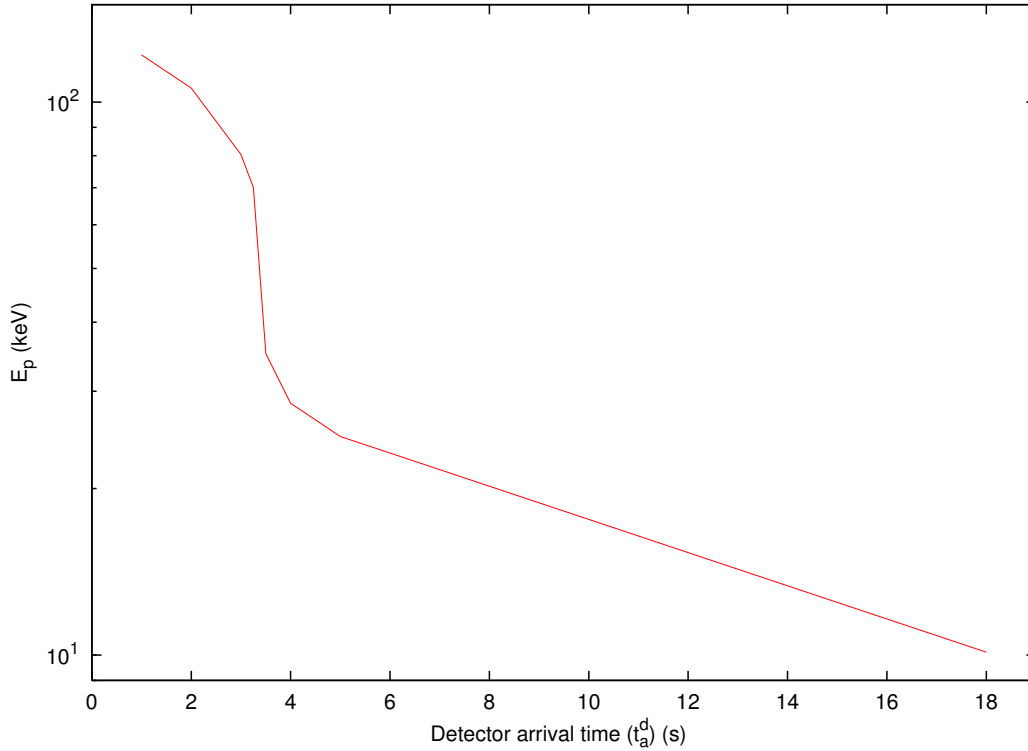


**Figure C.15.:** The energy of the peak of the instantaneous photon number spectrum  $N(E)$  is here represented as a function of the arrival time during the “prompt emission” phase. The clear hard to soft behavior is shown.

$E_p$  drift monotonically to softer frequencies with time (see Fig. C.15). This feature explains the change in the power-law low energy spectral index  $\alpha$  (Band et al., 1993) which at the beginning of the prompt emission of the burst ( $t_a^d = 2$  s) is  $\alpha = 0.75$ , and progressively decreases for later times (see Fig. C.14). In this way the link between  $E_p$  and  $\alpha$  identified by Crider et al. (1997) is explicitly shown. This theoretically predicted evolution of the spectral index during the event unfortunately cannot be detected in this particular burst by INTEGRAL because of the not sufficient quality of the data (poor photon statistics, see Sazonov et al., 2004a).

### C.5.5. The time-integrated spectrum: comparison with the observed data

The time-integrated observed GRB spectra show a clear power-law behavior. Within a different framework Shakura, Sunyaev and Zel’dovich (see e.g. Pozdniakov et al., 1983, and references therein) argued that it is possible to obtain such power-law spectra from a convolution of many non power-law instantaneous spectra evolving in time. This result was recalled and applied

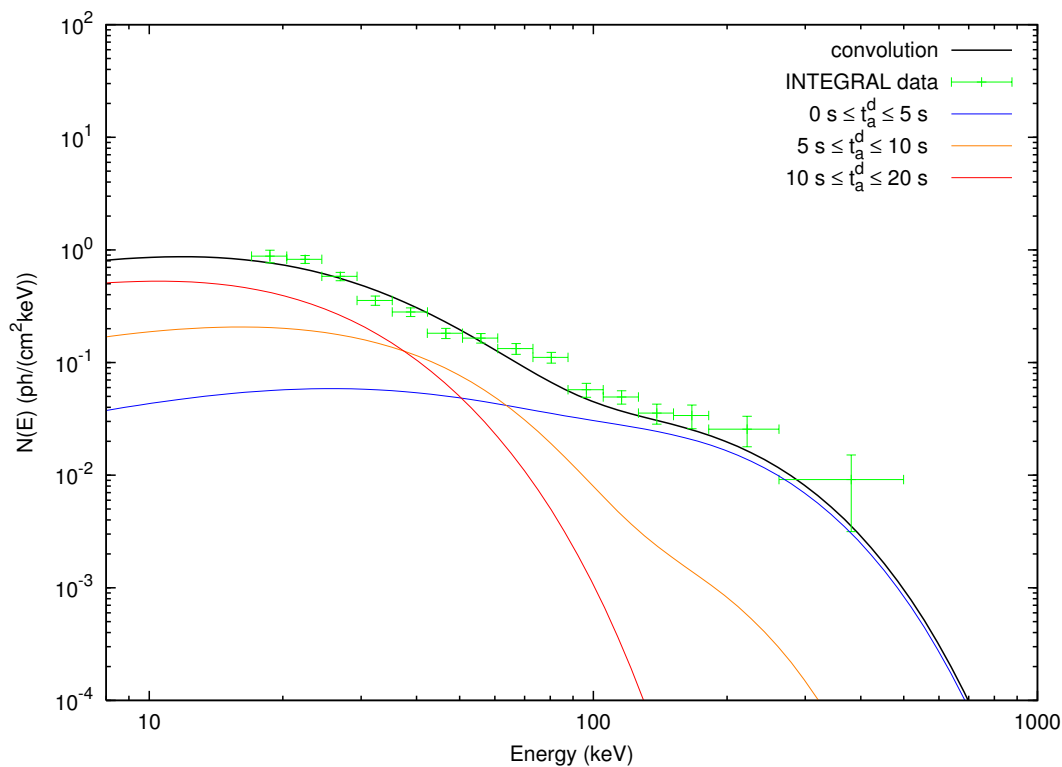


**Figure C.16.:** Three theoretically predicted time-integrated photon number spectra  $N(E)$  are here represented for  $0 \leq t_a^d \leq 5$  s,  $5 \leq t_a^d \leq 10$  s and  $10 \leq t_a^d \leq 20$  s (colored curves). The hard to soft behavior presented in Fig. C.15 is confirmed. Moreover, the theoretically predicted time-integrated photon number spectrum  $N(E)$  corresponding to the first 20 s of the “prompt emission” (black bold curve) is compared with the data observed by INTEGRAL (green points, see Sazonov et al., 2004a,b). This curve is obtained as a convolution of 108 instantaneous spectra, which are enough to get a good agreement with the observed data.

to GRBs by Blinnikov et al. (1999) assuming for the instantaneous spectra a thermal shape with a temperature changing with time. They showed that the integration of such energy distributions over the observation time gives a typical power-law shape possibly consistent with GRB spectra.

Our specific quantitative model is more complicated than the one considered by Blinnikov et al. (1999): as pointed out in previous sections, the instantaneous spectrum here is not a black body. Each instantaneous spectrum is obtained by an integration over the corresponding EQTS: it is itself a convolution, weighted by appropriate Lorentz and Doppler factors, of  $\sim 10^6$  thermal spectra with variable temperature. Therefore, the time-integrated spectra are not plain convolutions of thermal spectra: they are convolutions of convolutions of thermal spectra (see Fig. C.14).

The simple power-law shape of the integrated spectrum is more evident if we sum tens of instantaneous spectra, as in Fig. C.16. In this case we divided the prompt emission in three different time interval, and for each one we integrated on time the energy distribution. The resulting three time-integrated spectra have a clear non-thermal behavior, and still present the characteristic hard to soft transition.

Finally, we integrated the photon number spectrum  $N(E)$  over the whole duration of the prompt event (see again Fig. C.16): in this way we obtain a typical non-thermal power-law spectrum which results to be in good agreement with the INTEGRAL data (see Sazonov et al., 2004a,b) and gives a clear evidence of the possibility that the observed GRBs spectra are originated from a thermal emission.

The precise knowledge we have here acquired on GRB 031203 helps in clarifying the overall astrophysical system GRB 031203 - SN 2003lw - the 2 – 10 keV XMM and Chandra data (see sections A.3 and A.5, where the late 2 – 10 keV XMM and Chandra data are also discussed).

## C.6. Application to GRB 050315

GRB 050315 (Vaughan et al., 2006) has been triggered and located by the BAT instrument (Barthelmy, 2004; Barthelmy et al., 2005a) on board of the *Swift* satellite (Gehrels et al., 2004) at 2005-March-15 20:59:42 UT (Parsons et al., 2005). The narrow field instrument XRT (Burrows et al., 2004, 2005a) began observations  $\sim 80$  s after the BAT trigger, one of the earliest XRT observations yet made, and continued to detect the source for  $\sim 10$  days (Vaughan et al., 2006). The spectroscopic redshift has been found to be  $z = 1.949$  (Kelson and Berger, 2005).

We present here the results of the fit of the *Swift* data of this source in 5 energy bands in the framework of our theoretical model, pointing out a new step toward the uniqueness of the explanation of the overall GRB structure. We first recall the essential features of our theoretical model; then we fit the GRB 050315 observations by both the BAT and XRT instruments; we also present the instantaneous spectra for selected values of the detector arrival time ranging from 60 s (i.e. during the so called “prompt emission”) all the way to  $3.0 \times 10^4$  s (i.e. the latest afterglow phases).

### C.6.1. The fit of the observations

The best fit of the observational data leads to a total energy of the black hole dyadosphere, generating the  $e^\pm$  plasma,  $E_{e^\pm}^{tot} = 1.46 \times 10^{53}$  erg (the observational *Swift*  $E_{iso}$  is  $> 2.62 \times 10^{52}$  erg, see Vaughan et al., 2006), so that the plasma is created between the radii  $r_1 = 5.88 \times 10^6$  cm and  $r_2 = 1.74 \times 10^8$  cm with an initial temperature  $T = 2.05 MeV$  and a total number of pairs  $N_{e^+e^-} =$

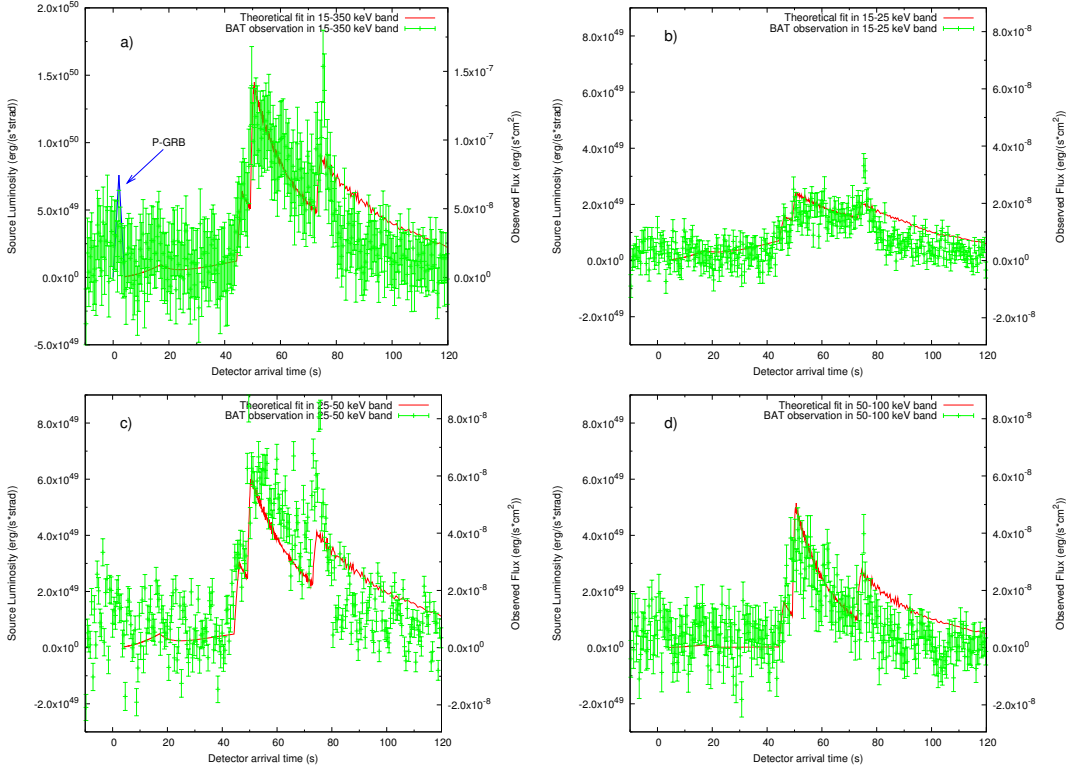


**Figure C.17.:** Our theoretical fit (red line) of the BAT observations (green points) of GRB 050315 in the 15–350 keV (a), 15–25 keV (b), 25–50 keV (c), 50–100 keV (d) energy bands (Vaughan et al., 2006). The blue line in panel (a) represents our theoretical prediction for the intensity and temporal position of the P-GRB.

$7.93 \times 10^{57}$ . The second parameter of the theory, the amount  $M_B$  of baryonic matter in the plasma, is found to be such that  $B \equiv M_B c^2 / E_{\text{dya}} = 4.55 \times 10^{-3}$ . The transparency point and the P-GRB emission occurs then with an initial Lorentz gamma factor of the accelerated baryons  $\gamma_o = 217.81$  at a distance  $r = 1.32 \times 10^{14}$  cm from the black hole.

### The BAT data

In Fig. C.17 we represent our theoretical fit of the BAT observations in the three energy channels 15–25 keV, 25–50 keV and 50–100 keV and in the whole 15–350 keV energy band.

In our model the GRB emission starts at the transparency point when the P-GRB is emitted; this instant of time is often different from the moment in which the satellite instrument triggers, due to the fact that sometimes the P-GRB is under the instrumental noise threshold or comparable with it. In order to compare our theoretical predictions with the observations, it is important to estimate and take into account this time shift. In the present case

of GRB 050315 it has been observed (see Vaughan et al., 2006) a possible precursor before the trigger. Such a precursor is indeed in agreement with our theoretically predicted P-GRB, both in its isotropic energy emitted (which we theoretically predict to be  $E_{P-GRB} = 1.98 \times 10^{51}$  erg) and its temporal separation from the peak of the afterglow (which we theoretically predicted to be  $\Delta t_a^d = 51$  s). In Fig. C.17a the blue line shows our theoretical prediction for the P-GRB in agreement with the observations.

After the P-GRB emission, all the observed radiation is produced by the interaction of the expanding baryonic shell with the interstellar medium. In order to reproduce the complex time variability of the light curve of the prompt emission as well as of the afterglow, we describe the CBM filamentary structure, for simplicity, as a sequence of overdense spherical regions separated by much less dense regions. Such overdense regions are nonhomogeneously filled, leading to an effective emitting area  $A_{eff}$  determined by the dimensionless parameter  $\mathcal{R}$  (see previous sections and Ruffini et al., 2004b, 2005c, for details). Clearly, in order to describe any detailed structure of the time variability an authentic three dimensional representation of the CBM structure would be needed. However, this finer description would not change the substantial agreement of the model with the observational data. Anyway, in the “prompt emission” phase, the small angular size of the source visible area due to the relativistic beaming makes such a spherical approximation an excellent one (see also for details Ruffini et al., 2002).

The structure of the “prompt emission” has been reproduced assuming three overdense spherical CBM regions with width  $\Delta$  and density contrast  $\Delta n / \langle n \rangle$ : we chose for the first region, at  $r = 4.15 \times 10^{16}$  cm,  $\Delta = 1.5 \times 10^{15}$  cm and  $\Delta n / \langle n \rangle = 5.17$ , for the second region, at  $r = 4.53 \times 10^{16}$  cm,  $\Delta = 7.0 \times 10^{14}$  cm and  $\Delta n / \langle n \rangle = 36.0$  and for the third region, at  $r = 5.62 \times 10^{16}$  cm,  $\Delta = 5.0 \times 10^{14}$  cm and  $\Delta n / \langle n \rangle = 85.4$ . The CBM mean density during this phase is  $\langle n_{cbm} \rangle = 0.81$  particles/cm<sup>3</sup> and  $\langle \mathcal{R} \rangle = 1.4 \times 10^{-7}$ . With this choice of the density mask we obtain agreement with the observed light curve, as shown in Fig. C.17. A small discrepancy occurs in coincidence with the last peak: this is due to the fact that at this stage the source visible area due to the relativistic beaming is comparable with the size of the clouds, therefore the spherical shell approximation should be duly modified by a detailed analysis of a full three-dimensional treatment of the CBM filamentary structure. Such a topic is currently under investigation (see also for details Ruffini et al., 2002). Fig. C.17 shows also the theoretical fit of the light curves in the three BAT energy channels in which the GRB has been detected (15–25 keV in Fig. C.17b, 25–50 keV in Fig. C.17c, 50–100 keV in Fig. C.17d).

### The XRT data

The same analysis can be applied to explain the features of the XRT light curve in the afterglow phase. It has been recently pointed out (Nousek et al.,

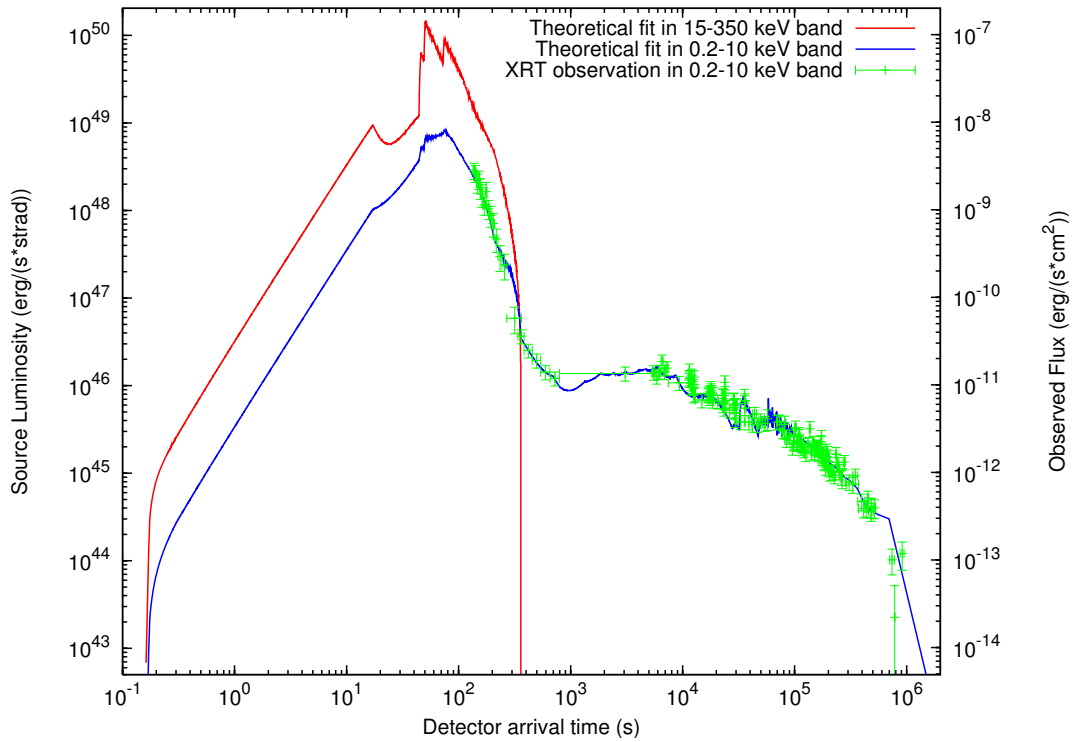


**Figure C.18.:** Our theoretical fit (blue line) of the XRT observations (green points) of GRB 050315 in the 0.2–10 keV energy band (Vaughan et al., 2006). The theoretical fit of the BAT observations (see Fig. C.17a) in the 15–350 keV energy band is also represented (red line).

2006) that almost all the GRBs observed by *Swift* show a “canonical behavior”: an initial very steep decay followed by a shallow decay and finally a steeper decay. In order to explain these features many different approaches have been proposed (Meszaros, 2006; Nousek et al., 2006; Panaitescu et al., 2006; Zhang et al., 2006). In our treatment these behaviors are automatically described by the same mechanism responsible for the prompt emission described above: the baryonic shell expands in an CBM region, between  $r = 9.00 \times 10^{16}$  cm and  $r = 5.50 \times 10^{18}$  cm, which is significantly at lower density ( $\langle n_{cbm} \rangle = 4.76 \times 10^{-4}$  particles/cm<sup>3</sup>,  $\langle \mathcal{R} \rangle = 7.0 \times 10^{-6}$ ) then the one corresponding to the prompt emission, and this produces a slower decrease of the velocity of the baryons with a consequent longer duration of the afterglow emission. The initial steep decay of the observed flux is due to the smaller number of collisions with the CBM. In Fig. C.18 is represented our theoretical fit of the XRT data, together with the theoretically computed 15–350 keV light curve of Fig. C.17a (without the BAT observational data to not overwhelm the picture too much).

What is impressive is that no different scenarios need to be advocated in order to explain the features of the light curves: both the prompt and the afterglow emission are just due to the thermal radiation in the comoving frame produced by inelastic collisions with the CBM duly boosted by the relativistic transformations over the EQTSs.

### C.6.2. The instantaneous spectrum

In addition to the the luminosity in fixed energy bands we can derive also the instantaneous photon number spectrum  $N(E)$  starting from the same assumptions. In Fig. C.19 are shown samples of time-resolved spectra for eight different values of the arrival time which cover the whole duration of the event. It is manifest from this picture that, although the spectrum in the comoving frame of the expanding pulse is thermal, the shape of the final spectrum in the laboratory frame is clearly non thermal. In fact, as explained in Ruffini et al. (2004b), each single instantaneous spectrum is the result of an integration of thousands of thermal spectra over the corresponding EQTS. This calculation produces a non thermal instantaneous spectrum in the observer frame (see Fig. C.19).

A distinguishing feature of the GRBs spectra which is also present in these instantaneous spectra is the hard to soft transition during the evolution of the event (Crider et al., 1997; Piran, 1999; Frontera et al., 2000; Ghirlanda et al., 2002). In fact the peak of the energy distribution  $E_p$  drifts monotonically to softer frequencies with time. This feature is linked to the change in the power-law low energy spectral index  $\alpha$  (Band et al., 1993), so the correlation between  $\alpha$  and  $E_p$  (Crider et al., 1997) is explicitly shown.

It is important to stress that there is no difference in the nature of the spec-

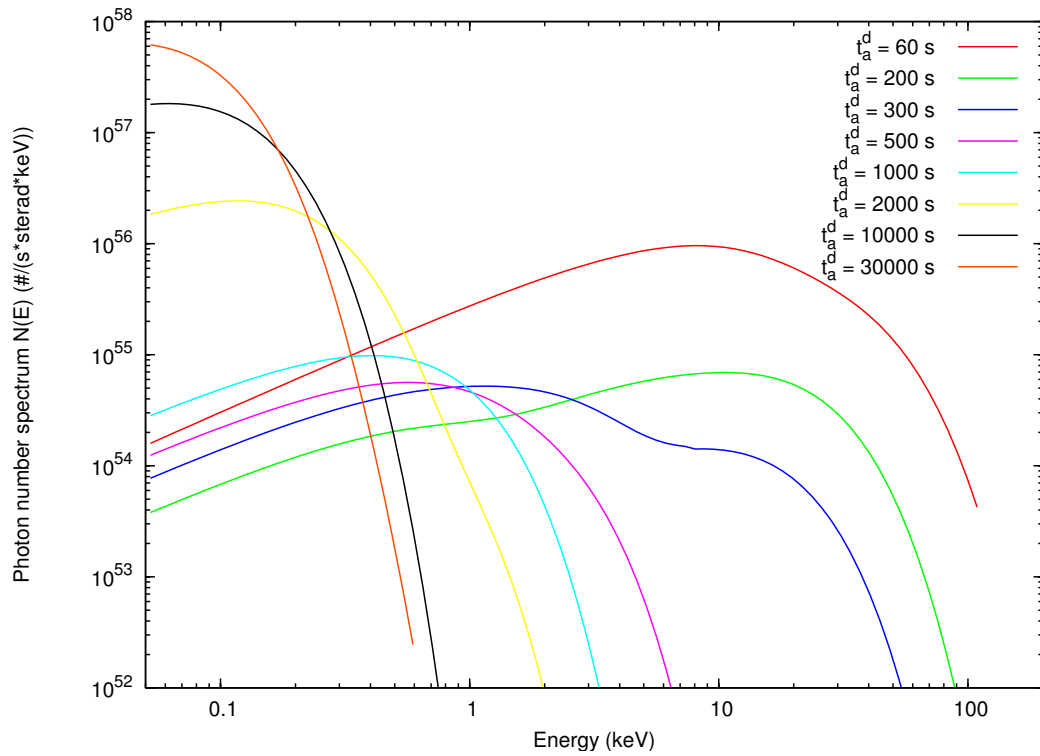


**Figure C.19.:** Eight theoretically predicted instantaneous photon number spectra  $N(E)$  are here represented for different values of the arrival time (colored curves). The hard to soft behavior is confirmed.

trum during the prompt and the afterglow phases: the observed energy distribution changes from hard to soft, with continuity, from the “prompt emission” all the way to the latest phases of the afterglow.

### C.6.3. Problems with the definition of “long” GRBs

The confirmation by *Swift* of our prediction of the overall afterglow structure, and especially the coincidence of the “prompt emission” with the peak of the afterglow, opens a new problematic in the definition of the long GRBs. It is clear, in fact, that the identification of the “prompt emission” in the current GRB literature is not at all intrinsic to the phenomenon but is merely due to the threshold of the instruments used in the observations (e.g. BATSE in the 50–300 keV energy range, or BeppoSAX GRBM in 40–700 keV, or *Swift* BAT in 15–350 keV). As it is clear from Fig. C.20, there is no natural way to identify in the source a special extension of the peak of the afterglow that is not the one purely defined by the experimental threshold. It is clear, therefore, that long GRBs, as defined till today, are just the peak of the afterglow and there is no way, as explained above, to define their “prompt emission” duration as a characteristic signature of the source. As the *Swift* observations show, the duration of the long GRBs has to coincide with the duration of the entire afterglow. A Kouveliotou - Tavani plot of the long GRBs, done following our interpretation which is clearly supported by the recent *Swift* data (see Fig. C.20), will present enormous dispersion on the temporal axis.

We recall that in our theory both “short” and “long” GRBs originate from the same process of black hole formation. The major difference between the two is the value of the baryon loading parameter  $B$  (see Fig. 3.8). In the limit of small baryon loading, all the plasma energy is emitted at the transparency in the P-GRB, with negligible afterglow observed flux. For higher values of the baryon loading, the relative energy content of the P-GRB with respect to the afterglow diminishes (see Ruffini et al., 2005a, and references therein).

## C.7. Application to GRB 060218

GRB 060218 triggered the BAT instrument of *Swift* on 18 February 2006 at 03:36:02 UT and has a  $T_{90} = (2100 \pm 100)$  s (Cusumano et al., 2006). The XRT instrument (Kennea et al., 2006; Cusumano et al., 2006) began observations  $\sim 153$  s after the BAT trigger and continued for  $\sim 12.3$  days (Sakamoto et al., 2006). The source is characterized by a flat  $\gamma$ -ray light curve and a soft spectrum (Barbier et al., 2006). It has an X-ray light curve with a long, slow rise and gradual decline and it is considered an X-Ray Flash (XRF) since its peak energy occurs at  $E_p = 4.9^{+0.4}_{-0.3}$  keV (Campana et al., 2006a). It has been observed by the *Chandra* satellite on February 26.78 and March 7.55 UT ( $t \simeq 8.8$  and 17.4 days) for 20 and 30 ks respectively (Soderberg et al., 2006b).

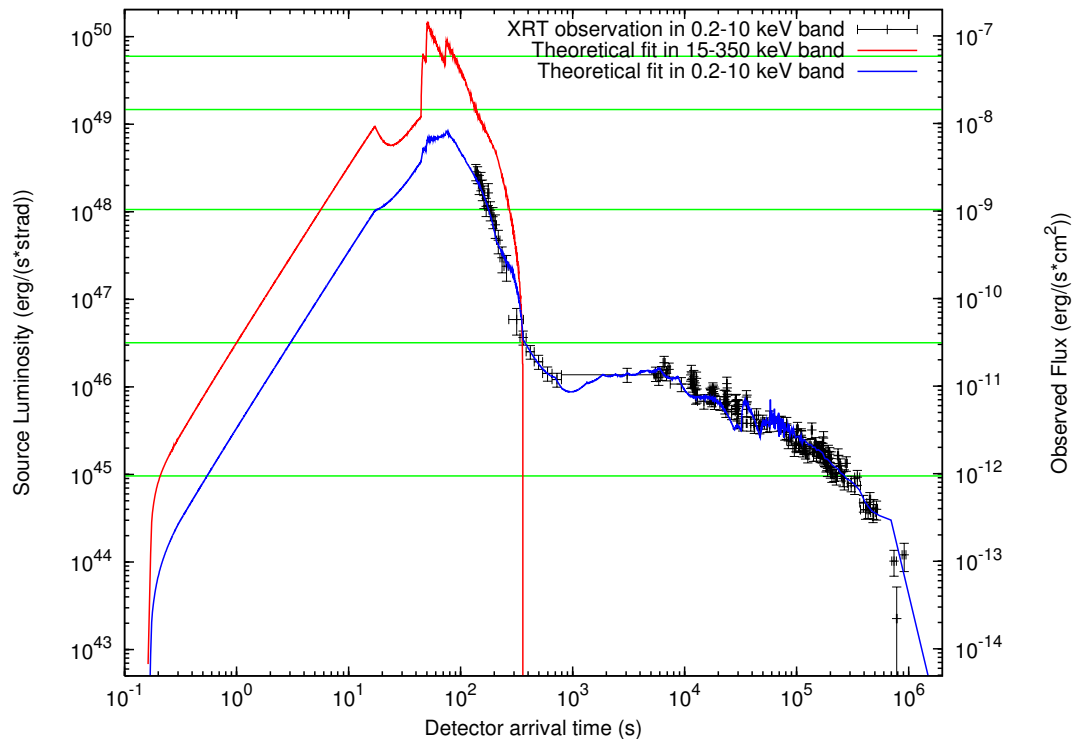


**Figure C.20.:** Same as Fig. C.18. The horizontal green lines corresponds to different possible instrumental thresholds. It is clear that long GRB durations are just functions of the observational threshold.

The spectroscopic redshift has been found to be  $z = 0.033$  (Sollerman et al., 2006; Mirabal et al., 2006). The corresponding isotropic equivalent energy is  $E_{iso} = (1.9 \pm 0.1) \times 10^{49}$  erg (Sakamoto et al., 2006) which sets this GRB as a low luminous one, consistent with most of the GRBs associated with SNe (Liang et al., 2007; Cobb et al., 2006; Guetta and Della Valle, 2007).

GRB 060218 is associated with SN2006aj whose expansion velocity is  $v \sim 0.1c$  (Pian et al., 2006; Fatkhullin et al., 2006; Soderberg et al., 2006a; Cobb et al., 2006). The host galaxy of SN2006aj is a low luminosity, metal poor star forming dwarf galaxy (Ferrero et al., 2007) with an irregular morphology (Wiersema et al., 2007), similar to the ones of other GRBs associated with SNe (Modjaz et al., 2006; Sollerman et al., 2006).

### C.7.1. The fit of the observed data

In this section we present the fit of our fireshell model to the observed data (see Figs. C.21, C.24). The fit leads to a total energy of the  $e^\pm$  plasma  $E_{e^\pm}^{tot} = 2.32 \times 10^{50}$  erg, with an initial temperature  $T = 1.86$  MeV and a total number of pairs  $N_{e^\pm} = 1.79 \times 10^{55}$ . The second parameter of the theory,  $B = 1.0 \times 10^{-2}$ , is the highest value ever observed and is close to the limit for the stability of the adiabatic optically thick acceleration phase of the fireshell (for further details see Ruffini et al., 2000). The Lorentz gamma factor obtained solving the fireshell equations of motion (Bianco and Ruffini, 2005b,a) is  $\gamma_o = 99.2$  at the beginning of the afterglow phase at a distance from the progenitor  $r_o = 7.82 \times 10^{12}$  cm. It is much larger than  $\gamma \sim 5$  estimated by Kaneko et al. (2007) and Toma et al. (2007).

In Fig. C.21 we show the afterglow light curves fitting the prompt emission both in the BAT (15–150 keV) and in the XRT (0.3–10 keV) energy ranges, as expected in our “canonical GRB” scenario (Dainotti et al., 2007). Initially the two luminosities are comparable to each other, but for a detector arrival time  $t_a^d > 1000$  s the XRT curves becomes dominant. The displacement between the peaks of these two light curves leads to a theoretically estimated spectral lag greater than 500 s in perfect agreement with the observations (see Liang et al., 2006b). We obtain that the bolometric luminosity in this early part coincides with the sum of the BAT and XRT light curves (see Fig. C.24) and the luminosity in the other energy ranges is negligible.

We recall that at  $t_a^d \sim 10^4$  s there is a sudden enhancement in the radio luminosity and there is an optical luminosity dominated by the SN2006aj emission (see Campana et al., 2006a; Soderberg et al., 2006b; Fan et al., 2006). Although our analysis addresses only the BAT and XRT observations, for  $r > 10^{18}$  cm corresponding to  $t_a^d > 10^4$  s the fit of the XRT data implies two new features: **1**) a sudden increase of the  $\mathcal{R}$  factor from  $\mathcal{R} = 1.0 \times 10^{-11}$  to  $\mathcal{R} = 1.6 \times 10^{-6}$ , corresponding to a significantly more homogeneous effective CBM distribution (see Fig.C.25b); **2**) an XRT luminosity much smaller

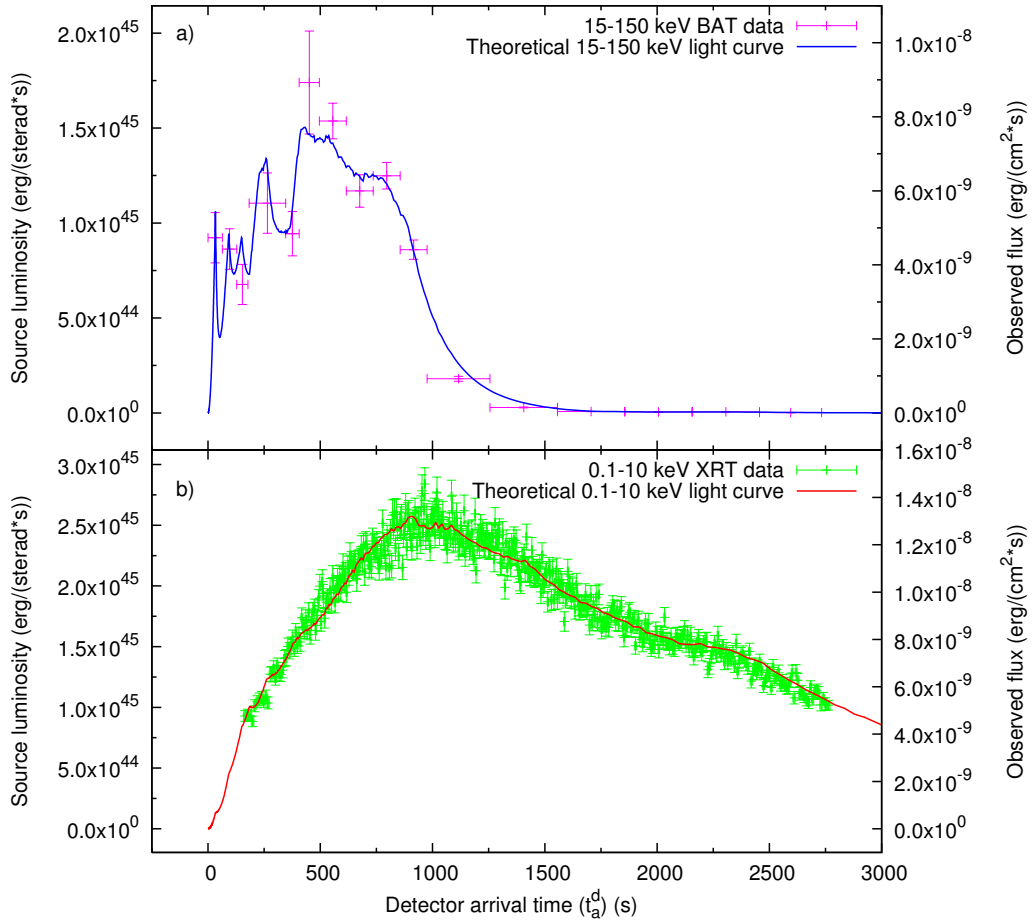


**Figure C.21.** GRB 060218 prompt emission: a) our theoretical fit (blue line) of the BAT observations in the 15–150 keV energy band (pink points); b) our theoretical fit (red line) of the XRT observations in the 0.3–10 keV energy band (green points) (Data from: Campana et al., 2006a).

than the bolometric one (see Fig. C.24). These theoretical predictions may account for the energetics of the enhancement of the radio and possibly optical and UV luminosities. Therefore, we identify two different regimes in the afterglow, one for  $t_a^d < 10^4$  s and the other for  $t_a^d > 10^4$  s. Nevertheless, there is a unifying feature: the determined effective CBM density decreases with the distance  $r$  monotonically and continuously through both these two regimes from  $n_{cbm} = 1$  particle/cm<sup>3</sup> at  $r = r_o$  to  $n_{cbm} = 10^{-6}$  particle/cm<sup>3</sup> at  $r = 6.0 \times 10^{18}$  cm:  $n_{cbm} \propto r^{-\alpha}$ , with  $1.0 \lesssim \alpha \lesssim 1.7$  (see Fig. C.25a).

Our assumption of spherical symmetry is supported by the observations which set for GRB 060218 an opening beaming angle larger than  $\sim 37^\circ$  (Liang et al., 2007; Campana et al., 2006a; Soderberg et al., 2006b; Guetta and Della Valle, 2007).

### C.7.2. The procedure of the fit

The arrival time of each photon at the detector depends on the entire previous history of the fireshell (Ruffini et al., 2001c). Moreover, all the observables depends on the EQTS (Bianco and Ruffini, 2004, 2005b) which, in turn, depend crucially on the equations of motion of the fireshell. The CBM engulfment has to be computed self-consistently through the entire dynamical evolution of the fireshell and not separately at each point. Any change in the CBM distribution strongly influences the entire dynamical evolution of the fireshell and, due to the EQTS structure, produces observable effects up to a much later time. For example if we change the density mask at a certain distance from the black hole we modify the shape of the lightcurve and consequently the evolution changes at larger radii corresponding to later times. Anyway the change of the density is not the only problem to face in the fitting of the source, in fact first of all we have to choose the energy in order to have Lorentz gamma factor sufficiently high to fit the entire GRB. In order to show the sensitivity of the fitting procedure I also present two examples of fits with the same value of  $B$  and different value of  $E_{e^\pm}^{tot}$ .

The first example has an  $E_{e^\pm}^{tot} = 1.36 \times 10^{50}$  erg . This fit resulted unsuccessfully as we see from the Fig.C.22, because the bolometric lightcurve is under the XRT peak of the afterglow. This means that the value of the energy chosen is too small to fit any data points after the peak of the afterglow. So we have to increase the value of the Energy to a have a better fit. In fact the parameters values have been found with various attempt in order to obtain the best fit.

The second example is characterized by  $E_{e^\pm}^{tot} = 1.61 \times 10^{50}$  erg and the all the data are fitted except for the last point from  $2.0 \times 10^2$ s to the end (see Fig. C.23). I attempt to fit these last points trying to diminishes the  $R$  values in order to enhance the energy emission, but again the low value of the Lorentz gamma factor, that in this case is 3 prevent the fireshell to expand. So again in this case the value of the Energy chosen is too small, but it is better than

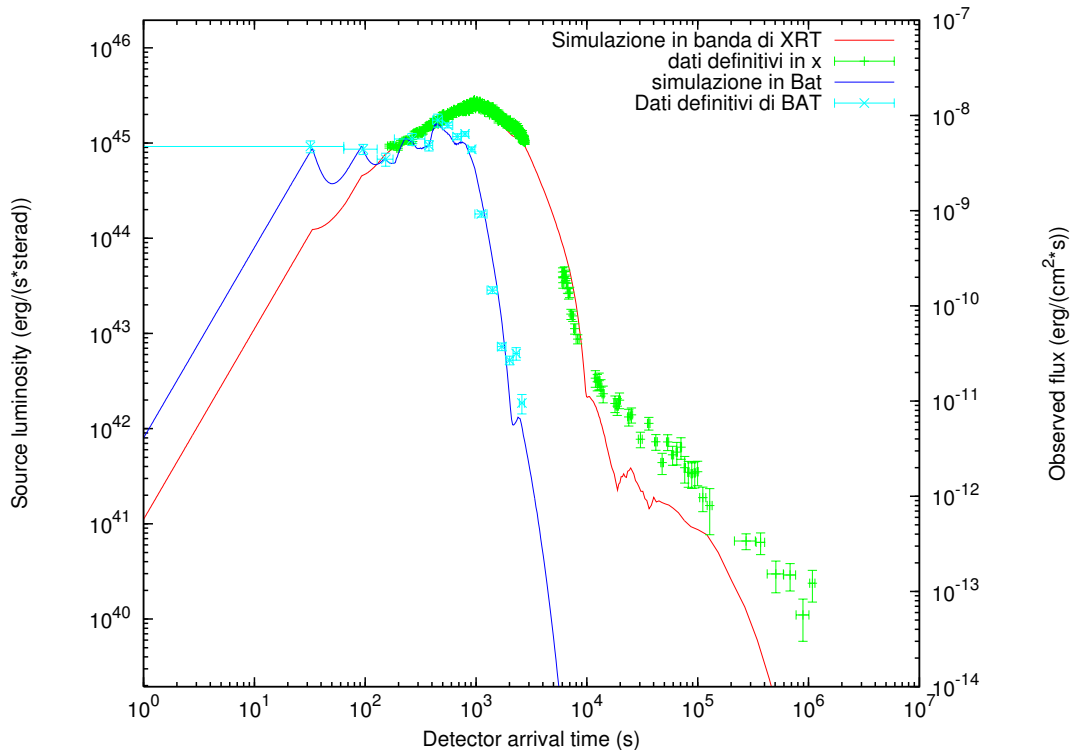


**Figure C.22.:** GRB 060218 light curves with  $E_{e^\pm}^{tot} = 1.36 \times 10^{50}$  erg: our theoretical fit (blue line) of the 15–150 keV BAT observations (pink points), our theoretical fit (red line) of the 0.3–10 keV XRT observations (green points) and the 0.3–10 keV *Chandra* observations (black points) are represented together with our theoretically computed bolometric luminosity (black line) (Data from: Campana et al. (2006a); Soderberg et al. (2006b)).

the previous attempt. In this case we increased the energy value of the 24%, but it is not enough so we decide to increase 16%.

So the final fit is characterized by the  $B = 1.0 \times 10^{-2}$  and by the  $E_{e^\pm}^{tot} = 2.32 \times 10^{50}$  erg. With this value of the energy we are able to fit all the experimental points.

### C.7.3. The fireshell fragmentation

GRB 060218 presents different peculiarities: the extremely long  $T_{90}$ , the very low effective CBM density decreasing with the distance and the largest possible value of  $B = 10^{-2}$ . These peculiarities appear to be correlated. Following Ruffini et al. (2007b), we propose that in the present case the fireshell is fragmented. This implies that the surface of the fireshell does not increase any longer as  $r^2$  but as  $r^\beta$  with  $\beta < 2$ . Consequently, the effective CBM density

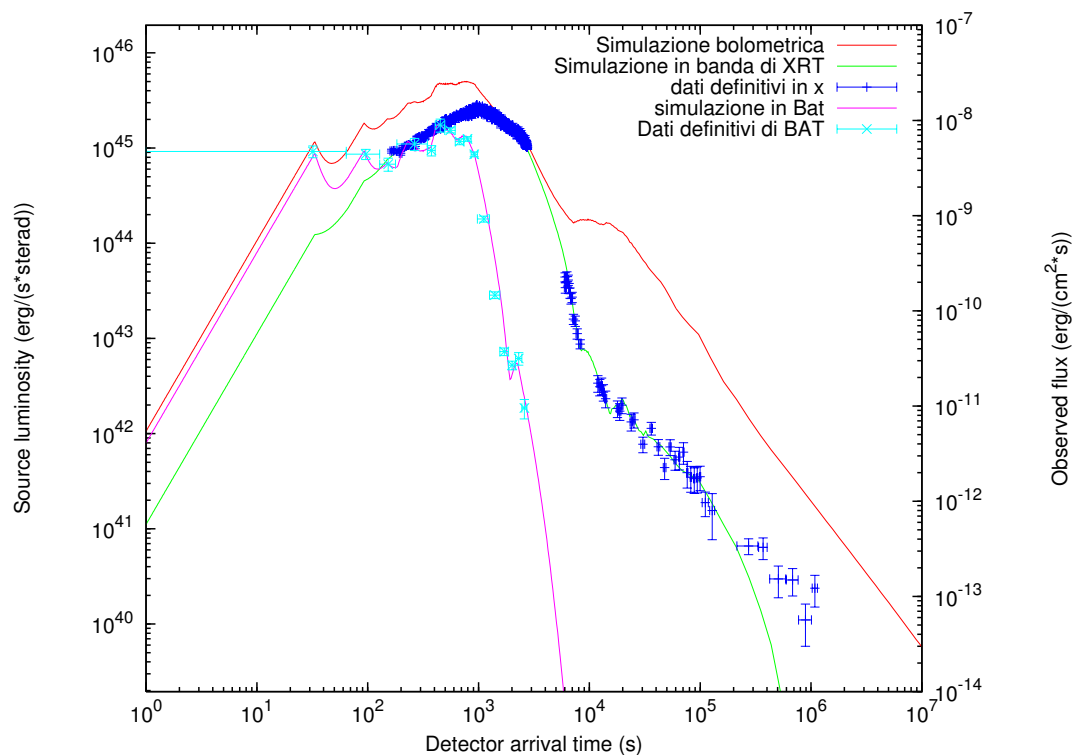


**Figure C.23.:** GRB 060218 light curves with  $E_{e^{\pm}}^{tot} = 1.61 \times 10^{50}$  erg: our theoretical fit (blue line) of the 15–150 keV BAT observations (pink points), our theoretical fit (red line) of the 0.3–10 keV XRT observations (green points) and the 0.3–10 keV *Chandra* observations (black points) are represented together with our theoretically computed bolometric luminosity (black line). Data from: Campana et al. (2006a); Soderberg et al. (2006b).

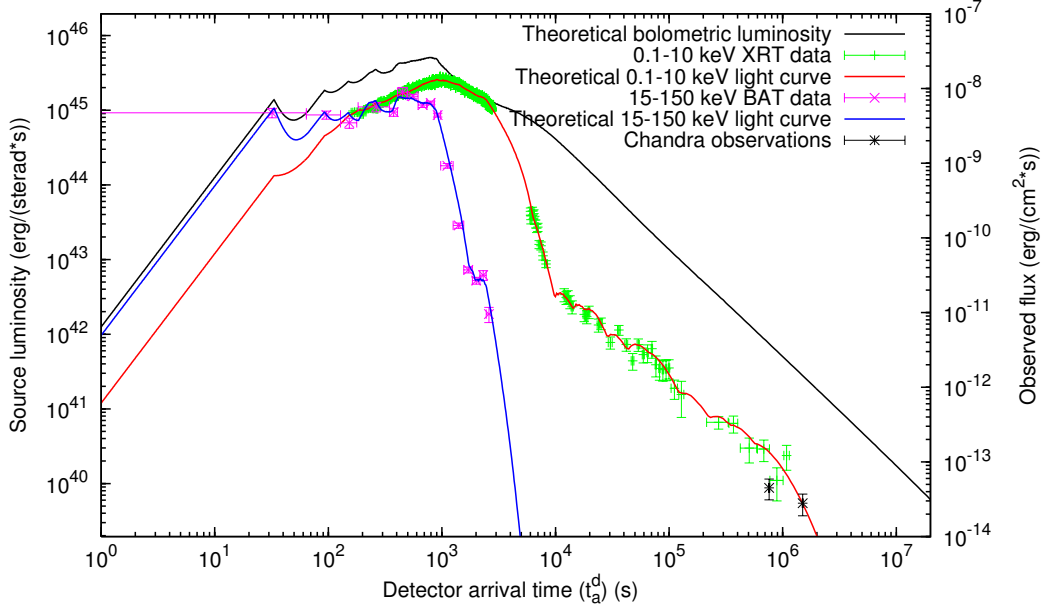


**Figure C.24.:** GRB 060218 complete light curves: our theoretical fit (blue line) of the 15–150 keV BAT observations (pink points), our theoretical fit (red line) of the 0.3–10 keV XRT observations (green points) and the 0.3–10 keV *Chandra* observations (black points) are represented together with our theoretically computed bolometric luminosity (black line) (Data from: Campana et al., 2006a; Soderberg et al., 2006b).

$n_{cbm}$  is linked to the actual one  $n_{cbm}^{act}$  by:

$$n_{cbm} = \mathcal{R}_{shell} n_{cbm}^{act}, \quad \text{with} \quad \mathcal{R}_{shell} \equiv (r^*/r)^\alpha, \quad (\text{C.7.1})$$

where  $r^*$  is the starting radius at which the fragmentation occurs and  $\alpha = 2 - \beta$  (see Fig. C.25a). For  $r^* = r_o$  we have  $n_{cbm}^{act} = 1$  particles/cm<sup>3</sup>, as expected for a “canonical GRB” (Ruffini et al., 2007a) and in agreement with the apparent absence of a massive stellar wind in the CBM (Soderberg et al., 2006b; Fan et al., 2006; Li, 2007).

The  $\mathcal{R}$  parameter defined in Eq.(C.7.2) has to take into account both the effect of the fireshell fragmentation ( $\mathcal{R}_{shell}$ ) and of the effective CBM porosity ( $\mathcal{R}_{cbm}$ ):

$$\mathcal{R} \equiv \mathcal{R}_{shell} \times \mathcal{R}_{cbm}. \quad (\text{C.7.2})$$

The phenomenon of the clumpiness of the ejecta, whose measure is the filling factor, is an aspect well known in astrophysics. For example, in the case of Novae the filling factor has been measured to be in the range  $10^{-2}$ – $10^{-5}$  (Ederoclite et al., 2006). Such a filling factor coincides, in our case, with  $\mathcal{R}_{shell}$ .

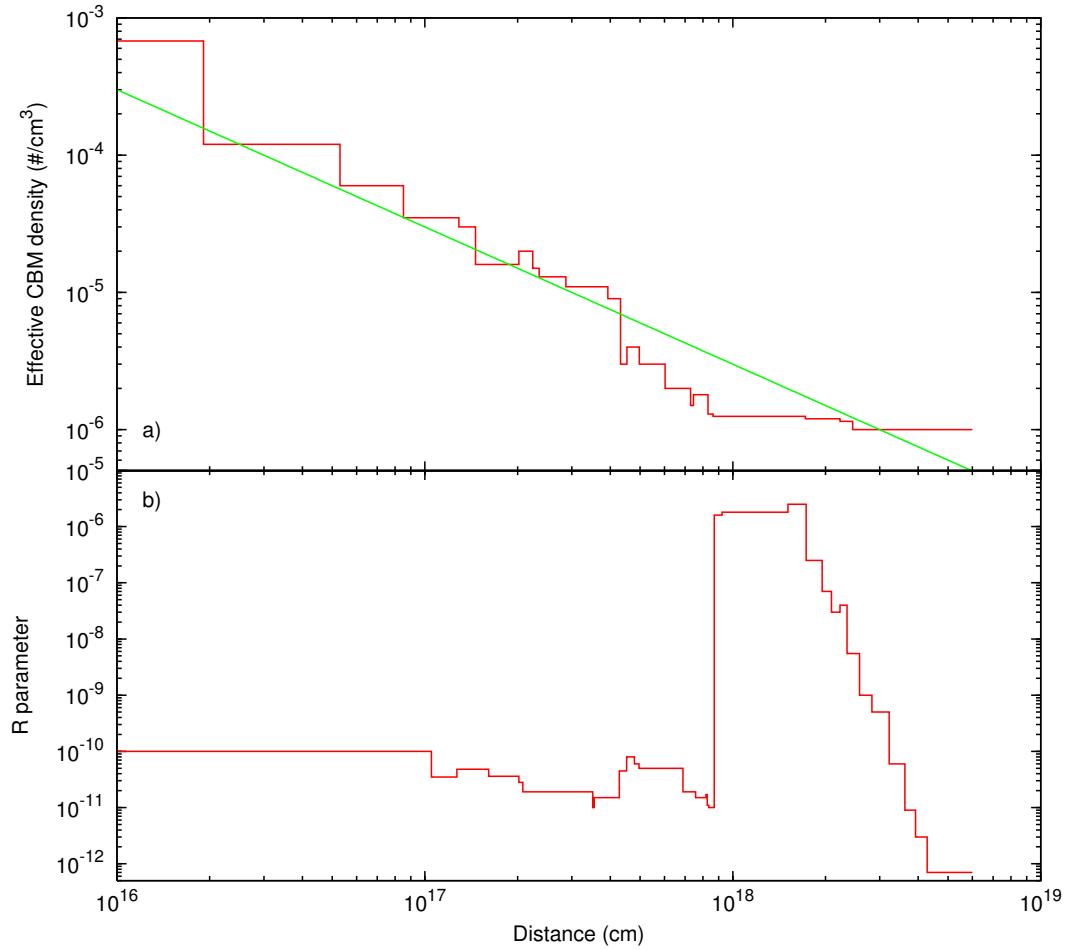


**Figure C.25.:** The CBM distribution parameters: a) the effective CBM number density (red line) monotonically decreases with the distance  $r$  following Eq.(C.7.1) (green line); b) the  $\mathcal{R}$  parameter vs. distance.

#### C.7.4. Binaries as progenitors of GRB-SN systems

The majority of the existing models in the literature appeal to a single astrophysical phenomenon to explain both the GRB and the SN (“collapsar”, see e.g. Woosley and Bloom, 2006). On the contrary, a distinguishing feature of our theoretical approach is to differentiate between the SN and the GRB process. The GRB is assumed to occur during the formation process of a black hole. The SN is assumed to lead to the formation of a neutron star (NS) or to a complete disruptive explosion without remnants and, in no way, to the formation of a black hole. In the case of SN2006aj the formation of such a NS has been actually inferred by Maeda et al. (2007) because of the large amount of  $^{58}\text{Ni}$  ( $0.05M_{\odot}$ ). Moreover the significantly small initial mass of the SN progenitor star  $M \approx 20M_{\odot}$  is expected to form a NS rather than a black hole when its core collapses (Maeda et al., 2007; Ferrero et al., 2007; Mazzali et al., 2006; Nomoto et al., 2007). In order to fulfill both the above requirement, we assume that the progenitor of the GRB and the SN consists of a binary system formed by a NS close to its critical mass collapsing to a black hole, and a companion star evolved out of the main sequence originating the SN. The temporal coincidence between the GRB and the SN phenomenon is explained in term of the concept of “induced” gravitational collapse (Ruffini et al., 2001a, 2007b). There is also the distinct possibility of observing the young born NS out of the SN (see e.g. Ruffini et al., 2007b, and references therein).

It has been often proposed that GRBs associated with SNe Ib/c, at smaller redshift  $0.0085 < z < 0.168$  (see e.g. Della Valle, 2006, and references therein), form a different class, less luminous and possibly much more numerous than the high luminosity GRBs at higher redshift (Pian et al., 2006; Soderberg et al., 2004; Maeda et al., 2007; Della Valle, 2006). Therefore they have been proposed to originate from a separate class of progenitors (Liang et al., 2007; Cobb et al., 2006). In our model this is explained by the nature of the progenitor system leading to the formation of the black hole with the smallest possible mass: the one formed by the collapse of a just overcritical NS (Ruffini et al., 2008b, 2007b).

The recent observation of GRB 060614 at  $z = 0.125$  without an associated SN (Della Valle et al., 2006; Mangano et al., 2007) gives strong support to our scenario, alternative to the collapsar model. Also in this case the progenitor of the GRB appears to be a binary system composed of two NSs or a NS and a white dwarf.

#### C.7.5. Conclusions

GRB 060218 presents a variety of peculiarities, including its extremely large  $T_{90}$  and its classification as an XRF. Nevertheless, a crucial point of our analysis is that we have successfully applied to this source our “canonical GRB” scenario.

Within our model there is no need for inserting GRB 060218 in a new class of GRBs, such as the XRFs, alternative to the “canonical” ones. This same point recently received strong observational support in the case of GRB 060218 (Liang et al., 2006b) and a consensus by other models in the literature (Kaneko et al., 2007).

The anomalously long  $T_{90}$  led us to infer a monotonic decrease in the CBM effective density giving the first clear evidence for a fragmentation in the fireshell. This phenomenon appears to be essential in understanding the features of also other GRBs (see e.g. GRB 050315 in Ruffini et al., 2007b; Bernardini et al., 2007).

Our “canonical GRB” scenario originates from the gravitational collapse to a black hole and is now confirmed over a  $10^6$  range in energy (see e.g. Ruffini et al., 2007a, and references therein). It is clear that, although the process of gravitational collapse is unique, there is a large variety of progenitors which may lead to the formation of black holes, each one with precise signatures in the energetics. The low energetics of the class of GRBs associated with SNe, and the necessity of the occurrence of the SN, naturally leads in our model to identify their progenitors with the formation of the smallest possible black hole originating from a NS overcoming his critical mass in a binary system. For GRB 060218 there is no need within our model for a new or unidentified source such as a magnetar or a collapsar.

GRB 060218 is the first GRB associated with SN with complete coverage of data from the onset all the way up to  $\sim 10^6$  s. This fact offers an unprecedented opportunity to verify theoretical models on such a GRB class. For example, GRB 060218 fulfills the Amati et al. (2002) relation unlike other sources in its same class. **This is particularly significant, since GRB 060218 is the only source in such a class to have an excellent data coverage without gaps. We are currently examining if the missing data in the other sources of such a class may have a prominent role in their non-fulfillment of the Amati et al. (2002) relation (Dainotti et al., in preparation; see also Ghisellini et al., 2006).**

## C.8. Application to GRB060607A: prompt emission, X-ray flares and late afterglow phase.

GRB060607A is a very distant ( $z = 3.082$ , Ledoux et al., 2006) and energetic event ( $E_{iso} \sim 10^{53}$  erg, Molinari et al., 2007). Its BAT light curve shows a double-peaked structure with a duration of  $T_{90} = (100 \pm 5)$  s (Tueller et al., 2006). The time-integrated spectrum over the  $T_{90}$  is best fit with a simple power-law model with an index  $\Gamma = 1.45 \pm 0.08$  (Guidorzi, private communication). The XRT light curve shows a prominent flaring activity (at least

two flares) superimposed to the normal afterglow decay (Page et al., 2006).

GRB060607A main peculiarity is that the peak of the near-infrared (NIR) afterglow has been observed with the REM robotic telescope (Molinari et al., 2007). Interpreting the NIR light curve as corresponding to the afterglow onset as predicted by the fireball forward shock model (Sari and Piran, 1999; Meszaros, 2006), it is possible to infer the initial Lorentz gamma factor of the emitting system that results to be  $\Gamma_0 \sim 400$  (Molinari et al., 2007; Covino et al., 2008; Jin and Fan, 2007). Moreover, these measurements seem to be consistent with an interstellar medium environment within the standard fireball scenario, ruling out the wind-like medium predicted by the Collapsar model (Molinari et al., 2007; Jin and Fan, 2007).

We analyze GRB060607A within the fireshell model (Ruffini et al., 2001c,b, 2007a). We deal only with the BAT and XRT observations, that are the basic contribution to the extended afterglow emission up to a distance from the progenitor  $r \sim 4 \times 10^{17}$  cm. Such observations are usually neglected in the treatments adopted in current literature to characterize the fireball dynamics (Molinari et al., 2007; Sari and Piran, 1999). The complete numerical modeling of the fireshell dynamics (see e.g. Ruffini et al., 2007a), from the creation of the initial plasma up to the interaction of the optically thin fireshell with the surrounding medium, allows to calculate all its characteristic quantities. In particular, the exact value of the Lorentz gamma factor of the fireshell at the transparency can be therefore calculated ( $\gamma_0 = 328$ ) once we fix the two free parameter from the gamma and X-ray light curves analysis.

According to the “canonical GRB” scenario (Ruffini et al., 2001b, 2007a) we interpret the whole prompt emission as the joint contribution of both the Proper-GRB (P-GRB), emitted at the fireshell transparency, and the peak of the extended afterglow, which follows the P-GRB emission. While the variability of the P-GRB is linked to the collapse mechanism of the progenitor (Caito et al., 2009), the observed temporal variability of the peak of the extended afterglow is shown to be produced by the interaction of the fireshell with CircumBurst Medium (CBM) clumps with density contrast  $\delta n/n \sim 2$ . The corresponding theoretical light curves obtained are in good agreement with the observations in all the *Swift* BAT energy bands.

We analyze the GRB060607A prompt emission time-integrated spectrum. The fireshell model postulates that the GRB spectrum is thermal in the comoving frame, and that the non-thermal power-law observed spectrum can be recovered by integrating over the EQuiTemporal Surfaces (EQTS, see Bianco and Ruffini, 2004, 2005b) and the observation time. The assumption of a pure thermal spectrum in the comoving frame has been chosen for simplicity as an *ansatz* on general thermal emission processes expected in high energy collisions. It can be subject to improvements when data on instantaneous spectra are available (Patricelli et al., in preparation). Indeed the resulting time-integrated spectrum is compatible with the one observed by BAT in different time intervals covering the whole prompt emission, despite a small discrep-

ancy at low energy.

We turn to the analysis of the X-ray flares observed by *Swift* XRT in the early part of the decaying phase of the X-ray afterglow (Page et al., 2006). According to the fireshell model these flares have the same nature than the peaks observed in the prompt emission, namely they are produced by the interaction of the fireshell with different CBM clumps. This idea is consistent with the correlation between the late peaks in the gamma-ray light curve and the X-ray flares when they are observed simultaneously (Molinari et al., 2007; Ziaeeepour et al., 2008). What is peculiar in the late afterglow phases is that the typical dimensions of the clumps become smaller than the visible area of the fireshell. Under this condition, a three dimensional description would be necessary to substitute the assumption of spherical symmetry and to take into due account the structure of the clumps. We propose here a simplified bi-dimensional model for the CBM clump along the line of sight, the emission being limited to a small fraction of the entire EQTS. We show that even with this simplified model it is possible to fully explain flares with  $\Delta t / t$  compatible with the observations.

The NIR emission shows no significant evidence for correlation with the prompt emission (Ziaeeepour et al., 2008): while the common gamma and X-ray flares light curves appear to be very close and correlate (Ziaeeepour et al., 2008), in the NIR band the flaring activity, if any, is much weaker (Molinari et al., 2007). On the contrary, when both the NIR and X-ray light curve are decaying regularly, these curves appear to be correlated (Molinari et al., 2007). We propose a possible scenario in which this second decaying phase arises from the injection of slower material into the fireshell. This leads to a collision which is assumed to be responsible for the X-ray plateau, producing a modification in the comoving thermal spectrum, as well as in the equations of the dynamics of the afterglow. This phase characterized by high level of instabilities may account for both the observed X-ray and NIR emission.

### C.8.1. GRB060607A prompt emission light curve

It is commonly believed that the observed temporal variability of the prompt emission and the X-ray flares are related to the activity of a “central engine” and originate from internal rather than external shocks (Sari and Piran, 1995; Daigne and Mochkovitch, 1998; Fenimore et al., 1999; Panaitescu and Mészáros, 1999; Liang et al., 2006a; Chincarini et al., 2007a). This interpretation claims that it can account for both the duration ( $\delta t / t \ll 1$ ) and the observed spectral properties of such a variability (Norris et al., 1996; Chincarini et al., 2007a; Falcone et al., 2007b). Indeed the internal shock model reveals some problems in the radiation mechanisms assumed for the gamma-ray emission: recently it has been pointed out that the synchrotron mechanisms apply successfully only for the late afterglow (Kumar and McMahon,

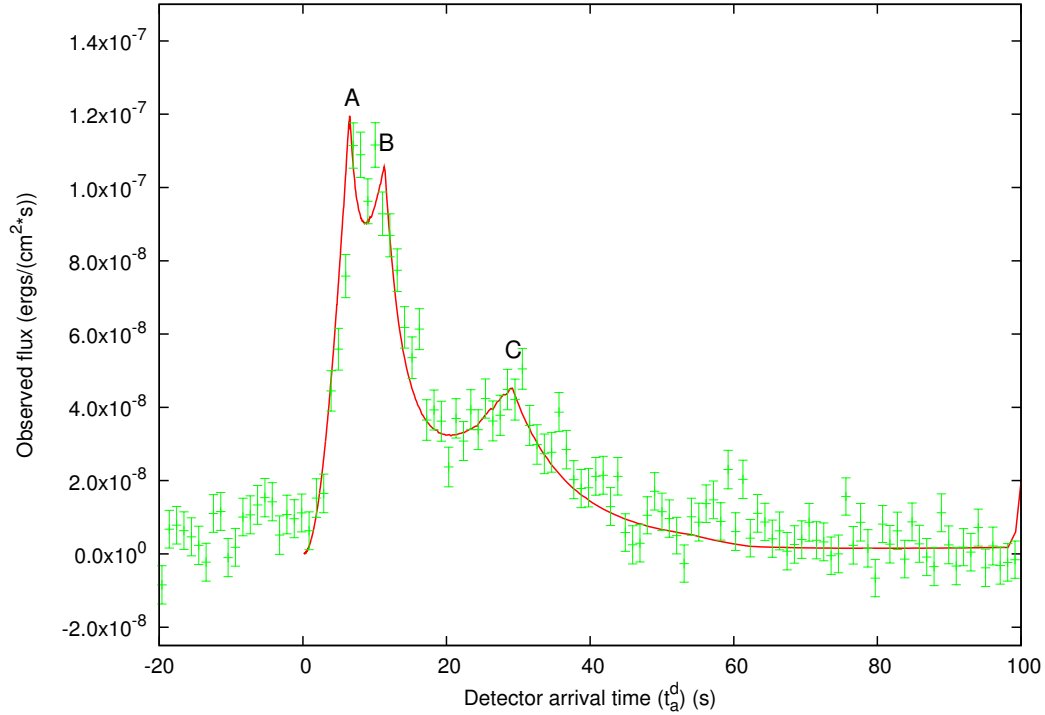


**Figure C.26.:** *Swift* BAT 15–150 keV light curve (green points) compared with the theoretical one (red line). The labels A, B, C identifies the three major peaks.

2008) and the inverse Compton scattering suffers of “energy crisis” (Piran et al., 2009).

Unlike treatments in the current literature, we recall that within the fireshell model the prompt emission consists of two sharply different components: the P-GRB and the peak of the extended afterglow (Ruffini et al., 2001b, 2007a). The variability of the P-GRB is linked to the collapse mechanism of the progenitor (Caito et al., 2009), while the observed temporal variability of the peak of the extended afterglow is described by the interaction of the fireshell with different CBM clumps (Ruffini et al., 2002).

We identify the whole prompt emission with the peak of the extended afterglow emission, and the remaining part of the light curve with the decaying tail of the afterglow, according to our “canonical GRB” scenario (Ruffini et al., 2001b, 2007a). The temporal variability of the light curve has been reproduced assuming spherical CBM regions with different densities (Ruffini et al., 2002). The structure of the CBM adopted is presented in Fig. C.27. This distribution of the CBM is just an approximation of the real one, where the CBM density shows some smooth fluctuations around its trend during the fireshell evolution. Nevertheless it is representative of the global properties of the medium and it is sufficient to account for the observed variability

in the luminosity. The decreasing trend of the CBM density up to very low values (see Fig. C.27) is not real but it is probably the result of the fragmentation occurring in the fireshell, as already proposed by Dainotti et al. (2007):  $n_{cbm} = n_{cbm}^{\circ} (r^*/r)^{\alpha}$ , with in this case  $\alpha \sim -2.5$ . The adopted density contrast with respect to the real CBM density  $n_{cbm}^{\circ}$  is  $\delta n/n \sim 2$  or less (see Fig. C.26).

For the two parameters characterizing the initial dynamics of the fireshell we adopt  $E_{tot}^{e^{\pm}} = 2.5 \times 10^{53}$  erg and  $B = 3.0 \times 10^{-3}$ . This choice is motivated by the requirement that the total energy of the system should account for the GRB isotropic emission up to the latest phase of the afterglow ( $E_{iso} = 1.1 \times 10^{53}$  erg, Tueller et al., 2006). The baryonic content of the fireshell ( $B$ ) determines how much kinetic energy should be dissipated during the afterglow that, we recall, in the fireshell model encompasses the prompt emission as well. Then, it is involved in the determination of the total energy emitted in the P-GRB and in the afterglow, in the determination of the overall duration of the phenomenon and in the occurrence of the peak of the afterglow emission (see Sec. 6). The baryon loading adopted for this GRB is fixed by the requirement that the P-GRB is under the BAT threshold: the total isotropic energy emitted in the P-GRB is expected to be  $E_{P-GRB}^{iso} = 1.9\% E_{tot}^{e^{\pm}} = 4.7 \times 10^{51}$  erg, hence it is below the BAT threshold if we assume an observed duration  $\Delta t_{p-grb} \gtrsim 10$  s. Therefore this is the minimum  $B$  acceptable. Larger values of  $B$  would result in an afterglow peak emission with a much slower rise time than the observed one. In Fig. C.26 we present a simulation of the light curve of GRB060607A in the *Swift* BAT (15–150 keV) energy band obtained with this choice of the parameters.

The initial conditions adopted for the optically thick fireshell ( $E_{tot}^{e^{\pm}}$  and  $B$ ) estimated from the simultaneous analysis of the BAT and XRT light curves imply an initial number of  $e^{\pm}$  pairs  $N_{e^{\pm}} = 2.6 \times 10^{58}$  and an initial temperature  $T = 1.7$  MeV. After the transparency point at  $r_{\circ} = 1.4 \times 10^{14}$  cm from the progenitor, the initial Lorentz gamma factor of the fireshell is  $\gamma_{\circ} = 328$ . This value confirms that the fireshell is highly relativistic, as expected to avoid the “compactness problem” (Piran, 2005). The Lorentz factor at the transparency  $\gamma_{\circ}$  is an exact value calculated by solving numerically the equation of motion of the fireshell. In particular this is the maximum value of  $\gamma_{\circ}$  since it has been obtained with the minimum baryon loading acceptable for this GRB (see sec. 6 and e.g. Ruffini et al., 2008a). The value of 400 that has been claimed in the literature within the fireball forward shock model (Molinari et al., 2007; Covino et al., 2008; Jin and Fan, 2007) cannot be reached by the fireshell, otherwise the P-GRB would be visible.

### C.8.2. GRB spectrum

We turn now to the analysis of the GRB060607A prompt emission time-integrated spectrum. As discussed in previous works (Ruffini et al., 2004b, 2005c; Bernar-

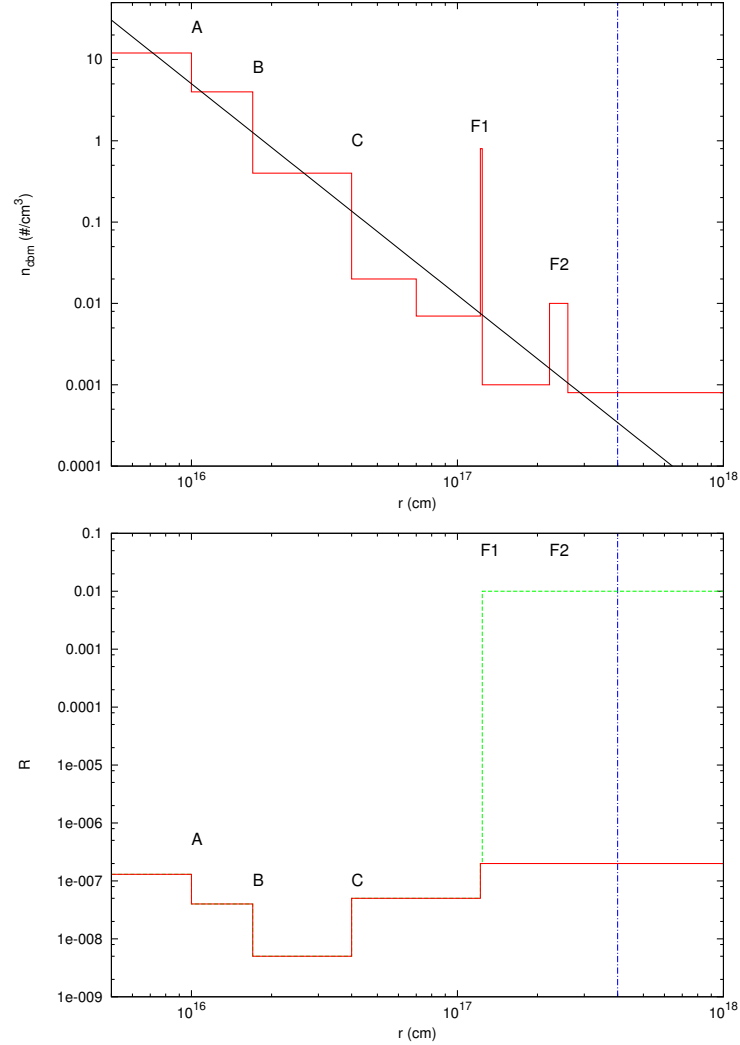


**Figure C.27.:** Structure of the CBM adopted: effective particle number density  $n_{cbm}$  (upper panel) and fraction of effective emitting area  $\mathcal{R}$  (lower panel) versus distance from the progenitor. The labels A, B, C indicate the values corresponding to the peaks in the BAT light curve (see Fig. C.26). The black solid line represents the decreasing trend of the CBM density that probably reflects a fragmentation in the fireshell. The two X-ray flares, indicated by the labels F1, F2, corresponds in the upper panel to the huge increase in the CBM density that departs from the roughly power-law decrease observed. In the lower panel, the X-ray flares produce an increase of the emitting area which is not real but due to the lack of a complete three-dimensional treatment of the interaction between the fireshell and the CBM (green dashed line). In fact if we adopt a bi-dimensional structure for the CBM clumps responsible for the flares we obtain a constant value (red solid line, see Sec. C.8.3). The blue vertical dashed-dotted line sets the limit of our analysis (for details see Sec. C.8.4).

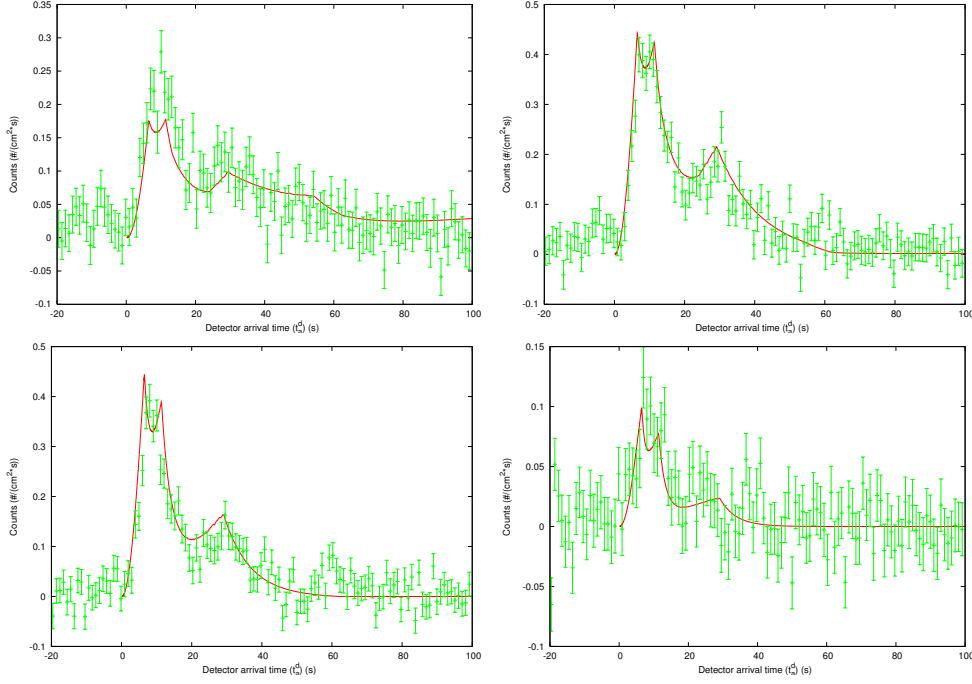


**Figure C.28.:** *Swift* BAT (15–25 keV, 25–50 keV, 50–100 keV, 100–150 keV) light curves (green points) compared with the theoretical ones (red lines).

dini et al., 2005a), the fireshell model postulates that:

- the resulting radiation as viewed in the comoving frame has a thermal spectrum
- the CBM swept up by the front of the optically thin fireshell is responsible for this thermal emission.

In our case the radiation is produced in the inelastic collision between the accelerated baryons and the CBM. The structure of the collision is determined by mass, momentum and energy conservation, i.e. by the constancy of the specific enthalpy, which are standard conditions in the expanding matter rest frame (Zeldovich and Raizer, 1966). The only additional free parameter to model this emission process is the size of the “effective emitting area” of the fireshell:  $A_{eff}$ .

The power emitted in the interaction of the fireshell with the CBM measured in the comoving frame is:

$$\frac{dE_{int}}{dt} = 4\pi r^2 \mathcal{R} \sigma T^4, \quad (C.8.1)$$

where  $dE_{\text{int}}$  is the internal energy developed in the collision,  $T$  is the black body temperature,  $\sigma$  is the Stefan-Boltzmann constant and

$$\mathcal{R} = \frac{A_{\text{eff}}}{A_{\text{tot}}} \quad (\text{C.8.2})$$

is the “surface filling factor” which accounts for the fraction of the shell surface becoming active, being the ratio between the “effective emitting area” and the total area  $A_{\text{tot}}$ . The ratio  $\mathcal{R}$  is a priori a function that varies as the system evolves so it is evaluated at every given value of the radius  $r$  (for the variability of  $\mathcal{R}$  in the case of GRB060607A see Fig. C.27).

We are now ready to calculate the source luminosity in a given energy band (Ruffini et al., 2004b). The source luminosity at a detector arrival time  $t_a^d$ , per unit solid angle  $d\Omega$  and in the energy band  $[\nu_1, \nu_2]$  is given by:

$$\frac{dE^{[\nu_1, \nu_2]}}{dt_a^d d\Omega} = \int_{\text{EQTS}} \frac{\Delta\varepsilon}{4\pi} v \cos\vartheta \Lambda^4 \frac{dt}{dt_a^d} W(\nu_1, \nu_2, T_{\text{arr}}) d\Sigma, \quad (\text{C.8.3})$$

where  $\Delta\varepsilon = \Delta E_{\text{int}}/V$  is the energy density released in the comoving frame assuming, for simplicity, that all the shell is emitting,  $\Lambda = 1/(\gamma(1 - (v/c) \cos\vartheta))$  is the Doppler factor,  $d\Sigma$  is the surface element of the EQTS at detector arrival time  $t_a^d$  on which the integration is performed and  $T_{\text{arr}}$  is the observed temperature of the radiation emitted from  $d\Sigma$ :

$$T_{\text{arr}} = \frac{\Lambda T}{(1+z)}. \quad (\text{C.8.4})$$

The “effective weight”  $W(\nu_1, \nu_2, T_{\text{arr}})$  is given by the ratio of the integral over the given energy band of a Planckian distribution at a temperature  $T_{\text{arr}}$  to the total integral  $aT_{\text{arr}}^4$  (Ruffini et al., 2004b):

$$W(\nu_1, \nu_2, T_{\text{arr}}) = \frac{\frac{2}{h^2 c^3} \int_{\nu_1}^{\nu_2} \frac{(h\nu)^3}{\exp^{h\nu/(kT_{\text{arr}})} - 1} d\nu}{aT_{\text{arr}}^4}. \quad (\text{C.8.5})$$

Fig. C.28 shows the simulations performed with the parameters derived in Sec. C.8.1 and with a variable surface filling factor  $\mathcal{R}$  as in Fig. C.27: they match quite well the observed prompt emission light curves of GRB060607A in all the BAT sub-energy bands, with just a small discrepancy in the first few seconds in the lowest channel (15 – 25 keV).

Once we have the luminosity in a given energy band in the same way we can obtain the instantaneous and the time-integrated photon number spectrum. It is clear from Eq. C.8.3 that each single instantaneous spectrum is the result of a convolution of thermal spectra since photons observed at the same arrival time are emitted at different comoving time, hence with dif-

ferent temperatures. This calculation produces a non-thermal instantaneous spectrum in the observer frame. This effect is enhanced if we calculate the time-integrated spectrum: we perform two different integrations, one on the observation time and one on the EQTSs, and what we get is a non-thermal spectrum that is comparable with the one observed by BAT in different time intervals covering the whole prompt emission (see Fig. C.29).

It is clear that this description attempts to identify the leading process of the GRB spectrum, and more details will be needed as soon as instantaneous spectra will become available. It is also clear that, in case of GRBs with Lorentz gamma factor well above the ones considered in the present source ( $\gamma_0 > 10^3$ ), additional high energy processes have to be considered, eventually including hadronic interactions.

### C.8.3. The X-ray flares

The last step to the understanding of the prompt emission of GRB060607A is the analysis of the X-ray flares observed by *Swift* XRT (0.3 – 10 keV) in the early part of the decaying phase of the afterglow. As already mentioned, in the current literature this emission is associated to the prompt emission due to their temporal and spectral behavior (Burrows et al., 2005b; Falcone et al., 2006; Zhang et al., 2006; Chincarini et al., 2007a; Falcone et al., 2007b). Even GRB060607A reveals a close correlation between the light curve observed by BAT and the X-ray flares observed by XRT (Ziaeeepour et al., 2008).

Accordingly with these observations, the fireshell model predicts that these flares have the same origin of the prompt emission, namely they are produced by the interaction of the fireshell with overdense CBM, and their appearance in the X-ray energy band depends on the hard-to-soft evolution of the GRB spectrum. Initially, the result obtained is not compatible with the observations (we choose as an example the second flare labeled as F2, see Fig. C.30, upper panel). This discrepancy is due to the simple “radial approximation” adopted, namely the CBM inhomogeneities are assumed to be in spherical shells (Ruffini et al., 2002). Clearly this approximation fails when the visible area of the fireshell is comparable with the size of the CBM clump. This is indeed the case of the X-ray flares, since at those times the fireshell visible area (defined by the condition  $\cos \theta \geq v/c$ , where  $\theta$  is the angle between the emitted photon and the line of sight, and  $v$  is the fireshell velocity) is much larger than during the prompt phase (for F2 see Fig. C.30, lower panel).

Following the results obtained for GRB011121 (Caito et al., 2008), we simulated the flare F2 light curve assuming a bi-dimensional structure of the CBM clump along the line of sight. We integrate over the emitting surface only up to a certain angle  $\theta_c$  from the line of sight, corresponding to the transverse dimension of the CBM clump which in this case results  $d_c = 2r_c \sin \theta_c \sim 10^{15}$  cm  $\sim 0.5 d_f$ , where  $d_c$  and  $d_f$  are respectively the CBM clump and the fireshell

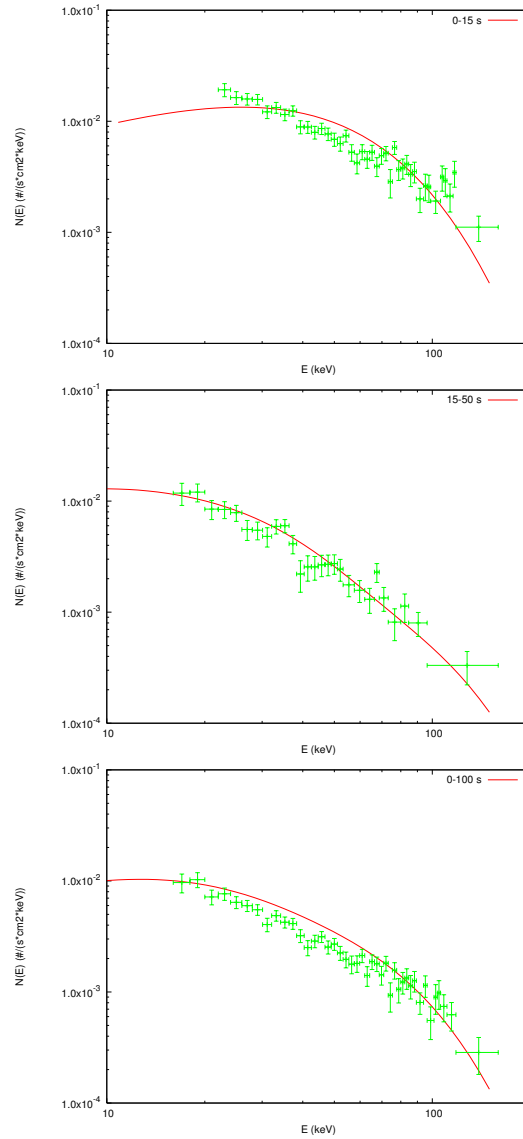


**Figure C.29.:** Theoretically predicted time-integrated photon number spectrum  $N(E)$  corresponding to the 0 – 15 s (upper panel), 15 – 50 s (middle panel), and to the whole duration ( $T_{90} = 100$  s, lower panel) of the prompt emission (solid lines) compared with the observed spectra integrated in the same intervals.

transverse dimensions, and  $r_c$  is the distance of the clump from the source. We obtain in this way a flare whose duration  $\Delta t/t$  is compatible with the observation (see Fig. C.30, middle panel). In general, we expect that the ratio  $\Delta t/t$  would be approximately constant for flares occurring at different times (as observationally found Chincarini et al., 2010) if the corresponding CBM clumps have similar size. This is due to the decrease of the Lorentz gamma factor of the fireshell.

It is worth to observe that with this procedure the value of  $\mathcal{R}$  remains constant during the flare (see Fig. C.27, lower panel, red solid line). Hence the increase in  $\mathcal{R}$  that we obtained in our previous analysis (see Fig. C.27, lower panel, green dashed line) was only a compensation for the failure of the radial approximation.

At this preliminary stage this procedure does not affect the dynamics of the fireshell in the proper way since the “cut” at  $\theta_c$  is performed only on the emitted flux, but the fireshell is supposed to interact still with a spherical CBM shell. Nevertheless, it is a confirmation that it is possible to obtain arbitrarily short flares when a fully three dimensional code for the CBM is implemented.

#### C.8.4. The decaying afterglow regime

The NIR emission shows no significant evidence for correlation with the prompt emission (Ziaeeepour et al., 2008): while the common gamma and X-ray light curves appear to be very close and correlate (Ziaeeepour et al., 2008), in the NIR band the flaring activity, if any, is much weaker (Molinari et al., 2007). Even if in GRB060607A it is not possible to perform a comparison between the NIR light curve and the X-ray one after the plateau phase (Molinari et al., 2007), generally they show similar trends (see e.g. Rykoff et al., 2009).

We propose a possible scenario in which the plateau phase and the following decaying phase of the X-ray afterglow originate from a delayed emission produced by a “second component” of the fireshell. This component can be identified with the trailing edge of the matter distribution inside the fireshell (see Sec. 6) that, being slower than the main shell, engulfs it at later times. We tried to analyze the dynamics of this second shell and we found that its Lorentz factor is correlated with the one of the fireshell at the moment of transparency, thus confirming that the second shell is not erratic, emitted in a distinct episode of the engine activity, but it is intertwined with the main fireshell until the transparency (Bernardini et al., 2010).

We expect that during the collision a turbulent regime onsets and the description of the fireshell dynamics presented in Sec. 6 does not hold anymore. Therefore we limit our analysis to the onset of the plateau, which in the case of GRB060607A occurs at a radius  $r_{on} \sim 4.0 \times 10^{17}$  cm (see Fig. C.27). The existence of these collisions implies that the subsequent expansion of the fireshell

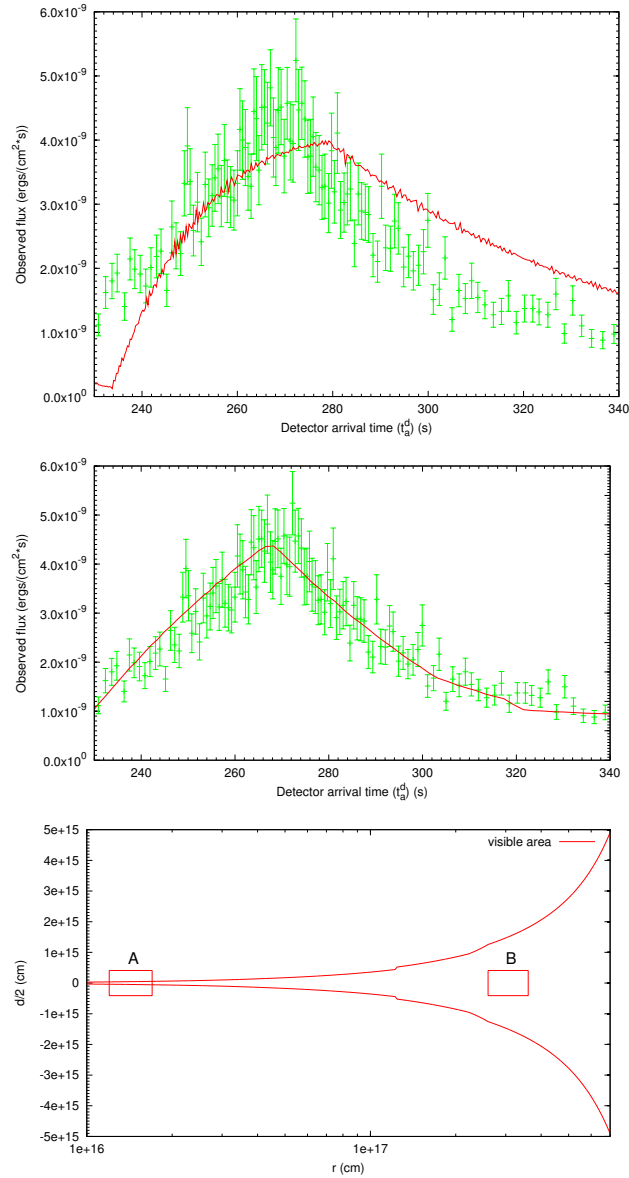


**Figure C.30.:** Upper panel: *Swift* XRT (0.3–10 keV) light curve of flare F2 compared with the theoretical one obtained under the “radial approximation” assumption (red line). Middle panel: *Swift* XRT (0.3–10 keV) light curve of flare F2 compared with the theoretical one obtained imposing a finite transverse dimension for the CBM clump (red line). Lower panel: the boundaries of the fireshell visible area ( $\cos \theta = v/c$ ) compared with the dimensions of two CBM clumps corresponding to the first spike of the prompt emission (A) and of the flare (B). It is manifest how similar clumps produce different observational results depending on the evolution of the fireshell visible area (see text).

will not follow a ballistic description. Therefore, any inference on the nature of the emitting process based on a ballistic picture of the expanding shell and power-law extrapolations will be necessarily incorrect.

### C.8.5. Conclusions

The “canonical GRB” scenario (Ruffini et al., 2001b, 2007a) implies that the GRB prompt emission is formed by two different components: the P-GRB and the peak of the extended afterglow. Therefore the analysis of the prompt emission light curve and spectrum is necessary and sufficient in order to fix the initial parameters which characterize the dynamics of the fireshell both in the optically thick and in the optically thin regimes through the equations of motion that we explicitly derived. This is one major difference between our approach and the ones in the current literature, where emphasis is usually given to the latest parts of the GRB emission (Optical, NIR) and the dynamics of the early phases is just extrapolated backwards by power-laws (Molinari et al., 2007; Sari and Piran, 1999).

In this paper we explicitly show in the case of GRB060607A how the analysis of the prompt emission spectra and luminosities in different energy bands allows to determine the total energy of the electron positron pairs  $E_{tot}^{e^{\pm}} = 2.5 \times 10^{53}$  erg. The engine powering the GRB is the gravitational collapse to a black hole and from our analysis this energetics points to a binary neutron star merger as the progenitor (Ruffini et al., 2009; Cherubini et al., 2009; Caito et al., 2009). The complete numerical modeling of the fireshell dynamics allows to calculate also the value of its Lorentz gamma factor at the transparency:  $\gamma_o = 328$ .

According to the fireshell model the X-ray flares have the same nature than the peaks observed in the prompt emission, namely they are produced by the interaction of the fireshell with different CBM clumps. What is peculiar in the late afterglow phases is that the typical dimensions of the clumps become smaller than the visible area of the fireshell. Under these conditions, we propose a bi-dimensional model for the CBM clump along the line of sight, the emission being limited to a small fraction of the entire EQTS, to substitute the assumption of spherical symmetry and to take into due account the structure of the clumps. We show that in this condition it is possible to obtain flares with  $\Delta t/t_{tot}$  compatible with the observations. In order to fully describe all the X-ray flares properties a three dimensional description will be necessary.

We stop our analysis at the starting of the X-ray plateau. We propose a possible scenario in which this phase arises from the injection of slower material into the fireshell. This phase is characterized by high level of instabilities and may account for both the observed X-ray and NIR emission. Clearly its dynamics does not follow a simple ballistic law. Therefore, any backward extrapolation based on power-law equations of motion approximating a bal-

listic dynamics may lead to unphysical results.



# Bibliography

ABDO, A.A., ACKERMANN, M., AJELLO, M., ASANO, K., ATWOOD, W.B., AXELSSON, M., BALDINI, L., BALLEST, J., BARBIELLINI, G., BARING, M.G. ET AL.

«Fermi Observations of GRB 090902B: A Distinct Spectral Component in the Prompt and Delayed Emission».

*ApJ*, **706**, pp. L138–L144 (2009a).

ABDO, A.A., ACKERMANN, M., ARIMOTO, M., ASANO, K., ATWOOD, W.B., AXELSSON, M., BALDINI, L., BALLEST, J., BAND, D.L., BARBIELLINI, G. ET AL.

«Fermi Observations of High-Energy Gamma-Ray Emission from GRB 080916C».

*Science*, **323**, p. 1688 (2009b).

AKSENOV, A., RUFFINI, R. AND VERESHCHAGIN, G.

«Thermalization of nonequilibrium electron-positron-photon plasmas».

*Phys. Rev. Lett.*, **99(12)**, p. 125003 (2007).

AKSENOV, A., RUFFINI, R. AND VERESHCHAGIN, G.

*submitted to Phys. Rev. D* (2008).

AKSENOV, A.G., RUFFINI, R. AND VERESHCHAGIN, G.V.

«Thermalization of the mildly relativistic plasma».

*Phys. Rev. D*, **79(4)**, p. 043008 (2009).

AMATI, L.

«The  $e_{p,i}$ - $e_{iso}$  correlation in gamma-ray bursts: updated observational status, re-analysis and main implications».

*MNRAS*, **372**, pp. 233–245 (2006).

AMATI, L.

talk presented at the congress “10<sup>th</sup> Italian-Korean Meeting”, Pescara, Italy, June 25-29 (2007).

AMATI, L.

«The  $E_{p,i}$  -  $E_{iso}$  correlation and Fermi Gamma-Ray Bursts».

*ArXiv:1002.2232* (2010).

- AMATI, L., DELLA VALLE, M., FRONTERA, F., MALESANI, D., GUIDORZI, C., MONTANARI, E. AND PIAN, E.  
«On the consistency of peculiar grbs 060218 and 060614 with the  $e_{p,i} - e_{iso}$  correlation».  
*A&A*, **463**, pp. 913–919 (2007).
- AMATI, L., FRONTERA, F. AND GUIDORZI, C.  
«Extremely energetic Fermi gamma-ray bursts obey spectral energy correlations».  
*A&A*, **508**, pp. 173–180 (2009).
- AMATI, L., FRONTERA, F., TAVANI, M., IN'T ZAND, J.J.M., ANTONELLI, A., COSTA, E., FEROCI, M., GUIDORZI, C., HEISE, J., MASETTI, N. ET AL.  
«Intrinsic spectra and energetics of bepposax gamma-ray bursts with known redshifts».  
*A&A*, **390**, pp. 81–89 (2002).
- AMATI, L., GUIDORZI, C., FRONTERA, F., DELLA VALLE, M., FINELLI, F., LANDI, R. AND MONTANARI, E.  
«Measuring the cosmological parameters with the  $E_{p,i} - E_{iso}$  correlation of gamma-ray bursts».  
*MNRAS*, **391**, pp. 577–584 (2008).
- ANTONELLI, L.A., D'AVANZO, P., PERNA, R., AMATI, L., COVINO, S., CUTINI, S., D'ELIA, V., GALLOZZI, S., GRAZIAN, A., PALAZZI, E. ET AL.  
«GRB 090426: the farthest short gamma-ray burst?»  
*A&A*, **507**, pp. L45–L48 (2009).
- ARNETT, W.D. AND MEAKIN, C.  
«Toward Realistic Progenitors of Core-collapse Supernovae».  
*ApJ*, **733**, p. 78 (2011).
- ATWOOD, W.B., ABDO, A.A., ACKERMANN, M., ALTHOUSE, W., ANDERSON, B., AXELSSON, M., BALDINI, L., BALLEST, J., BAND, D.L., BARBIELLINI, G. ET AL.  
«The Large Area Telescope on the Fermi Gamma-Ray Space Telescope Mission».  
*ApJ*, **697**, pp. 1071–1102 (2009).
- BAND, D., MATTESON, J., FORD, L., SCHAEFER, B., PALMER, D., TEEGARDEN, B., CLINE, T., BRIGGS, M., PACIESAS, W., PENDLETON, G. ET AL.  
«Batse observations of gamma-ray burst spectra. i - spectral diversity».  
*ApJ*, **413**, pp. 281–292 (1993).
- BARBIER, L., BARTHELMEY, S., CUMMINGS, J., CUSUMANO, G., FENIMORE, E., GEHRELS, N., HULLINGER, D., KRIMM, H., MARKWARDT, C., PALMER, D. ET AL.

- «Preliminary refined analysis of the swift-bat trigger 191157.»  
*GCN Circ.*, **4780** (2006).
- BARTHELMY, S.D.  
«Burst alert telescope (bat) on the swift midex mission».  
In K.A. Flanagan and O.H.W. Siegmund (eds.), *X-Ray and Gamma-Ray Instrumentation for Astronomy XIII.*, volume 5165 of *Society of Photo-Optical Instrumentation Engineers (SPIE) Conference Proceedings*, pp. 175–189 (2004).
- BARTHELMY, S.D., BARBIER, L.M., CUMMINGS, J.R., FENIMORE, E.E., GEHRELS, N., HULLINGER, D., KRIMM, H.A., MARKWARDT, C.B., PALMER, D.M., PARSONS, A. ET AL.  
«The burst alert telescope (bat) on the swift midex mission».  
*Space Science Reviews*, **120**, pp. 143–164 (2005a).
- BARTHELMY, S.D., CHINCARINI, G., BURROWS, D.N., GEHRELS, N., COVINO, S., MORETTI, A., ROMANO, P., O'BRIEN, P.T., SARAZIN, C.L., KOUVELIOTOU, C. ET AL.  
«An origin for short  $\gamma$ -ray bursts unassociated with current star formation».  
*Nature*, **438**, pp. 994–996 (2005b).
- BECK, R.  
«Observations of Magnetic Fields in Galaxies».  
In E. M. de Gouveia dal Pino, G. Lugones, & A. Lazarian (ed.), *Magnetic Fields in the Universe: From Laboratory and Stars to Primordial Structures.*, volume 784 of *American Institute of Physics Conference Series*, pp. 343–353 (2005).
- BELCZYNSKI, K., PERNA, R., BULIK, T., KALOGERA, V., IVANOVA, N. AND LAMB, D.Q.  
«A Study of Compact Object Mergers as Short Gamma-Ray Burst Progenitors».  
*ApJ*, **648**, pp. 1110–1116 (2006).
- BERGER, E.  
«The Host Galaxies of Short-Duration Gamma-Ray Bursts: Luminosities, Metallicities, and Star Formation Rates».  
*ApJ*, **690**, pp. 231–237 (2009).
- BERGER, E.  
«The Environments of Short-Duration Gamma-Ray Bursts and Implications for their Progenitors».  
*ArXiv:1005.1068* (2010).
- BERGER, E.  
«The environments of short-duration gamma-ray bursts and implications for their progenitors».

- New. Astron. Rev.*, **55**, pp. 1–22 (2011).
- BERGER, E., SHIN, M.S., MULCHAEY, J.S. AND JELTEMA, T.E.  
«Galaxy clusters associated with short grbs. i. the fields of grbs 050709, 050724, 050911, and 051221a».  
*ApJ*, **660**, pp. 496–503 (2007).
- BERNARDINI, M.G., BIANCO, C.L., CAITO, L., DAINOTTI, M.G., GUIDA, R. AND RUFFINI, R.  
«Grb 970228 and a class of grbs with an initial spikelike emission».  
*A&A*, **474**, pp. L13–L16 (2007).
- BERNARDINI, M.G., BIANCO, C.L., CAITO, L., DAINOTTI, M.G., GUIDA, R. AND RUFFINI, R.  
«Grb970228 and the class of grbs with an initial spikelike emission: do they follow the amati relation?»  
In C.L. Bianco and S.S. Xue (eds.), *Relativistic Astrophysics*, volume 966 of *American Institute of Physics Conference Series*, pp. 7–11 (2008).
- BERNARDINI, M.G., BIANCO, C.L., CAITO, L., IZZO, L., PATRICELLI, B. AND RUFFINI, R.  
«The end of the prompt emission within the fireshell model».  
In G. Chincarini, P. D’Avanzo, R. Margutti and R. Salvaterra (eds.), *The Shocking Universe*, volume 102 of *SIF Conference Proceedings*, p. 489 (2010).
- BERNARDINI, M.G., BIANCO, C.L., CHARDONNET, P., FRASCHETTI, F., RUFFINI, R. AND XUE, S.S.  
«A new astrophysical “trptych”: Grb030329/sn2003dh/urca-2».  
In E. Fenimore and M. Galassi (eds.), *Gamma-Ray Bursts: 30 Years of Discovery*, volume 727 of *American Institute of Physics Conference Series*, pp. 312–315 (2004).
- BERNARDINI, M.G., BIANCO, C.L., CHARDONNET, P., FRASCHETTI, F., RUFFINI, R. AND XUE, S.S.  
«Theoretical interpretation of the luminosity and spectral properties of grb 031203».  
*ApJ*, **634**, pp. L29–L32 (2005a).
- BERNARDINI, M.G., BIANCO, C.L., RUFFINI, R., XUE, S.S., CHARDONNET, P. AND FRASCHETTI, F.  
«General features of grb 030329 in the embh model».  
In M. Novello, S. Perez Bergliaffa and R. Ruffini (eds.), *The Tenth Marcel Grossmann Meeting. On recent developments in theoretical and experimental general relativity, gravitation and relativistic field theories*, p. 2459 (Singapore: World Scientific, 2005b).

- BERSIER, D., FRUCHTER, A., RHOADS, J., LEVAN, A. AND TANVIR, N.  
«Limits on a SN in the field of GRB 050509b.»  
*GCN Circ.*, **3521** (2005).
- BIANCO, C.L., BERNARDINI, M.G., CAITO, L., DAINOTTI, M.G., GUIDA, R.  
AND RUFFINI, R.  
«The “fireshell” model and the “canonical” grb scenario.»  
In C.L. Bianco and S.S. Xue (eds.), *Relativistic Astrophysics*, volume 966 of  
*American Institute of Physics Conference Series*, pp. 12–15 (2008a).
- BIANCO, C.L., BERNARDINI, M.G., CAITO, L., DAINOTTI, M.G., GUIDA, R.  
AND RUFFINI, R.  
«Short and canonical grbs».  
In M. Galassi, D. Palmer and E. Fenimore (eds.), *GAMMA-RAY BURSTS  
2007: Proceedings of the Santa Fe Conference*, volume 1000 of *American Insti-  
tute of Physics Conference Series*, pp. 305–308 (2008b).
- BIANCO, C.L., BERNARDINI, M.G., CAITO, L., DAINOTTI, M.G., GUIDA, R.  
AND RUFFINI, R.  
«The “fireshell” model and the “canonical GRB” scenario».  
In Y.F. Huang, Z.G. Dai and B. Zhang (eds.), *2008 Nanjing Gamma-Ray Burst  
Conference*, volume 1065 of *American Institute of Physics Conference Series*, pp.  
223–226 (2008c).
- BIANCO, C.L., CAITO, L. AND RUFFINI, R.  
«Theoretical interpretation of grb 011121».  
*Il Nuovo Cimento B*, **121**, p. 1441 (2006a).
- BIANCO, C.L. AND RUFFINI, R.  
«Exact versus approximate equitemporal surfaces in gamma-ray burst af-  
terglows».  
*ApJ*, **605**, pp. L1–L4 (2004).
- BIANCO, C.L. AND RUFFINI, R.  
«Exact versus approximate solutions in gamma-ray burst afterglows».  
*ApJ*, **633**, pp. L13–L16 (2005a).
- BIANCO, C.L. AND RUFFINI, R.  
«On the exact analytic expressions for the equitemporal surfaces in  
gamma-ray burst afterglows».  
*ApJ*, **620**, pp. L23–L26 (2005b).
- BIANCO, C.L. AND RUFFINI, R.  
«Exact versus approximate beaming formulae in gamma-ray burst after-  
glows».  
*ApJ*, **644**, pp. L105–L108 (2006).

- BIANCO, C.L., RUFFINI, R., VERESHCHAGIN, G. AND XUE, S.S.  
«Equations of motion and initial and boundary conditions for gamma-ray burst».  
*Journal of the Korean Physical Society*, **49**, p. 722 (2006b).
- BIANCO, C.L., RUFFINI, R. AND XUE, S.S.  
«The elementary spike produced by a pure  $e^+e^-$  pair-electromagnetic pulse from a black hole: The pem pulse».  
*A&A*, **368**, pp. 377–390 (2001).
- BISSALDI, E. AND CONNAUGHTON, V.  
«GRB 090902B: Fermi GBM detection of a bright burst.»  
*GRB Coordinates Network*, **9866**, pp. 1–+ (2009).
- BLANDFORD, R.D. AND MCKEE, C.F.  
«Fluid dynamics of relativistic blast waves».  
*Physics of Fluids*, **19**, pp. 1130–1138 (1976).
- BLINNIKOV, S.I., KOZYREVA, A.V. AND PANCHENKO, I.E.  
«Gamma-ray bursts: When does a blackbody spectrum look non-thermal?»  
*Astronomy Reports*, **43**, pp. 739–747 (1999).
- BLINNIKOV, S.I., NOVIKOV, I.D., PEREVODCHIKOVA, T.V. AND POLNAREV, A.G.  
«Exploding neutron stars in close binaries».  
*Soviet Astronomy Letters*, **10**, p. 177 (1984).
- BLOOM, J., BLAKE, C., PROCHASKA, J.X., HENNAWI, J., GLADDERS, M. AND KOESTER, B.  
«GRB 050509b: PAIRITEL and WIYN observations.»  
*GCN Circ.*, **3386** (2005a).
- BLOOM, J.S., DJORGOVSKI, S.G. AND KULKARNI, S.R.  
«The redshift and the ordinary host galaxy of grb 970228».  
*ApJ*, **554**, pp. 678–683 (2001).
- BLOOM, J.S., FOLEY, R.J., POOLEY, D., FILIPPENKO, A.V., CHORNOCK, R., BLAKE, C., PROCHASKA, J.X., HENNAWI, J., GLADDERS, M., KOESTER, B. ET AL.  
«GRB 050509b: Keck/Chandra cross-correlation.»  
*GCN Circ.*, **3417** (2005b).
- BLOOM, J.S., PROCHASKA, J.X., POOLEY, D., BLAKE, C.H., FOLEY, R.J., JHA, S., RAMIREZ-RUIZ, E., GRANOT, J., FILIPPENKO, A.V., SIGURDSSON, S. ET AL.

- «Closing in on a Short-Hard Burst Progenitor: Constraints from Early-Time Optical Imaging and Spectroscopy of a Possible Host Galaxy of GRB 050509b».  
*ApJ*, **638**, pp. 354–368 (2006).
- BOËR, M., ATTEIA, J.L., DAMERDJI, Y., GENDRE, B., KLOTZ, A. AND STRATTA, G.  
«Detection of a Very Bright Optical Flare from the Gamma-Ray Burst GRB 050904 at Redshift 6.29».  
*ApJ*, **638**, pp. L71–L74 (2006).
- BURLON, D., GHIRLANDA, G., GHISELLINI, G., LAZZATI, D., NAVA, L., NARDINI, M. AND CELOTTI, A.  
«Precursors in Swift Gamma Ray Bursts with Redshift».  
*ApJ*, **685**, pp. L19–L22 (2008).
- BURROWS, A. AND LATTIMER, J.M.  
«The birth of neutron stars».  
*ApJ*, **307**, pp. 178–196 (1986).
- BURROWS, D.N., HILL, J.E., NOUSEK, J.A., KENNEA, J.A., WELLS, A., OSBORNE, J.P., ABBEY, A.F., BEARDMORE, A., MUKERJEE, K., SHORT, A.D.T. ET AL.  
«The swift x-ray telescope».  
*Space Science Reviews*, **120**, pp. 165–195 (2005a).
- BURROWS, D.N., HILL, J.E., NOUSEK, J.A., WELLS, A.A., CHINCARINI, G., ABBEY, A.F., BEARDMORE, A.P., BOSWORTH, J., BRÄUNINGER, H.W., BURKERT, W. ET AL.  
«The swift x-ray telescope».  
In K.A. Flanagan and O.H.W. Siegmund (eds.), *X-Ray and Gamma-Ray Instrumentation for Astronomy XIII*, volume 5165 of *Society of Photo-Optical Instrumentation Engineers (SPIE) Conference Proceedings*, pp. 201–216 (2004).
- BURROWS, D.N., ROMANO, P., FALCONE, A., KOBAYASHI, S., ZHANG, B., MORETTI, A., O'BRIEN, P.T., GOAD, M.R., CAMPANA, S., PAGE, K.L. ET AL.  
«Bright x-ray flares in gamma-ray burst afterglows».  
*Science*, **309**, pp. 1833–1835 (2005b).
- CAITO, L., AMATI, L., BERNARDINI, M.G., BIANCO, C.L., DE BARROS, G., IZZO, L., PATRICELLI, B. AND RUFFINI, R.  
«GRB 071227: an additional case of a disguised short burst».  
*A&A*, **521**, p. A80 (2010).
- CAITO, L., BERNARDINI, M.G., BIANCO, C.L., DAINOTTI, M.G., GUIDA, R. AND RUFFINI, R.

- In R.T. Jantzen, H. Kleinert and R. Ruffini (eds.), *The Eleventh Marcel Grossmann Meeting*. (Singapore: World Scientific, 2008).
- CAITO, L., BERNARDINI, M.G., BIANCO, C.L., DAINOTTI, M.G., GUIDA, R. AND RUFFINI, R.  
«GRB060614: a “fake” short GRB from a merging binary system».  
*A&A*, **498**, pp. 501–507 (2009).
- CAMPANA, S., MANGANO, V., BLUSTIN, A.J., BROWN, P., BURROWS, D.N., CHINCARINI, G., CUMMINGS, J.R., CUSUMANO, G., DELLA VALLE, M., MALESANI, D. ET AL.  
«The association of grb 060218 with a supernova and the evolution of the shock wave».  
*Nature*, **442**, pp. 1008–1010 (2006a).
- CAMPANA, S., TAGLIAFERRI, G., LAZZATI, D., CHINCARINI, G., COVINO, S., PAGE, K., ROMANO, P., MORETTI, A., CUSUMANO, G., MANGANO, V. ET AL.  
«The x-ray afterglow of the short gamma ray burst 050724».  
*A&A*, **454**, pp. 113–117 (2006b).
- CANUTO, V.  
«Neutron stars».  
In R. Giacconi and R. Ruffini (eds.), *Physics and Astrophysics of Neutron Stars and Black Holes*, pp. 448–527 (1978).
- CASTRO-TIRADO, A.J., DE UGARTE POSTIGO, A., GOROSABEL, J., FATHKULLIN, T., SOKOLOV, V., BREMER, M., MÁRQUEZ, I., MARÍN, A.J., GUZIY, S., JELÍNEK, M. ET AL.  
«GRB 050509b: the elusive optical/nIR/mm afterglow of a short-duration GRB».  
*A&A*, **439**, pp. L15–L18 (2005).
- CENKO, S.B., SOIFER, B.T., BIAN, C., DESAI, V., KULKARNI, S.R., BERGER, E., DEY, A. AND JANNUZI, B.T.  
«GRB 050509b: further analysis of Keck LRIS images.»  
*GCN Circ.*, **3401** (2005).
- CHERUBINI, C., GERALICO, A., J. A. RUEDA, H. AND RUFFINI, R.  
« $e^-e^+$  pair creation by vacuum polarization around electromagnetic black holes».  
*Phys. Rev. D*, **79(12)**, p. 124002 (2009).
- CHIANG, J. AND DERMER, C.D.  
«Synchrotron and synchrotron self-compton emission and the blast-wave model of gamma-ray bursts».  
*ApJ*, **512**, pp. 699–710 (1999).

- CHINCARINI, G., MAO, J., MARGUTTI, R., BERNARDINI, M.G., GUIDORZI, C., PASOTTI, F., GIANNIOS, D., DELLA VALLE, M., MORETTI, A., ROMANO, P. ET AL.  
«Unveiling the origin of X-ray flares in gamma-ray bursts».  
*MNRAS*, **406**, pp. 2113–2148 (2010).
- CHINCARINI, G., MORETTI, A., ROMANO, P., FALCONE, A.D., MORRIS, D., RACUSIN, J., CAMPANA, S., COVINO, S., GUIDORZI, C., TAGLIAFERRI, G. ET AL.  
«The First Survey of X-Ray Flares from Gamma-Ray Bursts Observed by Swift: Temporal Properties and Morphology».  
*ApJ*, **671**, pp. 1903–1920 (2007a).
- CHINCARINI, G., MORETTI, A., ROMANO, P., FALCONE, A.D., MORRIS, D., RACUSIN, J., CAMPANA, S., GUIDORZI, C., TAGLIAFERRI, G., BURROWS, D.N. ET AL.  
«The first survey of x-ray flares from gamma ray bursts observed by swift: Temporal properties and morphology».  
*ArXiv:astro-ph/0702371* (2007b).
- COBB, B.E., BAILYN, C.D., VAN DOKKUM, P.G. AND NATARAJAN, P.  
«Sn 2006aj and the nature of low-luminosity gamma-ray bursts».  
*ApJ*, **645**, pp. L113–L116 (2006).
- COSTA, E., FRONTERA, F., HEISE, J., FEROCI, M., IN'T ZAND, J., FIORE, F., CINTI, M.N., DAL FIUME, D., NICASTRO, L., ORLANDINI, M. ET AL.  
«Discovery of an x-ray afterglow associated with the  $\gamma$ -ray burst of 28 february 1997».  
*Nature*, **387**, pp. 783–785 (1997).
- COVINO, S., VERGANI, S.D., MALESANI, D., MOLINARI, E., D'AVANZO, P., CHINCARINI, G., ZERBI, F.M., ANTONELLI, L.A., CONCONI, P., TESTA, V. ET AL.  
«The Afterglow Onset for GRB 060418 and GRB 060607A».  
*Chinese Journal of Astronomy and Astrophysics Supplement*, **8**, pp. 356–360 (2008).
- CRIDER, A., LIANG, E.P., SMITH, I.A., PREECE, R.D., BRIGGS, M.S., PENDLETON, G.N., PACIESAS, W.S., BAND, D.L. AND MATTESON, J.L.  
«Evolution of the low-energy photon spectral in gamma-ray bursts».  
*ApJ*, **479**, p. L39 (1997).
- CUMMINGS, J., ANGELINI, L., BARTHELMI, S., CUCCHIARA, A., GEHRELS, N., GRONWALL, C., HOLLAND, S.T., MANGANO, V., MARSHALL, F., PAGANI, C. ET AL.  
«GRB050904: Swift-BAT detection of a probable burst.»

- GCN *Circ.*, **3910**, pp. 1–+ (2005).
- CUSUMANO, G., BARTHELMY, S., GEHRELS, N., HUNSBERGER, S., IMMLER, S., MARSHALL, F., PALMER, D. AND SAKAMOTO, T.  
«Grb 060218: Swift-bat detection of a possible burst.»  
*GCN Circ.*, **4775** (2006).
- CUSUMANO, G., MANGANO, V., CHINCARINI, G., PANAITESCU, A., BURROWS, D.N., LA PAROLA, V., SAKAMOTO, T., CAMPANA, S., MINEO, T., TAGLIAFERRI, G. ET AL.  
«Swift observations of GRB 050904: the most distant cosmic explosion ever observed».  
*A&A*, **462**, pp. 73–80 (2007).
- DAI, Z.G. AND LU, T.  
«Gamma-ray burst afterglows and evolution of postburst fireballs with energy injection from strongly magnetic millisecond pulsars».  
*A&A*, **333**, pp. L87–L90 (1998).
- DAIGNE, F. AND MOCHKOVITCH, R.  
«Gamma-ray bursts from internal shocks in a relativistic wind: temporal and spectral properties».  
*MNRAS*, **296**, pp. 275–286 (1998).
- DAINOTTI, M.G., BERNARDINI, M.G., BIANCO, C.L., CAITO, L., GUIDA, R. AND RUFFINI, R.  
«Grb 060218 and grbs associated with supernovae ib/c».  
*A&A*, **471**, pp. L29–L32 (2007).
- DAMOUR, T. AND RUFFINI, R.  
«Quantum electrodynamical effects in kerr-newman geometries.»  
*Physical Review Letters*, **35**, pp. 463–466 (1975).
- D’AVANZO, P., MALESANI, D., COVINO, S., PIRANOMONTE, S., GRAZIAN, A., FUGAZZA, D., MARGUTTI, R., D’ELIA, V., ANTONELLI, L.A., CAMPANA, S. ET AL.  
«The optical afterglows and host galaxies of three short/hard gamma-ray bursts».  
*A&A*, **498**, pp. 711–721 (2009).
- DAVIES, M.B., LEVAN, A.J., LARSSON, J., KING, A.R. AND FRUCHTER, A.S.  
«Progenitors of long gamma-ray bursts».  
In M. Axelsson and F. Ryde (eds.), *Gamma-Ray Bursts: Prospects for GLAST*, volume 906 of *American Institute of Physics Conference Series*, pp. 69–78 (2007).

- DELLA VALLE, M.  
«Supernova and grb connection: Observations and questions».  
In S.S. Holt, N. Gehrels and J.A. Nousek (eds.), *Gamma-Ray Bursts in the Swift Era*, volume 836 of *American Institute of Physics Conference Series*, pp. 367–379 (2006).
- DELLA VALLE, M., CHINCARINI, G., PANAGIA, N., TAGLIAFERRI, G., MALESANI, D., TESTA, V., FUGAZZA, D., CAMPANA, S., COVINO, S., MANGANO, V. ET AL.  
«An enigmatic long-lasting  $\gamma$ -ray burst not accompanied by a bright supernova».  
*Nature*, **444**, pp. 1050–1052 (2006).
- DEZALAY, J.P., BARAT, C., TALON, R., SYUNYAEV, R., TEREKHOV, O. AND KUZNETSOV, A.  
«Short cosmic events - a subset of classical grbs?»  
In W.S. Paciesas and G.J. Fishman (eds.), *American Institute of Physics Conference Series*, volume 265 of *American Institute of Physics Conference Series*, pp. 304–309 (1992).
- EDEROCLITE, A., MASON, E., DELLA VALLE, M., GILMOZZI, R., WILLIAMS, R.E., GERMANY, L., SAVIANE, I., MATTEUCCI, F., SCHAEFER, B.E., WALTER, F. ET AL.  
«Early spectral evolution of nova sagittarii 2004 (v5114 sagittarii)».  
*A&A*, **459**, pp. 875–883 (2006).
- EICHLER, D., LIVIO, M., PIRAN, T. AND SCHRAMM, D.N.  
«Nucleosynthesis, neutrino bursts and gamma-rays from coalescing neutron stars».  
*Nature*, **340**, pp. 126–128 (1989).
- EVANS, P.A., BEARDMORE, A.P., PAGE, K.L., OSBORNE, J.P., O'BRIEN, P.T., WILLINGALE, R., STARLING, R.L.C., BURROWS, D.N., GODET, O., VETTERE, L. ET AL.  
«Methods and results of an automatic analysis of a complete sample of Swift-XRT observations of GRBs».  
*MNRAS*, **397**, pp. 1177–1201 (2009).
- FALCONE, A.D., BURROWS, D.N., LAZZATI, D., CAMPANA, S., KOBAYASHI, S., ZHANG, B., MÉSZÁROS, P., PAGE, K.L., KENNEA, J.A., ROMANO, P. ET AL.  
«The Giant X-Ray Flare of GRB 050502B: Evidence for Late-Time Internal Engine Activity».  
*ApJ*, **641**, pp. 1010–1017 (2006).

- FALCONE, A.D., MORRIS, D., RACUSIN, J., CHINCARINI, G., MORETTI, A., ROMANO, P., BURROWS, D.N., PAGANI, C., STROH, M., GRUPE, D. ET AL.  
«The first survey of x-ray flares from gamma ray bursts observed by swift: Spectral properties and energetics».  
*ArXiv:0706.1564* (2007a).
- FALCONE, A.D., MORRIS, D., RACUSIN, J., CHINCARINI, G., MORETTI, A., ROMANO, P., BURROWS, D.N., PAGANI, C., STROH, M., GRUPE, D. ET AL.  
«The First Survey of X-Ray Flares from Gamma-Ray Bursts Observed by Swift: Spectral Properties and Energetics».  
*ApJ*, **671**, pp. 1921–1938 (2007b).
- FAN, Y.Z., PIRAN, T. AND XU, D.  
«The interpretation and implication of the afterglow of grb 060218».  
*Journal of Cosmology and Astro-Particle Physics*, **9**, p. 13 (2006).
- FATKHULLIN, T.A., SOKOLOV, V.V., MOISEEV, A.V., GUZIY, S. AND CASTRO-TIRADO, A.J.  
«Grb 060218: emergence of the underlying sn spectrum.»  
*GCN Circ.*, **4809** (2006).
- FENIMORE, E.E., COOPER, C., RAMIREZ-RUIZ, E., SUMNER, M.C., YOSHIDA, A. AND NAMIKI, M.  
«Gamma-ray bursts and relativistic shells: The surface filling factor».  
*ApJ*, **512**, pp. 683–692 (1999).
- FERRERO, P., PALAZZI, E., PIAN, E. AND SAVAGLIO, S.  
«Optical observations of grb 060218/sn 2006aj and its host galaxy».  
*In American Institute of Physics Conference Series*, volume 924 of *American Institute of Physics Conference Series*, pp. 120–125 (2007).
- FLETCHER, R.S., GAISSER, T.K., LIPARI, P. AND STANEV, T.  
«sibyll: An event generator for simulation of high energy cosmic ray cascades».  
*Phys. Rev. D*, **50**, pp. 5710–5731 (1994).
- FONG, W., BERGER, E. AND FOX, D.B.  
«Hubble Space Telescope Observations of Short Gamma-Ray Burst Host Galaxies: Morphologies, Offsets, and Local Environments».  
*ApJ*, **708**, pp. 9–25 (2010).
- FOX, D.B., FRAIL, D.A., PRICE, P.A., KULKARNI, S.R., BERGER, E., PIRAN, T., SODERBERG, A.M., CENKO, S.B., CAMERON, P.B., GAL-YAM, A. ET AL.  
«The afterglow of grb 050709 and the nature of the short-hard  $\gamma$ -ray bursts».  
*Nature*, **437**, pp. 845–850 (2005).

- FRONTERA, F., AMATI, L., COSTA, E., MULLER, J.M., PIAN, E., PIRO, L., SOFFITTA, P., TAVANI, M., CASTRO-TIRADO, A., DAL FIUME, D. ET AL.  
«Prompt and delayed emission properties of gamma-ray bursts observed with beposax».  
*ApJSS*, **127**, pp. 59–78 (2000).
- FRONTERA, F., COSTA, E., PIRO, L., MULLER, J.M., AMATI, L., FEROCI, M., FIORE, F., PIZZICHINI, G., TAVANI, M., CASTRO-TIRADO, A. ET AL.  
«Spectral properties of the prompt x-ray emission and afterglow from the gamma-ray burst of 1997 february 28».  
*ApJ*, **493**, p. L67 (1998).
- FYNBO, J.P.U., WATSON, D., THÖNE, C.C., SOLLERMAN, J., BLOOM, J.S., DAVIS, T.M., HJORTH, J., JAKOBSSON, P., JØRGENSEN, U.G., GRAHAM, J.F. ET AL.  
«No supernovae associated with two long-duration  $\gamma$ -ray bursts».  
*Nature*, **444**, pp. 1047–1049 (2006).
- GAL-YAM, A., FOX, D.B., PRICE, P.A., OFEK, E.O., DAVIS, M.R., LEONARD, D.C., SODERBERG, A.M., SCHMIDT, B.P., LEWIS, K.M., PETERSON, B.A. ET AL.  
«A novel explosive process is required for the  $\gamma$ -ray burst grb 060614».  
*Nature*, **444**, pp. 1053–1055 (2006).
- GALAMA, T.J., TANVIR, N., VREESWIJK, P.M., WIJERS, R.A.M.J., GROOT, P.J., ROL, E., VAN PARADIJS, J., KOUVELIOTOU, C., FRUCHTER, A.S., MASETTI, N. ET AL.  
«Evidence for a supernova in reanalyzed optical and near-infrared images of grb 970228».  
*ApJ*, **536**, pp. 185–194 (2000).
- GALAMA, T.J., VREESWIJK, P.M., VAN PARADIJS, J., KOUVELIOTOU, C., AUGUSTEIJN, T., BÖHNHARDT, H., BREWER, J.P., DOUBLIER, V., GONZALEZ, J.F., LEIBUNDGUT, B. ET AL.  
«An unusual supernova in the error box of the  $\gamma$ -ray burst of 25 april 1998».  
*Nature*, **395**, pp. 670–672 (1998).
- GAMOW, G.  
*My wordlines - an informal autobiography* (New York: Viking press, 1970).
- GAMOW, G. AND SCHOENBERG, M.  
«Neutrino theory of stellar collapse».  
*Physical Review*, **59**, pp. 539–547 (1941).

- GEHRELS, N., CHINCARINI, G., GIOMMI, P., MASON, K.O., NOUSEK, J.A., WELLS, A.A., WHITE, N.E., BARTHELMY, S.D., BURROWS, D.N., COMINSKY, L.R. ET AL.  
«The swift gamma-ray burst mission».  
*ApJ*, **611**, pp. 1005–1020 (2004).
- GEHRELS, N., NORRIS, J.P., BARTHELMY, S.D., GRANOT, J., KANEKO, Y., KOUVELIOTOU, C., MARKWARDT, C.B., MÉSZÁROS, P., NAKAR, E., NOUSEK, J.A. ET AL.  
«A new  $\gamma$ -ray burst classification scheme from grb060614».  
*Nature*, **444**, pp. 1044–1046 (2006).
- GEHRELS, N., RAMIREZ-RUIZ, E. AND FOX, D.B.  
«Gamma-Ray Bursts in the Swift Era».  
*ARAA*, **47**, pp. 567–617 (2009).
- GEHRELS, N., SARAZIN, C.L., O'BRIEN, P.T., ZHANG, B., BARBIER, L., BARTHELMY, S.D., BLUSTIN, A., BURROWS, D.N., CANNIZZO, J., CUMMINGS, J.R. ET AL.  
«A short  $\gamma$ -ray burst apparently associated with an elliptical galaxy at redshift  $z = 0.225$ ».  
*Nature*, **437**, pp. 851–854 (2005).
- GHIRLANDA, G., CELOTTI, A. AND GHISELLINI, G.  
«Time resolved spectral analysis of bright gamma ray bursts».  
*A&A*, **393**, pp. 409–423 (2002).
- GHISELLINI, G., GHIRLANDA, G., MEREGHETTI, S., BOSNJAK, Z., TAVECCHIO, F. AND FIRMANI, C.  
«Are grb980425 and grb031203 real outliers or twins of grb060218?»  
*MNRAS*, **372**, pp. 1699–1709 (2006).
- GOLENETSKII, S., APTEKAR, R., MAZETS, E., PAL'SHIN, V., FREDERIKS, D. AND CLINE, T.  
«Konus-wind observation of GRB 071227.»  
*GCN Circ.*, **7155**, pp. 1–+ (2007).
- GOLENETSKII, S., APTEKAR, R., MAZETS, E., PAL'SHIN, V., FREDERIKS, D. AND CLINE, T.  
«Konus-wind observation of GRB 080319B.»  
*GCN Circ.*, **7482** (2008).
- GOODMAN, J.  
«Are gamma-ray bursts optically thick?»  
*ApJ*, **308**, pp. L47–L50 (1986).

- GREINER, J., KLOSE, S., SALVATO, M., ZEH, A., SCHWARZ, R., HARTMANN, D.H., MASETTI, N., STECKLUM, B., LAMER, G., LODIEU, N. ET AL.  
«Grb 011121: A collimated outflow into wind-blown surroundings».  
*ApJ*, **599**, pp. 1223–1237 (2003).
- GUETTA, D.  
«Short grbs: Rates and luminosity function implications».  
*ArXiv:astro-ph/0610408* (2006).
- GUETTA, D. AND DELLA VALLE, M.  
«On the rates of gamma-ray bursts and type ib/c supernovae».  
*ApJ*, **657**, pp. L73–L76 (2007).
- GUIDA, R., BERNARDINI, M.G., BIANCO, C.L., CAITO, L., DAINOTTI, M.G. AND RUFFINI, R.  
In R.T. Jantzen, H. Kleinert and R. Ruffini (eds.), *The Eleventh Marcel Grossmann Meeting*. (Singapore: World Scientific, 2008a).
- GUIDA, R., BERNARDINI, M.G., BIANCO, C.L., CAITO, L., DAINOTTI, M.G. AND RUFFINI, R.  
«The amati relation in the “fireshell” model».  
*A&A*, **487**, pp. L37–L40 (2008b).
- HJORTH, J., SOLLERMAN, J., GOROSABEL, J., GRANOT, J., KLOSE, S., KOUVELIOTOU, C., MELINDER, J., RAMIREZ-RUIZ, E., STARLING, R., THOMSEN, B. ET AL.  
«GRB 050509B: Constraints on Short Gamma-Ray Burst Models».  
*ApJ*, **630**, pp. L117–L120 (2005).
- IBEN, JR., I. AND TUTUKOV, A.V.  
«Supernovae of type I as end products of the evolution of binaries with components of moderate initial mass (M not greater than about 9 solar masses)».  
*ApJSS*, **54**, pp. 335–372 (1984).
- INFANTE, L., GARNAVICH, P.M., STANEK, K.Z. AND WYRZYKOWSKI, L.  
«Grb011121: possible redshift, continued decay.»  
*GCN Circ.*, **1152** (2001).
- JIN, Z.P. AND FAN, Y.Z.  
«GRB 060418 and 060607A: the medium surrounding the progenitor and the weak reverse shock emission».  
*MNRAS*, **378**, pp. 1043–1048 (2007).
- KANEKO, Y., RAMIREZ-RUIZ, E., GRANOT, J., KOUVELIOTOU, C., WOOSLEY, S.E., PATEL, S.K., ROL, E., ZAND, J.J.M.I., VAN DER HORST, A.J., WIJERS, R.A.M.J. ET AL.

- «Prompt and afterglow emission properties of gamma-ray bursts with spectroscopically identified supernovae».  
*ApJ*, **654**, pp. 385–402 (2007).
- KANN, D.A., KLOSE, S., ZHANG, B., WILSON, A.C., BUTLER, N.R., MALESANI, D., NAKAR, E., ANTONELLI, L.A., CHINCARINI, G., COBB, B.E. ET AL.  
«The afterglows of swift-era gamma-ray bursts. ii. short/hard (type i) vs. long/soft (type ii) optical afterglows».  
*ArXiv:0804.1959* (2008).
- KATZ, J.I.  
«Delayed hard photons from gamma-ray bursts».  
*ApJ*, **432**, pp. L27–L29 (1994).
- KAWAI, N., YAMADA, T., KOSUGI, G., HATTORI, T. AND AOKI, K.  
«Grb 050904: Subaru optical spectroscopy.»  
*GCN Circ.*, **3937** (2005).
- KELSON, D. AND BERGER, E.  
«Grb 050315: absorption redshift.»  
*GCN Circ.*, **3101** (2005).
- KENNEA, J.A., BURROWS, D.N., CUSUMANO, G. AND TAGLIAFERRI, G.  
«Subject: Grb 060218: Swift xrt position.»  
*GCN Circ.*, **4776** (2006).
- KLEBESADEL, R.W.  
«The durations of gamma-ray bursts».  
In C. Ho, R.I. Epstein and E.E. Fenimore (eds.), *Gamma-Ray Bursts - Observations, Analyses and Theories*, pp. 161–168 (Cambridge University Press, 1992).
- KOUVELIOTOU, C., MEEGAN, C.A., FISHMAN, G.J., BHAT, N.P., BRIGGS, M.S., KOSHUT, T.M., PACIESAS, W.S. AND PENDLETON, G.N.  
«Identification of two classes of gamma-ray bursts».  
*ApJ*, **413**, pp. L101–L104 (1993).
- KOUVELIOTOU, C., WOOSLEY, S.E., PATEL, S.K., LEVAN, A., BLANDFORD, R., RAMIREZ-RUIZ, E., WIJERS, R.A.M.J., WEISSKOPF, M.C., TENNANT, A., PIAN, E. ET AL.  
«Chandra observations of the x-ray environs of sn 1998bw/grb 980425».  
*ApJ*, **608**, pp. 872–882 (2004).
- KRAMER, M.  
In R.T. Jantzen, H. Kleinert and R. Ruffini (eds.), *The Eleventh Marcel Grossmann Meeting* (Singapore: World Scientific, 2008).

- KUMAR, P. AND MCMAHON, E.  
«A general scheme for modelling  $\gamma$ -ray burst prompt emission».  
*MNRAS*, **384**, pp. 33–63 (2008).
- LATTIMER, J.M., VAN RIPER, K.A., PRAKASH, M. AND PRAKASH, M.  
«Rapid cooling and the structure of neutron stars».  
*ApJ*, **425**, pp. 802–813 (1994).
- LEDOUX, C., VREESWIJK, P., SMETTE, A., JAUNSEN, A. AND KAUFER, A.  
«VLT/UVES observations of GRB 060607.»  
*GCN Circ.*, **5237** (2006).
- LEWIS, A.D., BUOTE, D.A. AND STOCKE, J.T.  
«Chandra observations of a2029: The dark matter profile down to below  $0.01r_{vir}$  in an unusually relaxed cluster».  
*ApJ*, **586**, pp. 135–142 (2003).
- LI, L.X.  
«Shock breakout in type Ibc supernovae and application to grb 060218/sn 2006aj».  
*MNRAS*, **375**, pp. 240–256 (2007).
- LIANG, E., ZHANG, B., VIRGILI, F. AND DAI, Z.G.  
«Low-luminosity gamma-ray bursts as a unique population: Luminosity function, local rate, and beaming factor».  
*ApJ*, **662**, pp. 1111–1118 (2007).
- LIANG, E.W., ZHANG, B., O'BRIEN, P.T., WILLINGALE, R., ANGELINI, L., BURROWS, D.N., CAMPANA, S., CHINCARINI, G., FALCONE, A., GEHRELS, N. ET AL.  
«Testing the curvature effect and internal origin of gamma-ray burst prompt emissions and x-ray flares with swift data».  
*ApJ*, **646**, pp. 351–357 (2006a).
- LIANG, E.W., ZHANG, B.B., STAMATIKOS, M., ZHANG, B., NORRIS, J., GEHRELS, N., ZHANG, J. AND DAI, Z.G.  
«Temporal profiles and spectral lags of xrf 060218».  
*ApJ*, **653**, pp. L81–L84 (2006b).
- LYUTIKOV, M. AND BLANDFORD, R.  
«Gamma Ray Bursts as Electromagnetic Outflows».  
*arXiv:astro-ph/0312347* (2003).
- MAEDA, K., KAWABATA, K., TANAKA, M., NOMOTO, K., TOMINAGA, N., HATTORI, T., MINEZAKI, T., KURODA, T., SUZUKI, T., DENG, J. ET AL.  
«Sn 2006aj associated with xrf 060218 at late phases: Nucleosynthesis signature of a neutron star-driven explosion».

- ApJ*, **658**, pp. L5–L8 (2007).
- MANGANÒ, V., HOLLAND, S.T., MALESANI, D., TROJA, E., CHINCARINI, G., ZHANG, B., LA PAROLA, V., BROWN, P.J., BURROWS, D.N., CAMPANA, S. ET AL.  
«Swift observations of grb 060614: an anomalous burst with a well behaved afterglow».  
*A&A*, **470**, pp. 105–118 (2007).
- MANNUCCI, F., DELLA VALLE, M., PANAGIA, N., CAPPELLARO, E., CRESCI, G., MAIOLINO, R., PETROSIAN, A. AND TURATTO, M.  
«The supernova rate per unit mass».  
*A&A*, **433**, pp. 807–814 (2005).
- MARGUTTI, R., GUIDORZI, C., CHINCARINI, G., PASOTTI, F., COVINO, S. AND MAO, J.  
«Temporal variability of GRB early X-ray afterglows and GRB080319B prompt emission».  
In Y.F. Huang, Z.G. Dai and B. Zhang (eds.), *2008 Nanjing Gamma-Ray Burst Conference*, volume 1065 of *American Institute of Physics Conference Series*, pp. 259–262 (2008).
- MAZZALI, P.  
talk presented at the congress “Swift and GRBs: unveiling the relativistic universe”, Venice, Italy, June 5-9 (2006).
- MAZZALI, P.A., DENG, J., NOMOTO, K., SAUER, D.N., PIAN, E., TOMINAGA, N., TANAKA, M., MAEDA, K. AND FILIPPENKO, A.V.  
«A neutron-star-driven x-ray flash associated with supernova sn 2006aj».  
*Nature*, **442**, pp. 1018–1020 (2006).
- MEEGAN, C., LICHTI, G., BHAT, P.N., BISSALDI, E., BRIGGS, M.S., CONNAUGHTON, V., DIEHL, R., FISHMAN, G., GREINER, J., HOOVER, A.S. ET AL.  
«The Fermi Gamma-ray Burst Monitor».  
*ApJ*, **702**, pp. 791–804 (2009).
- MEREGHETTI, S. AND GOTZ, D.  
«Grb 031203: further analysis of integral data.»  
*GCN Circ.*, **2460** (2003).
- MESZAROS, P.  
«Gamma-ray bursts.»  
*Reports of Progress in Physics*, **69**, pp. 2259–2322 (2006).
- MESZAROS, P., LAGUNA, P. AND REES, M.J.

- «Gasdynamics of relativistically expanding gamma-ray burst sources - kinematics, energetics, magnetic fields, and efficiency».  
*ApJ*, **415**, pp. 181–190 (1993).
- MESZAROS, P. AND REES, M.J.  
«Relativistic fireballs and their impact on external matter - Models for cosmological gamma-ray bursts».  
*ApJ*, **405**, pp. 278–284 (1993).
- MESZAROS, P. AND REES, M.J.  
«Optical and Long-Wavelength Afterglow from Gamma-Ray Bursts».  
*ApJ*, **476**, pp. 232–237 (1997a).
- MESZAROS, P. AND REES, M.J.  
«Poynting Jets from Black Holes and Cosmological Gamma-Ray Bursts».  
*ApJ*, **482**, p. L29 (1997b).
- MIRABAL, N., HALPERN, J.P., AN, D., THORSTENSEN, J.R. AND TERNDRUP, D.M.  
«Grb 060218/sn 2006aj: A gamma-ray burst and prompt supernova at  $z = 0.0335$ ».  
*ApJ*, **643**, pp. L99–L102 (2006).
- MODJAZ, M., STANEK, K.Z., GARNAVICH, P.M., BERLIND, P., BLONDIN, S., BROWN, W., CALKINS, M., CHALLIS, P., DIAMOND-STANIC, A.M., HAO, H. ET AL.  
«Early-time photometry and spectroscopy of the fast evolving sn 2006aj associated with grb 060218».  
*ApJ*, **645**, pp. L21–L24 (2006).
- MOLINARI, E., VERGANI, S.D., MALESANI, D., COVINO, S., D’AVANZO, P., CHINCARINI, G., ZERBI, F.M., ANTONELLI, L.A., CONCONI, P., TESTA, V. ET AL.  
«REM observations of GRB 060418 and GRB 060607A: the onset of the afterglow and the initial fireball Lorentz factor determination».  
*A&A*, **469**, pp. L13–L16 (2007).
- NOMOTO, K., TOMINAGA, N., TANAKA, M., MAEDA, K., SUZUKI, T., DENG, J.S. AND MAZZALI, P.A.  
«Diversity of the supernova - gamma-ray burst connection».  
*ArXiv:astro-ph/0702472* (2007).
- NORRIS, J.P. AND BONNELL, J.T.  
«Short gamma-ray bursts with extended emission».  
*ApJ*, **643**, pp. 266–275 (2006).

- NORRIS, J.P., NEMIROFF, R.J., BONNELL, J.T., SCARGLE, J.D., KOUVELIOTOU, C., PACIASAS, W.S., MEEGAN, C.A. AND FISHMAN, G.J.  
«Attributes of Pulses in Long Bright Gamma-Ray Bursts».  
*ApJ*, **459**, pp. 393–412 (1996).
- NOUSEK, J.A., KOUVELIOTOU, C., GRUPE, D., PAGE, K.L., GRANOT, J., RAMIREZ-RUIZ, E., PATEL, S.K., BURROWS, D.N., MANGANO, V., BARTHELMY, S. ET AL.  
«Evidence for a canonical gamma-ray burst afterglow light curve in the swift xrt data».  
*ApJ*, **642**, pp. 389–400 (2006).
- PACZYNSKI, B.  
«Evolution of cataclysmic binaries».  
In D. Lamb and J. Patterson (eds.), *Cataclysmic Variables and Low-Mass X-ray Binaries*, volume 113 of *Astrophysics and Space Science Library*, pp. 1–12 (1985).
- PACZYNSKI, B.  
«Gamma-ray bursters at cosmological distances».  
*ApJ*, **308**, pp. L43–L46 (1986).
- PAGE, K., GOAD, M. AND BEARDMORE, A.  
«GRB 060607: Swift-XRT team refined analysis.»  
*GCN Circ.*, **5240** (2006).
- PAKMOR, R., KROMER, M., RÖPKE, F.K., SIM, S.A., RUITER, A.J. AND HILLEBRANDT, W.  
«Sub-luminous type Ia supernovae from the mergers of equal-mass white dwarfs with mass  $\sim 0.9M_{\text{solar}}$ ».  
*Nature*, **463**, pp. 61–64 (2010).
- PANAITESCU, A.  
«The energetics and environment of the short-grb afterglows 050709 and 050724».  
*MNRAS*, **367**, pp. L42–L46 (2006).
- PANAITESCU, A. AND MÉSZÁROS, P.  
«Dynamical evolution, light curves, and spectra of spherical and collimated gamma-ray burst remnants».  
*ApJ*, **526**, pp. 707–715 (1999).
- PANAITESCU, A., MÉSZÁROS, P., GEHRELS, N., BURROWS, D. AND NOUSEK, J.  
«Analysis of the x-ray emission of nine swift afterglows».  
*MNRAS*, **366**, pp. 1357–1366 (2006).

- PANAITESCU, A., MESZAROS, P. AND REES, M.J.  
«Multiwavelength Afterglows in Gamma-Ray Bursts: Refreshed Shock and Jet Effects».  
*ApJ*, **503**, pp. 314–+ (1998).
- PARSONS, A., BARTHELMY, S., BARBIER, L., CUMMINGS, J., FENIMORE, E., FINK, R., GEHRELS, N., HOLLAND, S., HULLINGER, D., HURLEY, K. ET AL.  
«Swift-bat detection of grb 050315.»  
*GCN Circ.*, **3094** (2005).
- PASTORELLO, A., DELLA VALLE, M., SMARTT, S.J., ZAMPIERI, L., BENETTI, S., CAPPELLARO, E., MAZZALI, P.A., PATAT, F., SPIRO, S., TURATTO, M. ET AL.  
«A very faint core-collapse supernova in M85».  
*Nature*, **449** (2007).
- PIAN, E., AMATI, L., ANTONELLI, L.A., BUTLER, R.C., COSTA, E., CUSUMANO, G., DANZIGER, J., FEROCI, M., FIORE, F., FRONTERA, F. ET AL.  
«BeppoSax observations of grb 980425: Detection of the prompt event and monitoring of the error box».  
*ApJ*, **536**, pp. 778–787 (2000).
- PIAN, E., GIOMMI, P., AMATI, L., COSTA, E., DANZIGER, J., FEROCI, M., FIOCCHI, M.T., FRONTERA, F., KOUVELIOTOU, C., MASETTI, N. ET AL.  
«Xmm-newton observations of the field of  $\gamma$ -ray burst 980425».  
*Advances in Space Research*, **34**, pp. 2711–2714 (2004).
- PIAN, E., MAZZALI, P.A., MASETTI, N., FERRERO, P., KLOSE, S., PALAZZI, E., RAMIREZ-RUIZ, E., WOOSLEY, S.E., KOUVELIOTOU, C., DENG, J. ET AL.  
«An optical supernova associated with the x-ray flash xrf 060218».  
*Nature*, **442**, pp. 1011–1013 (2006).
- PIRAN, T.  
«Gamma-ray bursts and the fireball model».  
*Phys. Rep.*, **314**, pp. 575–667 (1999).
- PIRAN, T.  
«The physics of gamma-ray bursts».  
*Reviews of Modern Physics*, **76**, pp. 1143–1210 (2005).
- PIRAN, T., SARI, R. AND ZOU, Y.C.  
«Observational Limits on Inverse Compton Processes in GRBs».  
*ArXiv:0807.3954* (2008).

- PIRAN, T., SARI, R. AND ZOU, Y.  
«Observational limits on inverse Compton processes in gamma-ray bursts».  
*MNRAS*, **393**, pp. 1107–1113 (2009).
- PIRAN, T., SHEMI, A. AND NARAYAN, R.  
«Hydrodynamics of relativistic fireballs».  
*MNRAS*, **263**, p. 861 (1993).
- PIRANOMONTE, S., D’AVANZO, P., COVINO, S., ANTONELLI, L.A., BEARDMORE, A.P., CAMPANA, S., CHINCARINI, G., D’ELIA, V., DELLA VALLE, M., FIORE, F. ET AL.  
«The short GRB 070707 afterglow and its very faint host galaxy».  
*A&A*, **491**, pp. 183–188 (2008).
- PIRO, L.  
«Astrophysics: Short-burst sources».  
*Nature*, **437**, pp. 822–823 (2005).
- PIRO, L., DE PASQUALE, M., SOFFITTA, P., LAZZATI, D., AMATI, L., COSTA, E., FEROCI, M., FRONTERA, F., GUIDORZI, C., IN’T ZAND, J.M.J. ET AL.  
«Probing the environment in gamma-ray bursts: The case of an x-ray precursor, afterglow late onset, and wind versus constant density profile in grb 011121 and grb 011211».  
*ApJ*, **623**, pp. 314–324 (2005).
- POZDNIAKOV, L.A., SOBOL, I.M. AND SYUNYAEV, R.A.  
«Comptonization and the shaping of x-ray source spectra - monte carlo calculations».  
*Astrophysics and Space Physics Reviews*, **2**, pp. 189–331 (1983).
- PREPARATA, G., RUFFINI, R. AND XUE, S.S.  
«The dyadosphere of black holes and gamma-ray bursts».  
*A&A*, **338**, pp. L87–L90 (1998).
- PRICE, P.A., BERGER, E., REICHART, D.E., KULKARNI, S.R., YOST, S.A., SUBRAHMANYAN, R., WARK, R.M., WIERINGA, M.H., FRAIL, D.A., BAILEY, J. ET AL.  
«Grb 011121: A massive star progenitor».  
*ApJ*, **572**, pp. L51–L55 (2002).
- PROCHASKA, J.X., BLOOM, J.S., CHEN, H.W., HURLEY, K.C., MELBOURNE, J., DRESSLER, A., GRAHAM, J.R., OSIP, D.J. AND VACCA, W.D.  
«The host galaxy of grb 031203: Implications of its low metallicity, low redshift, and starburst nature».  
*ApJ*, **611**, pp. 200–207 (2004).

- PROCHASKA, J.X., COOPER, M., NEWMAN, J., BLOOM, J.S., HURLEY, K., BLAKE, C., GERKE, B. AND CHEN, H.W.  
«Keck/DEIMOS spectrum of possible host galaxy for GRB050509b.»  
*GCN Circ.*, **3390** (2005).
- RACUSIN, J.L., KARPOV, S.V., SOKOLOWSKI, M., GRANOT, J., WU, X.F., PAL'SHIN, V., COVINO, S., VAN DER HORST, A.J., OATES, S.R., SCHADY, P. ET AL.  
«Broadband observations of the naked-eye  $\gamma$ -ray burst GRB080319B.»  
*Nature*, **455**, pp. 183–188 (2008).
- RAO, A.R., MALKAR, J.P., HINGAR, M.K., AGRAWAL, V.K., CHAKRABARTI, S.K., NANDI, A., DEBNATH, D., KOTOCH, T.B., SARKAR, R., CHIDAMBARAM, T.R. ET AL.  
«Detection of GRB 090618 with the RT-2 Experiment on Board the Coronas-Photon Satellite».  
*ApJ*, **728**, p. 42 (2011).
- REES, M., RUFFINI, R. AND WHEELER, J.A.  
*Black holes, gravitational waves and cosmology: an introduction to current research*, volume 10 of *Topics in Astrophysics and Space Physics* (New York: Gordon and Breach, Science Publishers, Inc., 1974).
- REES, M.J. AND MESZAROS, P.  
«Unsteady outflow models for cosmological gamma-ray bursts».  
*ApJ*, **430**, pp. L93–L96 (1994).
- REES, M.J. AND MESZAROS, P.  
«Refreshed shocks and afterglow longevity in gamma-ray bursts».  
*ApJ*, **496**, p. L1 (1998).
- RICHARDSON, D., BRANCH, D. AND BARON, E.  
«Absolute magnitude distributions and light curves of stripped-envelope supernovae».  
*AJ*, **131**, pp. 2233–2244 (2006).
- ROL, E., PAGE, K., BURROWS, D.N., GEHRELS, N., GOAD, M., HURKETT, C., KENNEA, J. AND BRIAN, P.  
«GRB 050509B: Swift/XRT refined analysis.»  
*GCN Circ.*, **3395** (2005).
- ROMANI, R.W.  
«Model atmospheres for cooling neutron stars».  
*ApJ*, **313**, pp. 718–726 (1987).
- RUFFINI, R.

talk presented at the congress “Eleventh Marcel Grossmann Meeting”, Berlin, Germany, July 23-29 (2006).

RUFFINI, R.

«The ergosphere and dyadosphere of black holes».

In D.L. Wiltshire, M. Visser and S. Scott (eds.), *The Kerr Spacetime* (Cambridge University Press, 2009).

RUFFINI, R., AKSENOV, A.G., BERNARDINI, M.G., BIANCO, C.L., CAITO, L., CHARDONNET, P., DAINOTTI, M.G., DE BARROS, G., GUIDA, R., IZZO, L. ET AL.

«The Blackholic energy and the canonical Gamma-Ray Burst IV: the “long,” “genuine short” and “fake-disguised short” GRBs».

In M. Novello and S. Perez Bergliaffa (eds.), *XIII Brazilian School on Cosmology and Gravitation*, volume 1132 of *American Institute of Physics Conference Series*, pp. 199–266 (2009).

RUFFINI, R., AKSENOV, A.G., BERNARDINI, M.G., BIANCO, C.L., CAITO, L., DAINOTTI, M.G., DE BARROS, G., GUIDA, R., VERESHCHAGIN, G.V. AND XUE, S.S.

«The canonical Gamma-Ray Bursts and their “precursors”».

In Y.F. Huang, Z.G. Dai and B. Zhang (eds.), *2008 Nanjing Gamma-Ray Burst Conference*, volume 1065 of *American Institute of Physics Conference Series*, pp. 219–222 (2008a).

RUFFINI, R., BERNARDINI, M.G., BIANCO, C.L., CAITO, L., CHARDONNET, P., DAINOTTI, M.G., FRASCHETTI, F., GUIDA, R., ROTONDO, M., VERESHCHAGIN, G. ET AL.

«The blackholic energy and the canonical gamma-ray burst».

In M. Novello and S.E. Perez Bergliaffa (eds.), *XII Brazilian School of Cosmology and Gravitation*, volume 910 of *American Institute of Physics Conference Series*, pp. 55–217 (2007a).

RUFFINI, R., BERNARDINI, M.G., BIANCO, C.L., CAITO, L., CHARDONNET, P., DAINOTTI, M.G., FRASCHETTI, F., GUIDA, R., VERESHCHAGIN, G. AND XUE, S.S.

«The role of grb 031203 in clarifying the astrophysical grb scenario».

In S. Grebenev, R. Sunyaev, C. Winkler, A. Parmar and L. Ouweland (eds.), *The 6<sup>th</sup> Integral Workshop - The Obscured Universe*, volume SP-622 of *ESA Special Publication*, p. 561 (2007b).

RUFFINI, R., BERNARDINI, M.G., BIANCO, C.L., CHARDONNET, P., FRASCHETTI, F., GUIDA, R. AND XUE, S.S.

«Grb 050315: A step toward the uniqueness of the overall grb structure».

*N.Cim.B*, **121**, pp. 1367–1372 (2006a).

- RUFFINI, R., BERNARDINI, M.G., BIANCO, C.L., CHARDONNET, P., FRASCHETTI, F., GUIDA, R. AND XUE, S.S.  
«Grb 050315: A step toward understanding the uniqueness of the overall gamma-ray burst structure».  
*ApJ*, **645**, pp. L109–L112 (2006b).
- RUFFINI, R., BERNARDINI, M.G., BIANCO, C.L., CHARDONNET, P., FRASCHETTI, F., GURZADYAN, V., VITAGLIANO, L. AND XUE, S.S.  
«The blackholic energy: long and short gamma-ray bursts (new perspectives in physics and astrophysics from the theoretical understanding of gamma-ray bursts, ii)».  
In M. Novello and S.E. Perez Bergliaffa (eds.), *XI Brazilian School of Cosmology and Gravitation*, volume 782 of *American Institute of Physics Conference Series*, pp. 42–127 (2005a).
- RUFFINI, R., BERNARDINI, M.G., BIANCO, C.L., CHARDONNET, P., FRASCHETTI, F. AND XUE, S.S.  
«Grb 980425, sn1998bw and the embh model».  
*Advances in Space Research*, **34**, pp. 2715–2722 (2004a).
- RUFFINI, R., BERNARDINI, M.G., BIANCO, C.L., VITAGLIANO, L., XUE, S.S., CHARDONNET, P., FRASCHETTI, F. AND GURZADYAN, V.  
«Black hole physics and astrophysics: The grb-supernova connection and urca-1 - urca-2».  
In M. Novello, S. Perez Bergliaffa and R. Ruffini (eds.), *The Tenth Marcel Grossmann Meeting. On recent developments in theoretical and experimental general relativity, gravitation and relativistic field theories*, p. 369 (Singapore: World Scientific, 2005b).
- RUFFINI, R., BIANCO, C.L., CHARDONNET, P., FRASCHETTI, F., GURZADYAN, V. AND XUE, S.S.  
«On the instantaneous spectrum of gamma-ray bursts».  
*IJMPD*, **13**, pp. 843–851 (2004b).
- RUFFINI, R., BIANCO, C.L., CHARDONNET, P., FRASCHETTI, F., GURZADYAN, V. AND XUE, S.S.  
«Emergence of a filamentary structure in the fireball from grb spectra».  
*IJMPD*, **14**, pp. 97–105 (2005c).
- RUFFINI, R., BIANCO, C.L., CHARDONNET, P., FRASCHETTI, F., VITAGLIANO, L. AND XUE, S.S.  
«New perspectives in physics and astrophysics from the theoretical understanding of gamma-ray bursts».  
In M. Novello and S.E. Perez Bergliaffa (eds.), *Cosmology and Gravitation*, volume 668 of *American Institute of Physics Conference Series*, pp. 16–107 (2003).

- RUFFINI, R., BIANCO, C.L., CHARDONNET, P., FRASCHETTI, F. AND XUE, S.S.  
«On a possible gamma-ray burst-supernova time sequence».  
*ApJ*, **555**, pp. L117–L120 (2001a).
- RUFFINI, R., BIANCO, C.L., CHARDONNET, P., FRASCHETTI, F. AND XUE, S.S.  
«On the interpretation of the burst structure of gamma-ray bursts».  
*ApJ*, **555**, pp. L113–L116 (2001b).
- RUFFINI, R., BIANCO, C.L., CHARDONNET, P., FRASCHETTI, F. AND XUE, S.S.  
«Relative spacetime transformations in gamma-ray bursts».  
*ApJ*, **555**, pp. L107–L111 (2001c).
- RUFFINI, R., BIANCO, C.L., CHARDONNET, P., FRASCHETTI, F. AND XUE, S.S.  
«On the structures in the afterglow peak emission of gamma-ray bursts».  
*ApJ*, **581**, pp. L19–L22 (2002).
- RUFFINI, R., CHAKRABARTI, S.K. AND IZZO, L.  
«Possible multiple components in a GRB: the case of GRB 090618».  
*Submitted to Adv. Sp. Res.* (2010).
- RUFFINI, R., FRASCHETTI, F., VITAGLIANO, L. AND XUE, S.S.  
«Observational signatures of an electromagnetic overcritical gravitational collapse».  
*IJMPD*, **14**, pp. 131–141 (2005d).
- RUFFINI, R., IZZO, L., PENACCHIONI, A.V., BIANCO, C.L., CAITO, L., CHAKRABARTI, S.K. AND NANDI, A.  
«GRB 090618: a possible case of multiple GRB?»  
*PoS(Texas2010)*, p. 101 (2011).
- RUFFINI, R., SALMONSON, J.D., WILSON, J.R. AND XUE, S.S.  
«On the pair electromagnetic pulse of a black hole with electromagnetic structure».  
*A&A*, **350**, pp. 334–343 (1999).
- RUFFINI, R., SALMONSON, J.D., WILSON, J.R. AND XUE, S.S.  
«On the pair-electromagnetic pulse from an electromagnetic black hole surrounded by a baryonic remnant».  
*A&A*, **359**, pp. 855–864 (2000).
- RUFFINI, R., VERESHCHAGIN, G. AND XUE, S.S.  
«Electron-positron production, annihilation and oscillation in electromagnetic fields».

- Phys. Rep.* (in press-).
- RUFFINI, R. AND WHEELER, J.A.  
«Introducing the black hole.»  
*Physics Today*, **24**, pp. 30–36 (1971).
- RUFFINI, R. ET AL.  
In R.T. Jantzen, H. Kleinert and R. Ruffini (eds.), *The Eleventh Marcel Grossmann Meeting*. (Singapore: World Scientific, 2008b).
- RYDE, F.  
«The Cooling Behavior of Thermal Pulses in Gamma-Ray Bursts».  
*ApJ*, **614**, pp. 827–846 (2004).
- RYKOFF, E.S., AHARONIAN, F., AKERLOF, C.W., ASHLEY, M.C.B.,  
BARTHELMY, S.D., FLEWELLING, H.A., GEHRELS, N., GÖĞÜŞ, E.,  
GÜVER, T., KIZILOĞLU, Ü. ET AL.  
«Looking Into the Fireball: ROTSE-III and Swift Observations of Early  
Gamma-ray Burst Afterglows».  
*ApJ*, **702**, pp. 489–505 (2009).
- SAHU, K.C., LIVIO, M., PETRO, L., MACCHETTO, F.D., VAN PARADIJS, J.,  
KOUVELIOTOU, C., FISHMAN, G.J., MEEGAN, C.A., GROOT, P.J. AND  
GALAMA, T.  
«The optical counterpart to  $\gamma$ -ray burst grb970228 observed using the hubble  
space telescope».  
*Nature*, **387**, pp. 476–478 (1997).
- SAKAMOTO, T., BARBIER, L., BARTHELMY, S., CUMMINGS, J., FENI-  
MORE, E., GEHRELS, N., HULLINGER, D., KRIMM, H., MARKWARDT, C.,  
PALMER, D. ET AL.  
«Grb 060218/sn 2006aj: Swift-bat fluence and peak flux.»  
*GCN Circ.*, **4822** (2006).
- SAKAMOTO, T., BARBIER, L., BARTHELMY, S., CUMMINGS, J., HULLINGER,  
D., FENIMORE, E., GEHRELS, N., KRIMM, H., MARKWARDT, C., PALMER,  
D. ET AL.  
«GRB 050904 BAT refined analysis of complete data set.»  
*GCN Circ.*, **3938** (2005).
- SAKAMOTO, T., NORRIS, J., UKWATTA, T., BARTHELMY, S.D., GEHRELS, N.  
AND STAMATIKOS, M.  
«Further Swift-BAT analysis of GRB 071227.»  
*GCN Circ.*, **7156**, p. 1 (2007).
- SARI, R. AND MÉSZÁROS, P.  
«Impulsive and Varying Injection in Gamma-Ray Burst Afterglows».

- ApJ*, **535**, pp. L33–L37 (2000).
- SARI, R. AND PIRAN, T.  
«Hydrodynamic Timescales and Temporal Structure of Gamma-Ray Bursts».  
*ApJ*, **455**, p. L143 (1995).
- SARI, R. AND PIRAN, T.  
«Predictions for the Very Early Afterglow and the Optical Flash».  
*ApJ*, **520**, pp. 641–649 (1999).
- SARI, R., PIRAN, T. AND NARAYAN, R.  
«Spectra and Light Curves of Gamma-Ray Burst Afterglows».  
*ApJ*, **497**, pp. L17–L20 (1998).
- SAVAGLIO, S., GLAZEBROOK, K. AND LEBORGNE, D.  
«The Galaxy Population Hosting Gamma-Ray Bursts».  
*ApJ*, **691**, pp. 182–211 (2009).
- SAZONOV, S.Y., LUTOVINOV, A.A. AND SUNYAEV, R.A.  
«An apparently normal  $\gamma$ -ray burst with an unusually low luminosity».  
*Nature*, **430**, pp. 646–648 (2004a).
- SAZONOV, S., LUTOVINOV, A. AND SUNYAEV, R.  
Private communication (2004b).
- SHEMI, A. AND PIRAN, T.  
«The appearance of cosmic fireballs».  
*ApJ*, **365**, pp. L55–L58 (1990).
- SODERBERG, A.M., BERGER, E. AND SCHMIDT, B.P.  
«Grb060218: optical spectroscopy of grb-sn.»  
*GCN Circ.*, **4804** (2006a).
- SODERBERG, A.M., KULKARNI, S.R., BERGER, E., FOX, D.W., SAKO, M.,  
FRAIL, D.A., GAL-YAM, A., MOON, D.S., CENKO, S.B., YOST, S.A. ET AL.  
«The sub-energetic  $\gamma$ -ray burst grb 031203 as a cosmic analogue to the  
nearby grb 980425».  
*Nature*, **430**, pp. 648–650 (2004).
- SODERBERG, A.M., KULKARNI, S.R., NAKAR, E., BERGER, E., CAMERON,  
P.B., FOX, D.B., FRAIL, D., GAL-YAM, A., SARI, R., CENKO, S.B. ET AL.  
«Relativistic ejecta from x-ray flash xrf 060218 and the rate of cosmic ex-  
plosions».  
*Nature*, **442**, pp. 1014–1017 (2006b).

- SOLLERMAN, J., JAUNSEN, A.O., FYNBO, J.P.U., HJORTH, J., JAKOBSSON, P., STRITZINGER, M., FÉRON, C., LAURSEN, P., OVALDSEN, J.E., SELJ, J. ET AL.  
«Supernova 2006aj and the associated x-ray flash 060218».  
*A&A*, **454**, pp. 503–509 (2006).
- STAMATIKOS, M., UKWATTA, T.N., SAKAMOTO, T., DHUGA, K.S., TOMA, K., PE'ER, A., MÉSZÁROS, P., BAND, D.L., NORRIS, J.P., BARTHELMY, S.D. ET AL.  
«The Correlation of Spectral Lag Evolution with Prompt Optical Emission in GRB 080319B».  
In C. Meegan, C. Kouveliotou and N. Gehrels (eds.), *GAMMA-RAY BURST: Sixth Huntsville Symposium*, volume 1133 of *American Institute of Physics Conference Series*, pp. 356–361 (2009).
- SUGITA, S., YAMAOKA, K., OHNO, M., TASHIRO, M.S., NAKAGAWA, Y.E., URATA, Y., PAL'SHIN, V., GOLENETSKII, S., SAKAMOTO, T., CUMMINGS, J. ET AL.  
«Suzaku-WAM, Konus-Wind, and Swift-BAT Observations of Prompt Emission of the High-Redshift GRB 050904».  
*PASJ*, **61**, p. 521 (2009).
- THOMPSON, C.  
«A Model of Gamma-Ray Bursts».  
*MNRAS*, **270**, p. 480 (1994).
- TIENGO, A., MEREGHETTI, S., GHISELLINI, G., ROSSI, E., GHIRLANDA, G. AND SCHARTEL, N.  
«The x-ray afterglow of grb 030329».  
*A&A*, **409**, pp. 983–987 (2003).
- TIENGO, A., MEREGHETTI, S., GHISELLINI, G., TAVECCHIO, F. AND GHIRLANDA, G.  
«Late evolution of the x-ray afterglow of grb 030329».  
*A&A*, **423**, pp. 861–865 (2004).
- TOMA, K., IOKA, K., SAKAMOTO, T. AND NAKAMURA, T.  
«Low-luminosity grb 060218: A collapsar jet from a neutron star, leaving a magnetar as a remnant?»  
*ApJ*, **659**, pp. 1420–1430 (2007).
- TROJA, E., KING, A.R., O'BRIEN, P.T., LYONS, N. AND CUSUMANO, G.  
«Different progenitors of short hard gamma-ray bursts».  
*MNRAS*, **385**, pp. L10–L14 (2008).
- TRÜMPER, J.E.

- «Observations of cooling neutron stars».  
In A. Baykal, S.K. Yerli, S.C. Inam and S. Grebenev (eds.), *NATO ASIB Proc. 210: The Electromagnetic Spectrum of Neutron Stars*, p. 117 (2005).
- TSURUTA, S.  
Ph.D. thesis, , Columbia Univ., (1964) (1964).
- TSURUTA, S.  
«Thermal properties and detectability of neutron stars. i. cooling and heating of neutron stars.»  
*Phys. Rep.*, **56**, pp. 237–277 (1979).
- TSURUTA, S. AND CAMERON, A.G.W.  
«Cooling and detectability of neutron stars».  
*Canadian Journal of Physics*, **44**, p. 1863 (1966).
- TSURUTA, S., TETER, M.A., TAKATSUKA, T., TATSUMI, T. AND TAMAGAKI, R.  
«Confronting neutron star cooling theories with new observations».  
*ApJ*, **571**, pp. L143–L146 (2002).
- TUELLER, J., BARBIER, L., BARTHELMI, S., CUMMINGS, J., FENIMORE, E., GEHRELS, N., HULLINGER, D., KOSS, M., KRIMM, H., MARKWARDT, C. ET AL.  
«GRB 060607: Swift-BAT refined analysis.»  
*GCN Circ.*, **5242** (2006).
- USOV, V.V.  
«Millisecond pulsars with extremely strong magnetic fields as a cosmological source of gamma-ray bursts».  
*Nature*, **357**, pp. 472–474 (1992).
- VAN DEN BERGH, S., LI, W. AND FILIPPENKO, A.V.  
«Classifications of the Host Galaxies of Supernovae, Set III».  
*PASP*, **117**, pp. 773–782 (2005).
- VAN PARADIJS, J., GROOT, P.J., GALAMA, T., KOUVELIOTOU, C., STROM, R.G., TELTING, J., RUTTEN, R.G.M., FISHMAN, G.J., MEEGAN, C.A., PETTINI, M. ET AL.  
«Transient optical emission from the error box of the  $\gamma$ -ray burst of 28 february 1997».  
*Nature*, **386**, pp. 686–689 (1997).
- VAN RIPER, K.A.  
«Magnetic neutron star atmospheres».  
*ApJ*, **329**, pp. 339–375 (1988).

- VAN RIPER, K.A.  
«Neutron star thermal evolution».  
*ApJSS*, **75**, pp. 449–462 (1991).
- VAUGHAN, S., GOAD, M.R., BEARDMORE, A.P., O'BRIEN, P.T., OSBORNE, J.P., PAGE, K.L., BARTHELMY, S.D., BURROWS, D.N., CAMPANA, S., CANNIZZO, J.K. ET AL.  
«Swift observations of the x-ray-bright grb 050315».  
*ApJ*, **638**, pp. 920–929 (2006).
- VILLASENOR, J.S., LAMB, D.Q., RICKER, G.R., ATTEIA, J.L., KAWAI, N., BUTLER, N., NAKAGAWA, Y., JERNIGAN, J.G., BOER, M., CREW, G.B. ET AL.  
«Discovery of the short  $\gamma$ -ray burst grb 050709».  
*Nature*, **437**, pp. 855–858 (2005).
- VREESWIJK, P.M., SMETTE, A., MALESANI, D., FYNBO, J.P.U., MILVANG-JENSEN, B., JAKOBSSON, P., JAUNSEN, A.O., OSLO, U. AND LEDOUX, C.  
«VLT/UVES redshift of GRB 080319B.»  
*GCN Circ.*, **7444** (2008).
- WATSON, D., HJORTH, J., JAKOBSSON, P., XU, D., FYNBO, J.P.U., SOLLERMAN, J., THÖNE, C.C. AND PEDERSEN, K.  
«Are short  $\gamma$ -ray bursts collimated? grb 050709, a flare but no break».  
*A&A*, **454**, pp. L123–L126 (2006a).
- WATSON, D., HJORTH, J., LEVAN, A., JAKOBSSON, P., O'BRIEN, P.T., OSBORNE, J.P., PEDERSEN, K., REEVES, J.N., TEDDS, J.A., VAUGHAN, S.A. ET AL.  
«A very low luminosity x-ray flash: Xmm-newton observations of grb 031203».  
*ApJ*, **605**, pp. L101–L104 (2004).
- WATSON, D., REEVES, J.N., HJORTH, J., FYNBO, J.P.U., JAKOBSSON, P., PEDERSEN, K., SOLLERMAN, J., CASTRO CERÓN, J.M., MCBREEN, S. AND FOLEY, S.  
«Outshining the Quasars at Reionization: The X-Ray Spectrum and Light Curve of the Redshift 6.29 Gamma-Ray Burst GRB 050904».  
*ApJ*, **637**, pp. L69–L72 (2006b).
- WIERSEMA, K., SAVAGLIO, S., VREESWIJK, P.M., ELLISON, S.L., LEDOUX, C., YOON, S.C., MØLLER, P., SOLLERMAN, J., FYNBO, J.P.U., PIAN, E. ET AL.  
«The nature of the dwarf starforming galaxy associated with grb 060218/sn 2006aj».  
*A&A*, **464**, pp. 529–539 (2007).

- WILLIAMS, J.P., BLITZ, L. AND MCKEE, C.F.  
«The Structure and Evolution of Molecular Clouds: from Clumps to Cores to the IMF».  
*Protostars and Planets IV*, pp. 97–+ (2000).
- WILLINGALE, R., O'BRIEN, P.T., OSBORNE, J.P., GODET, O., PAGE, K.L., GOAD, M.R., BURROWS, D.N., ZHANG, B., ROL, E., GEHRELS, N. ET AL.  
«Testing the standard fireball model of gamma-ray bursts using late x-ray afterglows measured by swift».  
*ApJ*, **662**, pp. 1093–1110 (2007).
- WOOSLEY, S.E.  
«Gamma-ray bursts from stellar mass accretion disks around black holes».  
*ApJ*, **405**, pp. 273–277 (1993).
- WOOSLEY, S.E. AND BLOOM, J.S.  
«The supernova gamma-ray burst connection».  
*ARAA*, **44**, pp. 507–556 (2006).
- XU, D., STARLING, R.L.C., FYNBO, J.P.U., SOLLERMAN, J., YOST, S., WATSON, D., FOLEY, S., O'BRIEN, P.T. AND HJORTH, J.  
«In search of progenitors for supernova-less GRBs 060505 and 060614: re-examination of their afterglows».  
*ArXiv:0812.0979* (2008).
- YAKOVLEV, D.G. AND PETHICK, C.J.  
«Neutron star cooling».  
*ARAA*, **42**, pp. 169–210 (2004).
- ZELDOVICH, Y.B. AND RAIZER, Y.P.  
*Elements of gasdynamics and the classical theory of shock waves* (New York: Academic Press, 1966, edited by Hayes, W.D.; Probstein, Ronald F., 1966).
- ZHANG, B., FAN, Y.Z., DYKS, J., KOBAYASHI, S., MÉSZÁROS, P., BURROWS, D.N., NOUSEK, J.A. AND GEHRELS, N.  
«Physical processes shaping gamma-ray burst x-ray afterglow light curves: Theoretical implications from the swift x-ray telescope observations».  
*ApJ*, **642**, pp. 354–370 (2006).
- ZHANG, B. AND KOBAYASHI, S.  
«Gamma-Ray Burst Early Afterglows: Reverse Shock Emission from an Arbitrarily Magnetized Ejecta».  
*ApJ*, **628**, pp. 315–334 (2005).
- ZHANG, B. AND MÉSZÁROS, P.  
«Gamma-Ray Burst Afterglow with Continuous Energy Injection: Signature of a Highly Magnetized Millisecond Pulsar».

*ApJ*, **552**, pp. L35–L38 (2001).

ZHANG, B., ZHANG, B.B., LIANG, E.W., GEHRELS, N., BURROWS, D.N.  
AND MÉSZÁROS, P.

«Making a short gamma-ray burst from a long one: Implications for the  
nature of grb 060614».

*ApJ*, **655**, pp. L25–L28 (2007).

ZIAEPOUR, H., HOLLAND, S.T., BOYD, P.T., PAGE, K., OATES, S., MARK-  
WARDT, C.B., MÉSZÁROS, P., GEHRELS, N., MARSHALL, F.E., CUM-  
MINGS, J. ET AL.

«GRB 060607A: a gamma-ray burst with bright asynchronous early X-ray  
and optical emissions».

*MNRAS*, **385**, pp. 453–467 (2008).

ZOU, Y., PIRAN, T. AND SARI, R.

«Clues from the Prompt Emission of GRB 080319B».

*ApJ*, **692**, pp. L92–L95 (2009).